People at the tidal flats: coastal morphology and hazards in Iqaluit, Nunavut

by

©Scott Hatcher

A Thesis submitted to the School of Graduate Studies in partial fulfillment of the requirements for the degree of

Master of Science

Department of Geography

Memorial University of Newfoundland

May 2014

St. John's Newfoundland

Abstract

Rapid environmental change observed in the Canadian Arctic is driving efforts at federal, territorial, and municipal levels to adapt to the impacts of projected changes. Recent work with communities has shown that targeted and relevant scientific input can greatly enhance ongoing vulnerability assessments and policy planning around adaptation and sustainability. The Arctic coast is dynamic, creating risk to Arctic coastal infrastructure. Using GIS modelling and geoscientific data collected over three field seasons, this thesis reports on a project aimed at providing coastal hazard mapping for Iqaluit, Nunavut. Iqaluit is the capital city of Nunavut, and sits alongside a macrotidal embayment with extensive tidal flats, which influence many aspects of life in the community. Data collected include: detailed topography and bathymetry, elevations of the coastal setting, elevations of past extreme water levels, and morphological mapping. The results build on previous work in Iqaluit, showing a relatively stable boulder-strewn sand flat morphology in the macrotidal embayment. Modelling of the coastal topography indicates a recent (last century) period of quasi stable sea level, with possible slight emergence persisting. Hydrodynamic data reveal little evidence for significant erosion through wave and current input. Recorded nearshore current velocities were between 0.1 - 0.3 m/s, with greater velocities at the top 3 m of the water column. The hazard mapping then attempts to incorporate the morphological mapping into a GIS of coastal infrastructure in the city in order to provide detailed

information for city planners. Results show limited freeboard of 0.3-0.8 m for most coastal infrastructure under an upper-limit projection of 0.7 m relative sea-level rise from 2010 to 2100. Key infrastructure, and especially the subsistence infrastructure focused on the coast, is actually below past recorded maximum water levels during high spring tides. Lack of data, however, precludes any reasonable estimate of recurrence. Geomorphological mapping of the coastal setting provides crucial insight into the risks to infrastructure from storm waves, erosion, and sea-level rise. The study shows that the tidal flats are a source of coastal resilience in the form of wave dissipation, lowering ice pile-up/ride-up risk, and protection from rapid erosion.

Acknowledgements

I would like to acknowledge ArcticNet, SSHRC through C-Change, the Northern Scientific Training Program, Natural Resources Canada, and the Memorial University Department of Geography for funding the research for this thesis. I would also like to thank the Nunavut Research Institute and the Canada Nunavut Geoscience Office for their assistance while in Iqaluit. Deserved acknowledgements go to Don Forbes for providing me the opportunity to take my education from human history into natural history, and for trusting an untested student. Having taken that opportunity, my ability to produce a thesis was dependent largely on the support of the Geography department at Memorial, including my advisors Norm Catto and Trevor Bell, as well as the rest of my fellow graduate students. I'd also be a much more sullen student without the warmth and friendship of my dear wife Hilary, who motivated me by writing a far better thesis than I ever could (and in less time). Despite this I was still encouraged by my parents Bruce and Annamarie to finish, often reminding me of the slightly depressing thought that graduate school was one of the best times of their lives. Without them I would never have been able to take the opportunity.

On the more technical side, I really can't thank Gavin Manson enough for giving me on-site training in "doing science". The data provided by Paul Budkewitsch at the Canadian Centre for Remote Sensing was crucial to the project. I'd also like to acknowledge Anne-Marie Leblanc, and the whole team from Universite Laval, for

logistical support in the field. Finally, to Meagan Leach at the city of Iqaluit I owe thanks for data provided and for her encouraging collaboration.

Statement of co-authorship

The following people and institutions contributed to the publication of work undertaken as part of this thesis:

Hatcher, S.V. Memorial University, St.John's, NL.

Forbes, D.L.F. Memorial University, St.John's, NL, and Geological Survey of Canada, Dartmouth, NS.

Manson, G. Geological Survey of Canada, Dartmouth, NS.

Paper 1 - Coastal geomorphology of a low Arctic macrotidal embayment

- Located in chapter 2.
- Hatcher was the primary author, contributed to stakeholder consultation and data acquisition, undertook the data analysis, composed the visuals, and wrote the text.
- Forbes contributed to conceptual development, stakeholder consultation, data acquisition, and review and revision of the manuscript.

- Manson contributed to field work logistics, data acquisition, and discussion in the field.

Paper 2 - Assessing exposure to coastal hazards in Iqaluit

- Located in chapter 3.
- Hatcher was the primary author, contributed to stakeholder consultation and data acquisition, undertook the data analysis, composed the visuals, and wrote the text.
- Forbes contributed to conceptual development, stakeholder consultation, data acquisition, and review and revision of the manuscript.

Data report

- Located in Appendix.
- Hatcher was the primary author, contributed to stakeholder consultation and data acquisition, undertook the data analysis, composed the visuals, and wrote the text.
- Forbes contributed to project formulation, stakeholder consultation, data acquisition, and review and revision of the manuscript.
- Manson contributed to field work logistics, data acquisition, and discussion in the field.

Table of Contents

List of Tables

List of Figures

Chapter 1

Introduction

1.1 The Arctic coastal system

Communities in the Canadian Arctic are increasingly exposed to impacts from climate change. Those shifts in environmental norms are already being reported by and documented for the population of the Canadian Arctic (Anisimov et al., 2007), leading the Inuit Circumpolar Council to file a human rights violation petition in 2005 (ICC, 2005). A majority of Canadian Arctic communities are coastal and are considered one of the most critical groups in terms of the rapidity of environmental change, as well as the expected impacts from those changes to natural resources (Forbes, 2011). Among anticipated climate change impacts, decreased or less reliable sea ice impacts subsistence hunting and transportation networks (Laidler, 2006; Laidler et al., 2008), greater wave energy and rising sea levels impact coastal infrastructure (Ford et al., 2010; Forbes, 2011), and changes in storm patterns with associated storm surges and coastal erosion impact the sustainability of coastal settlements (Furgal & Prowse, 2007; Lynch & Brunner, 2007). The close coupling of these exposure-impact scenarios, as well as the effect projected changes to climate might have on these interactions,

forms an extensive avenue of research (Furgal & Prowse, 2007).

Assessing this vulnerability to climatic shifts within a complex social-ecological system is key in determining courses of action that reduce the negative impacts of these changes (adaptation). There is widespread recognition that communities of the Arctic will feel these climatic changes more acutely than other populations due to a number of inherent social attributes. These include Inuit reliance on the environment through subsistence activity, widespread socio-economic challenges that characterize northern life, as well as rapid settlement of the once nomadic population in communities where wage economies often compete with other forms of wealth pursuit (Ford, 2009). This work is plentiful in the literature (Bolton et al., 2011), much of it conducted through a framework for vulnerability assessment (Smit & Wandel, 2006; Champalle et al., 2013). Across a spectrum of academic output, and government-community partnerships, some key points have emerged and attracted broad agreement: (1) community-scale impact assessments, when done in close collaboration with communities, can provide invaluable knowledge to inform adaptation policies; (2) impacts and vulnerability are interrelated, but not the same; vulnerability is a function of exposure, sensitivity, and adaptive capacity (IPCC, 2001), which inevitably includes elements of the social fabric of the community; (3) the impacts experienced by communities vary widely across the Arctic, due to intricacies of the environment that require place-adjusted approaches to development and adaptation.

1.2 Climate change adaptation in Nunavut

1.2.1 Instability of coastal landscapes in Arctic communities

A project funded by the ArcticNet Network of Centres for Excellence (NCE) directly addresses the projection of responses to climate change within The Arctic coastal

system. This is seen as a prerequisite to effective adaptation policy. The goal is to "promote informed choices of adaptation measures and enhanced resilience in northern coastal communities" (Bell & Forbes, 2013). The driving philosophy is that better adaptation policy is formed in conjunction with sound geoscience mapping and regional modelling, a response mirrored in the Nunavut Climate Change Partnership (NCCP) proceedings (Mate & Reinhardt, 2011).

1.2.2 Nunavut Climate Change Partnership

Beginning in 2006, Natural Resources Canada (NRCan), the Government of Nunavut (GN), the Canadian Institute of Planners (CIP), and Indian and Northern Affairs Canada (INAC) developed a collaborative project to address some of the issues surrounding community vulnerability to climate change. The NCCP was set up to look at ways of improving the adaptive capacity of Nunavut communities through collaboration and research, beginning with a pilot project in Clyde River (Forbes et al., 2007). The stated goals were to "(1) create scientific information that is regionally and locally targeted to help communities adapt to climate change, (2) build capacity for climate change adaptation planning within the Government of Nunavut and in Nunavut communities, and (3) develop tools to collect, publish, share, and communicate climate change adaptation knowledge across Nunavut and beyond" (Mate & Reinhardt, 2011). A workshop held in Iqaluit, Nunavut, in February 2011 reviewed results and identified some central themes. One is the need for better communication amongst policy makers, researchers, and community members about expected changes brought on by climate change. Another is that research to quantitatively define expected coastal sensitivities and impacts at a community scale would be an asset for planners (Mate & Reinhardt, 2011). The interface of these two results is part of a continuing discussion on the best ways to deliver relevant and accessible applied

science to support adaptation efforts (Catto & Parewick, 2008; Lane & Watson, 2010; Lane et al., 2013; Champalle et al., 2013).

1.2.3 C-Change Adaptation Work in the city of Iqaluit

In recognition of limitations and challenges associated with coastal vulnerability and adaptation (IPCC, 2007), an International Community-University Research Alliance (ICURA) was established in 2009. C-Change (www.coastalchange.ca) was set up to address the needs for effective adaptation planning through partnerships with coastal communities in Canada and the Caribbean (Lane & Watson, 2010). One of the communities selected for the project was Iqaluit, Nunavut.

The City of Iqaluit had identified potential infrastructure vulnerability from sea-level rise and increased storm hazards as an important consideration in its 5-year administrative plan (City of Iqaluit, 2010). Local residents were noticing extended open-water seasons, and significant changes in local weather patterns, putting at risk the long-term sustainability of traditional livelihoods and hunter safety (Shirley, 2005). Also, flooding has occurred in the past (most recently in October 2003), inundating critical municipal and subsistence infrastructure (Nielsen, 2007). Included as well in the NCCP, the city's department of Engineering and Sustainability identified a knowledge gap in the impacts of these coastal hazards on current and future coastal infrastructure (Lewis & Miller, 2010).

The current research is directly related to this knowledge gap. Iqaluit sits within Koojesse Inlet, a macrotidal embayment of Frobisher Bay with extensive boulder tidal flats. The identification of coastal hazards under climate change as an important source of uncertainty for municipal planning suggested that directed geoscientific data collection and hazards mapping could make an important contribution to adaptation policy. Using a coastal geomorphology perspective to evaluate the coastal system,

including landforms and the built environment, this project provides a case study in applied hazard mapping and investigates the role of coastal morphology in determining exposure to coastal hazards along the Iqaluit waterfront.

1.3 The influence of coastal geomorphology and hazards on adaptation

The Arctic coast is changing rapidly. The Arctic Coastal Dynamics project reported coastal erosion ranging from 0 to 8 m/yr in parts of the Arctic (Lantuit et al., 2011). Communities on the Alaskan coast have had to relocate because of accelerated erosion (Bronen, 2009). The Beaufort sea coast is eroding rapidly due to thermal abrasion of its ice-rich unlithified coastline in a warming climate and increased wave energy from longer open-water seasons (Atkinson, 2005; Solomon, 2005; Manson et al., 2004; Manson & Solomon, 2007; Are et al., 2008; Overeem et al., 2011). Classification of the Arctic coastline into lithified and unlithified segments reveals more active erosion on ice-rich unlithified coasts due to the processes of thermal abrasion and the mobility of sediments in these sections (Lantuit & Pollard, 2008). The Arctic coast includes a range of morphologies, all of which exhibit differing rates of erosion, responses to relative sea-level change, and level of human development and interaction. Community infrastructure is often directly adjacent to the coast, and so is susceptible to changes in the Arctic coastal system (Forbes, 2011).

The field of coastal geomorphology, as a science of the dynamics and description of coastal landforms, is well situated to provide valuable information to coastal planners and developers. The implications of rapid coastal change from shifting sea-levels and storm patterns in recent decades has thrust this information into the realm of public policy. The unique challenges faced by communities in the Canadian Arctic

in a rapidly warming climate call for effective applied science and policy integration (Forbes, 2011). The field of coastal hazards, as a subset of natural hazards, involves the vulnerabilities of coastal populations to hazards (Finkl, 1994; Setterlund, 2003; Kron, 2012), including those imposed by landform dynamics (Viles & Spencer, 1995; Slaymaker et al., 2009; Liggins et al., 2010; Haslett, 2009; Woodroffe, 2003). It is the built environment, structures and properties that we position along the coast, that creates exposure and vulnerability to coastal hazards.

An understanding of the potential for infrastructure damage from natural hazards and climate change is fundamental to ongoing adaptation planning and vulnerability assessments in northern communities (Forbes, 2011). An estimated 5 trillion dollars worth of infrastructure is under threat from landscape hazards, both directly and indirectly attributable to rapid climate change, in the Canadian North (NRTEE, 2009). Unlike the people of the Arctic, who have adapted in the past to profound environmental shifts (AHDR, 2004), physical infrastructure is fixed, not readily adaptable, and costly to protect, modify, or replace (Larsen et al., 2008). The isolation and historical geography of communities in the north means that transportation infrastructure is generally focused on aviation or shipping. This is critical for food security, emergency access to medical services, and delivery of essential supplies, and thus is crucial to the sustainability of the communities (Forbes, 2011).

1.4 Research Objectives

The overall objective of this thesis is to contribute to the study of coastal hazards exposure in Iqaluit at the interface between residents and their environment. More specifically, the sub-objectives are, first, to evaluate the coastal impacts of climate change and sea-level change in Iqaluit, Nunavut. Second, to extend geomorphological

mapping of the Koojesse Inlet tidal flats into the nearshore in order to investigate the stability of the flats and their influence on sea ice and wave energy reaching shoreline infrastructure. Third, to assess the present and future exposure of community resources to coastal hazards in a changing climate, as a basis for informed adaptation planning and decision-making.

In order to meet these objectives, this thesis aims to do three things. The first is to describe the morphology and dynamics of the Koojesse Inlet tidal flats using data collected over three field seasons. Also, to develop plausible scenarios of extreme water levels based on the existing water level record, accumulating data on vertical motion, and global and local projections of sea-level change. And lastly, to assess and map the interaction of these evolving coastal hazards with the current coastal infrastructure of Iqaluit, Nunavut.

1.5 Thesis structure

This thesis follows a manuscript style, characterized by two research papers forming the core with an introductory chapter and a final chapter of discussion and conclusions aiming to synthesize the results and comment on the research as a whole. Though the two papers attempt to stand on their own, the data collection and analysis were cross-referenced and connected. After the title of each paper the authorship and target journal for submittal is listed.

The themes for each chapter are:

Chapter 1 Beginning with a brief introduction to commonalities in populated Arctic coastal systems, and moving on to descriptions of ongoing projects related to the implications of climate change for coastal Arctic communities, this section argues the validity of a coastal hazards assessment in Iqaluit.

Chapter 2 Paper 1 - Coastal geomorphology of a low Arctic macrotidal embayment.

Author: *Hatcher, S.V.*

Co-Authors: *Forbes, D.L.F., Manson, G.*

Target journal: *Journal of Coastal Research*

The purpose of this chapter is to present the results of a three year field work campaign to map the geomorphology and hydrodynamics of the Koojesse Inlet macrotidal flats located adjacent to Iqaluit, Nunavut. Data collected were elevations and depths describing the topography of the flats, currents and water levels both overtop the flats and in the nearshore, and ice thicknesses during the 2011 ice season. Using this dataset the paper argues that the topography of the flats, in corroboration with an ice-dominated forcing regime, suggests a close relationship between current sea level benchmarks and the morphology of the tidal flats.

Chapter 3 Paper 2 - Assessing coastal hazards to infrastructure in Iqaluit, Nunavut.

Author: *Hatcher, S.V.*

Co-Author: *Forbes, D.L.F.*

Target journal: *Arctic*

The purpose of this chapter is to present the results of the hazard mapping analysis conducted in Iqaluit, Nunavut. This analysis required detailed topographic mapping in the shoreface and backshore areas of the city, coupled with a projection of expected sea-level rise out to the year 2100. Using this, along

with observational data on short timescale hazard contributors such as sea-ice, waves, and tidal flooding, the paper argues that flooding risk in Iqaluit might have been previously overestimated. What is apparent, however, is that the infrastructure most at risk to future flooding is the subsistence infrastructure that lines the main coastline of the city.

Synthesis and Discussion The central question behind this chapter is "what is the contribution to coastal geomorphology and hazard analysis to informing climate-change adaptation and sustainability planning in a coastal municipality?" Drawing on a comparison of the geomorphology of the Koojesse Inlet tidal flats presented in chapter 2 and the coastal hazards in Iqaluit presented in chapter 3, what influence does the morphology have on the hazards? It is found that certain aspects of the morphology contribute to whatever risk of hazard there is, where as other aspects of the morphology present inherent sources of resilience to change. Scientific study of the morphology, therefore, can have a positive and essential contribution to ongoing adaptation and sustainability plans.

Appendix - Open file report on field work This appendix is formatted as a Geological Survey of Canada (GSC) open file report, aimed to be published in the next year. It provides detailed information on the data collected, the summary of field work activities, as well as graphical representations of all the data presented in the two papers. It is meant to be consulted in conjunction with the rest of the thesis so that a more detailed understanding of the data collected is provided in the thesis where it would not be in the paper format.

1.6 Terminology and Context

Specific terminology used in this thesis must be defined as clearly as possible in order to aid understanding. The approach is primarily pragmatic, and tries to be as consistent as possible. Within the central themes of the field - natural hazards, vulnerability, resilience, adaptation, environmental change - a large amount of work has been done on defining conceptual boundaries and frameworks (See Klein & Nicholls, 1999; Ford & Smit, 2004; Adger et al., 2005; Smit & Wandel, 2006; Cutter & Finch, 2008; Wolf, 2011), but the terms are still not cut in stone. A comparison of approaches reveals related but distinct definitions depending on originator fields of study (Wolf, 2011). The definitions here attempt a midway point between intuitive understanding of the terms and reference to the theoretical publications.

The term "hazard" here refers to a potential event that damages infrastructure. By extension, coastal hazards are potential damaging events that occur related to coastal processes. This event can have multiple triggers, including meteorological, geomorphological, hydrological, or tectonic. "Risk" refers to the "probability of a given hazard". Geophysical change in the system under study brought by climatic shifts, tectonic change, or morphodynamics comprises a vast majority of natural hazards studies. This study is, then, primarily concerned with describing potential hazards based on wider scale research that has identified likely increases of risk on a regional basis.

The term "infrastructure" here refers to hard infrastructure, which includes buildings, roadbeds, culverts, breakwaters, and piers. There is an implicit acknowledgement, though, that this infrastructure is being used by the communities. Also, that there is a spatial aspect to this use: that fishing sheds include the building itself, but also imply a buffer around which fishing activities happen. Planning around this infrastructure then must include proximity to high water lines, rather than simply the intersection

of foundations with high water limits.

This terminology establishes a distinction between vulnerability and hazards. In the IPCC (2001) WGII summary for policy-makers, vulnerability is defined as "the degree to which a system is susceptible to, or unable to cope with, adverse effects of climate change... [it] is a function of the character, magnitude, and rate of climate change and variation to which a system is exposed, its sensitivity, and its adaptive capacity." the term vulnerability implies consideration of human adaptive capacity, resilience, and reaction to hazards. The work presented in this thesis describing extents in which flooding will damage coastal infrastructure does not include the resilience of the community to those damages, and includes no relevant data on the community's ability to adapt to changing risk. In this sense it deviates from the common definition of vulnerability, as it has come to be understood in the dominant literature. Instead, it discusses explicitly the vulnerability of infrastructure to risks from the natural system, with a secondary classification of sensitivity based on assumed use of that infrastructure. This thesis, however, recognizes two important facets of this interpretation: first, that the interdisciplinary nature of the field benefits from common conventions despite the lens through which a specific case study is conducted, and secondly (and more importantly), that vulnerability assessment and adaptation planning is an ongoing and reflexive process involving collaboration and exchange between community planners, community members, researchers, and regional government. The goal of a useful hazards assessment should be to competently assess changing risk in the system in question using the available data in a way that is most transferable to this continuing forum of discussion.

1.7 References

Adger, W. N., Hughes, T. P., Folke, C., Carpenter, S. R., & Rockström, J. (2005). Social-ecological resilience to coastal disasters. *Science*, *309*, 1036–1039.

AHDR (2004). Arctic Human Development Report. Tech. rep., Stefansson Arctic Institute, Akureyri.
URL (http://www.svs.is/AHDR/)

Anisimov, O., Vaughan, D., Callaghan, T., Furgal, C., Marchant, H., Prowse, T., Vilhjálmsson, H., & Walsh, J. (2007). *Polar Regions (Arctic and Antarctic)*, (pp. 653–685). Cambridge University Press, Cambridge, UK.

Are, F., Reimnitz, E., Grigoriev, M., Hubberten, H., & Rachold, V. (2008). The influence of cryogenic processes on the erosional Arctic shoreface. *Journal of Coastal Research*, *24*(1), 110–121.

Atkinson, D. (2005). Observed storminess patterns and trends in the circum-Arctic coastal regime. *Geo-Marine Letters*, *25*(2), 98–109.

Bell, T., & Forbes, D. (2013). Instability of Coastal Landscapes in Arctic Communities and Regions.
URL http://www.arcticnet.ulaval.ca/research/summary.php?project_id=44

Bolton, K., Lougheed, M., Ford, J., Nickels, S., Grable, C., & Shirley, J. (2011). What we know, don't know, and need to know about climate change in Inuit Nunan-

gat. Tech. rep., The Department of Indian and Northern Affairs Canada, Climate Change Adaptation Program (CCAP).

Bronen, R. (2009). *Forced migration of Alaskan indigenous communities due to climate change: creating a human rights response*, (pp. 68–73). United Nations University (Institute of Environment and Human Security) and Munich Re, UNU-EHS Publication No. 12.

Catto, N., & Parewick, K. (2008). *Hazard and vulnerability assessment and adaptive planning: mutual and multilateral community-research communication, Arctic Canada*, vol. 305, (pp. 123–140). Gological Society, London, Special Publications 2008.

Champalle, C., Tudge, P., Sparling, E., Riedlsperger, R., Ford, J., & Bell, T. (2013). Adapting the Built Environment in a Changing Northern Climate. Tech. rep., Report for Natural Resources Canada, Climate Change Impacts and Adaptation.

City of Iqaluit (2010). Amended Version of the City of Iqaluit General Plan (Draft February 2010). Tech. rep., City of Iqaluit.

Cutter, S. L., & Finch, C. (2008). Temporal and spatial changes in social vulnerability to natural hazards. *Proceedings of the National Academy of Sciences of the United States of America*, *105*(7), 2301–2306.

Finkl, C. W. (1994). Preface. *Journal of coastal research*, *Special Issue No. 12 Coastal Hazards: perception, susceptibility and mitigation*, ix–xi.

Forbes, D., Mate, D., Bourgeois, J., Bell, T., Budkewitsch, P., Chen, W., Gearhard, S., Illauq, N., Irvine, M., & Smith, R. (2007). Integrated mapping and environmental change detection for adaptation planning in an Arctic coastal community, Clyde

River, Nunavut. In G. Flöser, H. Kremer, & V. Rachold (Eds.) *Arctic Coastal Zones at Risk: Workshop Proceedings*, (pp. 42–47).
URL http://coast.gkss.de/events/arctic07/docs/proceedings.pdf

Forbes, D. e. (2011). *State of the Arctic Coast 2010 - Scientific Review and Outlook*. Helmholtz-Zentrum, Geesthacht. Germany.: International Arctic Science Committee, Land-Ocean Interactions in the Coastal Zone, Arctic Monitoring and Assessment Programme, International Permafrost Association.
URL http://arcticcoasts.org

Ford, J., Bell, T., & St. Hilaire-Gravel, D. (2010). *Vulnerability of Community Infrastructure to Climate Change in Nunavut: A Case Study From Arctic Bay*, chap. 5, (pp. 107–130). Dordrecht: Springer Netherlands.

Ford, J., & Smit, B. (2004). A framework for assessing the vulnerability of communities in the Canadian Arctic to risks associated with climate change. *Arctic*, *57*(4), 389–400.

Ford, J. D. (2009). Dangerous climate change and the importance of adaptation for the Arctic's Inuit population. *Environmental Research Letters*, *4*(2), 024006.

Furgal, C., & Prowse, T. (2007). Northern Canada. In D. Lemmen, F. Warren, & J. Lacroix (Eds.) *From Impacts to Adaptation: Canada in a Changing Climate*, (pp. 57–118). Government of Canada, Ottawa, ON.

Haslett, S. (2009). *Coastal Systems*. Routledge, 2nd ed.

ICC (2005). Petition to the Inter American Commission on Human Rights Seeking Relief from Violations Resulting from Global Warming Caused by Acts and Omissions of the United States.

URL http://www.inuitcircumpolar.com/files/uploads/icc-files/FINALPetitionICC.pdf

IPCC (2001). *Climate Change 2001 - Summary for Policy-Makers*. Cambridge University Press, Cambridge, UK.

IPCC (2007). *Climate Change 2007: Synthesis Report. Contribution of Working Groups I, II and III to the Fourth Assessment Report of the Intergovernmental Panel on Climate Change*. Cambridge University Press, Cambridge, UK and New York, NY, USA.

Klein, R., & Nicholls, R. (1999). Assessment of coastal vulnerability to climate change. *Ambio*, *28*(2), 182–187.

Kron, W. (2012). Coasts: the high-risk areas of the world. *Natural Hazards*, *66*(3), 1363–1382.

Laidler, G. (2006). Inuit and Scientific Perspectives on the Relationship Between Sea Ice and Climate Change: The Ideal Complement? *Climatic Change*, *78*(2-4), 407–444.

Laidler, G., Ford, J. D., Gough, W. A., Ikummaq, T., Gagnon, A. S., Kowal, S., Qrunnut, K., & Irngaut, C. (2008). Travelling and hunting in a changing Arctic: assessing Inuit vulnerability to sea ice change in Igloolik, Nunavut. *Climatic Change*, *94*(3-4), 363–397.

Lane, D., Mercer Clarke, C., Forbes, D., & Watson, P. (2013). The gathering storm: managing adaptation to environmental change in coastal communities and small islands. *Sustainability Science*, *special issue on-line*.

Lane, D., & Watson, P. (2010). Managing adaptation to environmental change in coastal communities: Canada and the Caribbean. In *Proceedings of the 11th Annual Conference of SALISES*, (pp. 1–16). St. Augustine, Trinidad and Tobago.

Lantuit, H., Atkinson, D., Paul, P., Grigoriev, M., Rachold, V., Grosse, G., & Hubberten, H.-W. (2011). Coastal erosion dynamics on the permafrost-dominated Bykovsky Peninsula, north Siberia, 1951–2006. *Polar Research*, *30*(7341).

Lantuit, H., & Pollard, W. (2008). Fifty years of coastal erosion and retrogressive thaw slump activity on Herschel Island, southern Beaufort Sea, Yukon Territory, Canada. *Geomorphology*, *95*(1), 84–102.

Larsen, P., Goldsmith, S., Smith, O., Wilson, M., Strzepek, K., Chinowsky, P., & Saylor, B. (2008). Estimating future costs for Alaska public infrastructure at risk from climate change. *Global Environmental Change*, *18*(3), 442–457.

Lewis, J., & Miller, K. (2010). Climate Change Adaptation Action Plan for Iqaluit. Tech. rep., Report to Natural Resources Canada, Nunavut Climate Change Partnership. Atuliqtuq: Action and Adaptation in Nunavut.
URL `http://www.planningforclimatechange.ca/wwwroot/Docs/Library/CommAdptPlans/IQALUIT_REPORT_E.PDF`

Liggins, F., Betts, R. a., & McGuire, B. (2010). Projected future climate changes in the context of geological and geomorphological hazards. *Philosophical transactions. Series A, Mathematical, physical, and engineering sciences*, *368*(1919), 2347–2367.

Lynch, A. H., & Brunner, R. D. (2007). Context and climate change: an integrated assessment for Barrow, Alaska. *Climatic Change*, *82*(1-2), 93–111.

Manson, G., Solomon, S., Atkinson, D., & Craymer, M. (2004). Spatial Variability

of factors influencing coastal change in the western Canadian Arctic. *GeoMarine Letters*, *25*, 138–145.

Manson, G. K., & Solomon, S. M. (2007). Past and future forcing of Beaufort Sea coastal change. *Atmosphere-Ocean*, *45*(2), 107–122.

Mate, D., & Reinhardt, F. (Eds.) (2011). *Nunavut Climate Change Partnership Workshop, February 15-16*. Geological Survey of Canada, Open File 6867. 1 CD-ROM.

Nielsen, D. (2007). The City of Iqaluit's Climate Change Impacts, Infrastructure Risks & Adaptive Capacity Project. Tech. rep., City of Iqaluit, Iqaluit.

NRTEE (2009). True North: Adapting Infrastructure to Climate Change in Northern Canada. Tech. rep., National Round Table on the Environment and the Economy.

Overeem, I., Anderson, R., Wobus, C., Clow, G., Urban, F., & Matell, N. (2011). Sea ice loss enhances wave action at the Arctic coast. *Geophysical Research Letters*, *38*(17), L17503.

Setterlund, S. (2003). Coastal hazards: A guide to print, electronic and web resources. *Journal of coastal research*, *19*(1), 134–156.

Shirley, J. (2005). Inuit Qaujimajatuqangit of Climate Change in Nunavut. Tech. rep., Government of Nunavut, Dept of Environment.

Slaymaker, O., Spencer, T., & Embleton-Hamann, C. (2009). *Geomorphology and global environmental change*. Cambridge University Press.

Smit, B., & Wandel, J. (2006). Adaptation, adaptive capacity and vulnerability. *Global Environmental Change*, *16*(3), 282–292.

Solomon, S. (2005). Spatial and temporal variability of shoreline change in the Beaufort-Mackenzie region, Northwest Territories, Canada. *Geo-Marine Letters*, *25*(2), 127–137.

Viles, H., & Spencer, T. (1995). *Coastal Problems: Geomorphology and Ecology and Society at the Coast*. London: Edward Arnold.

Wolf, S. (2011). Vulnerability and risk: comparing assessment approaches. *Natural Hazards*, *61*(3), 1–15.

Woodroffe, C. (2003). *Coasts: Form, Process, and Evolution*. Cambridge University Press.

Chapter 2

Coastal geomorphology of a low Arctic macrotidal embayment

Hatcher, Forbes, Manson 2013. Formatted for the Journal of Coastal Research

2.1 Abstract

Our knowledge of coasts with tidal flats comes primarily with examples from temperate regions. High-latitude tidal flats, or cold zone tidal flats, occur in places where seasonal ice cover presents a new array of landforms and dynamic interactions. The coastal Arctic is changing rapidly, and a better understanding of its tidal flat coastlines might provide additional support in the drive to sustain its communities. The purpose of this study is to build on previous investigations of the macrotidal flats of Koojesse Inlet on southern Baffin Island in Canada's eastern subArctic by quantifying erosion/deposition over a three-year timespan, by extending morphological mapping into the nearshore, and by investigating the potential of currents and waves to alter the coast in comparison with the effects of sea-ice. Field work conducted over

five trips, which spanned all seasons, between 2009 and 2011 focused on producing a dataset of morphological mapping and drivers of change on the flats. Mapping was conducted by RTK-GPS coastal surveys, sonar and sub-bottom surveying, and surficial sampling throughout. Change is based on observations of currents and waves over short time periods, sea-ice surveys during and after freezeup, as well as changes in coastal transects from re-occupied GPS surveys. Results show a shoreface and intertidal that reflect the influence of wave events in beach formation, and ice influence through a lack of sediment zonation and boulder movement. The deeper basins in the harbour adjacent to the flats are characterized by ponded silty sediment, in contrast to the tidal flat surface which has a veneer of sand and boulders. Beneath this veneer is a unit of truncated glacio-marine sediment. Erosion and deposition is chaotic on the flats surface over this short timespan, but we found some morphological evidence for consistent mass wasting into the nearshore. The boulder mounds formed by sea-ice movement provide a protective barrier to significant wave input in the intertidal. The vast majority of currents measured were incapable of transporting the sand-dominated surface material, and were driven by a combination of tide and wind asymmetries. Sand ripples on the surface suggest the ability of shallow water wind currents to form the sand during low tides. This study supports the importance of postglacial uplift and sea-ice sediment entrainment in the formation of these high-latitude tidal flats.

2.2 Introduction

Tidal flats are low-slope, low-relief, unlithified coastal landforms alternately covered and exposed by the flood and ebb of tides (Bird & Schwartz, 1985; Amos, 1995). They are generally best developed and most extensive in meso- to macro-tidal settings (with tidal range >2 m), though many examples can be found in areas of more restricted tide

(Martini, 1991). There is wide geographic variability in the form and sedimentology of tidal flats, but generally they are considered to be depositional coastal systems dominated by finer sediments and found in protected embayments and estuaries (Amos, 1995). Macrotidal flats exhibit greater variation in sediment sizes, depending on the level of vegetation and the exposure to waves.

High-latitude tidal flats developed in cold climates display a number of distinctive characteristics (Dionne, 1988; Forbes & Taylor, 1994; Forbes & Hansom, 2012). Cold-region flats in areas of glacio-isostatic rebound are commonly erosional surfaces (McCann et al., 1981; Dale et al., 2002), which formed as uplifted marine deposits are reworked by shore-zone processes at lower sea levels (Ruz et al., 1998). High-latitude tidal flats typically exhibit morphological indicators of ice-dominance in sediment dynamics (Dionne, 1988; Forbes & Taylor, 1994). Ice action generally provides at once (1) a unique forcing that differentiates these flats from their temperate counterparts, and (2) an important, if not dominant, shaper of modern morphology (Dionne, 1988; Leech, 1998; Forbes & Taylor, 1994).

The boulder-strewn tidal flats of Koojesse Inlet in southeastern Baffin Island are one such example. Studies in the early 1980s provided an initial description of the flats in this macrotidal setting (McCann et al., 1981). This included documentation of ice and sediment dynamics during the annual ice break-up (McCann & Dale, 1986), a theoretical analysis of the mechanics of boulder transport by ice (Drake & McCann, 1982; Forbes & Taylor, 1994), and the role of ice in disrupting benthic biota, diminishing the role of biological processes (Gilbert, 1984; Dale et al., 2002). More recently investigation has focused on quantifying entrained sediment load (Leech, 1998), with results comparable to loads observed in other cold-region tidal flats (Dionne, 1993; Martini, 1991; Ruz et al., 1998). Leech (1998) directly measured boulder transport on the flats and found predominantly shoreward migration. This was in contrast to

the seaward transport hypothesized by the observation of well established boulder barricades and garlands in other cold-region tidal flats (Rosen, 1979; Lauriol & Gray, 1980). Previous work also considered the shore-normal zonation of the flats, showing the absence of the fining-landwards sediment grading typical of tidal flat deposition in mid- to low-latitude settings (Dale et al., 2002). The overall conclusion from previous work is the erosional nature of the Iqaluit flats. Given the ongoing environmental and developmental changes on the flats, better understanding of the rates of erosion is desirable. This study aims to quantify the capacity of waves and tidal currents, in addition to the influence of sea-ice, to erode or aggrade the flats surface.

2.2.1 Objectives

The objectives of this study are:

- to build on existing surficial geomorphological mapping by widening the area of investigation, including the nearshore.
- to assess the magnitude and significance of erosion over a three-year time span.
- to quantify the role of the tidal flats in dissipating incident wave energy; and to assess the potential for currents to transport sediments on the flats.

2.3 Area of Study

Koojesse inlet is a macro-tidal coastal embayment in the southern Canadian subArctic (64°44' N, 68°31' W). It is located on the northwestern shores of Frobisher Bay on southeastern Baffin Island (Fig. 2.1). Frobisher Bay is a half-graben developed in Precambrian gneiss, which gives Koojesse Inlet an underlying NW-SE bedrock orientation on which the surficial sediments are deposited (Hodgson, 2005). Koojesse Inlet is roughly 3.5 km long and 3 km wide at its mouth and opens to the southeast (Fig.

2.2). Due to the large tidal range, from 8 m at neap to 12 m springs, the shore zone is dominated by extensive boulder flats that vary in width from less than 200 m to more than 1000 m (McCann et al., 1981).

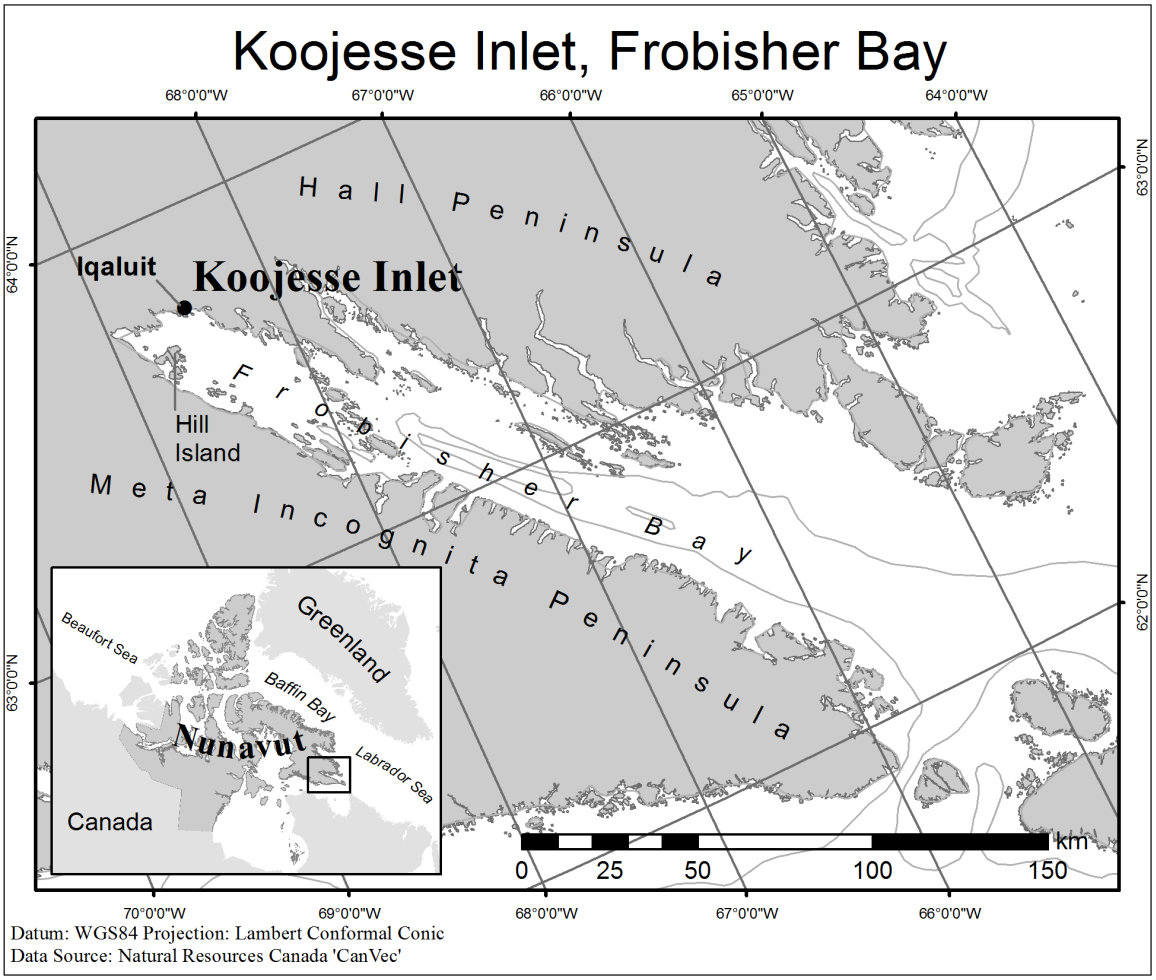

Figure 2.1: Koojesse Inlet is located within Frobisher Bay on south-eastern Baffin Island.

Koojesse Inlet has a coastal subarctic climate with an average temperature range between -32°C and 11°C and mean annual precipitation of 412 mm (57% snow) (Environment Canada, 2012) (Fig. 2.3). Increased precipitation is experienced here as a result of the increased influx of moisture from extra-tropical cyclone activity in the North Atlantic stormtrack (Maxwell, 1982). The local winds are subject to funnelling

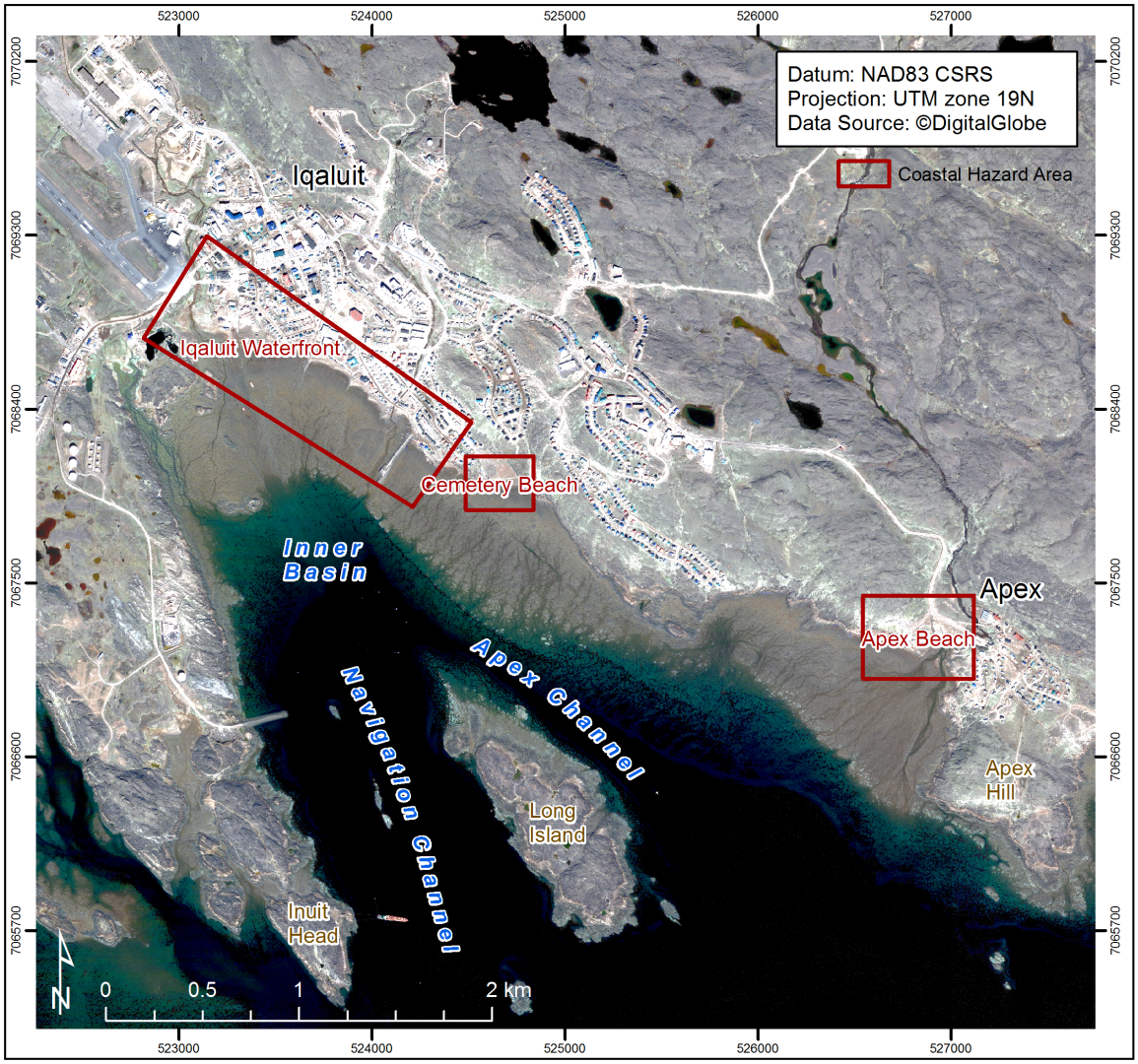

Figure 2.2: This is the location of Koojesse Inlet within inner Frobisher bay. Note Long Island located at the mouth of the inlet. All place names are taken from the CHS navigational chart of the area except for the channel names and the inner basin, which were created by the author.

from the surrounding topography (Deacu et al., 2010). The NW-SE oriented valley produces predominant winds in these directions, representing both offshore and onshore winds (Hanesiak et al., 2010). Proximity to the Labrador Sea means that this region is anomalously warm and wet for a subarctic environment (Maxwell, 1982). The mouth of the inlet is roughly defined by Inuit Head, the southern point of Long

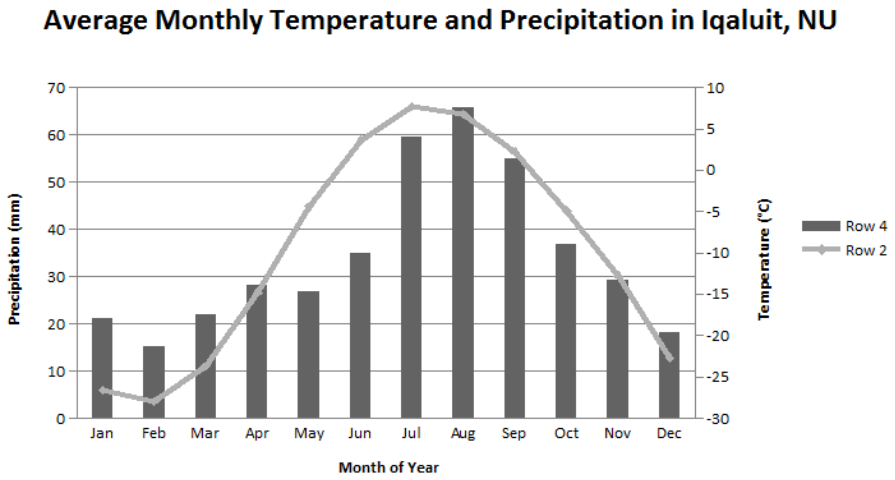

Figure 2.3: This climograph shows monthly mean temperatures and precipitation amounts from the Iqaluit climate station, located at the head of Koojesse Inlet. Data from Environment Canada climate normals 1990-2010 (Environment Canada, 2012)

Island, and Apex Hill (Fig. 2.2). Water depths in the approaches range from 20 m to 40 m at low tide. Shelter is provided by Long Island, which is roughly 200 m NE-SW and 500 m NW-SE. Channels on either side of Long Island lead into the inlet. East of the Island is 'Apex Channel' (narrow and shallow), while west of the Island is the 'Navigation Channel'. The latter is divided into two sections by bedrock outcrops parallel to the coast. At the confluence of the channels is an inner basin roughly 14 m deep, which provides sheltered anchorage for boats. Adjacent to the channels are extensive boulder-strewn tidal flats. Located on the shores of the inlet are the city of Iqaluit (capital of Nunavut), the former military airport (now the major civil aviation hub for the eastern Arctic) and the geographically separate suburban hamlet of Apex (the original settlement, now absorbed into Iqaluit) to the east of the main built-up area.

The ice season has a profound effect on the morphology of the flats. The ice season traditionally lasts from November to July (McCann et al., 1981; Dale et al., 2002). Previous work has focused exclusively on the dynamics and sedimentation of the

breakup period. Leech (1998) quantified the contribution of the freeze-up period to sediment transport for one season by estimating entrained sediment concentration trapped in the sea ice. The conclusion was that ice-entrained sediment is a dominant component of the sediment budget of the flats. Observations on the process of entrainment, however, have not previously been reported for Koojesse Inlet.

2.3.1 Geological setting and configuration of Koojesse Inlet

The geological setting and the paraglacial context are two important aspects of inheritance that shape the modern morphology of the coast (Forbes, 2012). The configuration of the bedrock is the foundation on which the sedimentary systems of the coast produce the landforms found today. Glacial history shapes the distribution of sediments on the modern coast and the region is dominated by exposed bedrock, with limited quantities of surficial sediment. Beaches are largely confined to paleodeltas, formed during the last deglaciation, at a time when the relative sea level was higher than today and glaciofluvial outwash provided sediment to the coast. The postglacial marine limit (highest relative sea level) is approximately 45 m above present sea level (Hodgson, 2005). GPS estimates of residual postglacial isostatic rebound in Iqaluit today range from 1.7 mm/yr to 7.6 mm/yr (continuous GPS 2010-2012) (J. Henton and T.S. James, pers. comm. 2012).

In Koojesse Inlet, there are two accumulations that continue to provide paraglacial sediment to the system: the Iqaluit and Apex paleodeltas. Formed in a proglacial setting during the last deglaciation, the Apex delta is now dissected by the outlet of the Apex River (Fig. 2.7), and the Iqaluit paleodelta underlies the current community of Iqaluit and its airport. The Iqaluit paleodelta is thought to have once been an outlet of the Sylvia Grinnell river during times of greater fluvial discharge at higher sea level (Hodgson, 2005). These rivers and smaller streams entering Koojesse Inlet continue

to provide inherited sediment to the bay in the study area.

The study area above the high-tide line is underlain by continuous permafrost. The depth of the 'active layer' (depth of seasonal thaw) is approximately 1 m (Short et al., 2012). It is unclear how far the permafrost extends beneath the tidal flats, but given the history of forced regression, it is unlikely that ice-bonding has developed in the sea-water-saturated clays of the modern tidal flats, except where bedrock is present at very shallow depth.

There are three river inlets in the system: 'Airport Creek', 'Geraldine Creek', and Apex River. 'Airport Creek' is a heavily modified waterway that snakes through the city on the west side. It mainly supports snow melt runoff and has no consistent source of flow. Further east is 'Geraldine Creek', which flows from Geraldine Lake directly north of the city (Fig. 2.7). As the city's water supply, the lake has been dammed, curtailing flow from the creek except during spring meltwater runoff or extreme precipitation events. On the eastern side is Apex River, which is the only input with a consistent flow year-round from a catchment further north. The Sylvia Grinnell River meets Frobisher Bay just west of the head of Koojesse Inlet, around Inuit Head.

Not much is known of the flats sedimentology. The sand and silt found on the surface of the flats is generally contained within a 10-20 cm layer that is actively reworked by water and ice (Dale et al., 2002). Below this, and in some places exposed at the surface by ice pressure on large boulders, is a layer of blue-grey silty clay interpreted as a glaciomarine unit (McCann et al., 1981; Hodgson, 2005; Allard et al., 2012). This sediment would have been sourced from the receding ice sheet and deposited during the late-glacial highstand of sea level up to 45 m above present MSL.

2.4 Methods

2.4.1 Mapping the boulder flats

A series of 22 coastal transects were surveyed using a Magellan Ashtech Z-Extreme survey-grade real-time kinematic (RTK) differential global positioning system (GPS) rover and fixed base station (Fig. 2.4). The position of transects were determined by a constant bearing that ran roughly shore-normal, except for two lines that ran shore parallel ("tn21" and "tn22", see Fig. 2.4). The numbering of cross-shore transects runs from 1 furthest west to 20 furthest east. The transects were spaced roughly 50 m apart, except between Apex and Iqaluit, where they are further apart. GPS points on the transect represent break-in-slope points, interpreted by the surveyor. Additionally, collection of many kinematic RTK-GPS points scattered across the flats between transects facilitated the topographic modelling of the surface.

Following establishment of a local network, the transect GPS points were connected to the Canadian Spatial Reference System (CSRS) high-precision network using benchmark "M009000" and Coast Guard tidal benchmark "FB1968" (See Table 2.2). The NtV2.0 geoid separation model is problematic in the Arctic due to the sparsity of control monuments, but here provides a geoid separation of 10.166 m from Ellipsoidal to Orthometric elevations. All mapping was conducted within the UTM projected grid coordinate system (UTM zone 19 N), using the NAD83 CSRS datum. Transect GPS points have a mean vertical RMS error of 0.04 m (σ= 0.02 m) and a horizontal RMS error of 0.02 m (σ= 0.01 m). These errors show ambiguity in positioning from signal error only, separate from error introduced from adjustments to the CSRS network, which averaged 0.05 m (σ= 0.08 m) horizontal and 0.05 m (σ= 0.06 m) vertical. Vertical accuracy between surveys averages 0.05 m.

Collected elevations are relative to the Orthometric datum established by the CGVD28

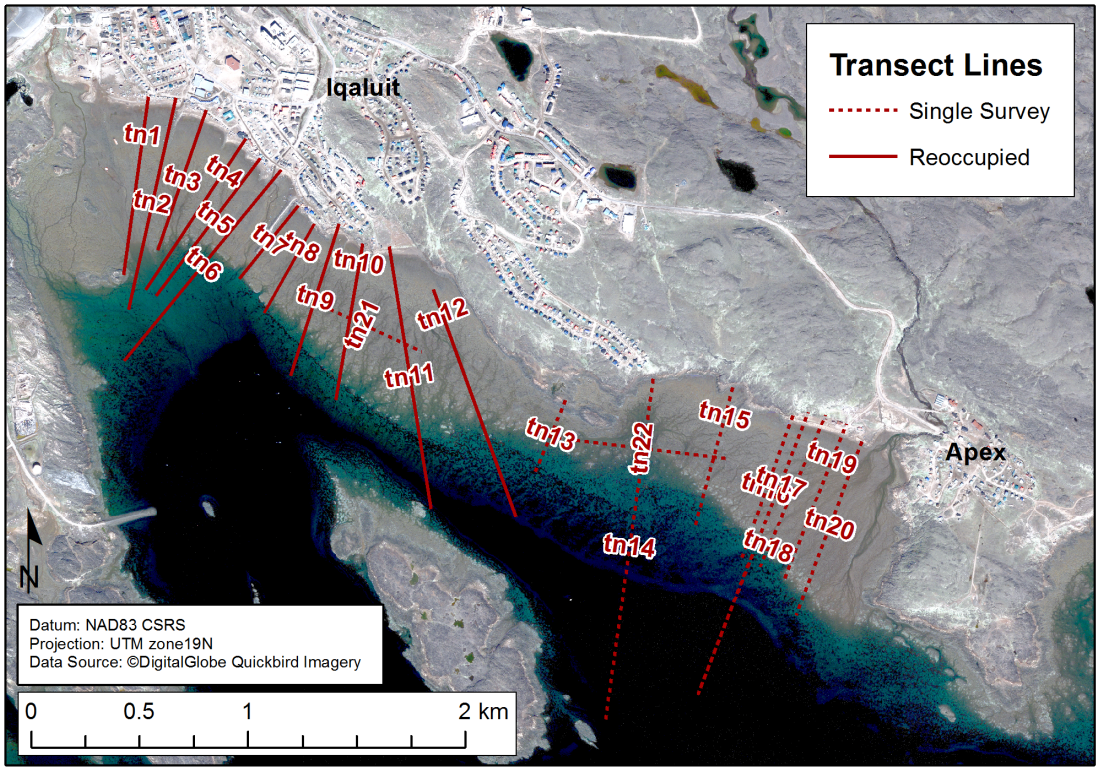

Figure 2.4: Layout of survey transects across Koojesse Inlet tidal flats.

separation model. Chart datum, established as the level of Lowest Low Water Large Tide (LLWLT) is 6.05 m below the orthometric datum zero point. This zero point is an approximation of mean sea level (MSL), and so elevations given in this paper can be considered to be above (positive) or below (negative) the mean tidal still water level.

In addition to mapping the flats, boatwork enabled the extension of mapping into the nearshore (Fig. 2.5). A few of the GPS transects were extended offshore using a single beam Lowrance LCX-25 (50/200 kHz) echo-sounder. Additionally, an Imagenex SportScan 330 kHz digital sidescan sonar was used to collect offshore seabed mapping information. Lastly, a SyQwest Stratabox 3.5/10 Khz system was used to survey 4 sub-bottom profile lines in the inlet (Fig. 2.5). Positioning information dur-

Table 2.1: Dates of surveys conducted on each coastal transect.

Transect	2009 (Aug. 7,9)	2010 (Aug. 18-24)	2011 (July 17-Aug. 3)	Ice 2011 (Feb. 8,9)	Nearshore (July 24-Aug. 3)
tn1	X	X	X	X	
tn2		X	X		
tn3	X	X	X	X	
tn4	X	X	X		
tn5		X	X		
tn6	X	X	X	X	X
tn7		X	X		X
tn8		X	X		X
tn9	X	X	X		X
tn10		X	X	X	X
tn11	X	X	X	X	X
tn12		X	X	X	X
tn13			X		
tn14			X		X
tn15	X	X	X	X	
tn16	X	X	X	X	
tn17	X	X	X	X	
tn18	X	X	X	X	
tn19	X	X	X	X	
tn20	X	X	X	X	
tn21	X	X	X	X	
tn22	X	X	X	X	

Table 2.2: Control positions used to correct RTK-GPS surveys in 2010 and 2011.

ID	Easting (m)	Northing (m)	Elevation (Ellipsoidal) (m)	Elevation (CGVD28) (m)
M009000	522372.23	7068886.14	22.34	32.506
FB1968	523304.52	7066785.48	-4.73	5.45
CAP	524511.59	7068063.94	3.524	13.69

ing all surveys was provided by a 12 channel Lowrance GPS with real-time WAAS corrections. This was complemented by a small dataset provided by the UNB Ocean

Mapping Group of a multi-beam survey conducted by the *MV Nuliajuk* in the inlet in October 2012.

Subtidal sediments were sampled using an Ekman grab and captured on underwater video from the boat. Surface samples were taken in the nearshore with depths from 0-5 cm. Samples were located along transects at different cross-shore distances, whereas grab samples were located in areas of different bottom return from the sonar mapping instruments (Fig. 2.6). Underwater video was recorded by a drop camera as the boat drifted. These digital videos were visually analyzed for substrate type, which directly fed into the substrate mapping.

Table 2.3: Schedule of single-beam and sidescan survey collection.

Instrument	Year	Period of Observation
Single-beam sonar	2011	July 26-30, Aug. 1-2
Stratabox sub-bottom	2011	July 30
Sidescan	2011	July 26-29, Aug. 1

Table 2.4: Start times for the underwater camera transects.

Transect file	Start time
DVR010101_0005_001.avi	July 26 2011 21:02 UTC
DVR010101_0022_001.avi	July 26 2011 21:18 UTC
DVR010104_1830_001.avi	July 30 2011 15:26 UTC
DVR010101_1906_001.avi	Aug 1 2011 16:03 UTC
DVR010106_2142_001.avi	Aug 1 2011 18:38 UTC
DVR010106_2226_001.avi	Aug 1 2011 19:22 UTC

A combination of RTK-GPS points, single-beam depths, and a previously created DEM from Natural Resources Canada produced a continuous DEM of bathymetry and topography in Koojesse Inlet. Concurrent water level measurements provided corrections for the single-beam echo sounder points, resulting in a database of point data that report Orthometric Elevations. Using surveyed control monuments, RTK-GPS elevations were corrected to Orthometric. These two datasets were combined

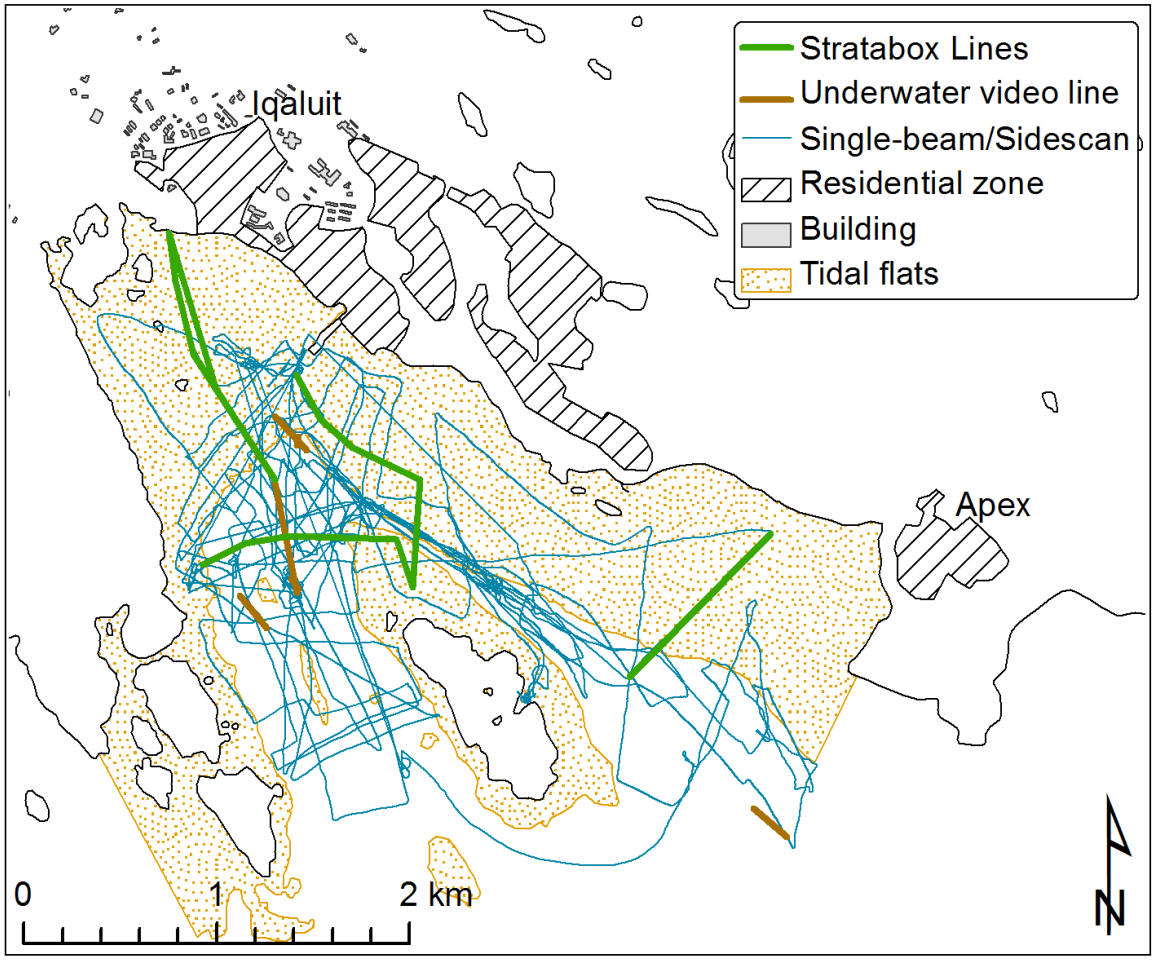

Figure 2.5: Vessel tracks of the nearshore surveys conducted in Koojesse Inlet. All boatwork was conducted in 2011, and so was not included in the change detection work, which only covered the intertidal.

using a tensioned spline interpolation (0.4 tension parameter) in GRASS GIS software to produce a continuous nearshore to intertidal bathymetric surface. Where the previously created terrestrial DEM overlapped this intertidal surface, the elevations were assumed to follow the terrestrial DEM due to its greater precision.

2.4.2 Coastal classification

The coastal classification follows up on work by McCann et al. (1981) and Dale et al. (2002), and is based on field work conducted between 2009 and 2011, as well as

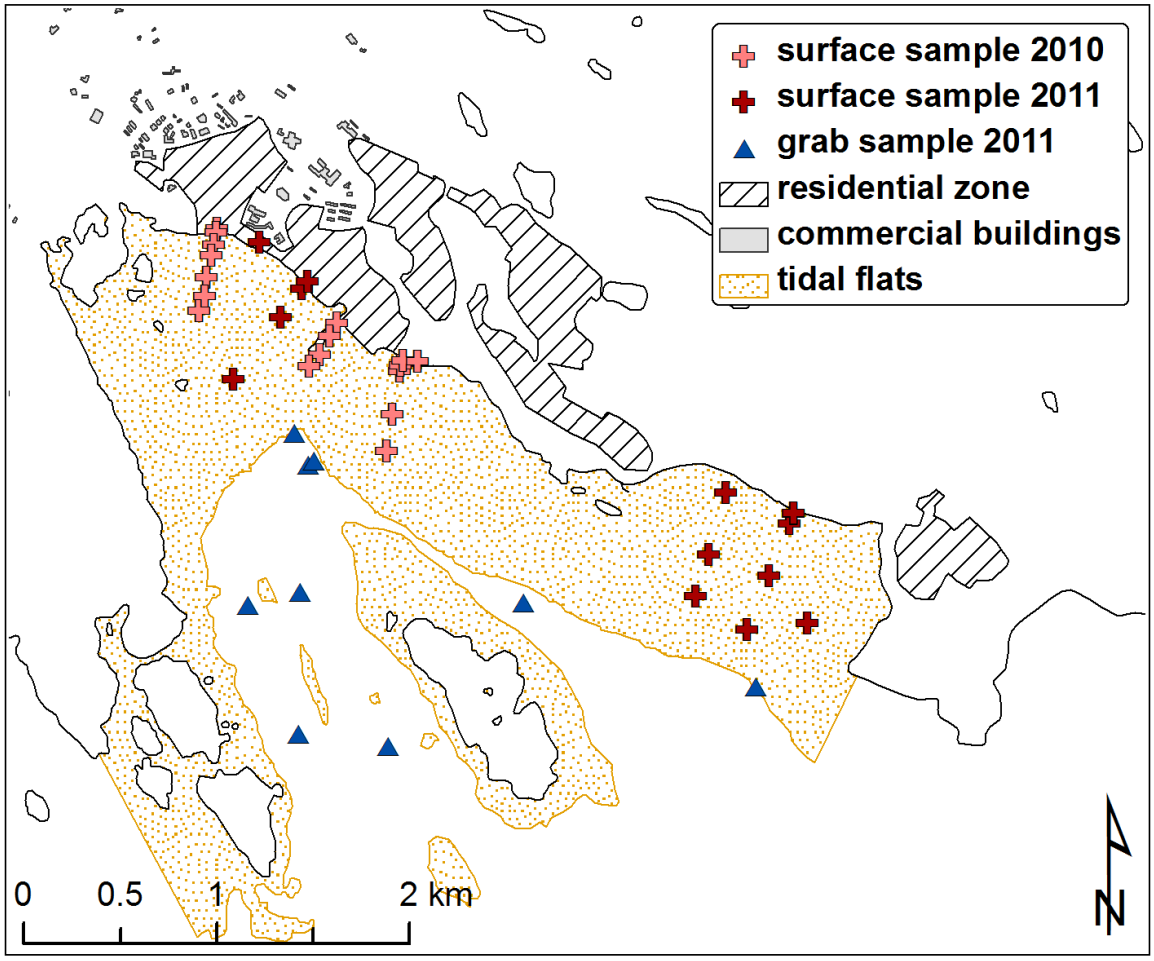

Figure 2.6: Sample locations in Koojesse Inlet showing intertidal surface samples and nearshore Ekman grab samples.

interpretation of imagery. Backshore form and material (rock, beach, anthropogenic features) were mapped as one-dimensional segments on the vector shoreline. Intertidal flats were classified as mudflat, upper sandflat, mid sandflat, graded sandflat, and disturbed flats and mapped as two-dimensional polygons. Classification mapping was done in ArcGIS software within a GIS that housed the products from the project.

2.4.3 Changes and forcing on the boulder flats

Resurveying of transects over the three year study enabled detection of elevation change by inter-year coincident point differencing. The differences are assumed to represent: elevation change due to natural sedimentation/erosion, vertical RMS error in the GPS points, and horizontal error from deviation of the compared points from the transect line. The largest of these is the error introduced by the horizontal difference between subsequent surveys. To obtain an estimate of valid change values, only coincident points within a 5 m radius were used, and for each of these a local roughness in the immediate vicinity was calculated to estimate the error introduced by horizontal separation from the comparison point. Local roughness is defined here as the standard deviation of the local slope, derived using the sample population of all survey points within a 10 m radius of each point on the transect. The 5 m search radius was chosen based on the point spacing, which followed breaks in slope and was generally 2-3 m apart. The 10 m radius for roughness coefficient is based on the general observation of the area over which the flats tend not to change. Additionally, surveys were conducted during a field visit in February of 2011 in order to measure the movement of the ice over the flats during full ice cover.

A total of six deployments of Tide and Wave Recorder (TWR) pressure sensors (RBR TWR-2050 instruments) and three deployments of a Nortek Aquadopp 1.0 MHz Acoustic Doppler Current Profiler (ADCP) were used to measure waves and currents. They spanned short intervals during the late summer and autumn in 2010 and 2011 (Fig. 2.5). This limited time was due to the constraints of ice and weather. More data could have been collected earlier in the summer, but winds capable of producing waves tend to be focused in the latter part of the summer in August and September, so this dataset is roughly representative of the maximum potential of these seasons to produce waves. The TWRs recorded simultaneous measurements

of wave characteristics and tidal water levels to a published accuracy of ±0.005 m (Gibbons et al., 2005). The ADCP recorded wave and current velocity profiles in three locations: one on the flats, and two in the nearshore channels. The velocity measurements have a published instrument uncertainty of 10% of the averaged ping velocity for each cell (Nortek, 2005).

Table 2.5: Schedule of TWR and ADCP deployments

Instrument	Year	Period of Observation
TWR	2010	Aug 18 - Oct 19
TWR	2011	Jul 16 - Sep 18
ADCP	2011	July 24 - Aug 3

Concurrent deployments of RBR tide and wave sensors in a cross-shore profile meant dissipation measurements could take place. The method of calculating the dissipation coefficient is given in Houser & Hill (2010b) as:

$$\frac{H_2}{H_1} = e^{-k_i \Delta x} \tag{2.1}$$

where $\frac{H_2}{H_1}$ represents the ratio between the significant wave heights at the first and second wave recording instrument, k_i represents the wave dissipation coefficient, and Δx represents the distance in metres between the two wave recorder instruments.

2.5 Results

2.5.1 Coastal geomorphology

The main coastal features can be classified into five types (Fig. 2.7: bedrock, beaches, boulder-strewn tidal flats, sparsely vegetated marsh, and anthropogenic features. Bedrock shores are characterized by steep to moderate slopes of largely unvegetated

and glacially smoothed bedrock meeting tidal flats below the high tide line. Between areas of bedrock exposure there are beaches formed from paraglacial sediments (sorted coarse quartz sands). Sparsely vegetated marsh occupies limited areas in sheltered embayments. The community of Iqaluit has extensive infrastructure along the waterfront, the proximity of which makes distinguishing fill from the natural beach difficult. Short sections of boulder revetment shoreline and boulder groynes are found along the urban waterfront. The intertidal zone seaward of this varied shoreline has extensive boulder-strewn tidal flats characteristic of high-latitude, glaciated, coasts, particularly in macrotidal settings (Forbes & Taylor, 1994; Forbes, 2012; Forbes & Hansom, 2012). The following sections describe each class of shoreline in more detail.

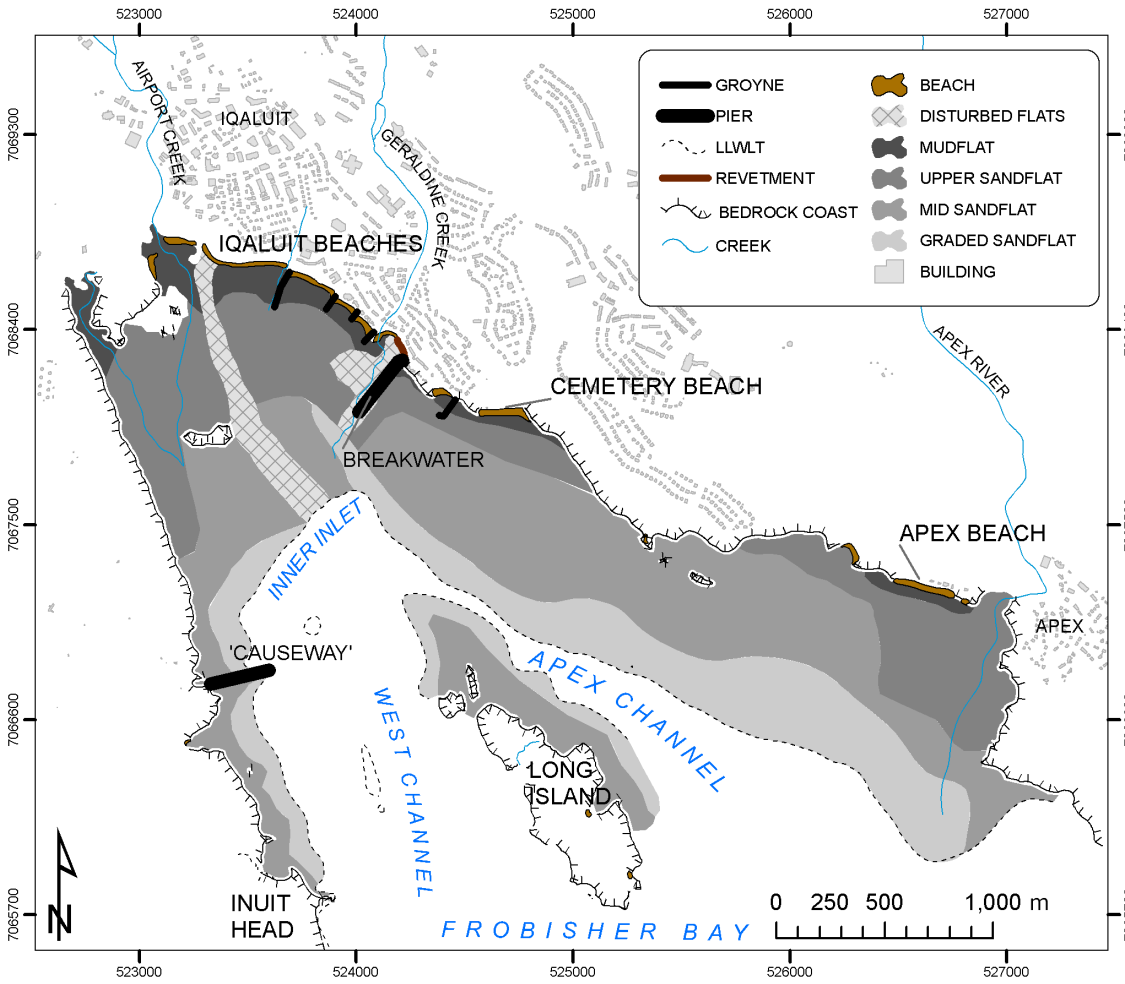

Figure 2.7: Shoreline classification done by the author showing various configurations of the coast of Koojesse Inlet. Coordinates are UTM zone 19N eastings and northings in metres.

Preliminary sub-bottom profiling conducted in this study revealed evidence of draped beds characteristic of nearshore proglacial marine deposition. This, however, was in only one spot near the tidal flats edge at the head of the inlet. Everywhere else the coarse sediments obstructed observation of sub-bottom patterns.

Rock Coast

The predominant rock type exposed in the Iqaluit area is a pinkish monzogranite orthogneiss of the Cumberland batholith, which has been glacially sculpted by south-easterly ice flow (St-Onge et al., 1999; Hodgson, 2005, p. 16). The bedrock's hummocky topography is partially infilled with glacial till, on which poorly vegetated surfaces have developed (Allard et al., 2012). The rock surface at the coast ranges from smooth steep slopes ($> 40°$) to frost fractured ramps ($< 40°$) (Hodgson, 2005) (Fig. 2.8). The high tide line is etched onto these surfaces by frost and ice action affecting the rock in the intertidal zone.

Figure 2.8: Typical bedrock coastal slope at high tide. Photo taken 50 m E of main breakwater, facing ESE. Photo: S Hatcher.

Beaches

Beaches have foreshore slopes of 1.8°-6.0°with poorly defined berms, composed of well sorted coarse sands. The beaches have concave-up profiles that merge seaward

with the boulder-strewn tidal flats. Their position at the edge of uplifted paleodeltas means that the backshore is composed of forced-regressive beaches from past higher sea levels. Active beach-ridge/berm elevations range from 5.7 to 5.9 m above MSL, roughly 0.1 to 0.3 m below highest high tide. These ridges, however, are poorly defined and hard to delineate due to the gradual transition from foreshore to backshore. In some cases, seasonal vegetation forms a line above the mean higher high tide level. The coarse sand composition implies intermittent wave energy capable of transporting such material (McCann et al., 1981; Dale et al., 2002). A gradual break in slope at the base of the beach marks the transition to a shoreface sand flat dominated by fine sand (Leech, 1998; Dale et al., 2002).

The Iqaluit waterfront beaches are heavily influenced by coastal infrastructure, unlike the Apex and cemetery beaches. The lateral confinement of the beaches is almost entirely artificial development, which has broken the previously continuous beach segment into smaller sub-system beaches. Five groynes and a single large pier break the once continuous beach into a series of pocket beaches (Fig. 2.9). In addition, a coastal revetment was placed on the west side of the large pier near the marina where small boat access is provided over the tidal flats.

Tidal Flats

Morphometry of the tidal flats shows topographical zonation. The surface of the flats ranges from 300 m to 1200 m wide in Koojesse Inlet (Fig. 2.10). A break in slope is consistently found at Lower Low Water Large Tide (LLWLT), which is here defined at 6.05 m below mean sea level (CGVD28). On the upper end, the flats merge with the lower beach shoreface above MSL. This transition is harder to define, as the base of the beach systems generally make a smooth transition to upper mudflats. The edge of the beach, therefore, is more a sedimentary feature than a topographic one. Considering the beaches to be a part of the tidal flat system, the range of elevations

Figure 2.9: (photo SVH 2011-07-11) Pocket beaches created by both natural and artificial lateral confinement (outcrop at feet, groyne at far end of foreground beach, outcrop beyond, and breakwater/jetty beyond that). Photo taken at W end of cemetery beach (524501 m E, 706851 m N, facing WNW.

is between -6.05 m and 5.90 m orthometric.

The tidal flats surface can be classified into four parts: mudflat, upper sandflat, mid sandflat, and graded sandflat. Boulder concentrations vary within each section depending on location within the inlet. Directly below the beach lies a mudflat, with few boulders (Fig. 2.7). It is continually reworked in winter by the ice and then slowly reworked during the open-water season to regain a regular tidal-flat morphology. Seaward of this zone is a boulder-strewn sandflat with intermixed sediments ranging from silt and fine sand to pebble, cobble, gravel, and boulders scattered throughout. Sediments in this area are reworked into ripple bedforms by flood and ebb tide currents. Further seaward are the dense boulder flats where the majority of the boulders are concentrated (as great as 30-40% coverage). In this zone, they form well defined boulder mounds with surrounding sediment ramps and drainage channels threading between the mounds. The graded flat reverses the trend of boulder density, which decreases with diminishing distance to the edge of the flats. The sediment in this zone is also more uniformly sandy, with fewer pebbles and cobbles. The transition between

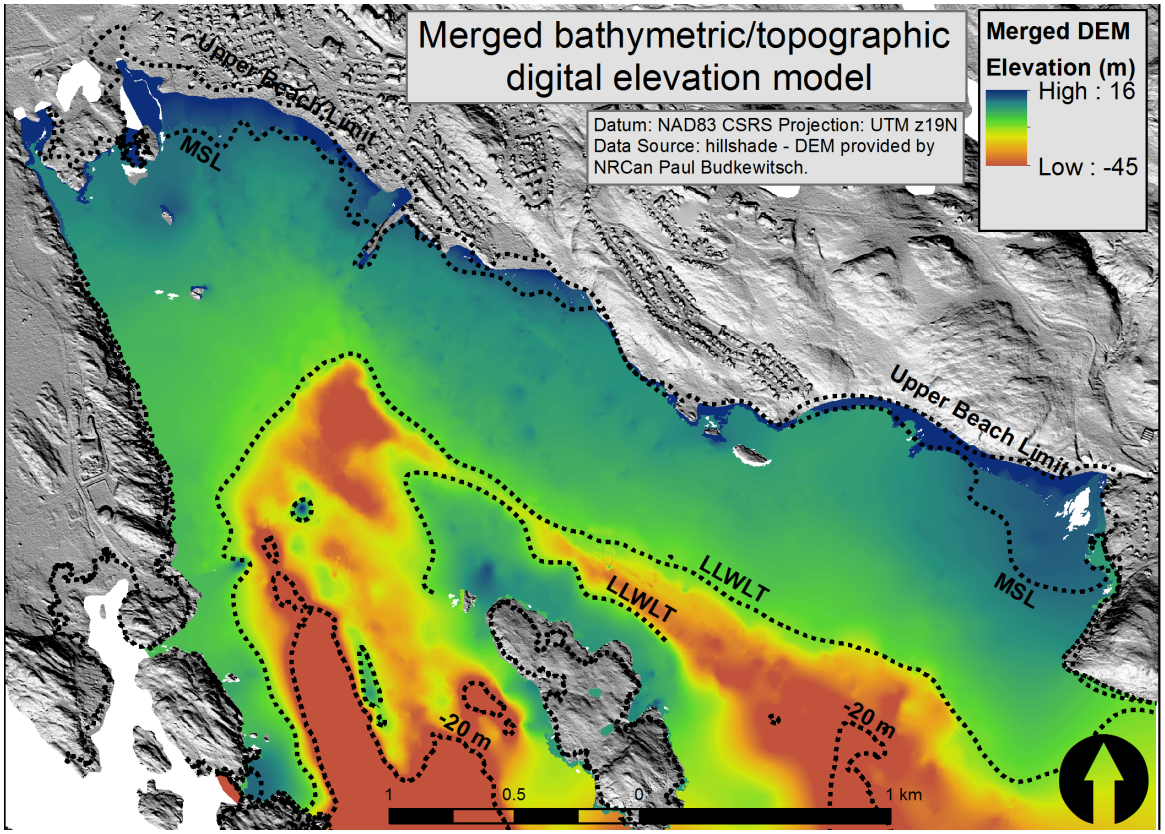

Figure 2.10: Digital Elevation Model showing the topography and nearshore bathymetry of the Koojesse Inlet tidal flats. Elevations are referenced to local Chart Datum.

the dense boulder and graded flats in places has the appearance of a boulder ridge.

Coastal infrastructure

Development along the coast can be classified into storage, access, municipal, and waste treatment. Three boat ramps exist where the coast is smoothed to allow access for small vessels. One is located at the base of the main pier from the city centre, one is at the coast guard base where large barges are landed to offload cargo, and the other is at the 'causeway' leading into the 'Navigation Channel' on the way out to Inuit Head (Fig. 2.7). The main pier rises 7 m above the tidal-flat surface, but is dry at low tide. The causeway, however, reaches into deeper waters, meaning it is accessible at all tides. These large structures are composed of large aggregate

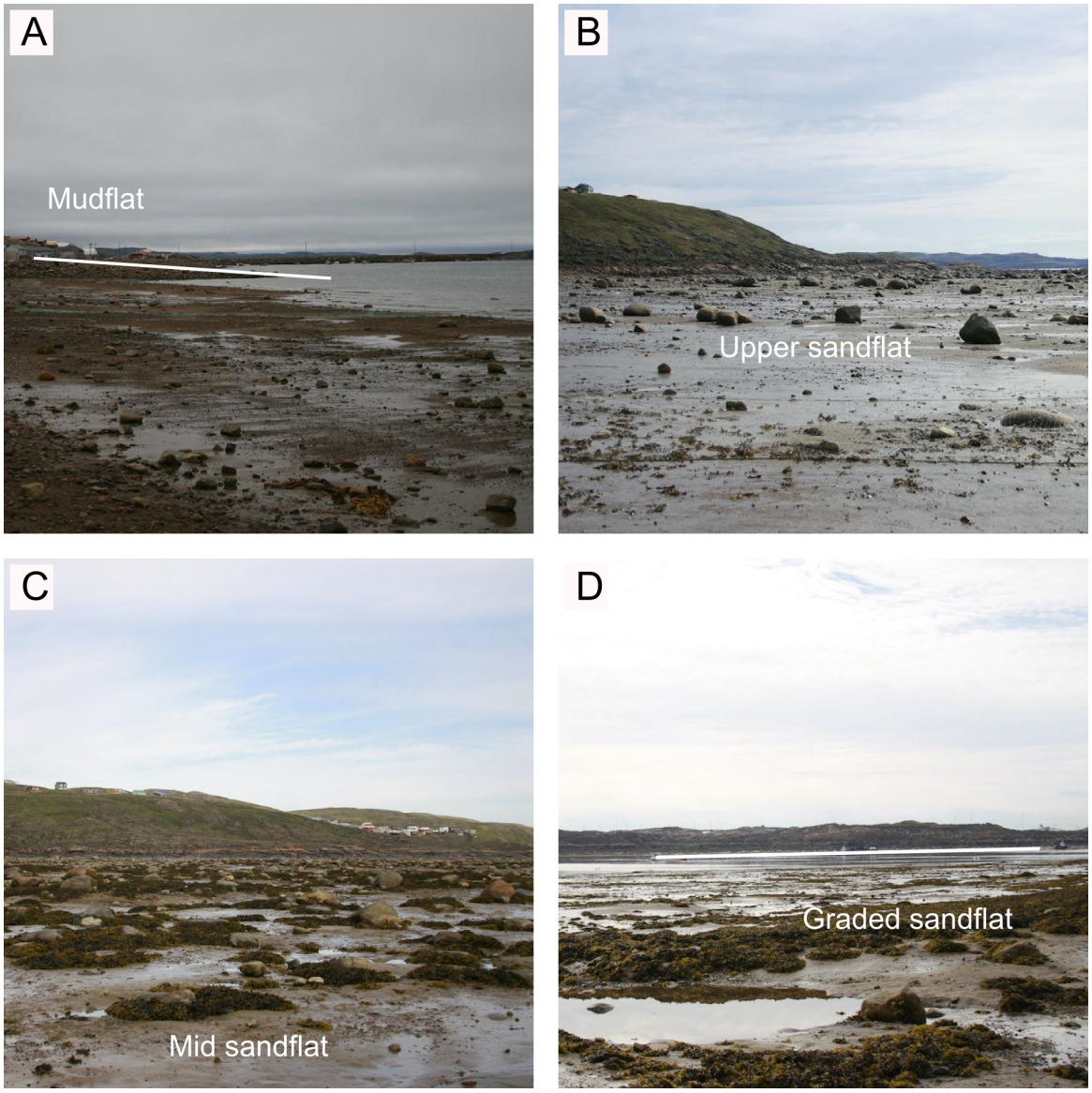

Figure 2.11: Collage of photos illustrating the zonation of the tidal flats. (A) Mudflat transition from the lower beachface into a fine sediment mud/sand flat surface with few boulders and sporadic cobbles. The distinction between beachface and flats is a coarsening of the sediment landward. (B) The upper sandflat where sparse medium sized boulders are scattered over saturated sand flats. (C) The mid sand flats have larger boulder mounds with one or a few large boulders with many smaller boulders arranged around the base. *Fucus evanescens* macro-algae are present below the mean water level. (D) At the edge of the outer boulder flats a break in slope is marked by a discontinuous boulder barricade, seaward of which there is a low-slope graded flat with few boulders.

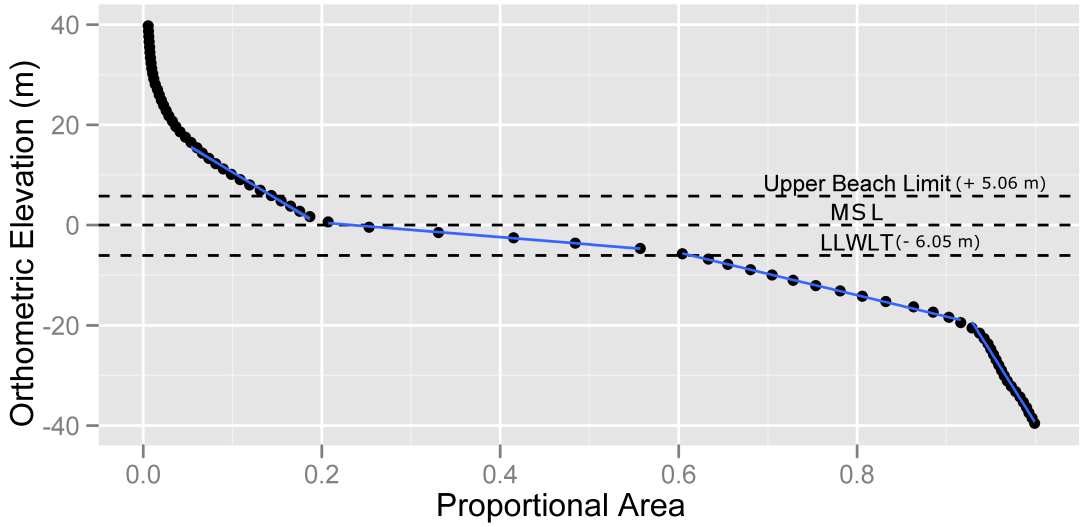

Figure 2.12: Hypsometric curve for the tidal flats, showing breaks in slope similar to those reported in Dale et al. (2002). The graph was constructed by cumulatively adding the areas made by 1-m contours derived from the merged DEM.

.

stone, and so represent littoral obstructions to sediment moving along the shoreline. This appears to have affected the composition of surficial sediments on the flats by trapping longshore transport. The coastal infrastructure is primarily used for access and storage in support of subsistence or recreational hunting and fishing activities. This infrastructure is placed by locals using experience of recent high water levels and by gauging the other sheds nearby. Interspersed with these sheds and containers is other municipal infrastructure (e.g. pumping stations) and buildings serving a variety of purposes. At the head of the inlet, seaward of the airport runway, is the sewage pond contained by two earthen dams on either side.

2.5.1.1 Seabed sediments and morphology

Bottom types

Offshore sediments fit three classes: a uniform sand/silt mixture with organic detritus,

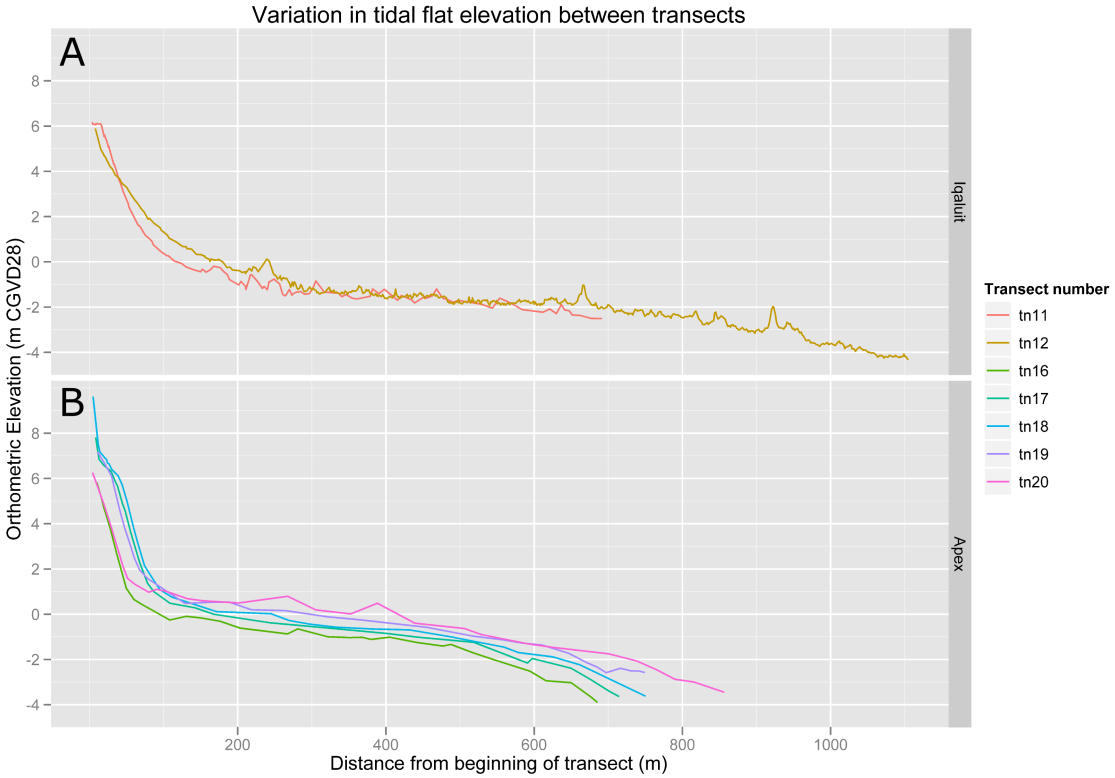

Figure 2.13: Difference in Orthometric elevations between transect lines. Transect numbers run from west-east (blue to orange), and are separated into Apex (A) and Iqaluit (B) lines. Note the depositional area at the base of the beach in the inner flats (blue lines), and the alluvial fan on the Apex flats (orange lines). Also, the lower elevations and truncated width of the flats between the two beach systems. Vertical exaggeration of 30.

coarse cobble clasts with interstitial sand, and brown mud/silt saturated bottom. The grab samples indicate that equal mixtures of mud and sand (40-60%) characterize the uniform bottom of the inner inlet, and are found at the bottom of the deeper channels west of Long Island (Fig. 2.14a). Sidescan sonar indicates that this bottom type is the most abundant in the study area (Fig. 2.17). Drop camera transects in these sections show drifting kelp and calm bottom conditions. Coarser material is present on the tidal flat edge. This zone forms a poorly sorted transition between the predominantly sandy tidal flat surface and the mud/sand mixture directly offshore (Fig. 2.15, and

Fig. 2.14b). Grab samples directly offshore of Apex, however, show a mixed sand and cobble seabed (Fig. 2.16c). At the base of the tidal flats on the western side of the inner inlet a brown silt/mud bottom, likely coloured by increased organic detritus, shows slightly different conditions than the sand/mud mixture sampled in the deeper parts of the channels west of Long Island.

Hard ground morphological features within the inlet are bedrock outcrops acting as reefs that are either exposed during low tide or continually submerged. They are spatially oriented with the surrounding bedrock, and are interpreted as exposures of the underlying monzogranite that composes the hard rock shoreline. The two primary outcrops are found between Long Island and Inuit Head, and are known as 'Polaris Reef' and 'Black Ledge'. West of Long Island at the mouth of the Inlet is Monument Island. Unlike Long Island, however, these bedrock reefs do not have tidal flat terraces at the periphery, meeting the seabed abruptly.

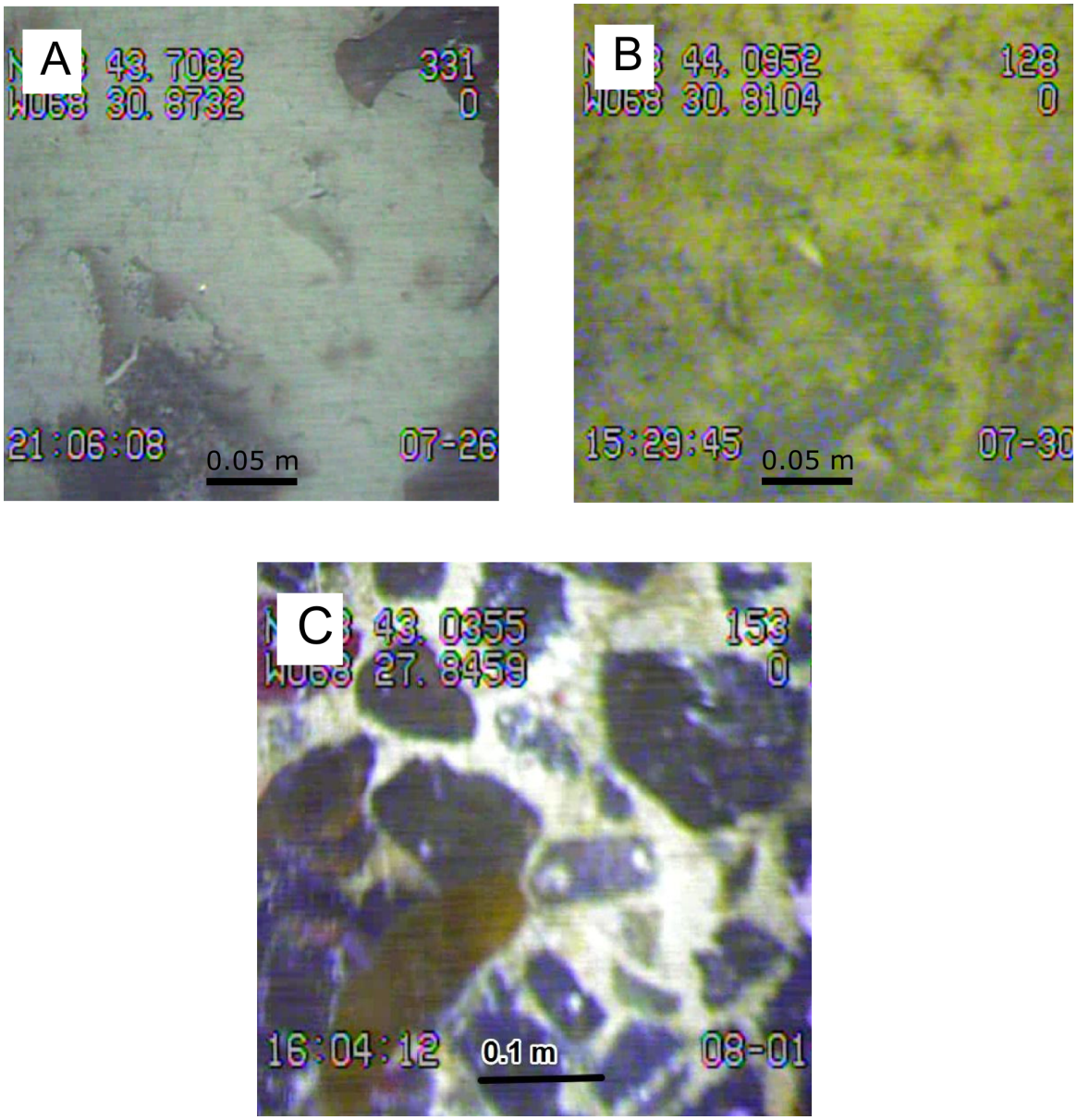

Figure 2.14: Images from the drop camera video transects showing (A) uniform mud bottom characterizing the inner nearshore basin of the inlet. Drifting kelp was observed in every transect taken in this area. Sporadic angular clasts (centre of image) are found in this area as well. (B) The base of the tidal flat edge, showing low slope mud with organic detritus and shell fragments. (C) Coarse angular cobble seabed observed directly offshore of Apex. Depths are slightly greater than the other two seabed types, and was only observed in this area within the inlet. Kelp was abundant, perhaps actively growing on the clasts.

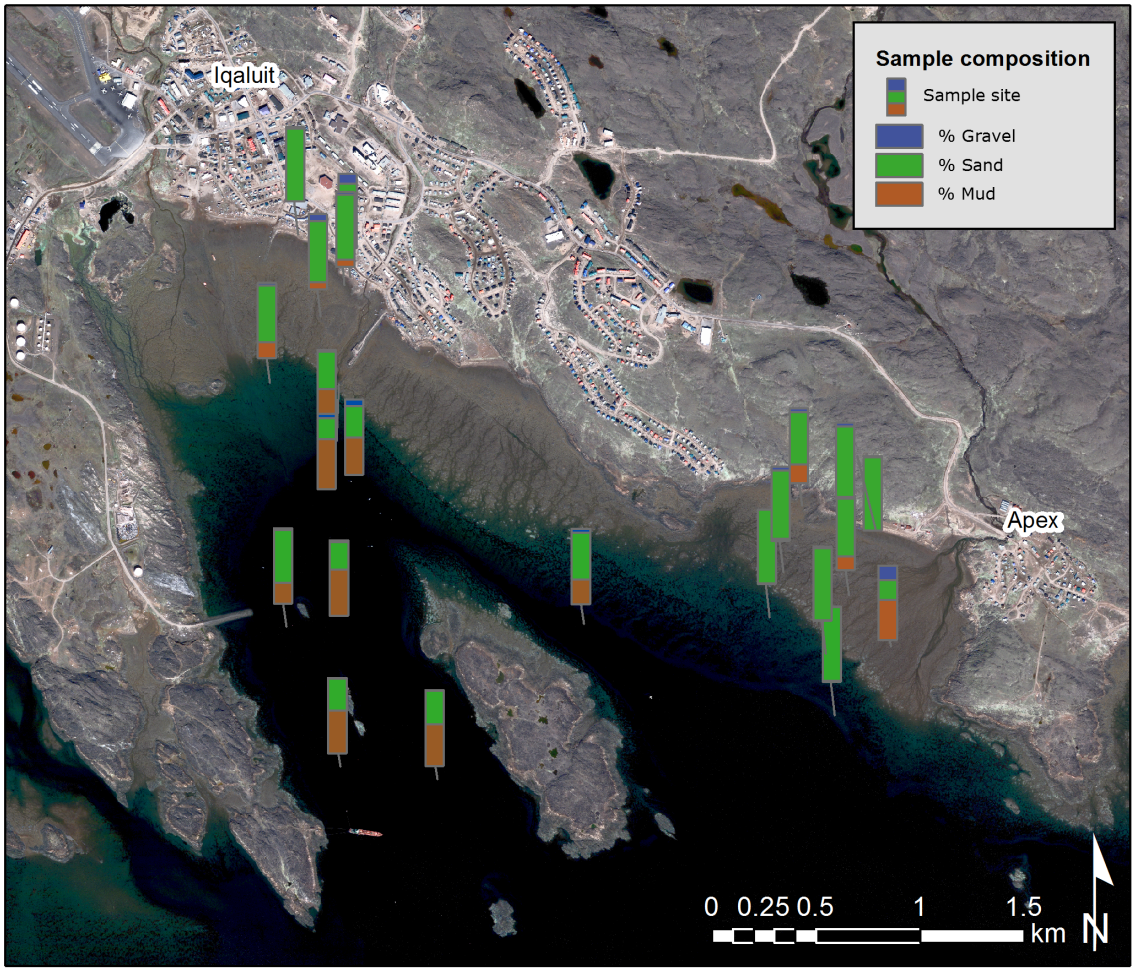

Figure 2.15: Sediment samples collected on the tidal flats and grab samples taken offshore. Each bar shows the percentage composition of sand, mud, and gravel in each sample. Location of sample is at the base of the bar.

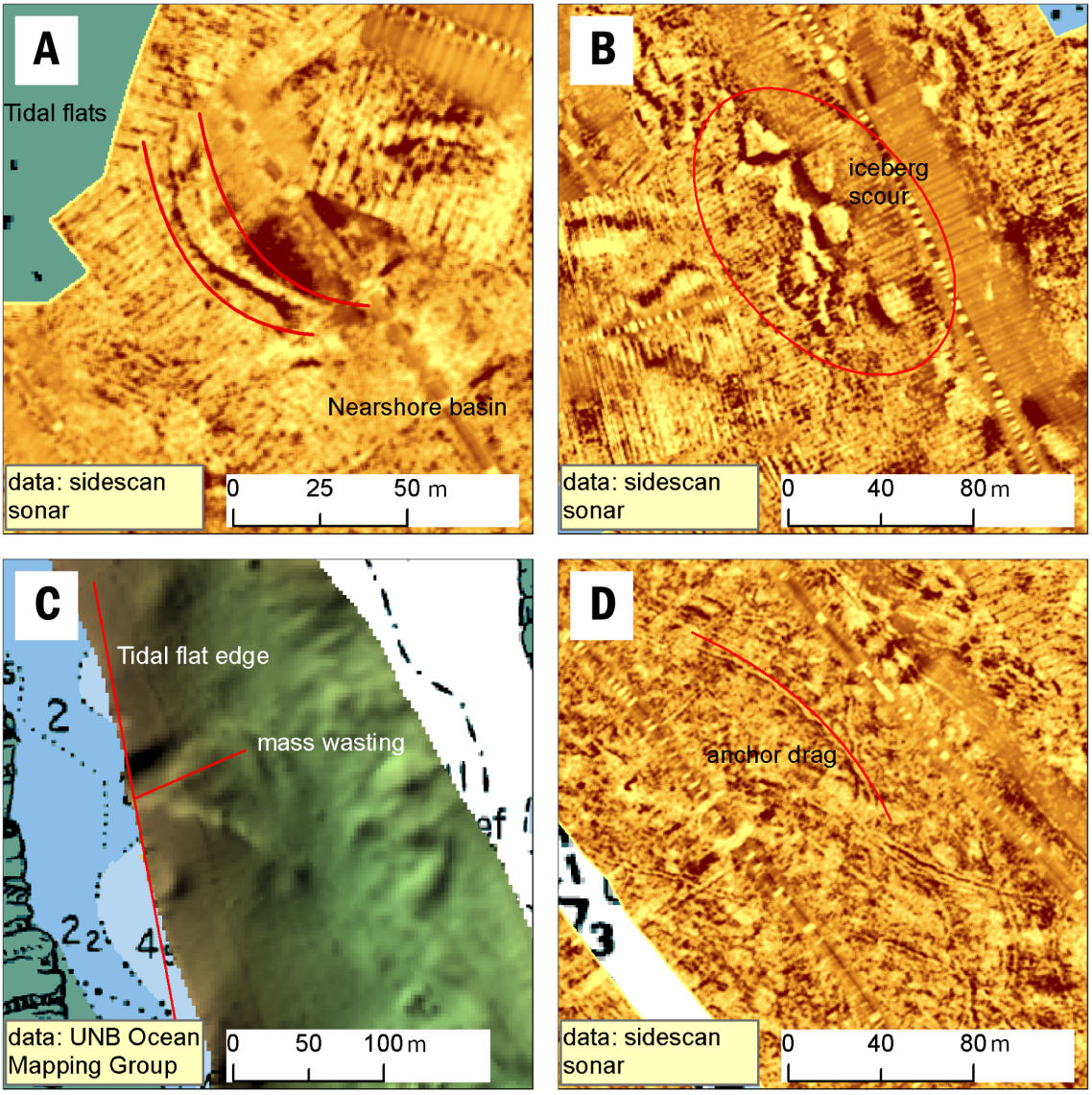

Figure 2.16: (A) Long narrow drainage fan located at the edge of the tidal flats at the head of the inlet. The sediment drains into the inner basin, where mud bottom predominates. (B) Sidescan sonar image showing circular scour features interpreted as products of ice grounding. (C) Multibeam sonar imagery from UNB Ocean Mapping Group showing slumping at the edge of the tidal flats off Inuit Head. Channels scoured in the higher slope portions of the tidal flat edge, with lobes in the deeper channel are interpreted as slumping features. (D) Sidescan sonar imagery showing curved linear features cut into uniform mud bottom in the protected inner inlet.

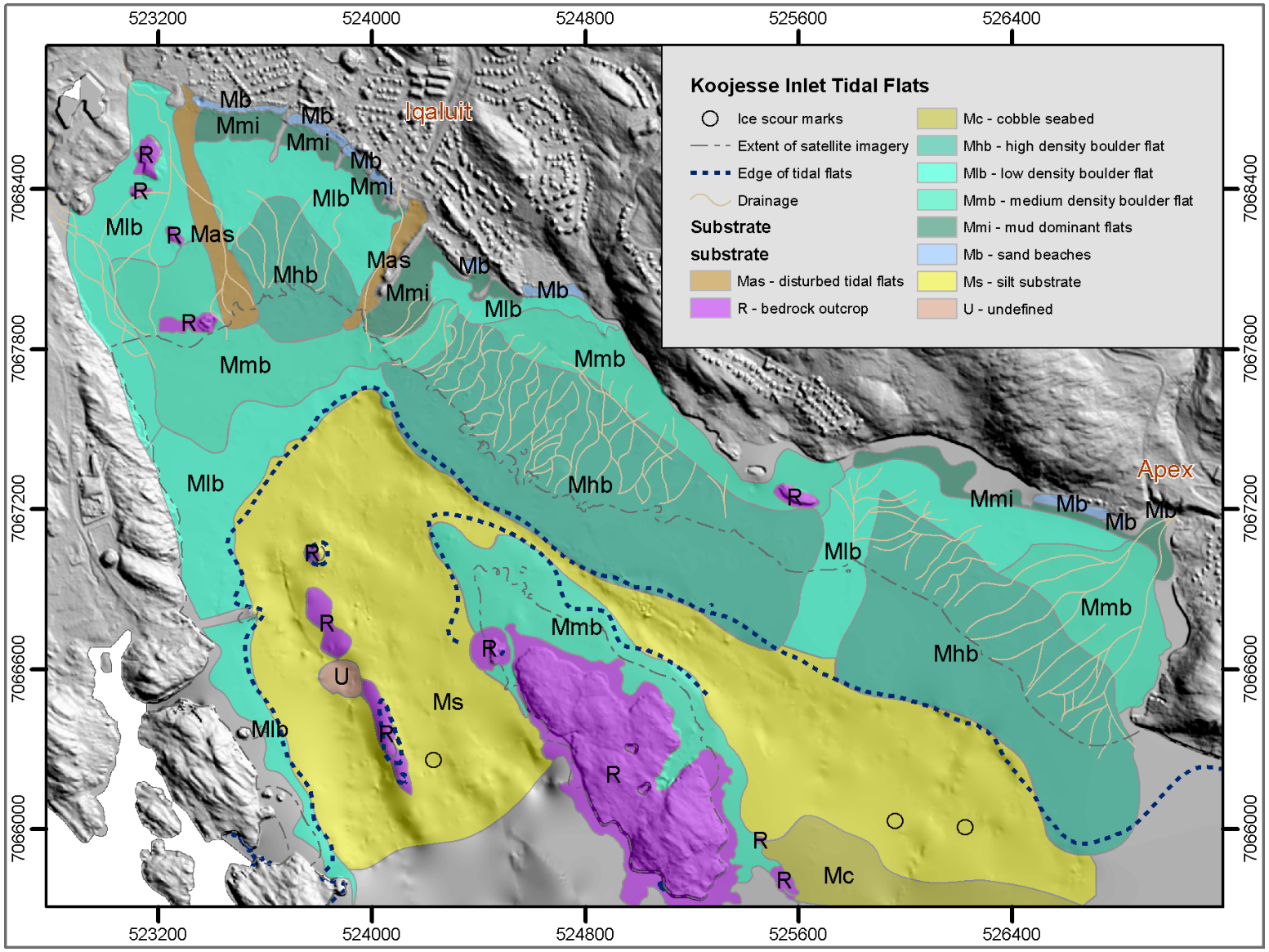

Figure 2.17: Marine and intertidal surficial geology of Koojesse Inlet showing the results of the 2010 and 2011 fieldwork. The channels in the inner inlet are typified by very fine silt substrate with sporadic kelp beds. Coordinates in NAD83CSRS UTM z19N.

Subtidal surficial types

Seaward of the lower-intertidal graded flats, the seabed descends into deeper water, forming a steep slope (ranging from 3° to 10°) that represents the seaward edge of the intertidal terrace. At the base of this slope is the offshore seabed, which is a uniform level bottom. Grab samples suggest a common equal mixture of sand and gravel, with little disturbance evident in the sidescan sonar. Two main channels, the 'Navigation Channel' and the 'Apex' channel, exhibit distinctive topographies and seabed types. The Navigation Channel is the deepest and widest channel, ranging from 20-35 m wide and 6-30 m below chart datum. At its landward end previous dredging has cleared a way to access the inner basin. This channel has the steepest walls between -0.17 and -0.07 (-9.65° and -3.8°). Apex channel is the narrowest, running SE between the hamlet of Apex and Long Island. It reaches a minimum of 2.7 m depth (chart datum) at low tide, where it is 50 m wide between the tidal flats off Cemetery Beach and the eastern side of Long Island.

The tidal-flat terrace face has slopes ranging from 2° to 8°, apparently controlled by the configuration of the offshore bathymetry. Areas where the steep face leads into the Apex and Navigation Channels show the greatest slopes. Where Long Island does not form an offshore barrier, however, the slopes are lowest, and the transition to the offshore is less abrupt. This occurs directly south of the hamlet of Apex (east of the mouth of Apex channel) (Fig. 2.17).

Hummocky fines were observed, and are interpreted to be silt and clay deposited as a veneer over underlying glacigenic deposits. These areas are found in deeper parts of the navigation channel. The hummocks are irregular and the lack of NW-SE orientation suggests no structural control from underlying bedrock. The underlying coarse clasts providing texture to the overlying seabed deposits are interpreted as relict moraine deposits. Depths range from 20 to 25 m below low tide, in the vicinity

of the Polaris Reef outcrop.

Sub-bottom profiling over the flats produced a single image that suggests sedimentary bedding layers underlying the flats (See Appendix A). Layers were measured at 2-3 m thick, and did not follow the shape of the eroded tidal flat surface. These are interpreted as glaciomarine deposits that form the structure of the flats, and are the source of the stiff blue-grey silt clay deposits underlying the sandy gravel veneer on the surface of the flats (Fig. 2.14c).

A number of anthropogenic deposits are found in the inlet. Within the inner basin where vessels commonly anchor, the seabed is marked by numerous anchor drag marks (Fig. 2.16d). The large number of drag marks suggests that they persist over a number of years, reflecting weak bottom currents in the inner basin. Additionally, sparse angular cobbles are scattered over the surface of the inner basin. Their source is unknown, but could be related to construction on the causeway nearby, or dropped from boats anchored above, or even non-anthropogenic sources such as importing by ice rafting. Lastly, there are a number of sunken barges filled with cobbles resting in the Navigation channel.

Disturbance features

Ice scour features are prominent near the mouth of the inlet, and on the edge of the flats on the southeast side of Long Island. Circular depressions roughly 6-8 m in diameter mark areas where icebergs have grounded at low tide (Fig. 2.16b). The locations of these features range from 5-7 m below low tide. Evidence of ice pressure ridges at the edge of the flats was not found.

There is some indication of submarine slumping on the slopes flanking the flats (Fig. 2.16c). Toe edge fans showing evidence of slump deposits were also found in transects from Apex Beach on the edge of the tidal flats. At the edge of the terrace, drainage fans were observed in the sidescan sonar imagery (See Fig. 2.16).

2.5.2 Processes driving morphological change on the flats

2.5.2.1 Erosion and sedimentation on the flats

Topographic surveys of the flats in 2009, 2010, and 2011 show spatially and temporally variable morphological change, generally of low magnitude (0.01-0.1 m change) alternating in some areas between erosion and deposition (Fig. 2.18). The outer flats show small amounts of erosion throughout the study period. The beaches show little evidence of change, despite an energetic storm in late November 2010. The focal point for sediment change is the interface between the base of the beach and the inner mudflats, although even here the changes are minor.

The frequency density functions of surface elevation change over the various cross-shore zones by year shows the spatial variability and differences between years (Fig. 2.19). The Iqaluit beaches show deposition on the order of 0.2 - 0.4 m between 2009 and 2010, with a reversal to erosion of equal magnitude the following year (Fig. 2.19). More data points in the 2010-2011 season show that the change is more widely distributed than was captured in 2009-2010. The 'Cemetery Beach' shows a mean slightly above zero, with skewed distributions representing erosion for both 2009-2010 and 2010-2011. The maps suggest this change is centred around the base of the beach, which experienced erosion throughout the study (Fig. 2.19). The inner flats have means slightly above zero, suggesting slight increase in bed height over the two years. The distributions show deposition followed by erosion. This, however, is found near the base of the beach, and therefore is a continuation of the same pattern found in the first graph. The outer flats show mean change near zero for both years, but with platykurtic distributions. This likely represents localized reworking from drainage and wave action.

The short duration of this study precludes long-term extrapolation. Its value is as a

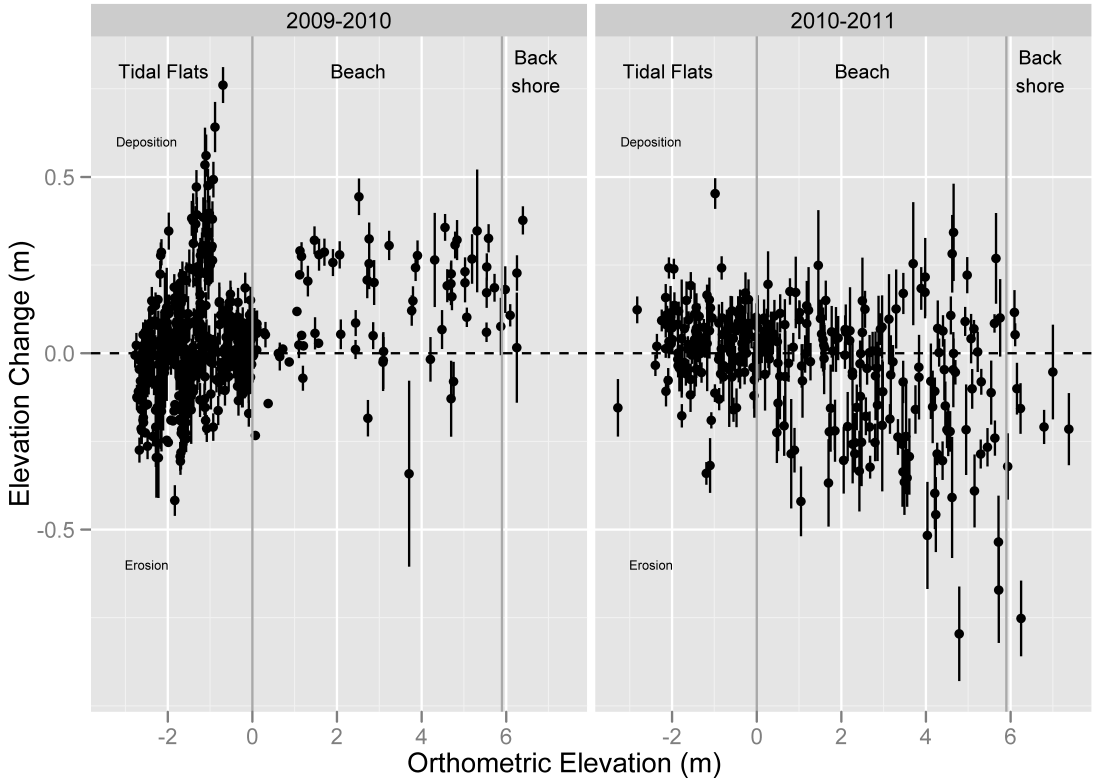

Figure 2.18: Scatterplot showing elevation changes between years measured by re-surveying GPS transects along the surface of the intertidal flats. The horizontal dashed line represents the differentiation between positive change (deposition) and negative change (erosion). The vertical grey lines represent the morphometric divisions derived from the hypsometric analysis of the inlet's topography (See Fig. 2.12). Lines intersecting each point of measurement show the derived error estimates for comparing the two GPS points.

baseline study, providing a basis for future comparison. A more detailed examination of sedimentation in the intertidal would be valuable in determining values and drivers at a few specific sites, but would require very fine resolution. The morphological change and variability observed over the two-year interval 2009-2011 is thought to represent a combination of storm wave events and seasonal reworking by ice.

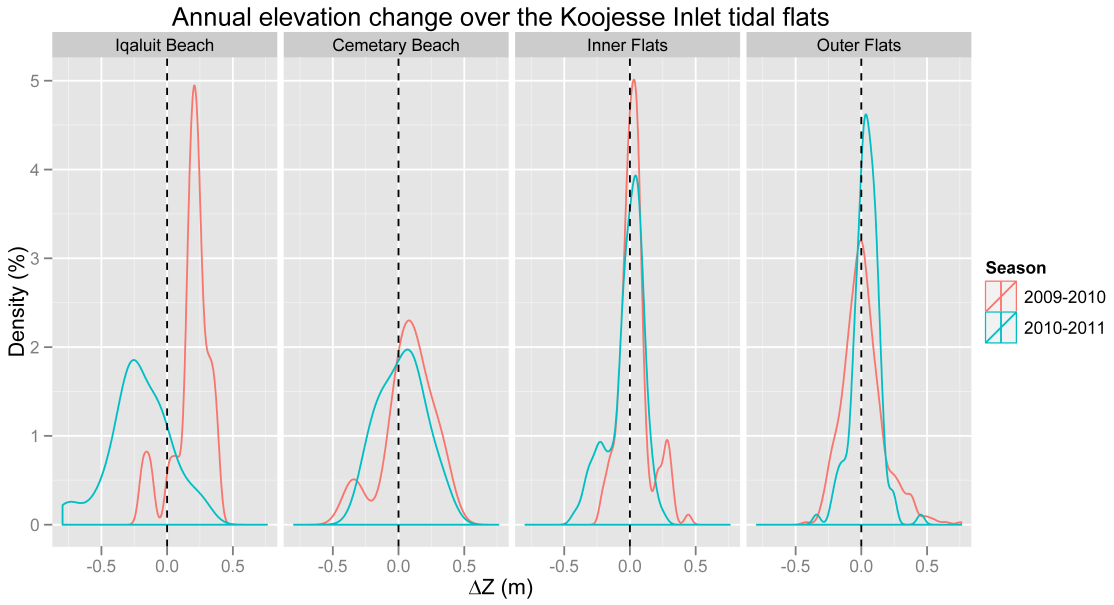

Figure 2.19: Probability density functions of annual elevation changes over thematic regions of the flats. Platykurtic distributions indicate a wide range of erosion/deposition values, and positive skew indicates mean erosion, negative skew indicates mean deposition. Some distributions are bi-modal, showing areas of distinct erosion or deposition.

2.5.2.2 Waves

A total of 4690 hours (195.4 days) of wave data were collected on the tidal flats, with concurrent observations from two TWR instruments in 2010 and four in 2011. The recorded waves varied in period between 1 and 7 s, and significant wave height ranged up to 0.7 m (Fig. 2.21). Instrument elevations were between -3.8 m and -2.5 m MSL, placing them in the mid-flats region characterized by the largest concentration of boulders. Waves were also observed using ADCP instruments in the harbour channels at elevations of -14.6 m and -9.2 m MSL. These recorded a maximum significant wave height of 1.06 m and wave periods between 4.7 s and 5.2 s. Waves in the inlet are generally low energy and range from localized chop to short-period wind-forced waves during high wind events from the southeast.

Concurrent measurements of waves at two locations over short time periods in 2010 (136 hours) and 2011 (174 hours) on two shore-normal lines enables estimates of wave dissipation over the flats. In 2010, two TWRs spaced 319 m apart showed a maximum of 81% dissipation of significant wave height over a change in elevation of 1.06 m. In 2011, two instruments 216 m apart measured a maximum of 66% dissipation of significant wave height over a change in elevation of 1.31 m. The 2010 data were collected over a section of the flats with a dense concentration of boulders. The 2011 data were collected over the inner basin directly off the main Iqaluit shoreline, where there is a lower concentration of boulders. This might account for the differences in measured dissipation. Dissipation from bottom friction of waves begins at a depth equal to half their wavelength. Waves of short period at high tide do not begin to feel the bottom and dissipate energy until much closer to the beach high tide line, and therefore the wave measurements show continued growth of energy over the flats.

A wave dissipation coefficient was calculated as the negative log of the ratio between the two measured wave heights divided by the distance between the two sensors (Houser & Hill, 2010b) (Equation 1). The attenuation coefficients approached 0.006 at times of greatest dissipation and greatest relative wave height. The coefficients also varied with position, showing greater wave attenuation on the cemetery transect, but with more energetic waves, perhaps due to the additional southeast fetch at this position. The linear model fit is poor, perhaps due to wave direction, wind direction, or (more importantly in this macro-tidal setting) the velocity and direction of tidal currents at the time. This dataset, however, only spans 310 hours, and was collected over a time interval without storm activity.

There is a slight difference in recorded wave periods between the Apex side and the sheltered inner basin off Iqaluit (Fig. 2.21). This is likely due to the exposure to larger open fetch on the Apex side. This dataset, however, is insufficient to determine

whether higher energy waves can propagate through the western and navigation channels during strong storm events. Photographs (courtesy David Mate, CNGO) of the surf zone off the city waterfront during a moderate storm in late November 2010 show energetic waves approaching through that passage. The storm produced 10 hours of sustained 70 - 90 km/hr winds from the east-southeast. Offshore waves calculated with these parameters following Hurdle & Stive (1989) were thus likely in the 0.5-0.7 m significant wave height (H_s) with 4-5 s range in dominant period (T_p). There is evidence outside Koojesse Inlet that larger storm waves can be produced. GPS static surveys on beach storm debris lines on Long Island (at the mouth of the inlet) show swash runup events beyond the limit of spring high tide levels. It is assumed that these storm events occur during the ice-free season, predominantly in early fall when cyclonic systems can produce strong southeasterly winds in the inlet.

2.5.2.3 Currents

A total of 232.8 hours (9.7 days) of current observations were collected in three separate deployments. The first was on the tidal flats at an elevation of -2.43 m MSL. The second and third were in the western channel, and the Apex channel respectively. Current observations on the flats spanned a neap cycle (tidal range ˜ 5 m), whereas observations in the channels were during a rising spring cycle (tidal range 9 - 12 m). Current speeds reached a maximum of 0.7 m/s, and averaged 0.07 m/s. Results show that currents in the channels reflect the rise and fall of the tides, and have higher speed than those observed over the flats (Fig. 2.23). Consistent with hydraulic theory, currents are generally faster near the surface than at the seabed. In the water column over the flats, the highest current speed was during the first day of observations. High NW winds at this time (>60 km/h) seemed to be driving this. The wind altered the alternation of flood/ebb direction of the currents, so that the currents

were unidirectional offshore through four tidal cycles (Fig. 2.23). The current speeds compare favourably with reported measurements in previous work (Dale et al., 2002). The data collected on the flats were restricted to a neap cycle, and so the potential velocities experienced under storm winds and a spring tide are not captured in this dataset.

The currents observed show greatest velocities near the surface and in the channels off the flats. This agrees with the data collected by Dale et al. (2002). The currents on the flats had velocities far lower than in the channels, and had directions determined more by the winds than by the tidal stage. Calculation of the threshold of sediment motion through the dimensionless skin friction coefficient described in Houser & Hill (2010b), and using the threshold value for 0.125 mm diameter sand from Swart (1974), almost no recorded currents were able to set sediment in motion (Fig. 2.24).

2.5.2.4 Sea Ice

Observations of freeze-up during November 2010 provided some insight into this highly dynamic seasonal transformation. The most dynamic period of freeze-up occurred before temperatures allowed a consolidation of the pack ice. In the beginning, the ice cover was characterized by two forms: anchor ice and thin pan ice. The interface between the two was ill-defined. Newly formed anchor ice on the seabed sometimes floated at high tide and joined the accumulation of floating thin pan ice fragments. Anchor ice formed at low tide levels when the tide waters receded, leaving depressions in the flat with thin pockets of water. By the next high tide, these sheets either had bonded sufficiently to the surface sediments to remain anchored to the seabed as tide water moved overtop, or were not sufficiently bonded, were therefore released and floated free as the tide rose. During the next low tide, these sheets would settle again in a different position, adding another entrained layer of sediment to their underside.

Amidst this interplay of anchor ice sections and expansive thin pan ice accumulations, there was also movement of small ice flows from the mouth of Airport Creek onto the flats. These were different from those formed on the flats because they were much thicker. Inundated only during spring high tides, and refreshed with freshwater input from precipitation over land, this ice formed separately from the ice forming on the flats. These thicker floes remained in the sheltered mouth of Airport Creek until offshore wind and a spring tide carried them out over the flats. In one case, overnight pile-up of this thicker ice on the boat-launch ramp formed an ice barrier more than 2.5 m high, which had to be cleared by a bulldozer (Fig. 2.25). Constant movement of these three types of ice around the flats characterized this early period of freeze-up, and seemed to be controlled primarily by the local winds.

It was followed by a middle period of freeze-up, when the discontinuous ice cover began to coalesce into the thick continuous cover that persists through the rest of the winter. Anchor ice sheets became larger and thicker (Fig. 2.26) and a sheet of ice roughly 5-10 cm thick covered most of the bay, except in patches where wind had pushed the ice away. Tide water continued to overtop the ice that was frozen to the ground. This produced swift currents over the ice as water slowly inundated the ice sheets. This, presumably, aided the further thickening of the ice, as well as the adhesion between adjacent sheets. Also of note during this middle period was the initial formation of the winter icefoot. This seemed to form where the larger pieces of ice from the creek input grounded during a high tide. Because of the flow size, however, this line developed seaward of the spring high tide water line, near the base of the beach. During subsequent high spring tides, water was able to overflow the icefoot and run onto the upper beachface (Fig. 2.27).

Previous work has shown that the last stage of freeze-up is marked by a continuous ice cover over the inlet, so that the ice becomes ‘set’ (McCann & Dale, 1986). Ice surveys

in February 2011 show the icefoot between 4.0 and 5.5 m orthometric elevation, and at the time of surveys 0.45 - 1.00 m thick, gaining thickness seaward. Over the flats, the ice formed to about the same thickness as the icefoot (Fig. 2.29). Seaward of the icefoot, however, the ice floated with the tide, and was broken up by settling over large boulders, producing a chaotic ice surface with numerous large circular ice pile configurations known as ballycatters. These ballycatters seemed to stabilize the ice, and provided hinge points on which large pieces could move up and down with the tides. At the outer edge of the flats, ballycatters gave way to a smooth and flat landfast ice covering the inner bay.

Initial observations of freeze-up in November of 2011 revealed a complex process that ended with consolidation of the sea-ice cover for that ice season (Fig. 2.28). This freeze-up process, which can vary year to year in response to variable temperatures and winds, in large part determines the sediment available for redistribution during the following spring breakup. The nature of freeze-up suggests variability not only in the volume of sediment entrained before consolidation, but also its position in the pack. These results support the previous work done on redistribution of sediment on the flats during breakup by showing the importance of local winds at freeze-up and the length of time over which freeze-up occurs.

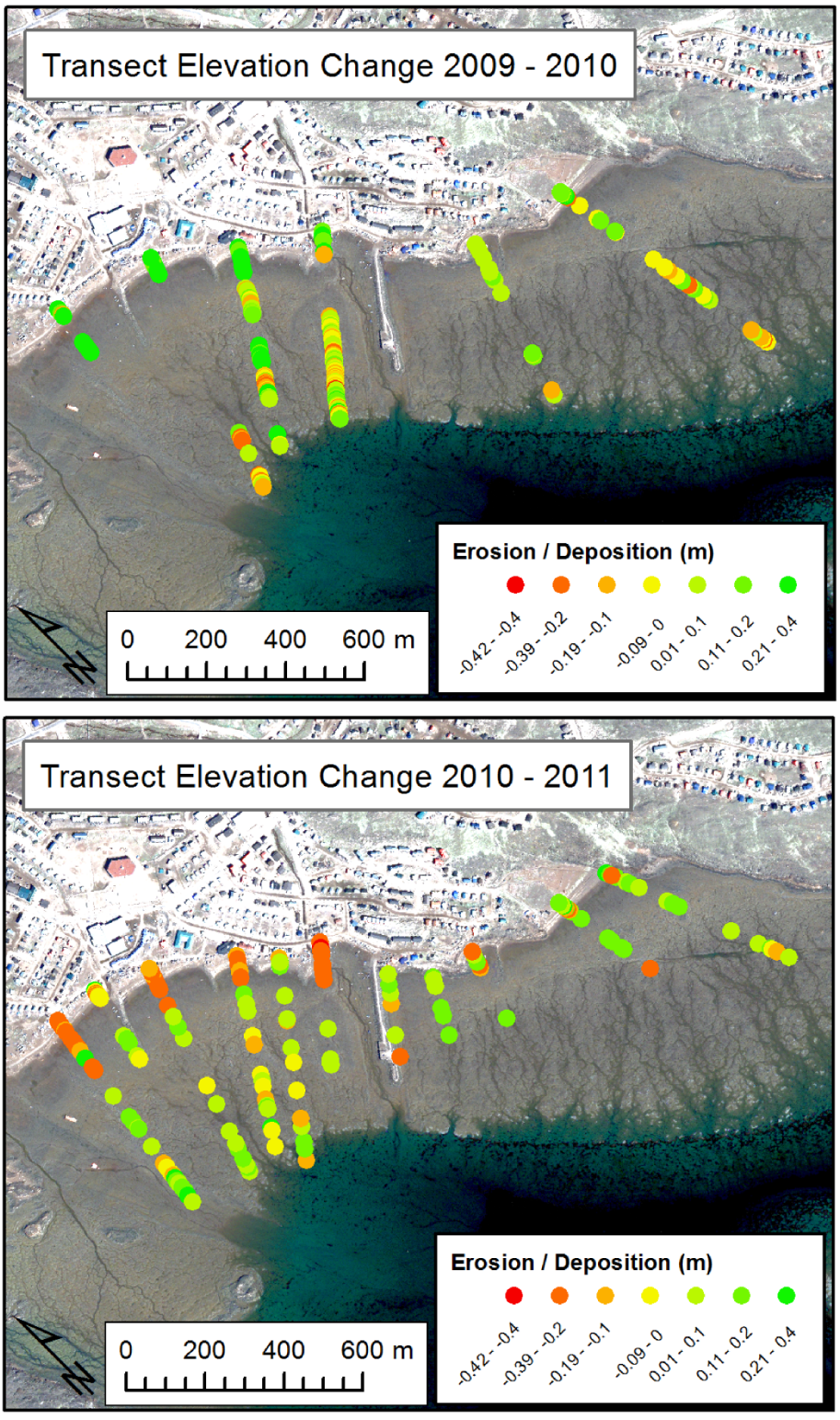

Figure 2.20: Localized elevation change on the flats between 2009-2010 and 2010-2011.

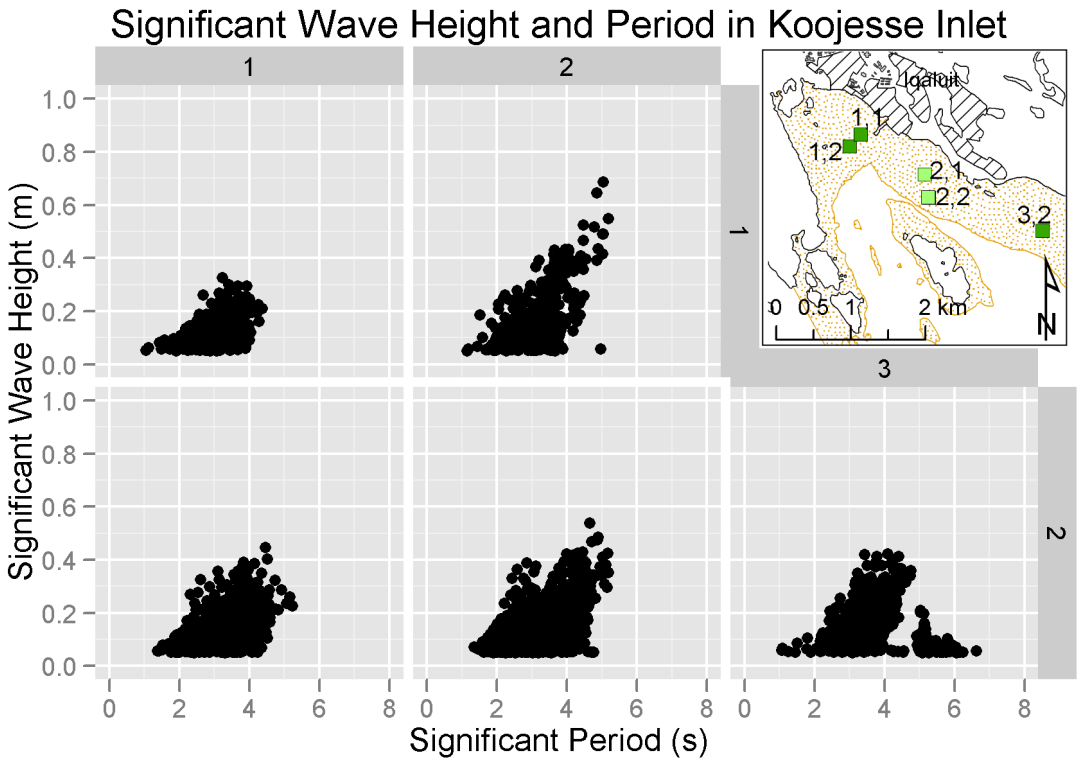

Figure 2.21: Wave spectrum from the five positions of TWR deployments on the flats. Greater period from more exposed southerly fetch is apparent in the 3,2 position off Apex.

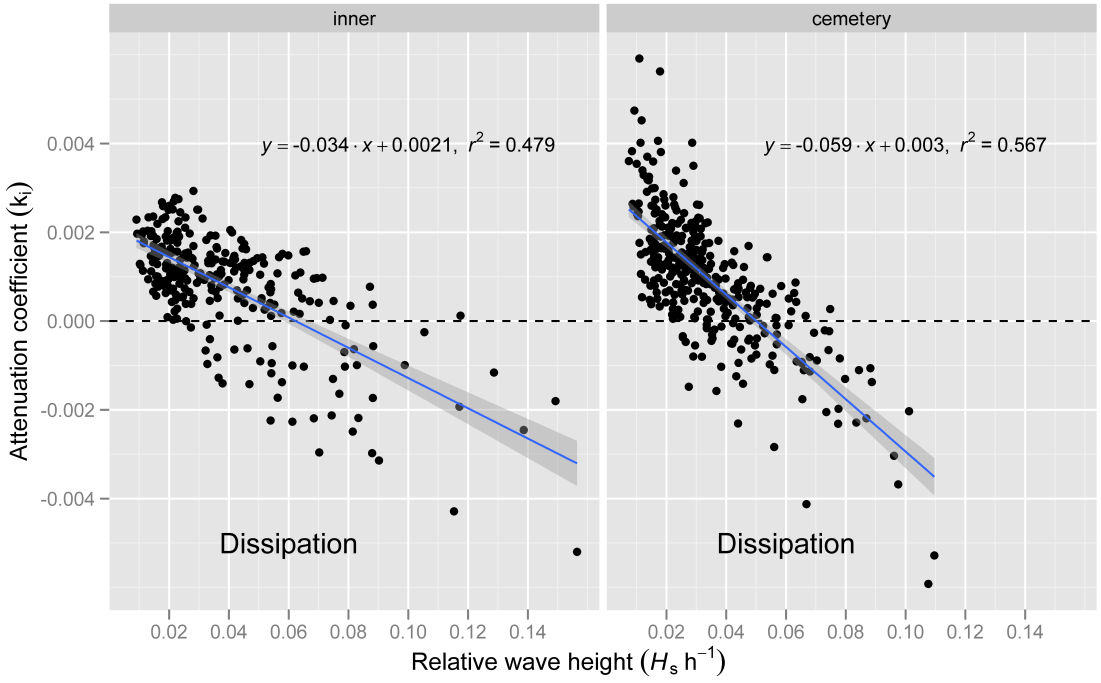

Figure 2.22: Wave attenuation over the flats in 2010 and 2011. The inner flats show a less marked attenuation of incoming waves, with less instance of wave growth over the flats. On the cemetery side, with a dense boulder field fronting the flats, the attenuation is more pronounced.

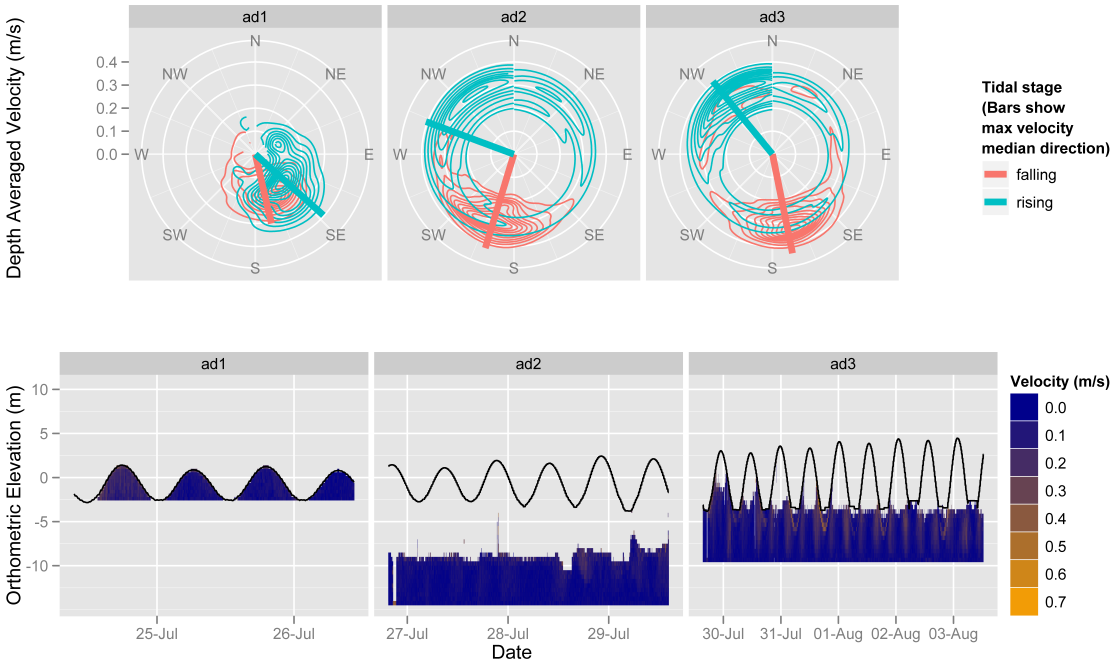

Figure 2.23: Visual representation of the collected current velocities and directions in late July and early August 2011. Above, directional spectra show depth averaged velocity contours with respect to direction. The measured velocities range from 0 to 0.4 m/s. The velocity measurements are further divided into rising (blue) and falling (red) tidal stages. Below, velocity measurements are shown with respect to depth. The values represent horizontal velocity components only, which range from 0 to 0.7 m/s. The thin black lines show the water level during collection. Clear water conditions made resolution of velocities near the surface difficult in the deep water deployments (ad2 and ad3).

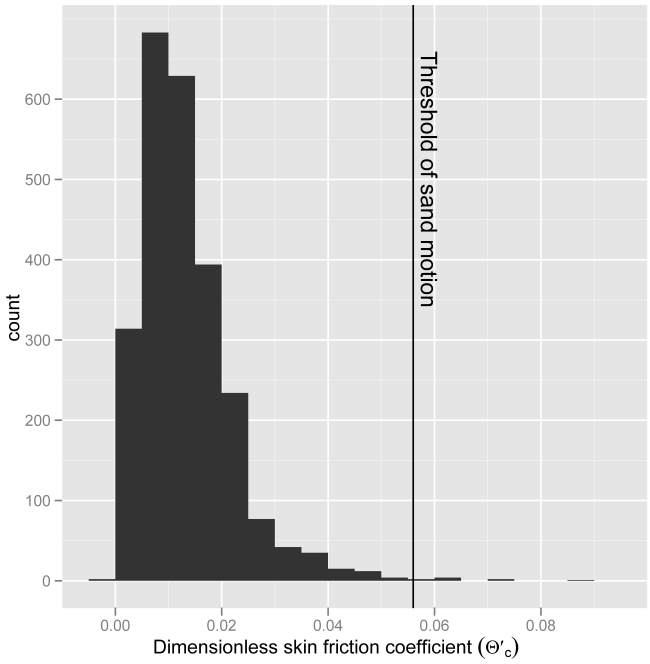

Figure 2.24: Dimensionless skin friction values from recorded current bed velocities on the Koojesse Inlet tidal flats in July/August of 2011.

Figure 2.25: Early development of the icefoot in November, 2011. The large chunks of ice come from the river mouth near the head of the bay, as the sea-ice forming on the flats had not yet reached that thickness.

Figure 2.26: Large anchor ice chunks removed from the seabed and transported by the high tide. They are redeposited elsewhere on the flats, determined mainly by the winds during high tide.

Figure 2.27: The early icefoot can be seen developing at the base of the beachface. The spring high tide water, however, came overtop and reached the upper level of the beachface, adding thickness to the underlying ice.

Figure 2.28: Extent of broken chaotic ballycatters (large conical protrusions of broken sea ice) overlying the tidal flats during the ice season. Person for scale. Photo: SVH, 2011-02-12

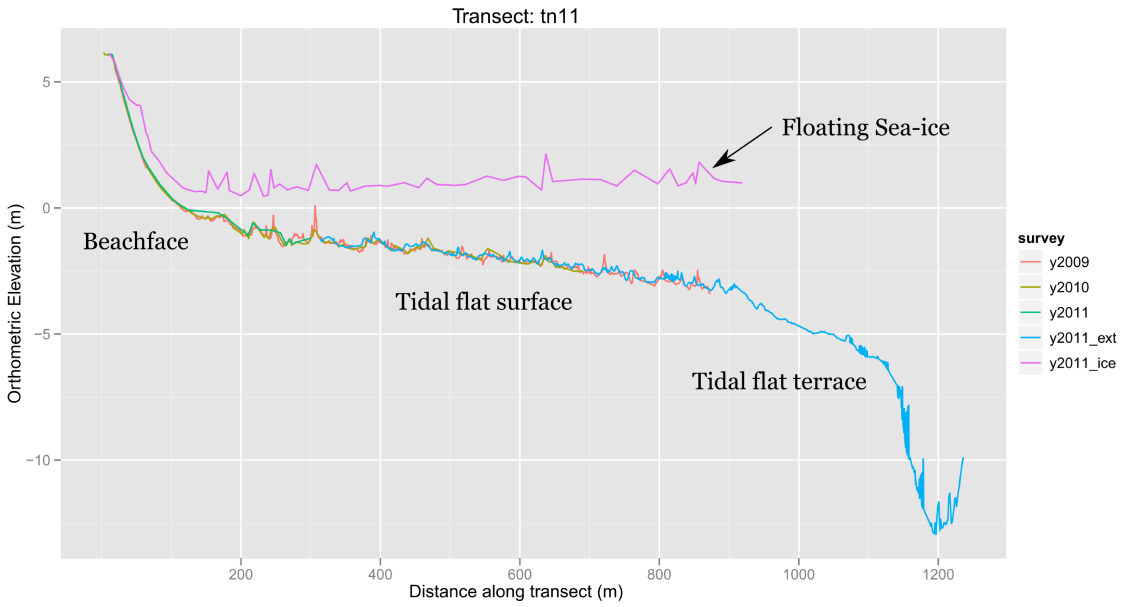

Figure 2.29: Transect showing solid sea ice over the tidal flat topography in February 2011. The icefoot is shown at the top of the beach, with draped ice approximately 1 m thick running out to sea level. Seaward of this the ice is floating with the tide as a solid cover, lifting and settling over 8 m (neap) and 12 m (spring) vertical twice daily. The ballycatters are evident as jags in the ice line, and follow the boulder mounds captured in the summer transects. Vertical exaggeration of 36.

2.6 Discussion

The boulder-strewn tidal flats in Koojesse Inlet were studied over three years (2009-2011) using GPS surveys, sonar (single-beam, sidescan, and sub-bottom), acoustic doppler current profilers, and tide and wave recorders. There were no distinctive berm or ridge features associated with the beaches near the high tide line as is seen in more energetic systems, where a distinct break in slope gives clear visual confirmation. Submarine slopes off the edge of the flats are comparable to the beachface slopes. The intervening flats have very low slopes, and show both convex-up and concave-up morphology. An integrated digital elevation model incorporating elevation data from field surveys and remote sensing photogrammetry allowed calculation of a hypsometric curve for the basin. This identified meaningful breaks in slope associated with the range of modern coastal processes. Additionally, elevation change between coincident points on GPS transects showed variable patterns of erosion and sedimentation over a short time series. Wave gauge data collected over the flats in the fall seasons of 2010 and 2011 showed wave periods of 2 - 7 s and significant wave heights reaching 0.7 m. A short time series in 2011 offshore of the flats recorded wave periods of 3 - 7 s and significant wave height reaching 1 m. Measured currents reached 0.46 m/s over the flats and 0.74 m/s in the harbour channels.

Placing these data in historical context is difficult due to scarce data, however some comparisons can be made. McCann et al. (1981) concluded the likely erosional origin of the flats, but was unable to identify or quantify change on a short time scale. Leech (1998) did so by estimating the amount of sediment entrained in a typical sea ice season from the flats at 68,000 $^{kg}/_{km^2}$. Historical water levels and climate records exist for the city, and a detailed study of the nature and changing patterns of storm weather in this area is provided by Hanesiak et al. (2010), which show that the period represented by this dataset does not capture the extremes but is fairly representative

of the norm. Further work on historical change would be invaluable, and could consist of detailed coastal change analysis on aerial photography as well as using entrainment estimates with sea ice season data to quantify an estimate of sediment moved. This was beyond the scope of this study.

Previous work on cold-region tidal flats has focused primarily on the role of ice in disrupting patterns typical of ice-free temperate settings. The work of McCann et al. (1981), McCann & Dale (1986) and Dale et al. (2002) established the dominant role of ice in determining sedimentary and biological zonation on the flats in Koojesse Inlet. Work in Ungava Bay (Lauriol & Gray, 1980), coastal Labrador (Rosen, 1979), the St. Lawrence Estuary (Dionne, 1988), Pangnirtung Fiord (Aitken et al., 1988), as well as in Koojesse Inlet (Leech, 1998), enriched our understanding of the distribution of boulders across the flats, a unique feature of northern tidal flats. Ruz et al. (1998) argued the dominant role of postglacial uplift in determining the morphology of northern tidal flats in glaciated regions. Results from this study can contribute to two discussions about northern tidal flats: their sediment transport mechanics, and their postglacial evolution.

2.6.1 Sediment Transport

2.6.1.1 Beaches

Formation of the beaches at the high tide line requires rare wave events at high water to rework paraglacial marine deposits. McCann et al. (1981) identified intermittent wave events as important shapers of the beach morphology in the inlet. Based on the well-sorted coarse-sand grain size, as well as the break in slope from the tidal flats, they suggested that the beaches are formed by waves during storm events. GPS transects surveyed in this study have shown that breaks in slope are gradual and the

beach berms are ill defined, indicating modest wave reworking. Since the work done in the 1980s, a number of groynes and a large pier have been placed in the littoral zone of the old Iqaluit beachfront. On the eastern side of these groynes, pocket beaches have developed with well-sorted coarse sand attesting to the effectiveness of the present wave climate, or perhaps the focusing of wave energy from altered tidal flat morphology. The elevations for the break in slope at the top of the beachface (the upper berm) and at the base are coincident with the shoreline levels at spring and neap high tides. The waves measured indicate the potential for reworking of sediment sizes found on the beach. The formation of the beach is dependent on storm wind events during high tides, when short-period wind waves can rework the upper beach through the high-tide cycle. The evidence for littoral circulation indicates the competence of storm waves to transport the beach sediment and reorient the pocket beaches. The difference between measured extreme tide levels and surveyed swash lines could either be a measure of maximum wave runup or evidence for past high spring tides or storm surges not recorded in the tidal data.

2.6.1.2 Sediment transport by Ice

Sediment transport by sea ice is thought to account for the boulder configuration on the flats and the minimal development of sedimentary zonation. Work in the St. Lawrence estuary by Dionne (1988), as well as theoretical and empirical work by Drake & McCann (1982) and Leech (1998) has established that ice is capable of moving boulders in Koojesse Inlet. This occurs mainly by ice push and shove rather than entrainment. Leech (1998) determined that boulder movement on the flats is chaotic and was primarily landward for the year of the study.

Boulder ridges, known as 'boulder barricades', are a common feature of many northern tidal flats. Rosen (1979) proposed three determinants for a barricade: ice capable

of transporting boulders, sufficient tidal range to permit transport by ice, and an identifiable break in slope near the low-tide line. All elements are found in Koojesse Inlet, but a well defined boulder barricade is not present. Instead, the break in slope at the edge of the flats is marked by a discontinuous array of boulder mounds, which extend shoreward into the flats. In some areas, a more defined ridge is present, but it is short ($<$ 100 m) and is oriented obliquely to the shoreline. Interestingly, there is a well defined boulder barricade in Pangnirtung Fiord 300 km further north in Cumberland Sound (Gilbert, 1984; Aitken et al., 1988; Forbes & Hansom, 2012), as well as more examples in Labrador and Ungava Bay (Rosen, 1979; Lauriol & Gray, 1980). Oblique photos from elsewhere in Frobisher Bay near Koojesse Inlet show a lack of obvious boulder ridges, and so it seems reasonable that this arrangement may be a product of the tidal range and climate of the area, though specific drivers remain unknown. The lack of a boulder barricade does make the Koojesse Inlet flats anomalous.

2.6.1.3 Transport by Waves and Currents

This study presented a small dataset on waves moving over the tidal flats. It was shown that at mid tides, the boulder-strewn flats effectively dissipate incident wave energy. However, because of low wave periods and short wavelengths resulting from restricted fetch, dissipation is not initiated until higher on the flats when the water level is high. Thus waves of intermediate period and wavelength forced by storm events during a high tide are able to propagate in over the flats. Comparing the wave heights and periods observed in this study with a theoretical calculation (following Hurdle & Stive (1989) with 45 km SE wind for 10 hours) of possible wave heights and periods, it appears that there is low probability of waves more than double the size of those observed occurring. This could account for the similar slopes found at the

outer edge of the flats, where waves rework coarser sediment near the low tide line. Dale et al. (2002) established the grain sizes of surficial sediments on the flats, and reported that the vast majority had mean sizes within the sand class, which is supported by samples taken in this study both on the Iqaluit flats and the Apex flats (Fig. 2.6). These intertidal flats are primarily sand flats, with areas of increased mud content. Houser & Hill (2010a) found that the sand flats at Roberts Bank, near Vancouver BC, were morphodynamically different from mudflats researched elsewhere (Houser & Hill, 2010a). This was because of the difference in transport dynamics of sand and mud. The fines typically found on mudflats are entrained into suspension by waves and can then be transported by the mean current. Therefore, they are susceptible to tidal current asymmetries. With much higher fall velocities, sand is less susceptible to transport by mean currents. Transport on sand flats, therefore, is thought to be based less on tidal current asymmetries, and instead more on the interplay between the incident wave field and the currents acting on them. Given the frequency of southeast winds onshore at the Koojesse Inlet flats, this dominance of oscillatory bedload transport landward in the absence of strong tidal currents may account partially for the sedimentation observed at the base of the beach. The ice-free season of 2010 was far longer in duration than that of 2011, and thus the area was exposed to greater magnitude southeast winds in the fall storm season. The deposition of sediment at the base of the beach between the 2009 and 2010 seasons might be related to the difference in wind activity.

The surficial sediments in the inlet are varied, but follow a pattern that seems to link forcing and depth. For surficial sediments throughout the bay, it seems reasonable that the sediment pattern represents a mixture of available fluvial fines, as well as the relative wave and current conditions. Long Island, by sheltering incident wave energy, likely contributes to the sediment composition of the inner inlet, while the sand and

cobble composition of the more exposed Apex shore is likely due to increased wave and current energy.

2.6.2 Evolution of the tidal flats

Data presented in this study support the interpretation proposed by McCann et al. (1981) for the evolution of the tidal flats. The silty clay underlying the flats indicates postglacial emergence which may be continuing today. Since the early 1980s, work on northern tidal flats has solidified the importance of uplifted glaciomarine deposits both in the evolution of the flats (Dionne, 1988; Martini, 1991), and in the modern sedimentary budgets of these systems (Ruz et al., 1998). In Koojesse Inlet, sub-bottom profiling in 2011 revealed stratigraphic layering under the flats interpreted as draped glaciomarine sediments (Fig. 2.30). Camera transects showed evidence of silty clay exposed at the edge of the flats, but without targeted sampling this can not be confirmed. This would be counter to the evidence of progradation at the edge of the terrace through channel drainage fans and slumping.

It appears the evidence for erosion of the flats is undeniable: outcropping of the underlying glaciomarine, coarse material intermixed with fines found in a thin veneer on the surface, evidence for runoff washing into the nearshore channels, and the concave profiles of the inner flats all indicate net erosion. This study, however, was unable to quantify significant erosion over a three year time series. In fact, deposition and erosion of equal magnitude were observed on the inner flats over two successive years. This is likely a reflection of the different scales of sediment dynamics involved in the landforms evolution, where year-to-year changes measured here are characteristic of ice entrainment and substantial wave reworking, and the morphological indicators of erosion point to decadal forces slowly reforming the broader morphology of the flats.

Three sources of information on this coastal system have been synthesized to produce a rough time-line of evolution for the system, presented in Figure 2.30. From previous work it relies on Hodgson (2005) for its postglacial time-line and sea level history. McCann et al. (1981) first suggested an erosional origin for the landform now present, and McCann & Dale (1986) furthered this by showing the present manifestations of ice entrainment on the flats. The boulders currently accumulated on the flats surface could either be transported from higher topographies as relative sea-level fell, as suggested by Lauriol & Gray (1980), or could be exhumed from the underlying glacio-marine deposit as the landform is eroded away. Partially buried boulders found throughout the flats support the latter, especially given the low amounts of deposition recorded and the transport of boulders reported by Leech (1998). Evidence for draped layering in the glacio-marine found in this study support the interpretation of proglacial marine deposition presented in figure 2.30. This diagram represents a culmination of current attempts to explain the evolution of the coastal landforms present in Koojesse Inlet.

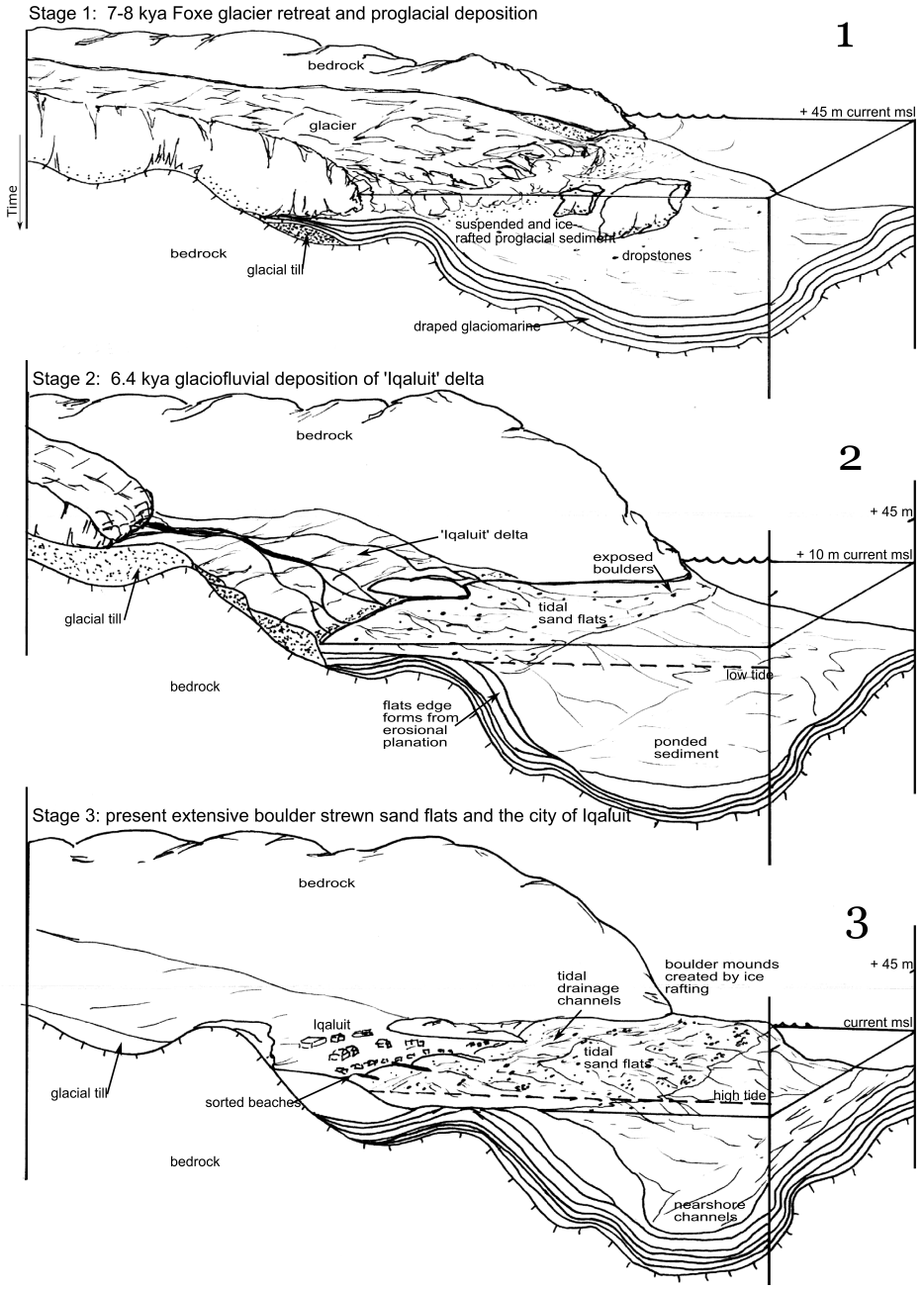

Figure 2.30: Theoretical steps in the evolution of the Koojesse Inlet tidal flats. Stage 1 shows conditions during the last sea level highstand roughly 45 m above current MSL (Hodgson, 2005). The proglacial deposition of boulder erratics and ice-rafted sediments created the draped glaciomarine layer of silty clay found underlying the flats today. Stage 2 is roughly during the glacial retreat stage about 6.4. kya when glaciofluvial deposition occurred in a previous tributary of the Sylvia Grinnell river (Hodgson, 2005). Deposition of the 'Iqaluit' delta is shown. Hodgson (2005) suggests that tides were similar to those today, and that the reworking and planation of the intertidal sediments created the sand flats found along most of the coast. Stage 3 is the present period where the flats show slow erosion through ice entrainment and the boulder erratics have had sufficient time to form a rough boulder garland near the edge of the flats. The figure was produced by S Hatcher.

2.7 Summary and Conclusions

Koojesse Inlet is an example of a macrotidal Arctic embayment with a complex erosional boulder-strewn tidal flat morphology. Previous work has mapped the sediment zonation of the tidal flats, measured boulder dynamics, described sedimentation processes during the dynamic breakup period, and quantified entrained sediment load from basal adfreezing. The continued growth of Iqaluit and Apex on the shores of Koojesse Inlet makes further description of the intertidal and nearshore morphology and sediment dynamics a priority for dealing with current environmental changes. Field work mapping the Koojesse Inlet tidal flats suggests:

- the importance of postglacial uplift in forming cold-region tidal flats
- a protective role for boulder mounds in wave and current energy dissipation
- that sedimentation over three years is focused on the inner flats near the base of the beachface, indicating a complex system of deposition, reworking, and export seaward
- current and wave energy is low and on the flats is related more to wind direction and duration then to tidal forcing
- the subtidal harbour seabed is characterized by locally ponded silty sediment probably derived from the tidal flats, and outcrops of glaciomarine draped sediment also found under the active layer on the flats

This work shows agreement with others in recognizing the dominant role of paraglacial sediments in the modern morphology and morphodynamics of cold-region tidal flats. Additionally, it suggests that improving understanding of these environments may require alteration of the traditional morphodynamic prism of tide-wave-river forcing to include varying degrees of sea-ice influence.

2.8 References

Aitken, A., Risk, M., & Howard, J. (1988). Animal-sediment relationships on a subarctic intertidal flat, Pangnirtung Fiord, Baffin Island, Canada. *Journal of Sedimentary Research*, *58*(6), 969–978.

Allard, M., Doyon, J., Mathon-Dufour, V., Leblanc, A.-M., L'Herault, E., Mate, D., Oldenborger, G., & Sladen, W. (2012). Surficial geology, Iqaluit, Nunavut. Geological Survey of Canada, Geoscience Map 64 (preliminary version), scale 1:15,000.

Amos, C. (1995). Siliciclastic tidal flats. In G. Perillo (Ed.) *Geomorphology and Sedimentology of Estuaries*, (pp. 273–306). Amsterdam: Elsevier Science.

Bird, E., & Schwartz, M. (Eds.) (1985). *The World's Coastline*. New York, Van Nostrand Reinhold.

Dale, J., Leech, S., McCann, S., & Samuelson, G. (2002). Sedimentary characteristics, biological zonation and physical processes of the tidal flats of Iqaluit, Nunavut. In K. Hewitt, M. Byrne, M. English, & G. Young (Eds.) *Landscapes in Transition: Landform Assemblages and Transformations in Cold Regions*, vol. 111, (pp. 205–234). Dordrecht: Kluwer.

Deacu, D., Zadra, A., & Hanesiak, J. (2010). Simulating Wind Channelling over Frobisher Bay and its Interaction with Downslope Winds during the 7-8 November 2006 Wind Event. *Atmosphere-Ocean*, *48*(2), 101–121.

Dionne, J. (1988). *Characteristic features of modern tidal flats in cold regions*, (pp. 301–332). Dordrecht: D. Reidel Publishing Company.

Dionne, J. (1993). Sediment load of shore ice and ice rafting potential, upper St. Lawrence estuary, Quebec, Canada. *Journal of coastal research*, *9*(3), 628–646.

Drake, J., & McCann, S. (1982). The movement of isolated boulders on tidal flats by ice floes. *Canadian Journal of Earth Sciences*, *19*(4), 748–754.

Environment Canada (2012). Climate Normals 1971-2000, Iqaluit.
URL `http://climate.weather.gc.ca/climate_normals/results_e.html?stnID=1758&lang=e&dCode=0&province=NU&provBut=Search&month1=0&month2=12`

Forbes, D. (2012). Glaciated Coasts. In E. Wolanski, & D. McClusky (Eds.) *Treatise on Estuarine and Coastal Science*, vol. 3, (pp. 223–243). Waltham: Academic Press.

Forbes, D., & Taylor, R. (1994). Ice in the shore zone and the geomorphology of cold coasts. *Progress in Physical Geography*, *18*(1), 59–89.

Forbes, D. L., & Hansom, J. (2012). *Polar Coasts*, vol. 3, (pp. 245–283). Waltham: Academic Press.

Gibbons, D., Jones, G., Siegel, E., Hay, A., & Johnson, F. (2005). Performance of a new submersible tide-wave recorder. In *Proceedings of MTS/IEEE Oceans Conference (17-23 Sept. 2005)*, vol. 15, (pp. 2–5).

Gilbert, R. (1984). The movement of gravel by the alga Fucus vesiculosus (L.) on an Arctic intertidal flat. *Journal of Sedimentary Research*, *54*(2), 463–468.

Hanesiak, J., Stewart, R., Barber, D., Liu, G., Gilligan, J., Desjardins, D., Dyck, R., Fargey, S., Hochheim, K., Martin, R., Taylor, P., Biswas, S., Gordon, M., Melzer, M. A., Moore, K., Field, R., Hay, C., Zhang, S., McBean, G., Strapp, W., Hudak, D., Scott, J., Wolde, M., Goodson, R., Hudson, E., Gascon, G., Greene, H., Henson,

W., & Laplante, A. (2010). Storm Studies in the Arctic (STAR). *Bulletin of the American Meteorological Society*, *91*(1), 47–68.

Hodgson, D. A. (2005). Quaternary Geology of Western Meta Incognita Peninsula and Iqaluit area, Baffin Island, Nunavut. Tech. rep., Geological Survey of Canada.

Houser, C., & Hill, P. (2010a). Sediment Transport on Roberts Bank: A Sandy Intertidal Flat on the Fraser River Delta. *Journal of Coastal Research*, *26*(2), 333–341.

Houser, C., & Hill, P. (2010b). Wave Attenuation across an Intertidal Sand Flat: Implications for Mudflat Development. *Journal of Coastal Research*, *263*(263), 403–411.

Hurdle, D., & Stive, R. (1989). Revision of PSM 1984 wave hindcast model to avoid inconsistencies in engineering applications. *Coastal Engineering*, *12*(4), 339–351.

Lauriol, B., & Gray, J. (1980). Processes responsible for the concentration of boulders in the intertidal zone in Leaf Basin, Ungava. In S. McCann (Ed.) *The Coastline of Canada*, vol. GSC paper 80-10, (pp. 281–292). Geological Survey of Canada.

Leech, S. (1998). *The transport of materials by ice in a subarctic macrotidal environment, Koojesse Inlet, southeast Baffin Island*. Master's thesis, M.Sc. Thesis, University of Regina, Regina.

Martini, I. (1991). *Sedimentology of subarctic tidal flats of western James Bay and Hudson Bay, Ontario, Canada*, chap. Memoir 16, (pp. 301–312). Canadian Society of Petroleum Geologists.

Maxwell, J. (1982). *The climate of the Canadian Arctic Islands and Adjacent Waters, Volume 2*. Toronto: Atmospheric Environment Service.

McCann, S., & Dale, J. (1986). Sea ice breakup and tidal flat processes, Frobisher Bay, Baffin Island. *Physical Geography*, *7*(2), 168–180.

McCann, S., Dale, J., & Hale, P. (1981). Subarctic Tidal Flats in Areas of Large Tidal Range, Southern Baffin Island, Eastern Canada. *Géographie physique et Quaternaire*, *35*(2), 183–204.

Nortek (2005). Aquadopp Current Profiler User Guide. Tech. rep., Nortek.

Rosen, P. (1979). Boulder barricades in central Labrador. *Journal of Sediment Petrology*, *49*(4), 1113–1123.

Ruz, M., Allard, M., & Michaud, Y. (1998). Sedimentology and evolution of subarctic tidal flats along a rapidly emerging coast, eastern Hudson Bay, Canada. *Journal of Coastal Research*, *14*(4), 1242–1254.

Short, N., Leblanc, A.-M., Sladen, W., Allard, M., & Mathon-Dufour, V. (2012). Seasonal Surface Displacement Derived from InSAR, Iqaluit, Nunavut. Geological Survey of Canada, Canadian Geoscience Map 66 (preliminary version), scale 1:15 000.

St-Onge, M., Scott, D., & Wodicka, N. (1999). Geology, Frobisher Bay, Nunavut. Map 1979A, scale 1:100 000.

Swart, D. (1974). *Offshore Sediment Transport and Equilibrium Beach Profiles*. Ph.D. thesis, Delfts University, Netherlands.

Chapter 3

Assessing exposure to coastal hazards in Iqaluit

3.1 Abstract

Recent changes in the Arctic coastal system present significant challenges to coastal infrastructure. In Iqaluit, the capital of the territory of Nunavut in Canada's Arctic, the city recognizes the need for adaptation planning to respond to rapid environmental change. This effort is challenged by a scarcity of data on which to base projections of future change. The purpose of this study is to provide baseline geoscience data and a knowledge base on coastal hazards to support adaptation planning along the waterfront in Iqaluit. Field work between 2010 and 2011, coupled with remotely sensed mapping data, focused on modelling the topography, mapping and classifying the coastal infrastructure on Iqaluit's coastline, and assessing hazards from sea ice, flooding, waves, and erosion. Coastal modelling consists of generating a terrestrial digital elevation model (DEM), coupled with an interpolated surface from extensive intertidal and nearshore GPS mapping. Infrastructure modelling consists of gener-

ating data on foundation and ground elevations of key coastal structures, as well as documenting their use. The modest wave climate has enabled development of built infrastructure close to the high tide line, a situation that leads to enhanced risk in the context of rising global sea levels. Taking a precautionary approach, under an upper-limit scenario of 0.7 m for relative sea-level rise from 2010 to 2100, key municipal infrastructure will have a remaining freeboard of 0.3-0.8 m above high spring tide. The ice-free season has been lengthening by 1-1.5 days/yr since 1979, and the ice has been getting thinner since then as well. Ice pile-up was observed to form a ridge of ice up to 2.5 m high at the high tide line during freeze-up in November 2011. The landfast icefoot, however, provides protection for coastal infrastructure, except where development artificially steepens the coast. Influence of storm waves is reduced by energy dissipation over the boulder tidal flats along the Iqaluit waterfront. Overtopping of critical infrastructure is a potential issue, dependent largely on the progress of relative sea-level. These results have implications for adaptation planning in the city, providing quantified limits for safe development. This study considers the information requirements for community-scale hazard mitigation and climate-change adaptation and the potential problems of down-scaling regional projections.

3.2 Introduction

3.2.1 Background and Objectives

Recent rapid changes within the Arctic climate system have exacted heavy tolls on the infrastructure of some Arctic coastal communities (Arehart, 2012). The effects of polar climate amplification mean that parts of the Arctic are warming at rates exceeding other regions of the globe (Serreze & Barry, 2011). Larsen et al. (2008) calculated an additional $5.6-$7.6 billion would be required, in excess of regular maintenance invest-

ment, to repair Alaskan infrastructure if projected climate change persists to 2030. A report investigating the impacts of climate change on infrastructure in Northern Canada estimated $5 trillion worth of infrastructure could be at risk from projected changes. Billions of dollars will be invested in new infrastructure in the coming decades, meaning the issue includes both an ageing base and a rapid expansion of infrastructure (NRTEE, 2009, pg. 18). The environment, isolation and transportation logistics of the Arctic raise costs, making infrastructure expensive to build and maintain (Forbes, 2011, pg. 34). Further work investigating potential impacts on infrastructure from projected environmental changes may provide a means to improve design and develop strategy to adapt and sustain Canada's northern infrastructure, now and in the future.

A significant proportion of infrastructure risks in the Canadian Arctic are coastal. All Canadian Inuit communities are coastal, meaning a great segment of Arctic infrastructure is therefore also coastal. Atmospheric warming has already led to changes such as increased thermal abrasion and coastal erosion (Are et al., 2008; Forbes, 2011). Arctic coastal communities are complex systems, and the threat to coastal infrastructure from changing coastal dynamics is only one source of risk amongst many (permafrost thaw subsidence, wind damage, increased precipitation). In some places potential impacts have already turned to hazards leading to relocation (`http://www.shishmarefrelocation.com/`) or retreat (Catto & Parewick, 2008). These challenges are exacerbated by sparse data and short time series, greatly inhibiting our ability to predict future impacts (NRTEE, 2009; Forbes, 2011; Strzelecki, 2011). Communities feel the pressure to adapt to change and protect their infrastructure, and this is often pursued with help from multiple bases of knowledge, including scientific research (Ford et al., 2010; Forbes, 2011). Responses are based on available information and are unique to the hazard and community infrastructure at risk.

The city of Iqaluit, Nunavut, is dealing with hazards from exposures on many fronts. Thawing permafrost has damaged city infrastructure (Nielsen, 2007), expanding population is putting strain on the food networks of the community (Lardeau et al., 2011), and occasional coastal flooding has occurred in the past (Fig. 3.1). Due to exacerbation of these issues by climate change, adaptation planning is ongoing and is mandated on both a territorial and municipal level (City of Iqaluit, 2010). The city has established a "sustainability subdivision" within the municipal administration to deal with questions of structural and cultural longevity of community resources under expected changes in the environment. Recent rapid growth of the city complicates this effort, as a $40 million infrastructure deficit owed creates an added burden for investment in solutions. One area identified as a research priority was hazards at the coast associated with sea-level change, high water levels, and changing sea-ice patterns (Nielsen, 2007; City of Iqaluit, 2010).

3.2.2 Study Area

Iqaluit sits at the head of Koojesse Inlet (63.7N, 68.5W) in the northwest corner of Frobisher Bay on Baffin Island (Fig. 3.2). This inlet is macrotidal, with spring tide range of 12 m (DFO, 2012). This produces a coast with extensive boulder-strewn tidal flats, which are found along much of Frobisher Bay's northern coast (Fig. 3.3). On the shoreward border of these flats, the coast is composed of mixed sand and gravel beaches between bedrock headlands that terminate near the high tide line of the tidal flats. On the seaward border, the flats fall off into deeper offshore channels. Navigation is therefore dictated by the tidal stage, and is complicated by bedrock reefs that are exposed only at low tide.

Wave action is limited in Koojesse Inlet by a number of factors. Incident swell is fetch limited due to the configuration of inner Frobisher Bay. The inlet opens to the

Figure 3.1: Flooding that occurred in October 2003. Photo courtesy of Rick Armstrong. The winds were light and offshore (northwest). The high water level was not associated with a storm, so was likely the result of an anomalously high tide. This photo was taken roughly 50 m from the base of the main breakwater, facing east.

southeast, and Long Island sits at the entrance, providing some shelter from incident waves (Fig. 3.2). The islands that separate inner and outer Frobisher Bay lie roughly 54 km straight line distance from the mouth of the inlet (Fig. 3.2). Strong southeast winds in the storm season (late August to early November), however, can produce wind waves and rough seas that can propagate into the inlet.

Erosion on this coastline is not rapid, and sediment movement is dominated by sea-ice dynamics. The configuration of sediment around groynes indicates a northwesterly alongshore drift along the Iqaluit waterfront. Accumulation of fine muds on the eastern side of the breakwaters suggests suspended sediments are transported alongshore

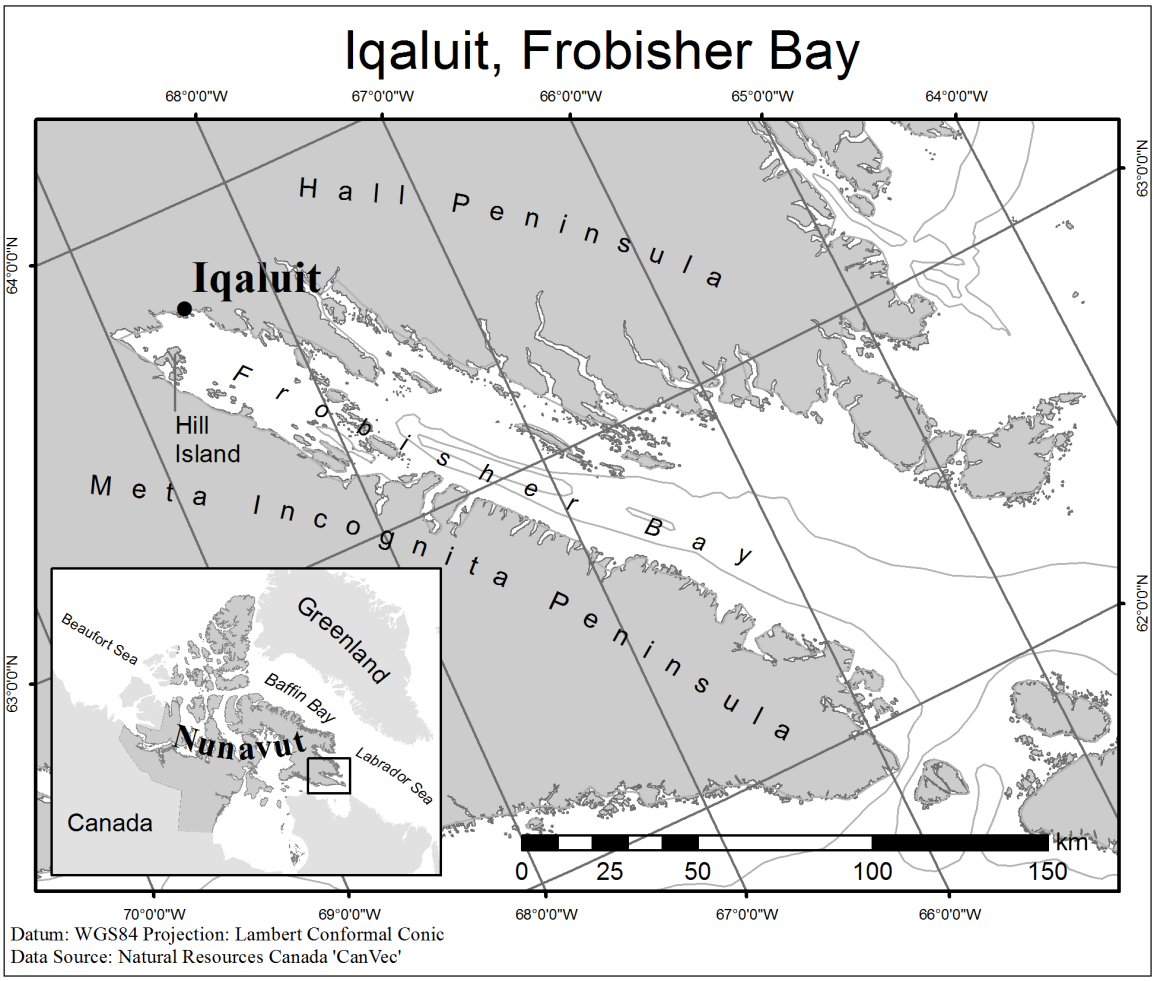

Figure 3.2: Iqaluit sits at the head of Frobisher Bay on the south-eastern side of Baffin Island.

in this direction, but the coarser sediments (sand and gravels) of the beaches are likely the result of reworking by combined waves and currents. Sea ice dominates the coast here for an average of 9 months of the year. During the ice season, thick intertidal ice is continually lifted and rested onto the flats by the alternating tides, which entrains sediment through basal adfreezing. This entrained sediment does not move offshore, but is instead recycled back onto the flats surface. This is due to preferential thawing of sediment laden ice in the spring and the solid offshore ice that contains the intertidal ice within the tidal flats zone (McCann & Dale, 1986).

Figure 3.3: The boulder-strewn tidal flats extend up to 1 km offshore of the beachface, and are very low slope with a complex network of shallow tidal drainage channels. The outskirts of the city are seen to the left of the photo.

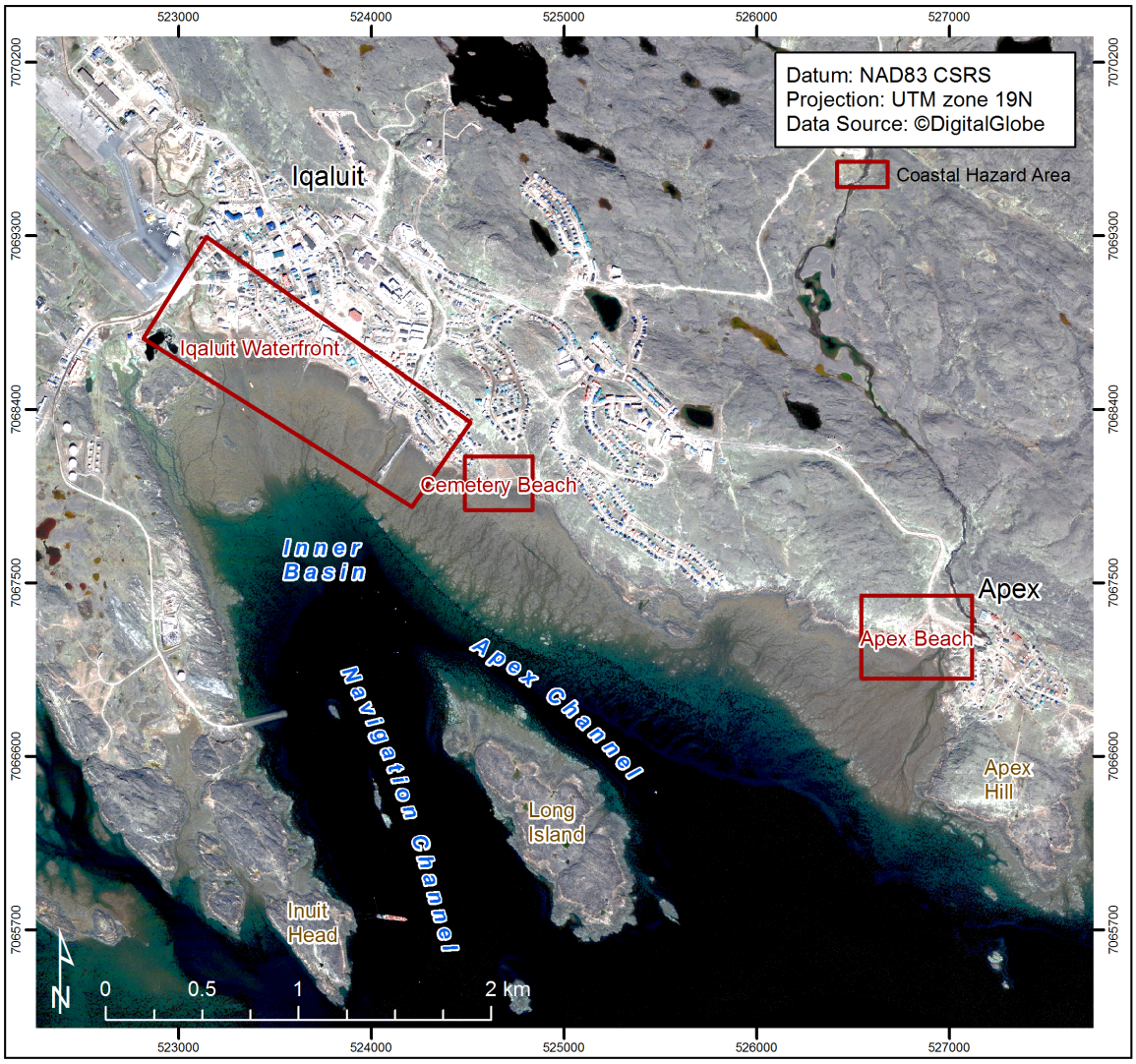

Figure 3.4: Quickbird imagery of Koojesse Inlet. The imagery was taken at low tide so the expansive tidal flats are shown off the Iqaluit and Apex waterfront. Surrounding the inner harbour is the industrial section of Iqaluit to the west, the airport to the northwest, and the main city commercial and residential areas to the east and north-east. Apex is located on the eastern side of Koojesse Inlet at the mouth of the Apex river. Contains material © DigitalGlobe.

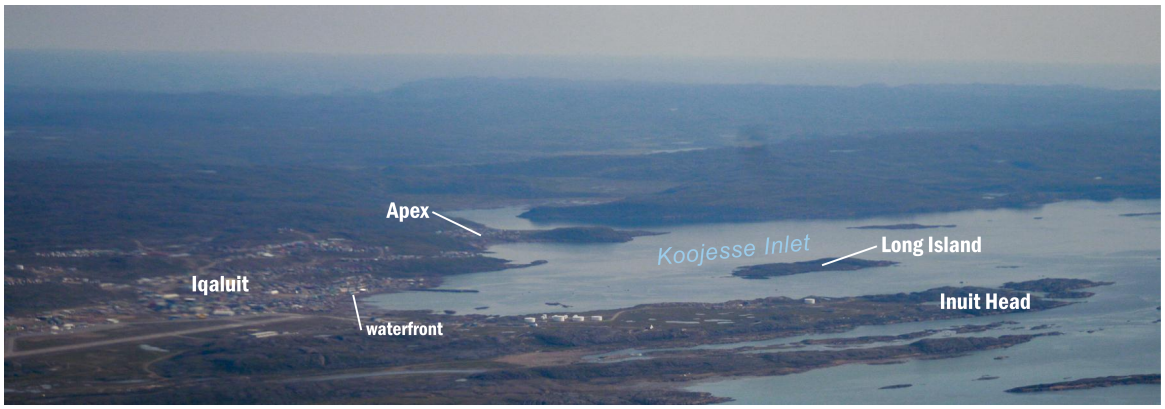

Figure 3.5: Oblique aerial photo showing the configuration of Koojesse Inlet (August 2010). Koojesse Inlet is roughly 3 km long and 2 km wide at its mouth, which opens facing south to south-west. Long Island shelters the Iqaluit waterfront from southerly swell. Apex is located 2 km east of Iqaluit. Iqaluit's main waterfront sits at the head of the inlet.

3.3 Urban development

The present City of Iqaluit developed as a hybrid settlement around the U.S. Strategic Air Command base at the head of the inlet. Inuit would seasonally occupy the beach in order to take advantage of both employment at the base and good fishing in the inlet (Eno, 2003). Iqaluit is an Inuktitut word that translates to "place of many fish". Because of this, the traditional grounds of the Inuit in Iqaluit were at the coast, where they would have seasonal camps close enough to the airbase to also work there (Fig. 3.6). The airbase acted as a nucleus of development, but infrastructure expanded to the shoreline in order to support the landing of supplies arriving by ship (Fig. 3.7).

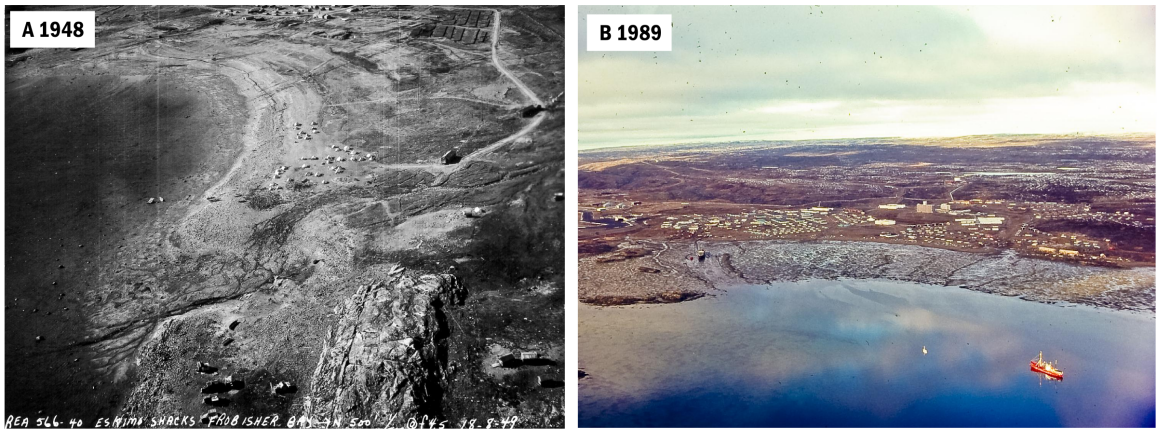

Figure 3.6: (A) Oblique aerial photo of Iqaluit settlement in 1948. In the foreground Inuit tents are shown. (Photo: National Air Photo Library) (B) Oblique aerial photograph from 1989 showing development toward the coast in Iqaluit. Note the clearing of boulders from a strip of the tidal flats to allow unloading of a ship. (Photo: SB McCann 1989)

The city of Iqaluit is now home to nearly 7000 people, and has been growing in population consistently since the 1991 census (Fig. 3.8). The larger buildings on the coast have all been built since 1970, and many were constructed in the late 1990s. The city now supports the territorial government of Nunavut, as well as a modern city administration. Municipal and federal infrastructure is found on the coast, while

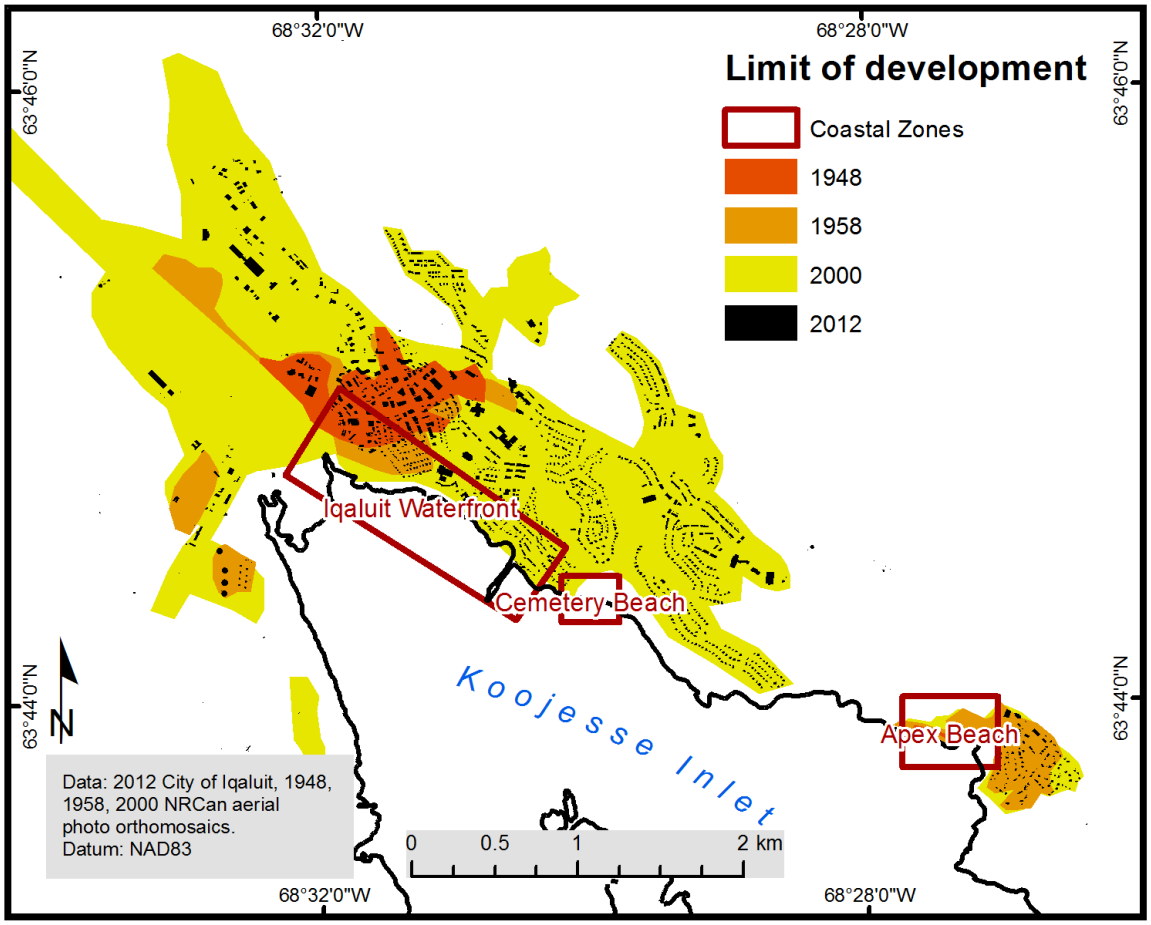

Figure 3.7: The development history in Iqaluit follows an expansion from the original airbase site near the head of Koojesse Inlet. The city now occupies the whole north-eastern coast of the inlet, with Apex found further east from Iqaluit's waterfront.

traditional activities and a subsistence economy continue along the coast.

By collecting scientific data on the coastal environment in Iqaluit, this study aims to contribute to an understanding of coastal hazards in the community. The two objectives of this study are (1) to evaluate the nature and severity of coastal hazards in inner Frobisher Bay, and (2) to investigate the sensitivity of coastal infrastructure in Iqaluit. Coastal hazards considered include sea-level change, storm waves, storm flooding, sea ice ride-up and pile-up, and shoreline erosion. These operate across a range of time scales and vary in severity and potential impacts at Iqaluit.

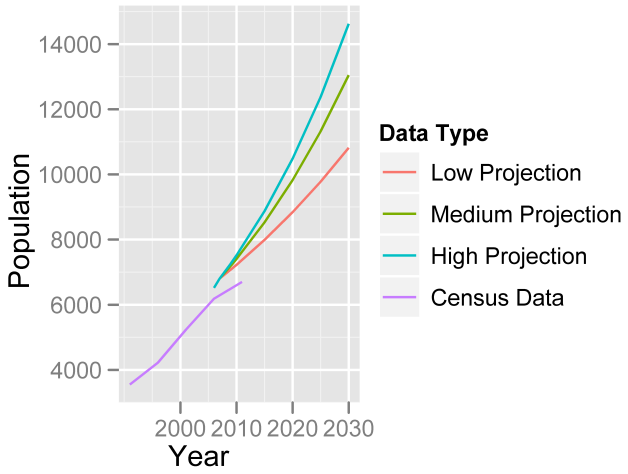

Figure 3.8: Population growth in Iqaluit. Projections taken from City of Iqaluit (2010).

Coastal flooding in Iqaluit remains poorly documented, but high spring tides from long-period oscillations provide one explanation for their occurrence. Additionally, no significant surges are recorded in the tide gauge record. Projections of sea-level change are constrained by uncertainties in the rate of vertical motion as well as the complexities of sea-level fingerprinting at this proximity to the Greenland Ice Sheet (James et al., 2011), but it is likely that a net positive change in relative sea level will be experienced by the end of the century. Storm wave energy is limited by the maximum 54 km open-water fetch in the inner bay and for much of the year wave generation is restricted by sea ice. Winter sea ice in the shore-zone is highly dynamic, rising and falling with the large tidal range, but the presence of an ice-foot provides some protection against ride-up and pile-up. Coastal retreat is minimal because much of the shore consists of resistant bedrock and, until very recently, if not to this day, the site has been emergent (falling relative sea level).

The climate and weather are crucial to coastal hazards because of their influence on coastal dynamics. In Iqaluit, this is primarily through two processes: storms and sea

ice. Here, storms capable of producing waves that can impact the coast are restricted to a narrow south-east fetch exposure, and are predominantly experienced during the fall season when extra-tropical cyclones propagating through the Labrador Sea and Baffin Bay tend to move westward over southern Baffin Island bringing relatively warm air masses north and producing precipitation. The impact of storms is dependent on the state of the sea ice, which divides the year into ice and ice-free seasons. The transition times during sea ice freeze-up (September - November) and break-up (May - June) are dynamic periods where ice is in constant motion at the coast, and significant amounts of sediment are being transported (McCann et al., 1981; Dale et al., 2002). Storms during these periods have the potential to cause sea ice ride-up and pile-up on the shore when strong onshore winds are present (Forbes & Taylor, 1994). Additionally, winds capable of producing waves can only do so in the absence of offshore sea ice.

3.4 Methods

Documenting coastal hazards in Iqaluit was essentially a mapping exercise enriched by analysis of relevant existing datasets. The data used in this study can be classified into seven categories:

- topography and bathymetry
- infrastructure
- climate and weather
- sea ice
- waves
- water levels
- geomorphology

Morphometry of the inlet and coastal zone was analyzed using data from two field seasons of topographic and bathymetric surveys (See Chapter 2). The elevation of infrastructure along the coast was surveyed to high precision (±0.05 m vertical). Infrastructure type was classified based on field observations and discussion with city staff. Climate records for the area from Environment Canada date back to 1949 (1953 hourly). Two datasets provide dates of freeze-up and break-up in the inlet, defining the ice season, which is crucial in assessing the impacts of storms. Analysis of meteorological data as well as break-up and freeze-up dates fed into consideration of wave potential in the inlet. Hindcast computations were validated by field measurement of inshore and offshore waves. Extreme water levels were investigated using the limited tide-gauge record supplemented by field measurement of water levels in the summer and fall of 2010 and 2011. Runup limits were determined by surveying storm debris lines.

Field work was conducted over five sessions between 2009 and 2011. The preliminary surveys in 2009 surveyed the flood water level reached in October 2003, segments of the main beach and four transects across the tidal flats. Subsequent surveys in 2010 and 2011 repeated and expanded the transect surveys across the full width of the tidal flats. In addition, foundation elevations for coastal infrastructure were surveyed and all surveys tied to geodetic and tidal datum control. Instrument moorings spanned the summer and fall of 2010 and 2011, with a total of nine wave and water level sensor deployments, seven in the intertidal and two in the subtidal harbour for short periods. A final trip in November 2011 to recover instruments before freeze-up coincidentally provided an opportunity to observe the freeze-up process (See Chapter 2).

3.4.1 Topography and bathymetry

Topographic elevation points were collected using survey-grade real-time kinematic (RTK) geographic positioning system (GPS) data. The system used in 2010 and 2011 was an Ashtech Z-Extreme receiver with an Ashtech dual band carrier-phase antenna. A comparable leased Magellan Promark 500 receiver with internal antenna was used in 2009. Originally, a local control point was established using a temporary benchmark near the coastline. This local coordinate system was then brought into the Canadian Spatial Reference System (CSRS) national grid by occupying three pillars (See Appendix A). Revisiting various control points established an estimated survey accuracy of ±0.15 m vertically and ±0.10 m horizontally (See Appendix A).

In addition to land-based surveys, boat work enabled the extension of mapping into the nearshore. Four GPS transects were extended offshore using a Lowrance LCX-25 (50/200 kHz) single beam echo-sounder. Positioning information was from a 12 channel Lowrance GPS with real time WAAS corrections. Horizontal positioning accuracy was approximately ±0.15 m, and vertical accuracy is ±0.25 m. The objective in mapping the nearshore and intertidal bathymetry, apart from completing the digital elevation model for the waterfront (see below), was to document erosion processes as well as the potential for wave energy loss across the boulder-strewn flats (See Chapter 2).

Elevations are always reported in reference to a vertical datum. In this study there are three used: the WGS84 ellipsoid, the CGVD28 orthometric datum, and Chart Datum (Fig. 3.9). All GPS positions were recorded as ellipsoidal elevations, which were subsequently converted to orthometric elevations using the separation value in the CGVD28 Ht v2.0 model, which in this area is 10.166 m. Chart Datum (the tide-gauge zero) is derived from the water level record and roughly coincides with the level of Lower Low Water Large Tide (LLWLT). Orthometric datum, which approximates

mean sea level, is 6.05 m above Chart Datum.

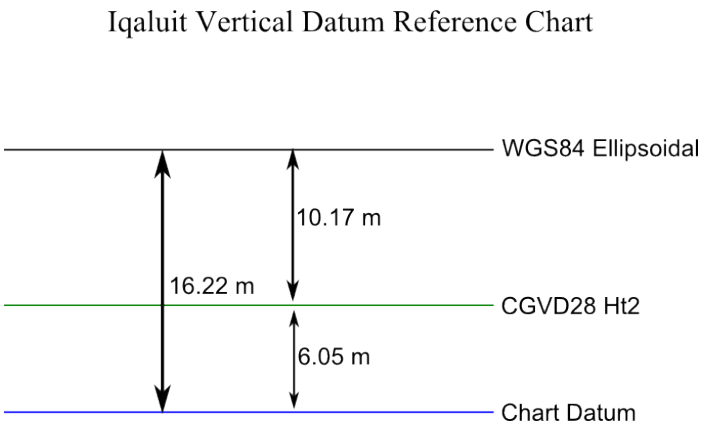

Figure 3.9: The vertical datums used in this paper. The original elevations were recorded in reference to the Ellipsoid, but were subsequently converted to Orthometric Elevations using the separation value from the Ht2.0 model for Canada. Chart Datum refers to LLWLT and is 6.05 m below mean sea level.

A digital elevation model (DEM) was used in conjunction with the coastal surveys. The DEM was provided by Natural Resources Canada (courtesy of Paul Budkewitsch), and was created to facilitate geoscience mapping and research in the area. It is a product of stereo pair photogrammetry using overlapping Worldview 2 satellite imagery. The DEM approaches the accuracy and resolution of LiDAR (Light Detection And Ranging) scanning airborne altimetry used in hazard studies elsewhere (Webster et al., 2004). Unfortunately, the imagery was captured at approximately mid tide, and as a result much of the intertidal area was obscured by water, precluding DEM coverage of the flats. Transects were surveyed with RTK-GPS at roughly 50 m spacing alongshore in order to extend the DEM into the intertidal. Coincident points (where GPS points overlap pixels of the DEM) were used to assess the relative accuracy of the elevations taken from the DEM (Fig. 3.10). Using the GPS points as reference the standard error was 0.4 m, but with some errors as large as 9 m. Larger errors occurred near the base of buildings as artifacts of the method employed in creating the DEM, but open-area elevations were much less prone to error. The accuracy of

the DEM is assessed to be ±1 m.

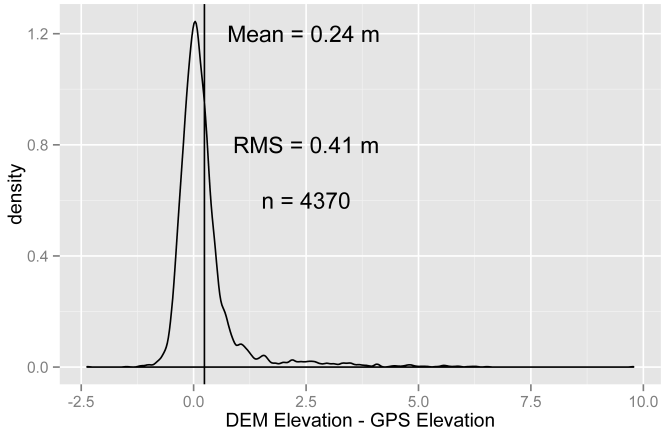

Figure 3.10: A selection of topographic survey points (n=4370) near the coast that were coincident with pixels of the DEM are used to assess the accuracy of the DEM. The differencing shows the DEM to be on average slightly lower in elevation than the GPS points (0.24 m below). In general the two sets of elevation points agree with one another to about 0.4 m.

Following field collection of points within the intertidal and nearshore (n = 89258), a tension splined interpolation method was employed within ArcGIS to build a continuous elevation surface. This method used a tension parameter as input (40 was used here), which is a dimensionless relative value representing the 'flatness' of the resulting interpolated surface (Mitasovä & Mitas, 1993). This allowed the modelling of smooth surfaces to be performed while still maintaining close alignment to the original GPS point elevations, a characteristic that was desirable for natural surface interpolation (Mitasovä & Drake, 2004). Following this the two surfaces (the NRCan topographic DEM and the coastal survey DEM) were integrated. Where they overlap the more accurate GPS-derived surface was used.

3.4.2 Infrastructure

Coastal infrastructure was divided into six categories: residential, commercial, municipal, cultural, federal, and subsistence. Residential includes housing near the coast. Commercial property near the coast includes the North Mart (grocery store) and the Grind and Brew Cafe. Municipal infrastructure includes the two pumping stations, as well as the sewage dam, road/culvert elevations, and the old territorial courthouse (now owned by the city). Cultural infrastructure refers to municipal buildings that are culturally significant including the Unikkaarvik visitor's centre, the museum, and the Hudson's Bay Company buildings on Apex Beach. Federal property includes the Coast Guard and the DFO buildings. Finally, subsistence infrastructure describes the sheds and sea cans (re-purposed shipping containers) used by local country food harvesters, who are organized under the Amarok Hunters & Trappers Association.

Infrastructure elevations were collected using RTK-GPS on key infrastructure as determined by this classification. Where the building was raised above ground elevation on piles (common in Iqaluit) we collected both ground and foundation elevation points. Piles are driven into the permafrost and are built on, which means flooding would have no direct impact on them, unless currents, waves, or ice impacted them during the high water event. Where the two elevations were equivalent, only one type of elevation was collected (Fig. 3.11A). For key infrastructure such as the courthouse or the pumping stations, elevations were generally taken on the corner of the building facing the coast. Some categories, such as the subsistence infrastructure or the roadbed elevations, include many points covering the range of elevations for that type of infrastructure along the length of the coastline.

The developed waterfront areas in Iqaluit and Apex were divided into two planning zones according to specifications in the Iqaluit general plan (City of Iqaluit, 2010). They are determined by horizontal distances of 30.5 m and 75 m from Higher High

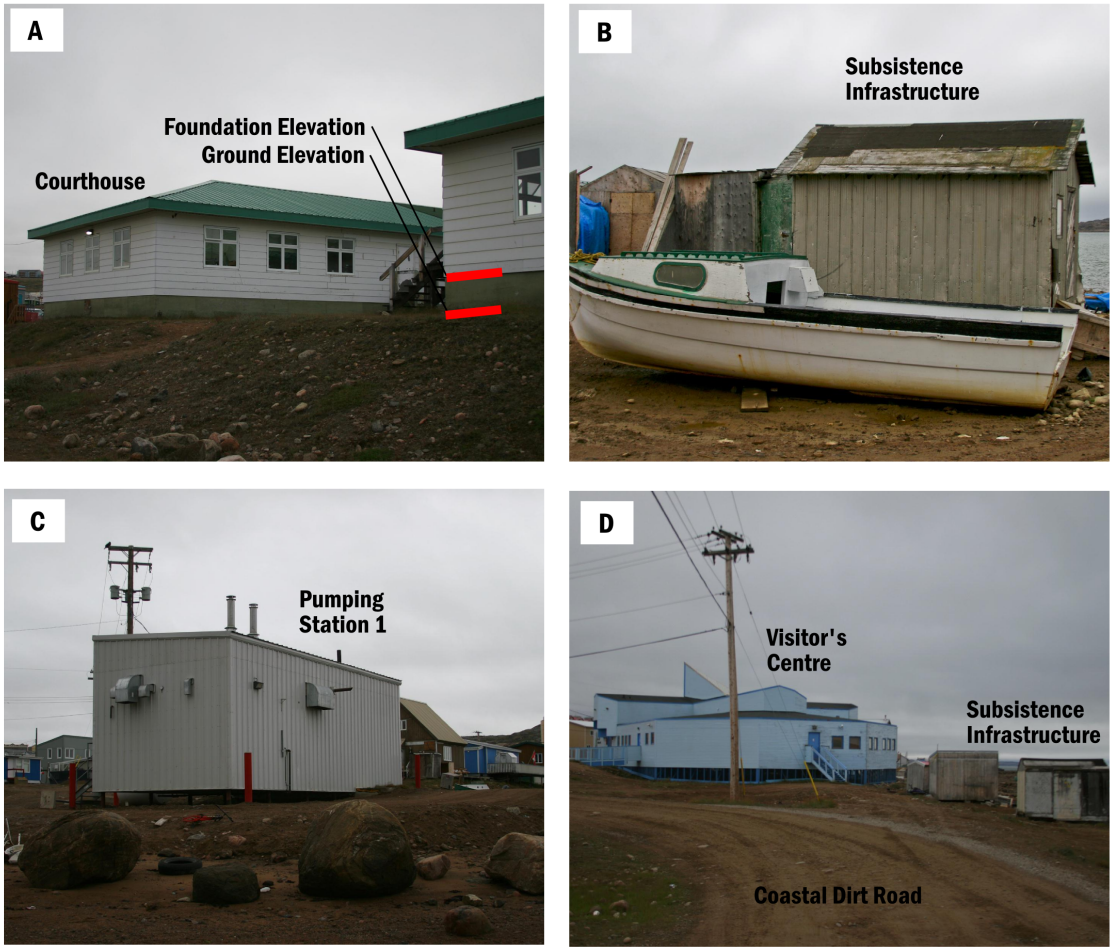

Figure 3.11: Examples of the different types of coastal infrastructure on the Iqaluit waterfront. (A) The territorial courthouse building sitting on pillars and graded land near the coast. (B) Subsistence infrastructure near the coast. This type varies from makeshift wood shacks to re-purposed 'sea cans' (old shipping containers). (C) The municipal pumping station located on the western end of the city. (D) The Unikkaarvik visitor's centre (blue building) sitting on the main waterfront amidst subsistence infrastructure. In the foreground is the coastal dirt access road running along the waterfront.

Water Large Tide (HHWLT). The first is designated as regulated "open space", and the second is a rough delineation of the coastal planning zone (named the "Sijjaanga district" in the general plan). This zone includes the major commercial and transportation infrastructure found near the coast. In order to quantify flood hazard for

Table 3.1: Available climate data for the Iqaluit area. Two of the stations are located at the airport, which is at the head of the inlet and near sea level. The other is from the climate station located on the road to Apex, which is above 100 m elevation.

Station ID	Hourly data	Daily data
2402590	1953-01-01 - 2011-05-11	1946-01-01 - 2008-07-31
2402591	2008-07-03 - 2011-05-11	2008-07-01 - 2011-05-31
2402592	2004-12-16 - 2012-01-01	2004-05-01 - 2011-05-31
2402594	NA	1997-04-01 - 2007-11-30

this study, an estimate of 75 m inland (which includes the infrastructure mentioned in the general plan) was used. Having the high water level and infrastructure data combined in a GIS allowed a quantification of change for the projected sea-level change in two ways: 1) by giving the amount of land lost in the two planning zones, and 2) giving a percentage of infrastructure affected. The use of these planning zones is meant to help city planners and administrators in defining areas of risk and help plan further coastal development.

3.4.3 Climate and weather

Environment Canada climate records near Iqaluit have been collected since 1946, with hourly measurements since 1953 (Table 3.1). Additional data have more recently been collected by the climate station located between Iqaluit and Apex. Reliable climate and weather information is therefore available in Iqaluit for the last 60 years. This allows the hindcasting of storms and estimation of wind events capable of producing waves that might affect coastal infrastructure.

Sea ice plays an integral part in defining the coastal morphology and the vulnerability of the community. McCann & Dale (1986) identified the break-up of sea ice occurring over a short period of time in the spring as the primary mover of sediment on the flats. Leech (1998) quantified this contribution at roughly 68,000 kg/km^2. It is evident that the timing of the freeze-up and break-up is largely dependent on local weather. The

longer the ice-free season, the more time hydrodynamic transport mechanisms have to rework sediment at the coast (Dale et al., 2002). The response of the morphology to shifts in season length is impossible to quantify adequately without more observations. No regional sea-ice trend analysis currently exists. Previous work on sea ice in the area has focused exclusively on the dynamics of break-up. This is a critical time for considering the sediment dynamics of the tidal flats (McCann & Dale, 1986; Leech, 1998). We know less, however, about the process of freeze-up. Community members generally describe it as a period of change when the sea ice 'sets up' on the coast. During this time, access is extremely difficult due to the thin ice and constant shifting in the intertidal zone over the tidal flats. In this study we rely on a single season of observations (November 2011) when the freeze-up was observed and photographed.

Part of the process of freeze-up involves forming the ice foot for the winter. The ice foot is the area near the high-tide line where sea ice is permanently frozen to the substrate, and where subsequent inundation during high spring tides builds thickness further and contributes to development of a flat ice terrace. The edge of the ice foot where it meets with mobile intertidal ice acts as a hinge point, and is the site of sea-ice ride-up and pile-up (Fig. 3.12). The ice foot along the main Iqaluit waterfront was surveyed in February 2011 using RTK-GPS to obtain elevations on the surface of the ice. These points were directly over transects surveyed in the summer. This allowed an estimation of ice foot thickness and elevation for the 2011 ice season.

We used two datasets to calculate possible trend in the dates of freeze-up and break-up. The two datasets used were the Canadian Ice Service Digital Archive (CISDA) (CIS, 2006) and the combined microwave sensor freeze-up/breakup analysis archive from the NASA Goddard Space Flight Center (Markus et al., 2009). The microwave sensor data directly measures the onset and completion of freeze-up/break-up by detecting water on the surface. The CISDA records report sea-ice concentrations as

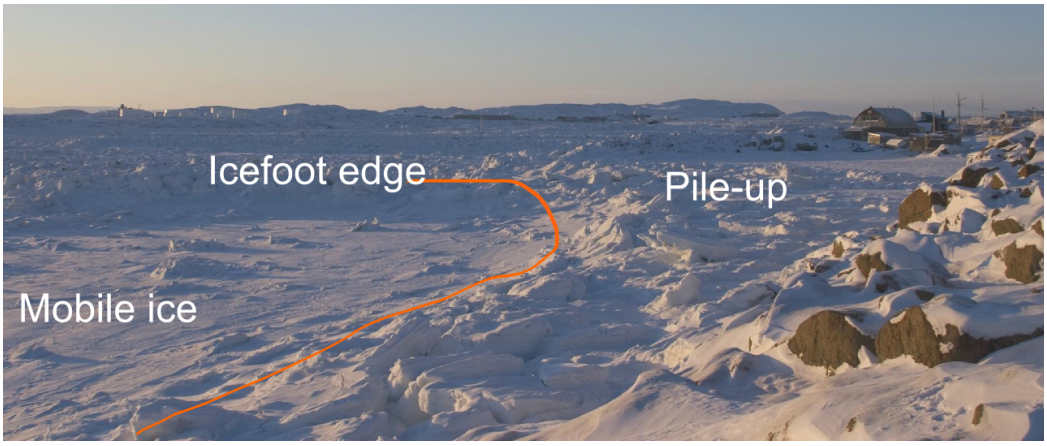

Figure 3.12: The icefoot establishes itself about half way down the beachface, and is evident by the change from a relatively smooth surface to a chaotic arrangement of ice blocks.

a fraction of 10 (10 being 100% concentration). We defined the timing of freeze-up and break-up following Gagnon & Gough (2010) as the point at which concentration permanently crosses 7/10 for that year.

The presence of a trend was determined using the non-parametric Mann-Kendall test for monotonic trends (Helsel & Hirsch, 1992), as used in sea-ice trend analysis elsewhere (Laidler et al., 2008; Gagnon & Gough, 2010). This test only detects the presence of a trend in the data, but the magnitude of that trend can be estimated using the Theil-Sen approach described in Gagnon & Gough (2010). This method simply reports the median of a distribution composed of slopes between every pair of points within the data moving forward in time.

There is difficulty in determining sea ice freeze-up/break-up trends due to the length and variability of these events. The CISDA dataset goes back to 1969, where as the NASA dataset goes back to 1979. These records capture a time of relative cooling in this area in the 1980s and 1990s, but since then warming has progressed rapidly. To add to the two datasets we also considered ice thickness from a time series initiated by Transport Canada in 1959, but now maintained by the Canadian Ice Service.

Thickness surveys were conducted multiple times during the ice season. By comparing this record to the ice season length records, as well as the winter temperature data, we can better assess the validity and potential impacts of changing sea ice dynamics.

3.4.4 Waves and run-up

Field work in 2010 and 2011 contributed information on incident waves and the configuration of sea ice. We collected wave data using seabed mounted pressure sensors (Fig. 3.13) and an acoustic doppler current profiler. The pressure sensors were located in the intertidal, and recorded wave information every 30 minutes. They were deployed from August to October of 2010 and 2011 in various positions in the intertidal zone. A total of six deployments of Tide and Wave Recorder (TWR) pressure sensors (RBR TWR-2050 instruments) and three deployments of a Nortek Aquadopp©1.0 MHz Acoustic Doppler Current Profiler (ADCP) were used to measure waves and currents. They spanned short intervals during the late summer and autumn in 2010 and 2011. The TWRs recorded simultaneous measurements of wave characteristics and tidal water levels to a published accuracy of ± 0.005 m (Gibbons et al., 2005). The ADCP recorded wave and current velocity profiles in three locations: one on the flats, and two in the nearshore channels. The velocity measurements have a published instrument uncertainty of 10% of the averaged ping velocity for each cell (Nortek, 2005).

Wave hindcasting for possible run-up heights was done using a combination of the climate records and the simple empirical wind-wave relationships presented in Hurdle & Stive (1989). The period of highest prolonged southeast winds occurred on 22 Sept 1960 when an average wind speed of 97 km/h occurred over a 3 hour period. The formulae derived in Hurdle & Stive (1989) are revised from SPM (1984), and are shown below:

Figure 3.13: The pressure sensors were RBR Tide and Wave Recorders. They were moored to the flats on small grates.

$$\tilde{H}_{rev} = 0.25 tanh(0.6\tilde{d}^{0.75}) tanh^{0.5}\left(\frac{4.3 \times 10^{-5}\tilde{F}}{tanh^2(0.6\tilde{d}^{0.75})}\right) \tag{3.1}$$

$$\tilde{T}_{rev} = 8.3 tanh(0.76\tilde{d}^{0.375}) tanh^{\frac{1}{3}}\left(\frac{4.1 \times 10^{-5}\tilde{F}}{tanh^3(0.76\tilde{d}^{0.375})}\right) \tag{3.2}$$

Where $\tilde{H}_{rev}$ is the dimensionless significant wave height (H_s) and $\tilde{T}_{rev}$ is the dimensionless spectral peak period (T_m). Conversion to dimensioned quantities is done by multiplying by a factor:

$\frac{U_a}{g}$

for spectral peak period, and:

$\frac{U_a^2}{g}$

for significant wave height. U_a represents the corrected wind-stress factor calculated according to SPM (1984) from the 10 m anemometer winds reported at the Iqaluit climate station.

3.4.5 Water levels and sea-level rise

Water-level records are available in two forms: the historical tide-gauge records provided by the Canadian Hydrographic Service (CHS), and the pressure sensor water levels recorded in 2010 and 2011 using the TWR instruments described above. The

CHS record is an irregular time series with 28 198 hours of data between 1963 and 1977 (Fig. 3.14). This means that in the 14 year span for which data exists, 77% are missing, averaging data for 84 days/year. The field data include 2 670 hours of data in the summer of 2010 and 2011 (Fig. 3.14). The data are sparse, and have a seasonal bias (the vast majority of the data were collected in the fall, see Fig. 3.14).

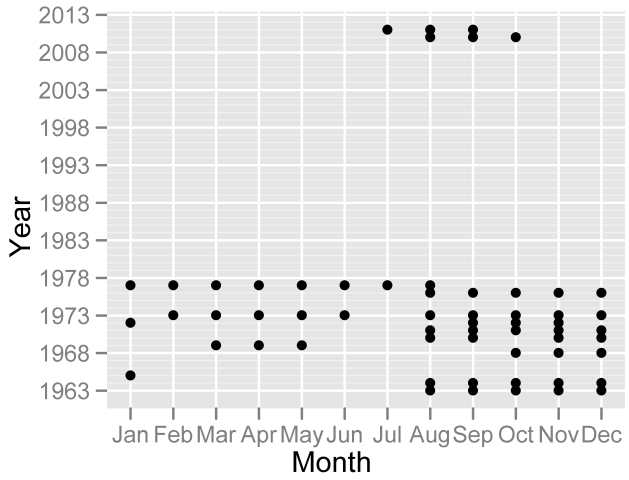

Figure 3.14: The tide gauge record ran intermittently between 1963 and 1977. The instrument data from 2010 and 2011 are shown at the top

Two types of record were surveyed with GPS to estimate past extreme water levels in the field:

- water levels taken from a photograph of a flood event in 2003
- storm swash limit lines preserved at various places within the inlet

A photograph from a flooding event in October of 2003 showed the water line against a boulder on the shore which allowed subsequent surveying of its elevation (Fig. 3.1, boulder surveyed is at centre of photo directly below red shed). Surveying past storm swash lines can provide additional information on high water levels (in this case including wave runup) in the area. Near Iqaluit, these storm swash lines are found

scattered around the outer limits of the inlet on undisturbed beaches (Fig. 3.15). Surveying elevations on these swash limits provides undated estimates of extreme high water limits. No correlation, however, can be made between two swash limits separated in space.

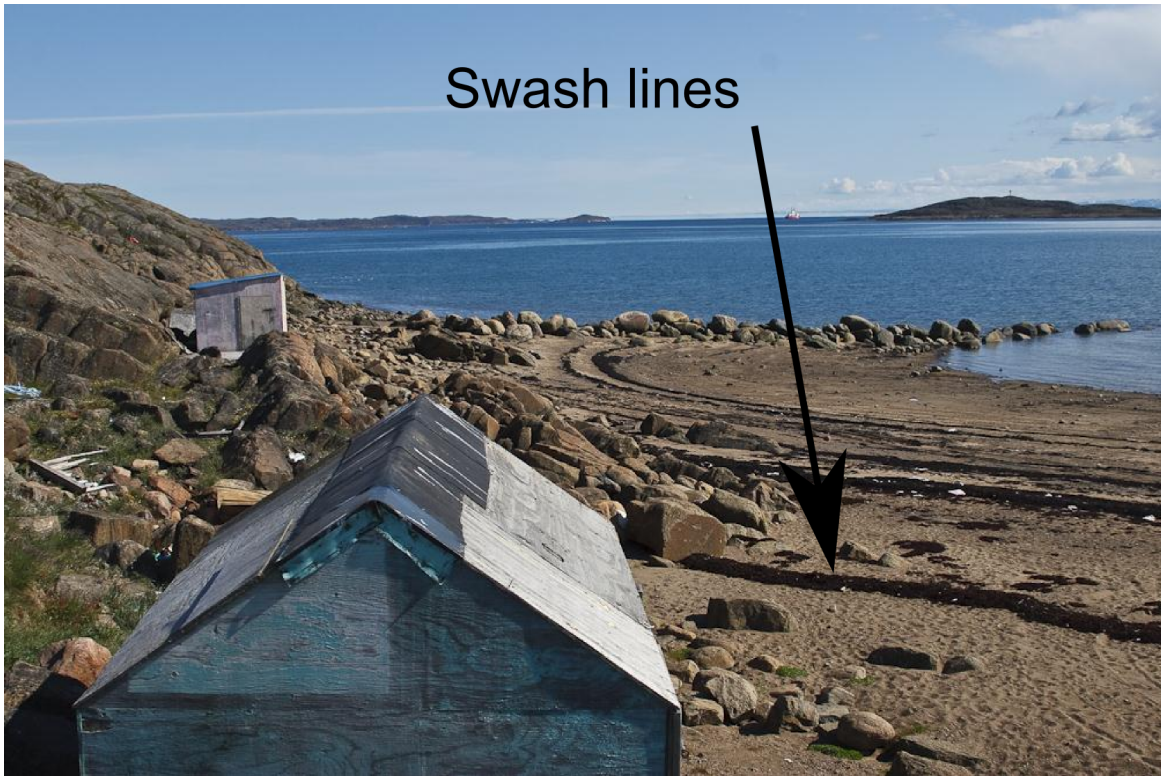

Figure 3.15: Storm swash lines on the beach

Aside from the uncertainty inherent in estimates of future global sea-level rise, projections for Iqaluit are also complicated by uncertainty in the vertical motion. A continuous GPS station has been operating for three years now, so estimates of the vertical motion and therefore also of sea-level change will improve over the coming few years. The most recent projections of 90 year (2010-2100) sea-level rise at Iqaluit have a range of 0 - 70 cm (James et al., 2011). New data on vertical motion indicates slight uplift continuing in Iqaluit, which will likely lower the upper limit of this estimate (J. Henton, pers. comm. 2012).

3.5 Results

3.5.1 Iqaluit topography and waterfront exposure

The coast is roughly divided into two classes: beaches and bedrock slopes. Development has been carried out almost exclusively on the low slope beaches between rock headlands and outcrop (Fig. 3.16). The main waterfront of the city is a large bay-head beach. Confined to the north side of the inlet, this is now fully backed by coastal infrastructure. The Apex side is different, where the beach is less than 500 m long and located adjacent to the outlet of the Apex River. At this site, there is only one residence amid a cluster of old Hudson Bay Company buildings, which were in use from 1949 to 1971.

Of all the coastal infrastructure surveyed, the subsistence structures are the most abundant, both in number and in extent. Key infrastructure facilities, including municipal utility buildings and residential buildings, are located in the backshore of Iqaluit's main beach, but the subsistence infrastructure sits on top of the beach crest along the entire length of the waterfront. A particular focus is around the dredged basin behind the main breakwater. This acts as a small boat launching area. Most of the subsistence structures are close to the spring high tide water line between the city and the sea.

Figure 3.17 maps out crucial infrastructure within the coastal zone of the three primary study areas: the Iqaluit waterfront, Apex beach, and Cemetery Beach. Excluding the fuel transfer facility, causeway, and dump, the urban waterfront of Iqaluit begins at the head of the inlet, where 'Airport Creek' flows onto the tidal flats just east of the sewage dam. The sewage lagoon is retained by two dams with limited freeboard under extreme tide conditions. East of this is the sealift barge landing facility and the Canadian Coast Guard property. Further along is a boat yard, housing and

Figure 3.16: Coastal development on Iqaluit's shoreline. Note the lack of obvious backshore, with development on the beach face.

subsistence infrastructure on the west side of Pumping Station 1. From this point, the unpaved coastal access land runs east along the backshore, with subsistence infrastructure on the seaward side, to the Elders Centre and the North Mart shopping complex. The coastal access land then continues eastward between the courthouse and the subsistence infrastructure on the beach crest, as far as the Visitors Centre. Sinaa Street continues east landward of the Visitors Centre, the museum, and the Amarok building, which all have subsistence infrastructure on their seaward side. Directly beyond this is the small craft launching area at the foot of the main breakwater. Across Sinaa Street is the Grind and Brew restaurant with Pumping Station 2 behind it. There are several residential properties in this area, including beachfront homes, multi-family structures, and a row of townhouses across from the breakwater and

boat launch. The road in this area has been flooded at extreme high tides. Moving on to the southeast into the Cemetery Beach area, a small pocket beach backed by a single-family home, lies between the cemetery and the breakwater. On Cemetery Beach itself, there is some subsistence infrastructure and the seaward edge of the cemetery, which is reported to have been flooded in the past (Shirley, 2005). The coast between Cemetery Beach and Apex is bold and rocky, with all structures located on high ground. Apex Beach is less than 500 m long, with four former Hudson's Bay Company buildings and a residence on the crest of the beach. The Apex River discharges to the flats at the east end of Apex Beach. The rest of the Apex coast is a steep bedrock slope or terraced sand gravel slopes.

Development on the Iqaluit waterfront occurs primarily in the area of the bayhead beaches. The extent of these beaches is defined by the distribution of the bedrock outcrop. There is a general pattern of coastal use on these stretches of beach that varies somewhat over their span, but is fairly consistent. Near the crest of the beach, subsistence infrastructure is scattered amongst small boats and equipment. Immediately landward of this, and in some cases mixed amongst it, are larger buildings such as residences, municipal, or commercial buildings.

The combination of extensive development and a low-slope regressive beach backshore on abandoned raised-beach deposits makes the measurement of beach crest elevation difficult. The backshore is generally a low-slope, poorly sorted, sand cobble veneer over glacio-fluvial sediments. Estimated beach crest elevations throughout the study area vary from beach to beach, largely as a function of exposure. The lowest crest elevations are found on the Iqaluit waterfront (5.1 m), with high crest levels at Cemetery Beach (6.1 m) and Apex Beach (6.2 m) relative the CGVD28 datum.

Backshore slopes are fairly consistent throughout, except where higher-relief bedrock is exposed. The mean slope of all the backshore transects (13) is 3.5°(Fig. 3.19). This

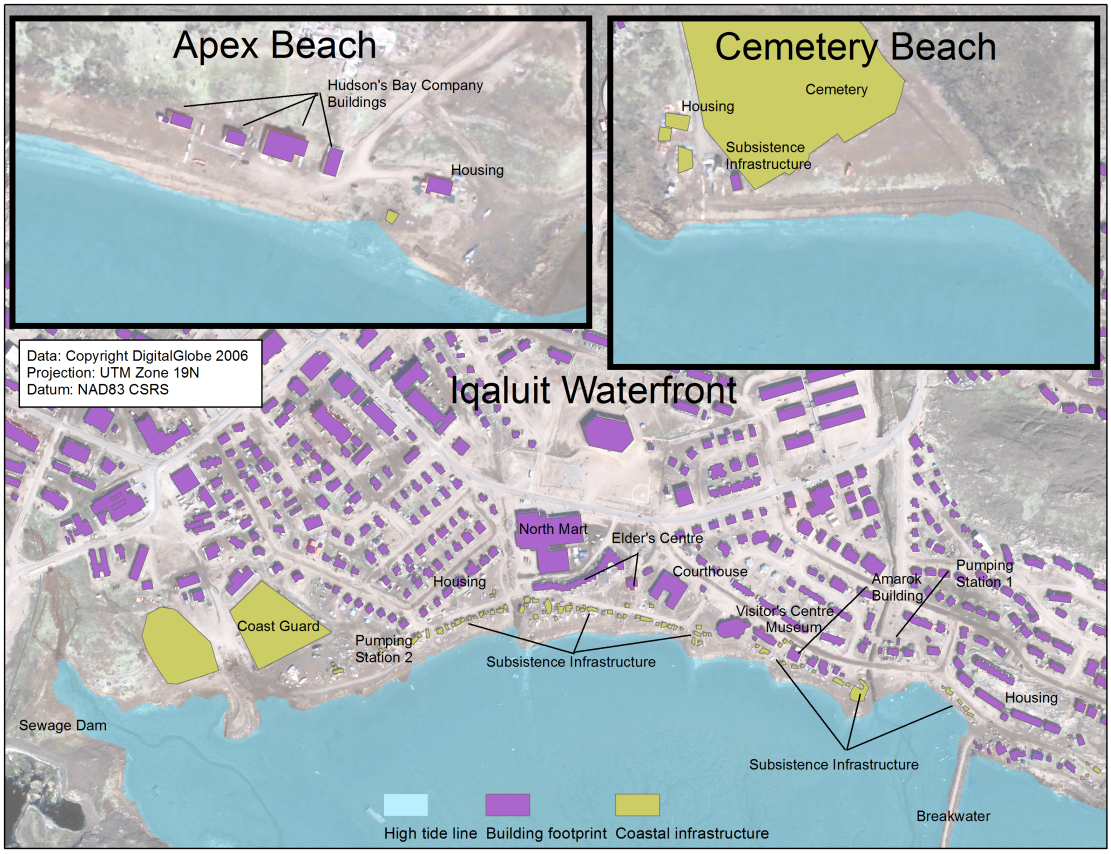

Figure 3.17: Detailed map showing the key infrastructure layout for the three main sections of coast in Iqaluit and Apex. Each section follows the insets labeled in fig. 3.4 and fig. 3.7. In general, subsistence infrastructure inhabits the beach berm of the main beaches, with larger infrastructure directly landward. There is little natural differentiation on the coast to divide the various uses.

translates to a 1:17 slope, where a 1 m rise in water level would inundate approximately 17 m horizontally into the backshore. This has implications for flood hazard projections, especially with a strong onshore wind that could drive additional wave runup.

Measured infrastructure foundation elevations in the waterfront zone range between 4.25 m and 10.13 m elevation. Subsistence infrastructure is predominantly located at the lowest elevations, closest to the water on the uppermost part of the beach. However, some structures are located as high as 8 m. Residential buildings are on

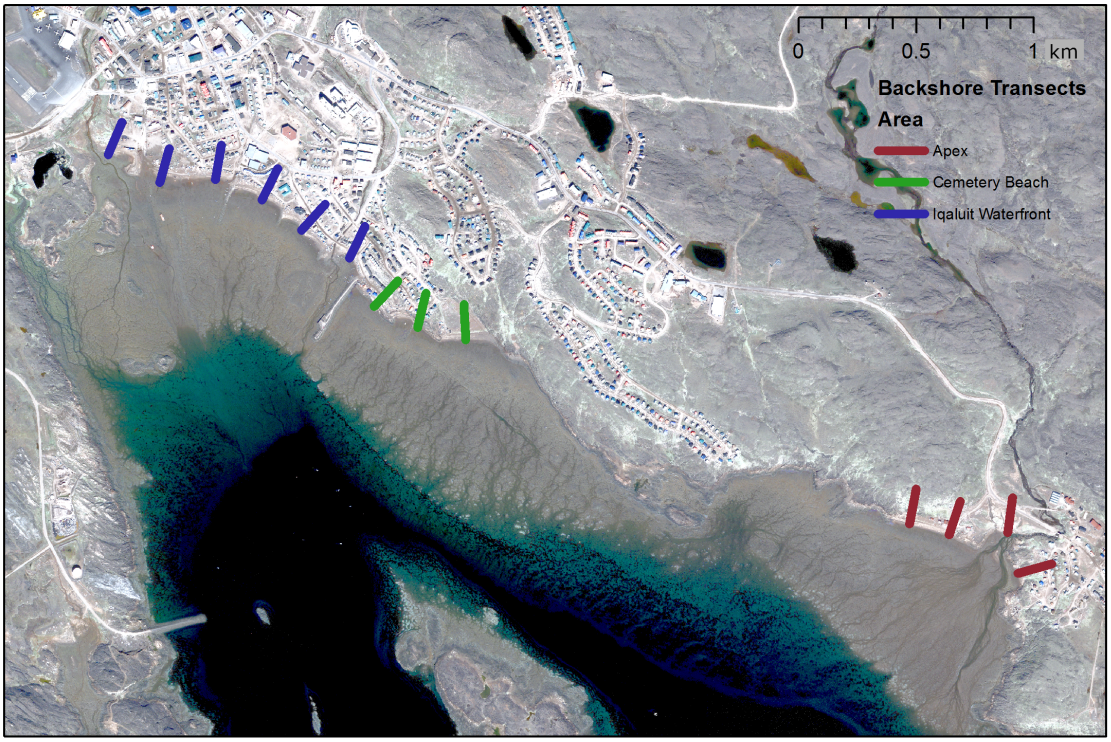

Figure 3.18: Grouping of backshore transects.

average at much higher elevations, although the lowest is a house at 5.6 m. Subsistence infrastructure is consistently found at the lowest elevations, and closest to the waterline (Fig. 3.20).

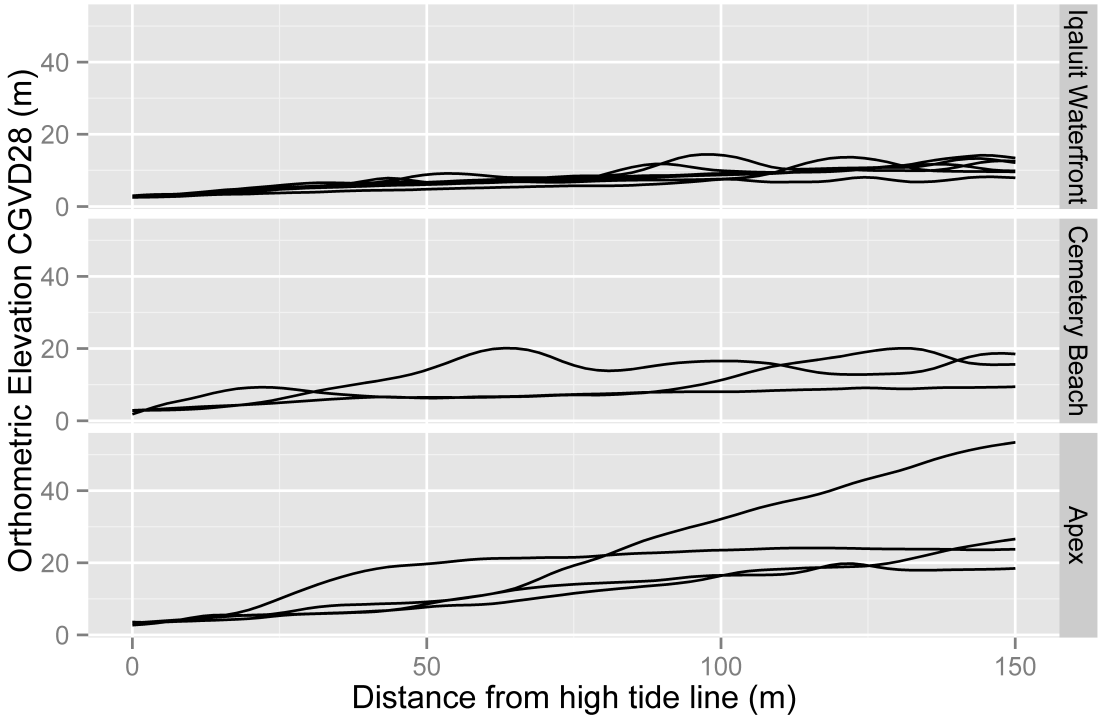

Figure 3.19: Backshore transects showing elevations 150 m back from the high tide shoreline. Steep slopes are where bedrock truncates the sandy backshore. Vertical exaggeration of 1.8.

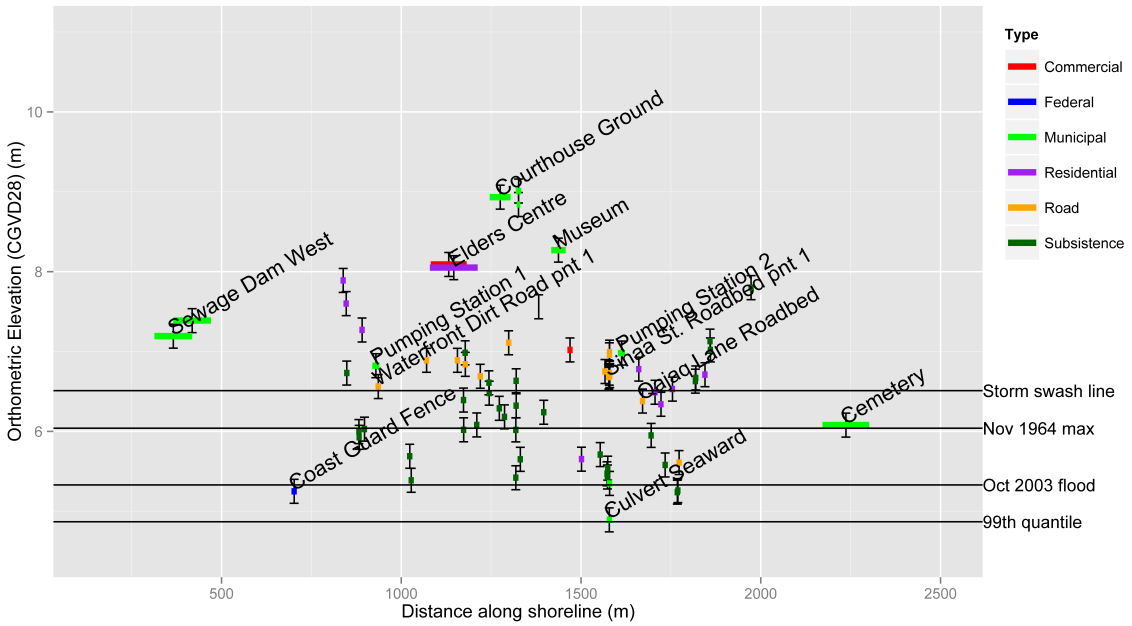

Figure 3.20: Elevation values for key infrastructure (text) and for all surveyed infrastructure points (lines) along the Iqaluit waterfront. The 99th percentile water level is defined as the 99th percentile level of the water level dataset described in Figure 3.14

3.5.2 Coastal hazards

3.5.2.1 Sea ice hazards

Using two datasets (the CISDA and NSIDC archives) that record the day of the time of freeze-up and break-up since 1969 and 1979 respectively, trends appear that show the open-water season to be lengthening within Frobisher Bay. Results of the sea ice freeze-up and break-up timing analysis are shown in Table 3.2, which shows the ice-free period to be lengthening by 1.58 days/year since 1969 (99% confidence). It is unclear whether this is happening equally on both ends of the open-water season. The dates of break-up and freeze-up as defined in the NASA data (Goddard Flight Centre) show comparable trends, toward earlier break-up (-0.55 days/year) and later freeze-up (±0.48 days/year). On the other hand, using the definition of break-up and freeze-up for the CISDA data results in trends of -0.95 days/year (breakup) and ±0.54 days/year (freeze-up) (See Fig. 3.21). Despite limitations imposed by a lack of satellite coverage prior to 1979, as well as ambiguity in the methods used to define the onset of breakup or freeze-up, this analysis provides evidence that Frobisher Bay is indeed following the rest of the Arctic in experiencing a decline in the length of the ice season.

Type	CISDA trend	NSIDC trend
Breakup	-0.95 **	-0.55 ***
Freezeup	0.54 **	0.49
Ice free period length	1.58 ***	1.05 ***

Table 3.2: Trends in two datasets for Frobisher Bay. Significance levels, taken from the Kendall Tau Rank Correlation Coefficient are shown by *** (99%) and ** (95%). Negative values show breakup earlier in the year (negative julian days), and positive values show freezeup later in the year (positive julian days). Positive length shows the lengthening of the ice free period.

Records of ice thickness indicate a trend to thinner ice. Fig. 3.22 shows a time series of maximum measured ice thickness every year within Koojesse Inlet from 1959 to

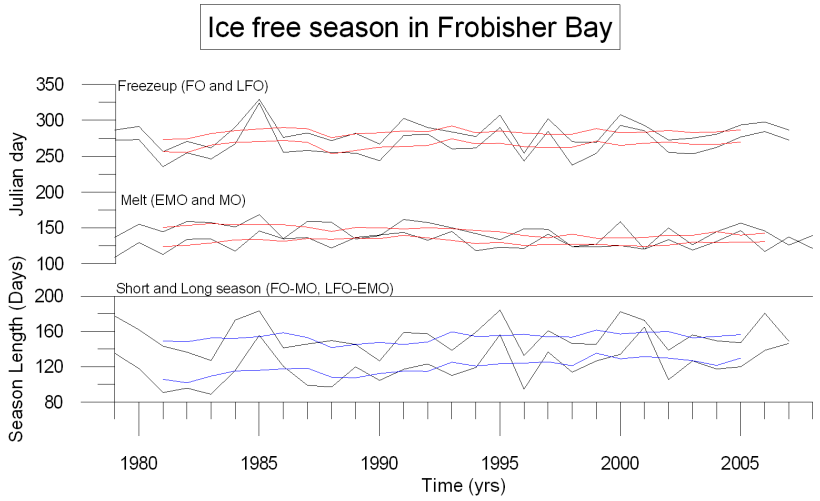

Figure 3.21: Sea-ice trend data from the NSIDC database. Annual data (red and blue lines show 5 year running means). The Freezeup graph shows the initiation of freezeup (lower line) and the last signs of freezeup (upper line). The melt graph shows early melt onset (lower line) and melt onset (upper line). The short and long season graph shows the two open-water seasons derived from subtracting late freezeup from early melt onset (short season) and freezeup onset from melt onset (long season).

2010. It shows a marked turn toward thinner ice in the early 1990s, with the thinnest maximum ice thickness measured in 2004. It is likely that this trend follows roughly the winter temperature trends (Fig. 3.22), but more detailed analysis might provide an estimate of the magnitude of this correlation. Combined, these two datasets (ice season length and ice thickness) provide ample evidence that local ice conditions have changed in the last half of the twentieth century, likely in response to larger scale climatic shifts measured on a circumpolar scale.

The large-scale effects can act in unexpected ways. Following break-up in 2012, significant amounts of multi-year sea ice (as much as 6 to 7 m thick) drifted in from Baffin Bay and grounded on the Iqaluit tidal flats. This caused problems with navigation within the bay. Changing Arctic sea ice regimes are releasing multi-year ice more often, and this could lead to an increased chance of large amounts of sea ice moving in during the open-water season in the decades to come.

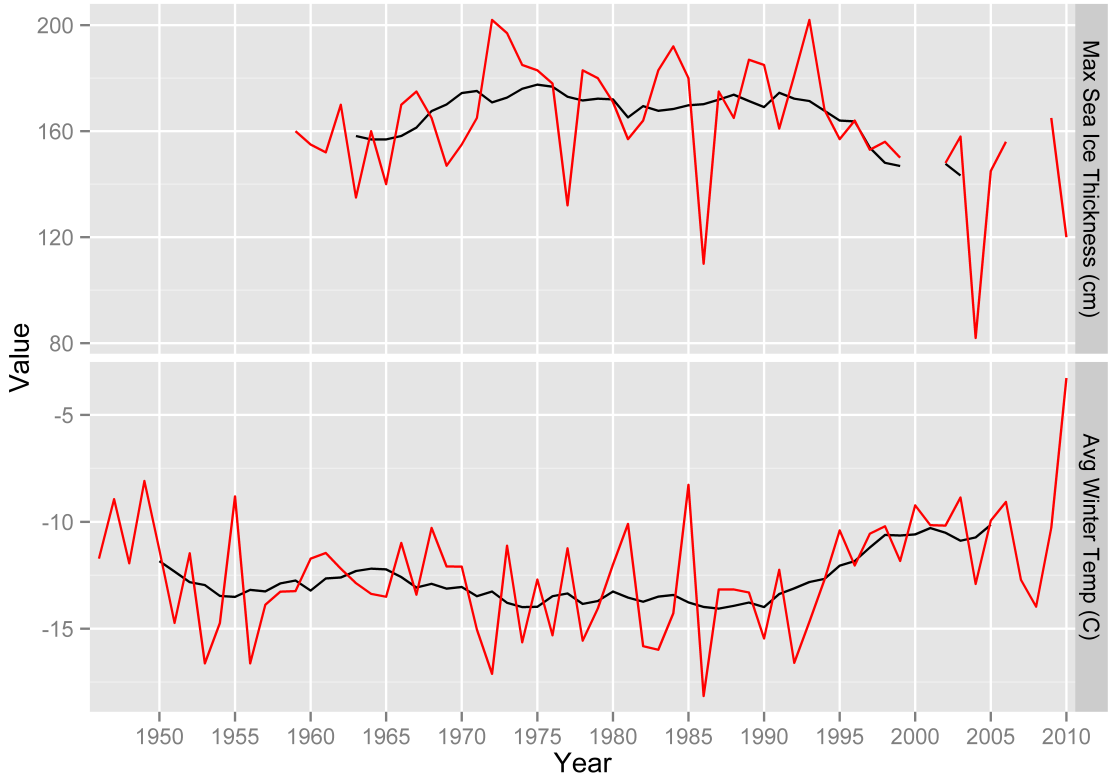

Figure 3.22: Ice thickness in cm collected by Transport Canada

Observations from the 2011 freeze-up suggest that early winter sea-ice ride-up and pile-up are widespread occurrences throughout the study area. Ride-up involves onshore incursion of an ice sheet that remains largely intact, whereas pile-up occurs when the ice fractures and builds up into a ridge of broken ice (Forbes & Taylor, 1994). In the 2011 freeze-up period, pile-up affected infrastructure in only one area near the base of the breakwater. In this case, ice pile-up exceeded 2 m in height, and was composed of blocks reaching 2 by 2 m dimensions and 0.75 m thickness. This ice remains mobile well into the freeze-up transition due to the diurnal settling of shifted ice pans onto the boulder mounds on the flats, creating a complex of interlocked but mobile ice. Onshore winds, combined with high spring tides, are known to produce substantial ice pile-up in other regions (Forbes & Taylor, 1994). Further field research, either by

interviewing community residents or from further observations, is needed to better describe the complex dynamics of the freeze-up period. Though no evidence now exists that points pile-up and ride-up events as being a significant problem for coastal infrastructure, this does not negate the potential for the phenomenon in the future. Most important in this situation is increased likelihood resulting from the push of freeze-up into the fall storm season caused by lengthening open water seasons, putting more onshore wind energy onto mobile ice conditions (Fig. 3.23).

Examples of ice pile-up and ride-up were widespread throughout the coast in November 2011, but the most significant occurrences were along a specific section of coast near the base of the breakwater where a revetment has been installed. Along the beaches, the establishment of the ice foot about halfway down the beach face restricted ice pile-up to the lower beach. In the section of the coast with revetments there was evidence both for thicker ice pans directly offshore, as well as more significant pile-up during spring-tide conditions (Fig. 3.24). Based on a single season, these results are not robust. However, a possible explanation for this localized effect might be the artificial steepening of the shoreline. The icefoot seems to be established on a depth-dependent basis: along the coast in 2011 the icefoot edge was at a consistent elevation of 3.5 - 4.0 m, presumably based on the relative inundation and exposure times for the tidal period during which the temperatures fell low enough to initiate the freeze-up process. On a low-slope coastline, where the beach extends out onto the tidal flat, the icefoot established near the high tide line is far enough down the beachface to negate frequent sea ice pile-up onto the upper crest area of the beach. However, where the coast has been artificially steepened by construction of revetments for shore protection, a narrow icefoot and deeper water close to the shore favour higher ice pile-up under appropriate ice, wind, and spring tide conditions. Due to the potential impacts and costs associated with sea ice pile-up, great care should

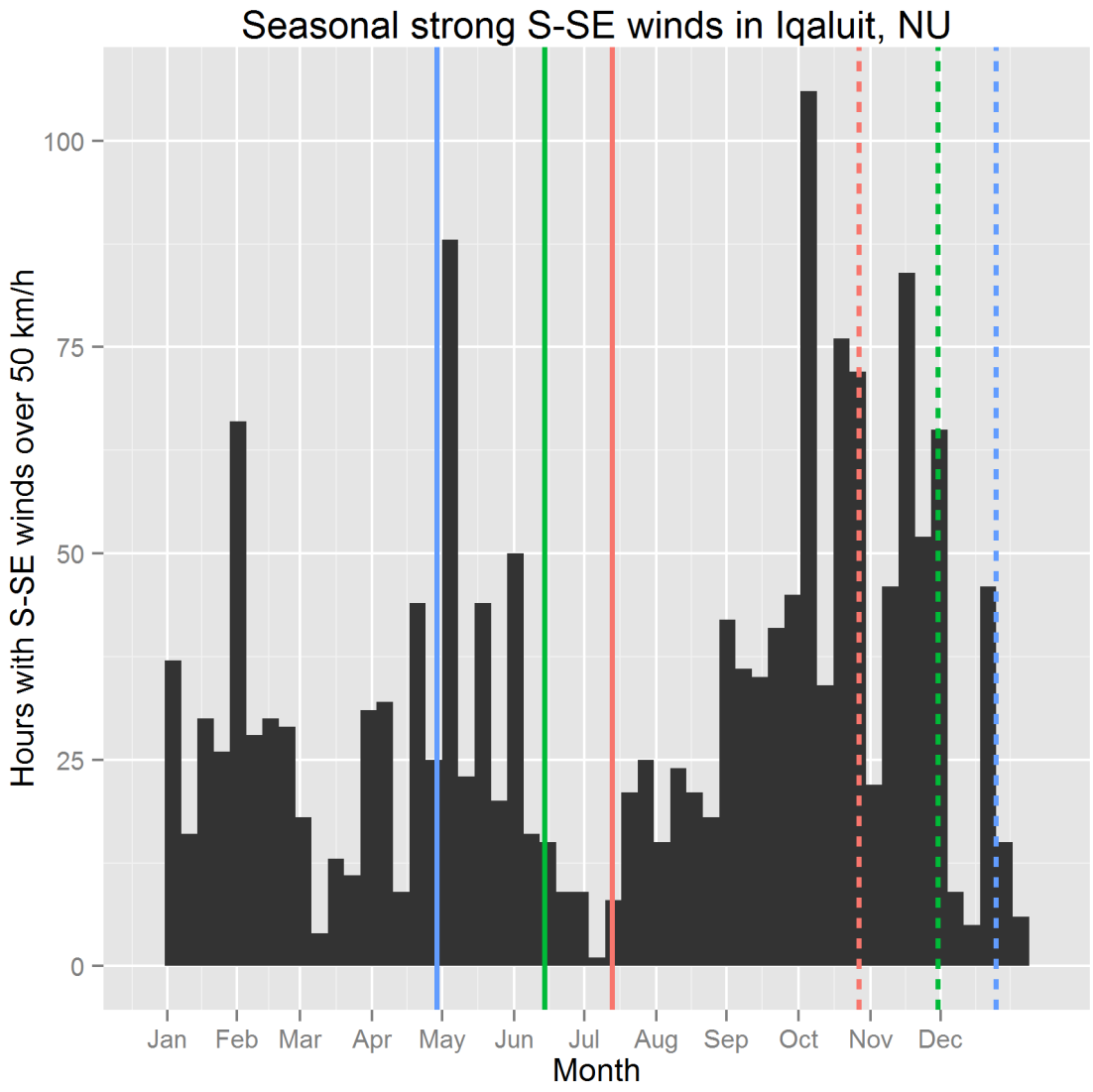

Figure 3.23: Weeks with observations of strong S-SE winds in Iqaluit. The y-axis shows observation counts extracted from the hourly observation data that exceeded 50 km/hr and were in the S-SE direction. The x-axis divides into bars showing the weeks of the year, labelled with months. The data show the dominance of strong S-SE winds in the fall storm season. The 2050 projection was derived from applying the breakup and freezeup trend reported in Table 3.2 to the 2013 dates out to 2050.

be taken to allow sufficient buffer areas behind any coastal areas that are steepened beyond the naturally set average (<1°).

Figure 3.24: Light onshore winds with large ice floes in the nearshore produced ice pile-up on the boat ramp near the main breakwater in November 2011. A front end loader spent the morning clearing the debris off the ramp, which was piled roughly 2-3 m high.

3.5.2.2 Flooding hazards and sea-level rise

There are three sources for historical high water levels: the tide-gauge record (Canadian Hydrographic Service), the instrumental record from 2010 and 2011 (this study), and the surveyed storm swash lines (this study). The 95th and 99th quantile water levels from the tide-gauge record are 4.00 m and 4.87 m CGVD28 respectively. The maximum level in the tide gauge record was 6.04 m on November 21, 1964. The range of elevations from surveyed storm lines (which do not necessarily record still-water levels) was from 5.16 m to 6.51 m. The surveyed level approximated from the October 2003 flood photograph was 5.33 m. A swash line found at the base of the Inuit head pipeline had an elevation of 5.66 m, and two other swash lines found further out Inuit Head were at 6.19 m and 6.06 m. The greatest elevation for swash lines on the outer shores of Long Island were at 6.48 m. Real-time corrections were unavailable for this survey, however, so a static post-processed point was used. This survey method is less accurate than the others, and so may represent a higher value than actually occurred.

Table 3.3: Type, elevation above mean sea level, and source of high water levels in Iqaluit.

Type	Elevation (m)	Source
95th quantile	4.00	tide gauge
99th quantile	4.87	tide gauge
max recorded	6.04	tide gauge
max instrumental	5.52	this study
Nov 2003 flood	5.33	photograph
cemetery beach	5.31	swash line
Inuit hd pipeline	5.66	swash line
Inuit hd station	6.06	swash line
Inuit hd station	6.19	swash line
Long Island	6.48	swash line
sewage lagoon	6.51	swash line

Lastly, swash lines surrounding the sewage lagoon at the head of the inlet were surveyed at 6.51 m, the highest elevation of all the swash lines. This is an interesting result, suggesting that the shape of the inlet may promote enhanced setup or runup at the head of the inlet, where the sewage lagoon is located.

Comparison of hindcast tidal water levels to the highest water levels recorded in the tide gauge record reveal discrepancies. Predicted water levels from the Canadian Hydrographic Service (CHS), based on a harmonic analysis of a subsection of the tide gauge record itself, have a maximum of 5.75 m, which is 0.29 m less than the maximum water level recorded. The WebTide Arctic model Collins et al. (2011) predicts a maximum tidal water level of 5.28 m. The macro-tidal conditions in Frobisher Bay, however, are known to create larger proportional errors in this model, and so accuracy is only said to be within 1 m. Using the CHS predicted water levels and the tide gauge record, residuals were assumed to be a product of storm surges, seicheing, or positional errors in the tide gauge occupation introduced by yearly installations.

The hazard maps show the extent of flooding from high water levels with the addition of a projected sea level rise of 0.7 m over 90 years. Lines of consecutively higher

water levels show a gradational pattern with no large incursions into backshore areas of lower elevation. Unlike many coastal beach systems where a defined storm ridge or dune line protects against periodic high water levels, the fairly even backshore slope in Iqaluit produces incremental incursions. Lack of a defined ridge, however, is evident in the proximity of infrastructure to spring tide levels (Fig. 3.26,3.27). With the addition of a rise in sea level of 0.7 m, usable land on the main coastline will decrease by 24458 m^2 representing 28% of the coastal "Open Space" and 14% of the coastal district land. Addition of projected sea level rise onto a repeated highest recorded water level would flood 46 of the 91 coastal structures (50%), and would flood 5 of the 61 municipal structures (8%) within the coastal district.

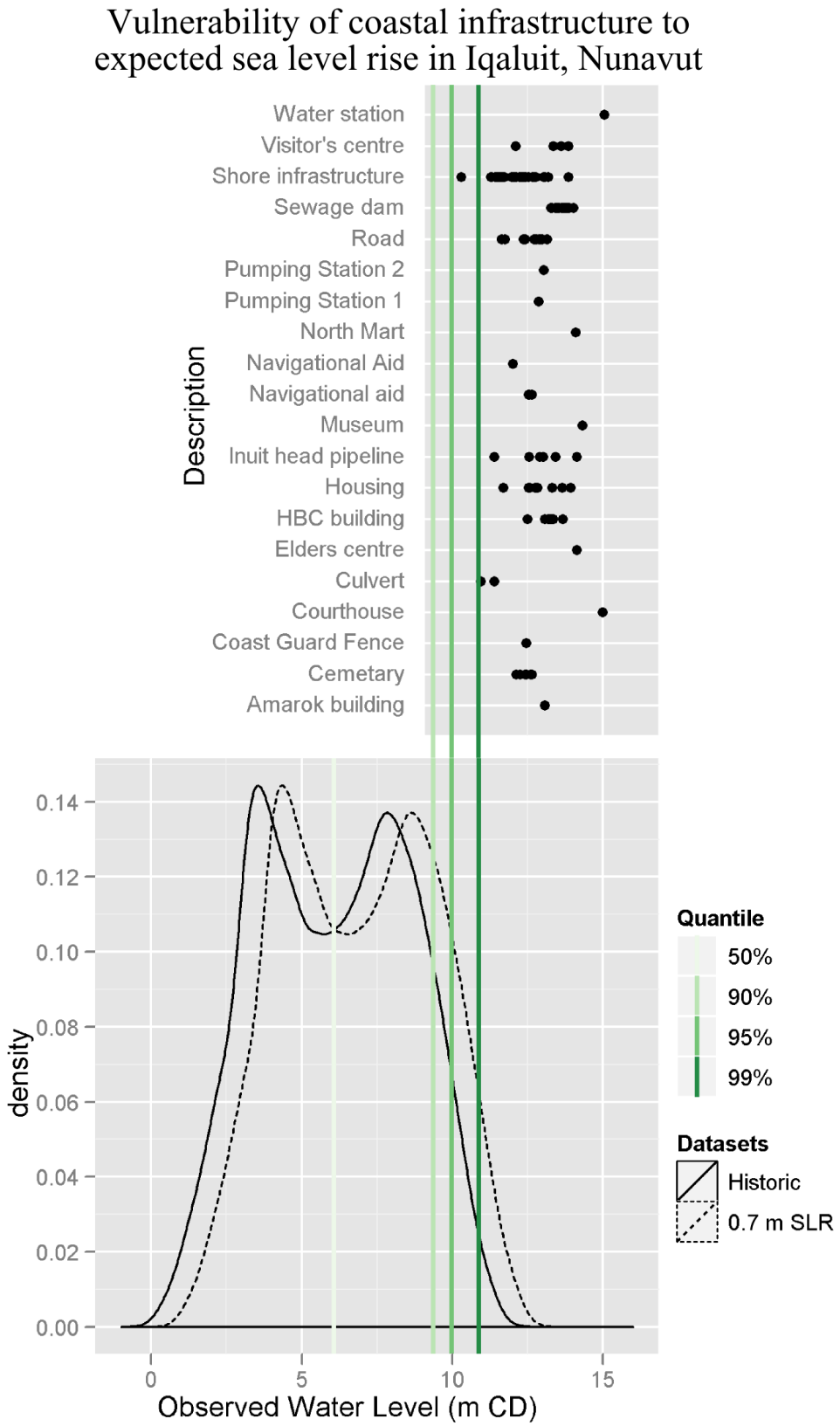

Figure 3.25: Elevation ranges for infrastructure groups with sea level descriptors plotted. Note the small buffer between high tide levels and the subsistence infrastructure.

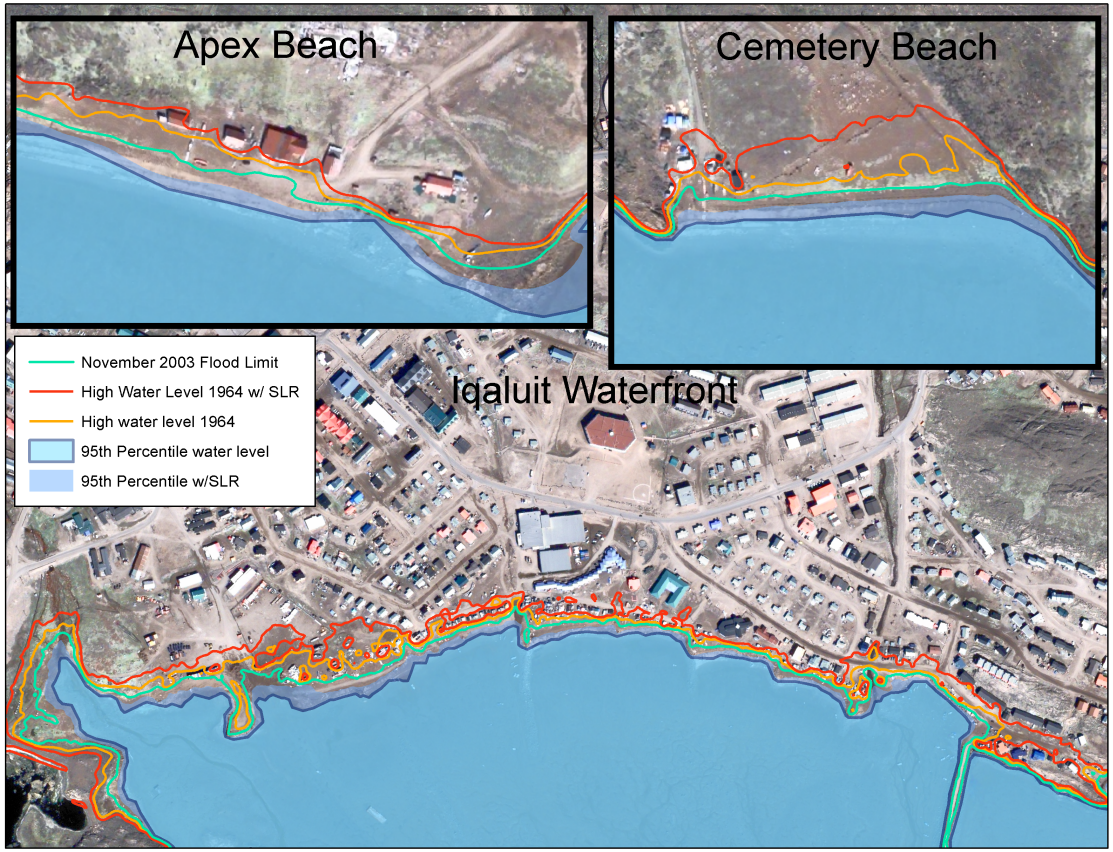

Figure 3.26: Flood hazard mapping along the main sections of the coast in Iqaluit and Apex. The three areas of the map follow the insets labeled in fig. 3.4 and fig. 3.7. The highest inundation line shows the addition of projected sea level to 2100 from James (2010) added on top of the highest recorded water level in November 1964 (6.04 m + 0.70 m).

Figure 3.27: High spring tide water levels during freeze up float ice right to the door steps of the coastal subsistence infrastructure. These buildings are vulnerable to even slight changes in the dynamics of storms or ice during the freeze up process.

3.5.2.3 Waves and run up hazards

Assuming an open-water fetch of 50 km, meteorological records from Iqaluit, and empirical wind-wave relations (SPM, 1984), the greatest wave-producing winds on record (22 Sept 1960, 97 km/h for 3 hours) give a hindcast significant wave height of $H_s = 1.9$ m with peak period $T_p = 5.6$ s. The potential runup from these waves on a beach slope of 5°typical of Koojesse Inlet was 0.6 m. Waves recorded during this study had significant heights up to 0.7 m over the flats and 1 m in deeper water with peak periods up to about 5 s. At a wave period of 5 s, the waves begin shoaling well out over the tidal flats (where the depth to wavelength ratio $h/L<1/4$, which is in 9 m depth for a 5 s wave). Up to 80% energy dissipation was observed in this study, suggesting that the flats serve a major shore protection function for Iqaluit. The hindcast 7.9 s waves for the 22 September 1960 event would begin to shoal in a depth of about 23 m and thus would suffer energy dissipation across the full width of the flats even at high spring tide. It is clear that the wave height at breaking and run-up

heights on the beaches depend to a large extent on the incoming wavelength and tide level, as well as on the roughness of the shoreface, the extent of energy dissipation during shoaling, and the slope of the beach. The largest waves observed during this study (H_s = 1 m, T_p = 5 s) coming in at high spring tide would suffer relatively little dissipation and would produce run-up of <1 m on beach slopes ranging up to 6°(Hunt, 1959).

3.5.2.4 Overtopping and erosion hazards

Overtopping of the sewage dam could have highly negative impacts on the health of the inlet ecosystem and do damage to the subsistence fishery. Our surveys show crest elevations of 7.7 m on the eastern dam and 7.3 m on the western dam. This is 1.3 m above the highest recorded water level in the tide gauge record. Surveys of storm swash lines near the dam walls, however, show a run-up limit of 6.5 m, 0.4 m above the highest recorded tide. With an RMS error on each survey point of 0.15 m, there is 0.9±0.3 m (0.5 to 1.1 m) of freeboard separating the sewage pond from the bay. At the low end of this range, a freeboard of 0.5 m leaves little allowance for more extreme events or sea-level rise.

The tidal flats are thought to be an erosional coastal landform, carved from glaciomarine sediments as relative sea level fell since the last glacial highstand McCann et al. (1981). Surveys conducted in the bay suggest a strong correlation between present-day coastal morphology and the tidal range, suggesting a rough equilibrium between current sea level and the coast. Erosion, however, is dependent now on the dynamics on the flats, which are dominated by sea ice action, but show little evidence of significant erosion on yearly time scales. The sea-ice, as well as tidal and wave currents currents have shaped the morphology of the beach, and any shifts in relative sea level will bring movement of the beach system back in line with the adjusted tidal limits.

3.6 Discussion

Results of this study investigating the major drivers of coastal hazards and severity of hazard exposure along the Iqaluit waterfront imply limited risk for much of the shorefront infrastructure. Nevertheless, some roads, structures, and other key facilities and resources are at risk from flooding, wave runup, or ice impacts. Detailed mapping of coastal infrastructure shows that development has been concentrated along the sand beach sections of the coast. In these areas some critical infrastructure is found in the backshore, and numerous subsistence-support resources (sheds, sea-cans, boats, motors, skidoos, komatiks, and other equipment) are concentrated on the uppermost part of the beach. The subsistence infrastructure is found primarily below the elevation of past extreme water levels. Much of the other waterfront infrastructure has a freeboard ranging from 1.0 to 1.5 m or more above the highest observed historical water level. At the upper limit of projected sea-level rise over the next century, this freeboard would be reduced to 0.3 - 0.8 m. Severe limitations of this conclusion, however, must be emphasized. The short time series of field work done here is inadequate for producing accurate estimates of long term change in influence of coastal erosion. Furthermore, a lack of long term data precludes many useful analyses that would greatly benefit this study.

Sea-ice hazards in the form of pile-up and ride-up are dependent on the freeze-up process, and the establishment of the ice foot in particular. The icefoot provides a buffer area for coastal infrastructure, except where there is artificial steepening of the coast. No severe damage from past onshore ice movement has been found, although a small pile-up ridge around the boat basin during freeze-up in November 2011 required heavy equipment to clear it away. The highly anomalous influx of thick multi-year ice at the beginning of the shipping season in 2012 caused severe disruption, damage to sealift vessels, and suspended landing operations.

The possibility of a fall in sea level might have implications for sediment transport in the inlet. The strongest currents we recorded in the intertidal zone were during offshore winds in shallow water. A decrease in mean sea level might enhance offshore transport of intertidal sediments, increasing erosion over the flats. Coupled with increased wave energy from an extended open-water season, this could affect the shoreline position. Houser & Hill (2010) have modelled changes in sedimentology on tidal sand flats from an increase in sea level, and shown that this may have a significant impact on the coastal use of the flats. As the tidal flats in Iqaluit have longer and longer open water seasons, there is a possibility that the same sorts of sediment dynamics could start to have more influence. The existence of the boulders, however, might negate the increased influence of waves here. During the lag response period following change in relative sea-level erosion might increase and sea ice dynamics may be more chaotic, leading to increased risk to navigation and shore infrastructure.

The current best guidance on relative sea-level change suggests a range of possible sea-level rise from 0 to 70 cm over 90 years from 2010 to 2100 (James et al., 2011). More recent analysis suggests that the upper limit could be significantly lower. Robust projections for Iqaluit are challenging because of the short GPS record (hence large uncertainty on the vertical motion), the lack of information on rates of glacier depletion in the South Baffin region, and the close proximity to the Greenland Ice Sheet. This study has shown that the tidal flats play an important role in shore protection during storms, dissipating a large proportion of incoming wave energy, except at the highest tides. Downward erosion (or sea-level rise) would diminish this effect, but the flats show little sign of significant erosion on short time scales. Wave run-up occurs in extreme events at high tides, but rough calculations suggest this is likely to be much less than 1 m (vertically) under most circumstances.

The use of the 0.7 m worst-case-scenario projection is reasonable in the context of

a precautionary approach to climate-change adaptation. Recent and ongoing data collection is suggesting changes in this projection toward lower values (Henton, pers. comm.). Flood hazard modelling in this study uses 0.7 m to define features susceptible to flooding. It is important to note, however, that the interactions are primarily with the morphology of the coastline and not on specific infrastructure. This is more vulnerable to hazards on a shorter timescale, such as storm hazards. Using this projection, however, allows the interpretation of possible changes to the morphology of the beaches where future development would be based. No conclusions are able to yet be drawn on this, but based on the current understanding of infrastructure one would need to make the unreasonable assumption that the infrastructure as it stands now would be similar to the infrastructure of 2100. The use of the 0.7 m level in flood risk modelling then is based on the current data, fits well with the planning discussion ongoing in the city, but comes with severe caveats due to sparse data in vertical land motion and no data on the nature of future infrastructure. It is currently the most reliable information on changing sea-level at this location.

The available data do not suggest impact from storm surges or wave run-up, which raises the question of whether floods are mainly attributable to high perigean spring tides? By analyzing output from a global tide model, Haigh et al. (2011) showed that the relative influences of long-period tidal constituents (8.85 yr lunar perigee cycle and the 18.6 yr lunar nodal cycle) are related to both tidal range and tidal form factor (relative influence of diurnal or semi-diurnal constituents). Higher spring tide levels are experienced when these two cycles coincide, sometimes adding an extra 0.2 m on top of high tide levels. In Iqaluit, with a macrotidal semi-diurnal setting, the influence of the 8.85 year perigee cycle dominates, but the effects of both are felt. The dominant cycle was last in place in 1997, and will not recur until 2014. The secondary cycle last occurred in 2006, and will not happen again until 2024. At these

times, especially during the dominant cycle, high-tide levels up to 0.2 m higher than the predicted tides (tide tables) can be expected. However it is also important to note that historical flooding events have occurred in other years, notably 1964 and 2003. Iqaluit's coastline is a complex zone of interaction with a range of key stakeholders (critical municipal infrastructure, sealift freight handling, and the subsistence hunters and fishers). Risk to the subsistence infrastructure is rooted in the incursion of urban development into the backshore zone, leaving limited space for hunters and fishers, who need to locate on land with direct access to the sea. This study shows the possibility of future flood water levels and sea ice incursion into the subsistence use zone. This is seen as the primary driver of coastal hazard for future planning. A general plan put out by the city in 2010 outlines policies for coastal development based around tourism (City of Iqaluit, 2010). It would seem that the handling of joint use between subsistence activities and tourism planning will be crucial in building coastal resilience along the city's spatially-constrained usable coastline.

Flood-hazard modelling based on topographic surfaces produces valuable inputs to adaptation and vulnerability analysis, but the parameterization of modelled water levels is produced with varying methods. In Clyde River, another community along the east coast of Baffin Island, Irvine (2010) showed the risks to infrastructure imposed by repeated high water levels from storm surges on top of high tides. Delimiting these zones was an important part of quantifying and mapping vulnerability of infrastructure throughout the community. Webster & Dias (2006), O'Reilly et al. (2005), and Bernatchez et al. (2011) emphasized the use of eyewitness data (through photographs of flooding) to validate measured high water levels, as they found discrepancies between water levels measured by the tide gauge and those surveyed from photographs. This, however, was in areas of high storm-wave action, and so represented fairly energetic conditions compared to the flooding experience in Iqaluit. Webster et al. (2004),

and Webster & Dias (2006), used GIS modelling over a topographic DEM to delimit flood hazard zones based on previous storm-surge water levels. Analysis of flood risk can use scenarios involving sea-level projections and storm surge or combined tide and surge probabilities (McCulloch et al., 2002; Daigle & Project Research Team, 2006; Bernier et al., 2007; Forbes et al., 2009). For such studies to be of most use to planners and other stakeholders of communities involved, the assessment methods must be tailored to the study site. This study in Iqaluit, where the tides are the dominant factor in defining high water levels, provides further support for site-specific approaches to the estimation of extreme water levels.

3.6.1 Implications for adaptation planning in Iqaluit

- Previous reports outlining challenges to sustainability and adaptation planning in Iqaluit have outlined the lack of data concerning coastal hazards as a source of vulnerability (Nielsen, 2007). Past reports have had to rely on cautionary recommendations for coastal assessment, but this study has provided some data on which to base decisions. This reduces some uncertainty inherent in applying regional or circumpolar projections (e.g. of sea-level rise) to the estimation of hazards in a local context. This report provides an update using the most recent data on the scientific understanding of hazards in Iqaluit.

- This study shows some indication that unrestricted steepening of the coastal profile through revetment or armouring will likely have a negative, rather than a positive, effect on hazards at the coast. We argue here that hazards are dominated by sea-ice dynamics during freeze-up and break-up. There is evidence to suggest that a steeper profile with a narrow icefoot allows higher ice pile-up. This puts infrastructure directly landward of the revetment at risk.

- The areal extent of flood risk from potential sea-level rise is significant, especially for the coastal subsistence infrastructure. Review of the city's planning literature suggests that this infrastructure is crucial to community sustainability, but its position on the coast means it is most at risk to any change in sea level or sea ice regime.

- Accurate surveys of coastal infrastructure have allowed the estimation of waterfront elevations and freeboard under various high-water scenarios. Uncertainty in deriving better estimates of sea-level rise will impact the adaptation planning process.

Serious limitations are imposed by the scarcity of some key data in this region. Estimates of erosion on the coast are temporally limited by the short time series. Further work looking at coastal change using aerial photography would greatly help determine the influence of coastline change. Also, a detailed analysis of storms and severe weather into the climate data would produce a better idea of how the expanding ice season might make the influence of waves a greater one in the future. Estimates of high water levels are constrained by the age, short duration, sporadic coverage, and seasonal bias of the tide-gauge data. The instrument moorings in 2010 and 2011 as part of this study provide the first measurements of waves in the vicinity of Iqaluit, but unfortunately did not include a major storm event. Remaining ambiguities in the rate of crustal uplift are a major limitation for projections of sea-level change in the area. However, ongoing data collection is expected to provide more reliable rates of uplift in the near future, when it will be possible to reassess the results of this study.

Table 3.4: The results and confidence of the coastal hazards assessment for Iqaluit.

Hazard	Data	Results	Confidence
Sea ice	• Ice thickness • freeze up/break up dates • field observations 2011	• Sea ice is generally thinner • Open water season is lengthening	Fairly confident
Flood hazard	• Survey extreme water levels • Hindcasting storm waves • Projections of SLR to 2100	• Uplift uncertain • Past extreme 0.75 m above HHWLT • Flooding from long-period tidal oscillations	Not confident
Wave run up	• 2010/11 field observations of waves	• Little evidence for wave runup hazard	Fairly Confident
Erosion	2010/11 field surveys and observations	• No signs of significant erosion • Hypsometry suggests stable conditions • Will change in the future.	Not very confident

More work within the city would benefit coastal development planning. This study suggests that, unlike in other areas, coastal monitoring might not focus on coastal erosion, but instead on sea ice dynamics, wave climate, wave shoaling, and run-up levels. Detailed surveys of pile-up ridges during freeze-up, as well as the conditions that caused them, would help to better define this phenomenon. Related monitoring of icefoot growth and dimensions, including year-to-year variability and trends, would complement this analysis. A significant proportion of Iqaluit's residents use the sea ice during the winter for hunting activities, and have accumulated considerable knowledge on the dynamics of ice over the tidal flats. Any coastal monitoring effort should not overlook this knowledge source.

3.7 Conclusions

The processes touched on to determine hazard and risk are working on timescales that are dependent both on the detailed three-year time series done through field work, but also on the longer term data that determines input to the system. In the case of longer term data, there exist massive gaps. The changing influence of coastal erosion would be lost in the three year time series, and the longer term data do not provide an adequate context. The flooding representing a significant hazard has a low probability, one which cannot be adequately determined with existing data. Though some components of waterfront infrastructure are at limited risk of ice incursion or flooding, the precautionary principle would dictate planning and action based on the best currently available estimates of future changes in hazards (high water levels, ice, wind, and waves) and associated risk under plausible upper limits of climate-change projections. This study has tried to provide part of this, to recommend further work that can be done, and to suggest monitoring work that would be most beneficial.

Coastal hazards in Iqaluit differ substantially from those faced by many other coastal communities. Sea level is likely stable, with limited rise in the coming century. Erosional shoreline retreat appears to be not an issue due to the coastal morphology and lithology (with extensive resistant rock), stable or falling sea level, limited wave climate, and wave-energy dissipation across the tidal flats. On the other hand, sea-ice dynamics in this macrotidal environment present continuing challenges to coastal users and infrastructure. This will likely undergo some change in a rapidly changing climate, although the specifics as they relate to hazards are difficult to predict. This study through investigation of characteristic components of hazards to coastal communities, has shown the importance of community-scale scientific research for informing planning and development policies.

3.8 References

Are, F., Reimnitz, E., Grigoriev, M., Hubberten, H., & Rachold, V. (2008). The influence of cryogenic processes on the erosional Arctic shoreface. *Journal of Coastal Research*, *24*(1), 110–121.

Arehart, M. (2012). Akiak Declares Erosion Disaster. Alaska Public Media. URL `http://www.alaskapublic.org/2012/10/04/akiak-declares-erosion-disaster/`

Bernatchez, P., Fraser, C., Lefaivre, D., & Dugas, S. (2011). Integrating anthropogenic factors, geomorphological indicators and local knowledge in the analysis of coastal flooding and erosion hazards. *Ocean & Coastal Management*, *54*(8), 621–632.

Bernier, N., Thompson, K., Ou, J., & Ritchie, H. (2007). Mapping the return periods of extreme sea levels: Allowing for short sea level records, seasonality, and climate change. *Global and Planetary Change*, *57*, 139–150.

Catto, N., & Parewick, K. (2008). *Hazard and vulnerability assessment and adaptive planning: mutual and multilateral community-research communication, Arctic Canada*, vol. 305, (pp. 123–140). Gological Society, London, Special Publications 2008.

CIS (2006). Canadian Ice Service Digital Archive – Regional Charts: History, Accuracy, and Caveats. Tech. rep., Canadian Ice Service, CIS Documentation Series No. 1.

URL `http://ice.ec.gc.ca/IA_DOC/cisads_no_001_e.pdf`

City of Iqaluit (2010). Amended Version of the City of Iqaluit General Plan (Draft February 2010). Tech. rep., City of Iqaluit.

Collins, A., Hannah, C., & Greenberg, D. (2011). Validation of a High Resolution Modelling System for Tides in the Canadian Arctic Archipelago. Tech. rep., Ocean Sciences Division, Maritimes Region, Fisheries and Oceans Canada: Canadian Technical Report of Hydrography and Ocean Sciences 273.

Daigle, R., & Project Research Team (2006). Impacts of Sea-level Rise and Climate Change on the Coastal Zone of Southeastern New Brunswick. Open file, Environment Canada, Ottawa.

URL `http://www.adaptation.nrcan.gc.ca/projdb/final_coastal_e.php`

Dale, J., Leech, S., McCann, S., & Samuelson, G. (2002). Sedimentary characteristics, biological zonation and physical processes of the tidal flats of Iqaluit, Nunavut. In K. Hewitt, M. Byrne, M. English, & G. Young (Eds.) *Landscapes in Transition:*

Landform Assemblages and Transformations in Cold Regions, vol. 111, (pp. 205–234). Dordrecht: Kluwer.

DFO (2012). Iqaluit (4140) 2012 Tide Tables. Tech. rep., Canadian Communication Group Publishing, Ottawa, Canada.

Eno, R. (2003). Crystal two: The origin of Iqaluit. *Arctic*, *56*(1), 63–75.

Forbes, D., Manson, G., Charles, J., Thompson, K., & Taylor, R. (2009). Halifax Harbour Extreme Water Levels in the Context of Climate Change : Scenarios for a 100-year planning horizon. Tech. rep., Geological Survey of Canada, Open File 6346.

Forbes, D., & Taylor, R. (1994). Ice in the shore zone and the geomorphology of cold coasts. *Progress in Physical Geography*, *18*(1), 59–89.

Forbes, D. e. (2011). *State of the Arctic Coast 2010 - Scientific Review and Outlook*. Helmholtz-Zentrum, Geesthacht. Germany.: International Arctic Science Committee, Land-Ocean Interactions in the Coastal Zone, Arctic Monitoring and Assessment Programme, International Permafrost Association.
URL `http://arcticcoasts.org`

Ford, J., Bell, T., & St. Hilaire-Gravel, D. (2010). *Vulnerability of Community Infrastructure to Climate Change in Nunavut: A Case Study From Arctic Bay*, chap. 5, (pp. 107–130). Dordrecht: Springer Netherlands.

Gagnon, A., & Gough, W. (2010). Trends in the dates of ice freeze-up and breakup over Hudson Bay, Canada. *Arctic*, *58*(4), 370–382.

Gibbons, D., Jones, G., Siegel, E., Hay, A., & Johnson, F. (2005). Performance

of a new submersible tide-wave recorder. In *Proceedings of MTS/IEEE Oceans Conference (17-23 Sept. 2005)*, vol. 15, (pp. 2–5).

Haigh, I. D., Eliot, M., & Pattiaratchi, C. (2011). Global influences of the 18.61 year nodal cycle and 8.85 year cycle of lunar perigee on high tidal levels. *Journal of Geophysical Research*, *116*.

Helsel, D., & Hirsch, R. (1992). *Statistical methods in water resources*, vol. 34. Amsterdam: Elsevier.

Houser, C., & Hill, P. (2010). Sediment Transport on Roberts Bank: A Sandy Intertidal Flat on the Fraser River Delta. *Journal of Coastal Research*, *26*(2), 333–341.

Hunt, A. (1959). Design of seawalls and breakwaters. *Journal of waterway, port, coastal and ocean division, ASCE*, (pp. 123–152).

Hurdle, D., & Stive, R. (1989). Revision of PSM 1984 wave hindcast model to avoid inconsistencies in engineering applications. *Coastal Engineering*, *12*(4), 339–351.

Irvine, M. (2010). *Living on Unstable Ground: Identifying Physical Landscape Constraints on and Planning and Infrastructure Development in Nunavut Communities*. Master's thesis, M.Sc. Thesis, Memorial University of Newfoundland, St. John's.

James, T. S., Simon, K. M., Forbes, D. L., Dyke, A. S., & Mate, D. J. (2011). Sea-level Projections for Five Pilot Communities of the Nunavut Climate Change Partnership. Tech. rep., Geological Survey of Canada, Open File 6715.

Laidler, G., Ford, J. D., Gough, W. A., Ikummaq, T., Gagnon, A. S., Kowal, S., Qrunnut, K., & Irngaut, C. (2008). Travelling and hunting in a changing Arctic: assessing Inuit vulnerability to sea ice change in Igloolik, Nunavut. *Climatic Change*, *94*(3-4), 363–397.

Lardeau, M.-P., Healey, G., & Ford, J. (2011). The use of Photovoice to document and characterize the food security of users of community food programs in Iqaluit, Nunavut. *Rural and remote health*, *11*(2), 1680.

Larsen, P., Goldsmith, S., Smith, O., Wilson, M., Strzepek, K., Chinowsky, P., & Saylor, B. (2008). Estimating future costs for Alaska public infrastructure at risk from climate change. *Global Environmental Change*, *18*(3), 442–457.

Leech, S. (1998). *The transport of materials by ice in a subarctic macrotidal environment, Koojesse Inlet, southeast Baffin Island*. Master's thesis, M.Sc. Thesis, University of Regina, Regina.

Markus, T., Stroeve, J. C., & Miller, J. (2009). Recent changes in Arctic sea ice melt onset, freezeup, and melt season length. *Journal of Geophysical Research*, *114*(C12), 1–14.
URL `http://neptune.gsfc.nasa.gov/csb/index.php?section=54`

McCann, S., & Dale, J. (1986). Sea ice breakup and tidal flat processes, Frobisher Bay, Baffin Island. *Physical Geography*, *7*(2), 168–180.

McCann, S., Dale, J., & Hale, P. (1981). Subarctic Tidal Flats in Areas of Large Tidal Range, Southern Baffin Island, Eastern Canada. *Géographie physique et Quaternaire*, *35*(2), 183–204.

McCulloch, M., Forbes, D., & Shaw, R. (2002). Coastal Impacts of Climate Change and Sea-Level Rise on Prince Edward Island. Tech. rep., Geological Survey of Canada, Open File 4261.

Mitasovä, H., & Drake, T. (2004). Quantifying Rapid Changes in Coastal Topography using Modern Mapping Techniques and Geographic Information System. *Environmental & Engineering Geoscience*, *X*(1), 1–11.

Mitasovä, H., & Mitas, L. (1993). Interpolation by regularized spline with tension: I. Theory and implementation. *Mathematical geology*, *25*(6), 641–655.

Nielsen, D. (2007). The City of Iqaluit's Climate Change Impacts, Infrastructure Risks & Adaptive Capacity Project. Tech. rep., City of Iqaluit, Iqaluit.

Nortek (2005). Aquadopp Current Profiler User Guide. Tech. rep., Nortek.

NRTEE (2009). True North: Adapting Infrastructure to Climate Change in Northern Canada. Tech. rep., National Round Table on the Environment and the Economy.

O'Reilly, C., Forbes, D., & Parkes, G. (2005). Defining and Adapting to Coastal Hazards in Atlantic Canada: Facing the Challenge of Rising Sea Levels, Storm Surges, and Shoreline Erosion in a Changing Climate. In A. Chircop, & M. McConnell (Eds.) *Ocean Yearbook 19*, (pp. 189 – 207). University of Chicago Press.

Serreze, M. C., & Barry, R. G. (2011). Processes and impacts of Arctic amplification: A research synthesis. *Global and Planetary Change*, *77*(1-2), 85–96.

Shirley, J. (2005). Inuit Qaujimajatuqangit of Climate Change in Nunavut. Tech. rep., Government of Nunavut, Dept of Environment.

SPM (1984). *Shore Protection Manual: U.S. Army Corps of Engineers*, vol. 1. Department of the Army Corps of Engineers.

Strzelecki, M. C. (2011). Cold shores in warming times - current state and future challenges in High Arctic coastal geomorphological studies. *Quaestiones Geographicae*, *30*(3), 101–113.

Webster, T., & Dias, G. (2006). An automated GIS procedure for comparing GPS and proximal LIDAR elevations. *Computers & Geosciences*, *32*(6), 713–726.

Webster, T. L., Forbes, D. L., Dickie, S., & Shreenan, R. (2004). Using topographic lidar to map flood risk from storm-surge events for Charlottetown, Prince Edward Island , Canada. *Canadian Journal of Remote Sensing*, *30*(1), 64–76.

Chapter 4

Synthesis and Discussion

This chapter is a synthesis of the two papers forming Chapters 2 and 3, with comment on the approach taken. The underlying question is essentially "What is the contribution of coastal geomorphology and hazard analysis to informing climate-change adaptation and sustainability planning in a coastal municipality?" How does the second paper benefit from the first? The answer to this follows three streams: first is the methodology, second the importance of physical context, and third understanding of coastal dynamics and inherent resilience of the morphological system in the face of changing climate.

Geomorphological and sub-bottom mapping in Koojesse inlet provides evidence for an erosional hypothesis of tidal-flat evolution and a baseline against which to measure future change. Acoustic profiles over the extensive boulder-strewn tidal flats at high tide revealed poorly defined draped bedding consistent with an interpretation of glaciomarine deposits truncated at the modern tidal-flat surface. Exposures of blue-grey silt-clay, partly encasing boulders on the flats, support this interpretation. A silty sand and sand-gravel veneer, as well as the numerous boulders, covers most of the intertidal surface. Sediment sampling was extended into the subtidal, where the

bottom sediment is mud. The fine grain size corroborates tidal current measurements in the channels, which revealed little evidence for significant scouring of the seabed or any bedforms in the tidal channels, despite the macrotidal setting. Some evidence of mass wasting was observed on the edge of the flats (the terrace front), but only in the areas of steeper slopes. This provides further insight into the slow erosion of the modern flats by a combination of slow mass wasting at the edges, abrasion by bedload transport of sand veneer during times of strong offshore winds and ebb tides, and the slow spillover of ice-entrained sediment into the subtidal channels. This project, conducted with modern GPS survey techniques and GIS modelling, represents a detailed case study of a subArctic geomorphic system and a baseline for analysis of coastal response to future change.

Delineation of past extreme water levels in Iqaluit, coupled with a GIS model of backshore topography, enabled mapping of flood water extents in relation to existing waterfront infrastructure. Levels associated with previous high-water event were determined from the tide gauge record, photos of past flooding, and proxy elevations from storm swash lines preserved around the inlet. Swash limits varied throughout the inlet, primarily due to the differences in exposure to offshore waves. Mapping the extents of the high water limits with the addition of the maximum projected sea-level rise (70 cm 2010-2100) showed a 28.9% loss of the municipal 'Open Space' zone (30.5 m from HHWLT) and 14.2% of the extended coastal zone (75 m from HHWLT). The infrastructure most affected was the private subsistence infrastructure, located on the upper beachface directly adjacent to the present-day high spring-tide level. Infrastructure flooded in the October 2003 event appears localized in the model reconstruction, isolated primarily to the armoured section of coast near the base of the main breakwater. Further analysis of the tide-gauge record reveals no evidence for significant storm surges in the area. Rather, the extreme water levels causing historical flooding have

been high spring tides with very limited meteorological enhancement. Nevertheless the swash lines attest to some wave action and runup to the levels they record. An expansion of the ice-free season with future warming, as projected by current local ice trends, may add exposure to surges during the fall storm season.

There are a number of ways to map flood hazards in communities. Studies in other locations have employed airborne Light Detection and Ranging (LiDAR) to develop high-resolution digital elevation models (DEMs) with which to visualize flood risk scenarios (Webster et al., 2004, 2006; Forbes et al., 2009). Integration of field surveys with aerial photography is widely used to derive shoreline change (e.g. Forbes et al., 1995, 2004; Mitasovä & Drake, 2004; Solomon, 2005; St-Hilaire-Gravel et al., 2012). In many cases, these have been used in a context that strives for close integration with planning authorities for use in policy decisions. It is a transferable model that spans latitudes and borders.

The choice of methods, however, is often constrained by financial and logistical limitations. LiDAR collection is expensive, technically complex, and requires logistics support from an airport. It is dependent on weather conditions and visibility. Field mapping with expensive GPS equipment is also not always realistic. This thesis has validated the use of a digital elevation model derived from high-resolution satellite stereo imagery for use in flood-hazard modelling, at resolutions and accuracies comparable to LiDAR-derived DEMs. The relatively modest cost of high-resolution satellite imagery, as well as the ability to remotely derive the DEM product, means this method could be a lower-cost alternative for smaller communities.

An understanding of the stability or resilience of natural morphological systems is important to an assessment of physical vulnerability and hazards in coastal settings (e.g. Forbes et al., 1995). Recent research in the geomorphological perspective on hazards has called for a greater integration of coastal evolution into impacts analysis

(Capobianco et al., 1999; Pethick & Crooks, 2002). The idea is that a geomorphological system can contain within it a form resilience - an ability to stabilize following a change. This is not often integrated into conventional scenario approaches to vulnerability assessment. If a true integration of physical and social perspectives is sought in vulnerability research, then this aspect of the systems under study may require further attention.

The case of Iqaluit provides evidence for the benefit of geomorphological study alongside hazards assessment. Dynamics in the Koojesse Inlet tidal-flat system operate on a range of timescales, but evidence suggests that decadal periods prevail in defining the current morphology. Data collected on currents and waves confirmed the earlier interpretation of an ice-dominated sediment budget. Also, the process of differential melting during break-up identified by McCann et al. (1981), which keeps a large proportion of entrained sediment within the flats zone, shows a control on erosion that is likely independent of changing sea levels. Changing ice season is also unlikely to affect this process. Shoreline change analysis revealed little evidence for a response in the system, likely due to a roughly static sea level at this time and the large proportion of rocky shoreline. Identification of this natural resilience within the coastal morphological system played into the hazards assessment when investigation of previous flooding revealed the area of most damage to be on the section of coastline that has been armoured. The connection to flooding is less obvious than in the case of sea-ice pile-up, also evidenced in the revetment area. With flooding, it is primarily a question of elevation (especially in this case with limited wave runup). The flooded structures, however, are on top of the revetment, which is lower than the naturally defined beach ridge and backshore.

Studies looking at hazards in Arctic communities can provide mutual benefit to two streams of research fairly seamlessly. The Arctic coast is expansive, diverse, and

relatively understudied (Forbes, 2011). Vulnerability research in the Arctic aims at integrating multiple perspectives to make outputs more useful to communities (Hovelsrud et al., 2010). The framework developed for vulnerability research in the Arctic most used treats geomorphological systems with a boundary condition approach. This study shows the capacity of integrated hazards and geomorphological research to better define these boundary conditions for adaptation planning and vulnerability assessment. At the same time, it allows for the establishment of baseline datasets for future analysis of change.

Studies looking at hazards to infrastructure in the Arctic from a natural sciences perspective are far less common than those employing social science methodologies. Ford et al. (2010) attempted a multi-perspective approach using a case study in Arctic Bay. Survey design and field work were conducted in concert with concerns from the community generated through stakeholder interviews and community engagement (Ford et al., 2010). Similar work by Irvine (2010) argued the importance of this aspect of vulnerability assessment in the north, which is echoed in findings from the social science perspective (Beaumier, 2010). The methods employed primarily rely on a geomorphological understanding of landscape processes, as well as survey-grade GPS positioning equipment. It is important to note, however, that these methods are equally crucial to impact analyses on systems with minimal human interaction (Jorgenson, 2001).

Past climate change adaptation reviews for Iqaluit have perhaps over-emphasized the coastal hazards due to limited data availability. No published projections of sea-level change, no assessment of the rates of erosion along the coast, and tacit assumptions about regional hazards from warming climates combined to force previous assessments into vague territory. A geomorphological understanding demonstrates the protective role of the tidal flats, dissipating a high proportion of wave energy at all but the

highest tides. The stability of the flats appears to be relatively insensitive to sea-level adjustment, although the effect of a change to rising sea level is uncertain. Ice pile-up hazards appear to be modest and easily managed. Although the record high water event occurred in 1964 before the waterfront was built up and its impacts are therefore hypothetical, a similar event today would flood some facilities. However, critical pumping station and sewage infrastructure appears to be high enough to avoid flooding, even under the highest sea-level rise scenario to 2100. On the other hand, most of the waterfront facilities supporting subsistence activities and an indigenous lifestyle are exposed to high-water events, even today. Thus, from a physical perspective, various classes of infrastructure have different levels of exposure and subsistence infrastructure is most at risk.

4.1 Limitations and future research

Further data collection would permit greater confidence in coastal planning in Iqaluit on two fronts: it would help to better resolve the sea-level change, and it would allow for more informative statistical modelling.

Subsurface geophysical profiling could reveal more about the sedimentation dynamics on the flats. No one has yet looked at the stratigraphy and facies characteristics of the sediments underlying the tidal flats. Some structure was revealed in this study using sub-bottom profiling, but higher resolution profiling would help to confirm the erosional nature of the flats and the character of deposition along the outer edge of the intertidal terrace. This would improve our understanding of the geomorphic system, and better place this baseline study in context.

Hazards on the coast in Iqaluit are differentiated by the varying coastal uses of the shoreline. Sewage treatment for the city is at the coast, and while this study showed

that flooding is unlikely to overtop the barriers, Leech (1998) suggested that the effects of microbial contamination could be carried by the mobile sea ice within the bay. This represents another aspect of coastal hazards in the city. Municipal infrastructure will come under increasing pressure as population continues to rise, and the flood risk for pumping stations will need regular reevaluation. At the present time, they appear to have a low probability of flooding.

The legal situation surrounding the subsistence infrastructure is ambiguous. At the same time, it is identified as an integral part of the city's sustainability initiatives. Because this sector looks to be affected most by any sea-level change, this will need to be an important aspect of coastal management for the city. High water levels currently reach the foundations of some of this infrastructure, and so under any change in sea level these will have to be moved. Vulnerability assessment using key stakeholder interviews would help to inform strategies for enhancing resilience along Iqaluit's waterfront.

The data currently available provide no evidence for significant storm surges, but further analysis and collection of more data might help at least to quantify surges into the future. A southwesterly storm thought capable of producing a surge was recorded in this study period, and no storm surge signature was recorded. The analysis presented in this thesis relies on a very short and sporadic tide gauge record. Previous studies have shown that extra-tropical cyclones occur in the region, providing opportunity for surge propagation into the inner parts of the bay (Roberts et al., 2009; Hanesiak et al., 2010). It is possible that tide-surge interaction works to hide surge signatures in phase modulation, as found by Horsburgh & Wilson (2007). Further work could combine the sea ice datasets mentioned in this thesis with sea-level pressure records for the area to test an ice-sensitive physically based surge model. This might help to estimate surge probability into the future.

4.2 Hazards and Vulnerability

Vulnerability assessments and adaptation strategies are best developed on a collaborative basis between social and physical disciplines, employing a range of expertise and close involvement of stakeholders. Infrastructure adaptation presents particular challenges that depend on a close understanding of the physical setting and hazard exposure. The sustainability of coastal infrastructure relies on the relative stability of the geomorphic system in which it resides. Identifying resilience remains a key goal for adaptation planning. Understanding the nature and limits of natural resilience in geomorphic systems is an important goal.

Further work at the interface of science and policy, of social and physical science, and of applied and pure research, will require true collaboration. The Arctic and subArctic coastal communities of Canada present a unique challenge to researchers. International effort has demonstrated the high exposure and sensitivity of Arctic communities to emerging and projected climate change, combined with a wide range of non-climate stresses, and the critical importance of multi- and transdisciplinary approaches (ACIA, 2005; Forbes, 2011). The International Polar Year promoted substantial research in a relatively data-poor part of the planet. There is a proliferation of work identifying the advantages and the fundamental importance of considering Inuit knowledge alongside scientific understanding (Ford & Smit, 2004; Smit & Wandel, 2006; Ford et al., 2010). Gaps remain and uncertainties inherent in conceptualizations of all aspects of the Arctic ecosystem continue to pervade investigations focusing on any one aspect. If a truly interdisciplinary investigation of vulnerability is to be achieved, then these uncertainties must remain a key component of the conversation. Humans have a unique opportunity to act on the question of adapting to climate change. Where better to meld disciplinary approaches than in the Arctic crucible facing some of the greatest challenges to human sustainability?

4.3 Conclusions

4.3.1 Stated Objectives

- Describe the morphology of the Koojesse Inlet tidal flats: Previous work describing the tidal flats in Koojesse Inlet has identified them as erosional, and established that the dominant sediment type is sand, but with an admixture of everything from fine silts to cobbles and large boulders (McCann et al., 1981; McCann & Dale, 1986; Dale et al., 2002). From this work, an erosional evolution was hypothesized, which would agree with interpretations of stratigraphic studies elsewhere (Ruz et al., 1998; Martini, 1991). The first paper in this thesis uses data collected over three field seasons to describe the morphology of the tidal flats, and it contributes to the ongoing study of their dynamics. The morphology indicates continued erosion, but fine-scale determination of this over three years was erased by the signature of reworking contributed by sea ice entrainment and redeposition over each ice season. Measurements on the flats surface show the influence of local winds in determining the dominant direction of currents, but we saw little evidence to suggest this mechanism of transport might be important. Hypsometric analysis of the embayment suggests a close relationship between breaks in bathymetry and current tidal limits, suggesting a relatively stable current sea level. Waves are dissipated by the flats such that little wave influence is recorded on the beachface, however, the coincidence of a high spring tide with strong onshore winds can produce wave runup and swash lines above water levels expected by tides. Bathymetry of the nearshore channels and sub-bottom profiles over the flats surface at high tide add weight to the earlier interpretation of the evolution of the flats as an erosional plain resultant from reworking of glaciomarine sediments deposited during the last highstand.

- Describe the influence of coastal hazards in Iqaluit: Past reports on landscape hazards in Iqaluit identify the lack of knowledge at the coast as a significant source of vulnerability to the city under continued climate change. This was largely driven by great uncertainty in sea-level rise estimates, the causes of past flooding, and the shifting sea-ice dynamics. The second paper of this thesis used GPS elevation measurements of infrastructure heights, as well as mapping of past extreme water levels and morphological mapping, to develop a better understanding of coastal hazards in the city. Estimation of past extreme water levels required elevations from the tide gauge record, as well as in situ survey measurements. A lack of evidence for surges, as well as the relatively small effect of waves and currents in the morphodynamics of the flats, suggests the past extreme water levels may have been a product of long period lunar cycles. This has significant impact on the predictability of extreme water events in the area, as opposed to the difficulty most coastal communities have in determining extreme water levels. Sea ice hazards at the coast include ride-up and pile-up with resulting damage to infrastructure. This was primarily observed to affect the subsistence infrastructure found along the waterfront. The observations collected indicate a possible link between artificial beachface steepening and increased probability of ice pile-up. This is assumed to be caused by the deeper water immediately offshore allowing larger ice blocks to congregate, as well as the inability of a protective icefoot to develop due to the artificial intertidal profile. Impacts from changing climate and coastal dynamics in Iqaluit are complex, and differ from other Arctic communities. Continued monitoring, as well as cautious development with respect to elevation and shoreline protection, will be needed to make sure unnecessary damage is not incurred.

- Map the hazards: the inclusion of an integrated coastal DEM with the GIS

data collected on high water levels and morphology allows an assessment of areal extents of potential damage, as well as a classification of the infrastructure most at risk in the event of long-term sea-level change. The subsistence infrastructure is found to be most at risk, due to its limitation to the beachface as well as its potential to be squeezed out by backshore development pressure. Of the recorded flood impacts, the most damage was done on the section of coast where armouring occurs. Crucial municipal infrastructure, such as the pumping stations and the sewage pond, appear to be at low risk of flooding. This mapping of flood inundation hazard is contingent on the current projections of sea-level rise, as well as the projection of sea-ice change. Because of this continued updates based on new information will prove useful. This will be possible using the GIS developed in this project.

4.4 Recommendations to the city

- Put in a tide gauge. The estimates of past extreme water levels are based on a very short time series of water levels that are almost 50 years old. Proper forecasting of potential flood hazard will greatly benefit from additional water level data.

- Do not allow infrastructure below the 5.3 m elevation line above mean sea level established by the October 2003 flooding. Work with subsistence hunters with infrastructure on the coast to develop a plan for coastal development that is mutually beneficial for the city as well as the hunters and trappers.

- Act on the opportunity to combine planning goals at the coast. The first is the stated objective of continued support for the subsistence economy acting in the city. The second relates to planning surrounding tourism, particularly at the

coast and the main waterfront areas. The third is the preservation of coastal access despite further development. A communal staging area at the coast with facilities setup to support animal processing (sealskin tanning, fish processing), community-run and supported by the Amarok Hunters & Trappers Association, could provide a sustainable means to accomplish these three goals. As a place to highlight traditional subsistence activities, it could serve as a source of tourism revenue, at the same time providing crucial support to those subsistence hunters currently using the sheds on the beach. Surrounding a communal building, with storage and equipment, could be coastal access, as well as the site for improved small vessel facilities. It is a model employed in small-scale fisheries in many parts of the Caribbean that, with appropriate adaptations, might prove beneficial to the City of Iqaluit.

4.5 References

ACIA (2005). *Arctic Climate Impact Assessment*. Cambridge, UK: Cambridge University Press.

Beaumier, M. (2010). Food insecurity among Inuit women exacerbated by socio-economic stresses and climate change. *Canadian Journal of Public Health*, *101*(3), 196–201.

Capobianco, M., DeVriend, H., Nicholls, R., & Stive, M. (1999). Coastal area impact and vulnerability assessment: the point of view of a morphodynamic modeller. *Journal of Coastal Research*, *15*(3), 701–716.

Dale, J., Leech, S., McCann, S., & Samuelson, G. (2002). Sedimentary characteristics, biological zonation and physical processes of the tidal flats of Iqaluit, Nunavut. In K. Hewitt, M. Byrne, M. English, & G. Young (Eds.) *Landscapes in Transition: Landform Assemblages and Transformations in Cold Regions*, vol. 111, (pp. 205–234). Dordrecht: Kluwer.

Forbes, D., Covill, R., Feindel, R., & Batterson, M. (1995). Preliminary Assessment of Coastal Erosion between Port au Port and Stephenville, St. George's Bay, West Newfoundland. Tech. rep., Geological Survey of Canada: Open File 3082.

Forbes, D., Manson, G., Charles, J., Thompson, K., & Taylor, R. (2009). Halifax Harbour Extreme Water Levels in the Context of Climate Change : Scenarios for a 100-year planning horizon. Tech. rep., Geological Survey of Canada, Open File 6346.

Forbes, D., Parkes, G., Manson, G., & Ketch, L. (2004). Storms and shoreline retreat in the southern Gulf of St. Lawrence. *Marine Geology*, *210*(1-4), 169–204.

Forbes, D. e. (2011). *State of the Arctic Coast 2010 - Scientific Review and Outlook*. Helmholtz-Zentrum, Geesthacht. Germany.: International Arctic Science Committee, Land-Ocean Interactions in the Coastal Zone, Arctic Monitoring and Assessment Programme, International Permafrost Association.
URL `http://arcticcoasts.org`

Ford, J., Bell, T., & St. Hilaire-Gravel, D. (2010). *Vulnerability of Community Infrastructure to Climate Change in Nunavut: A Case Study From Arctic Bay*, chap. 5, (pp. 107–130). Dordrecht: Springer Netherlands.

Ford, J., & Smit, B. (2004). A framework for assessing the vulnerability of communi-

ties in the Canadian Arctic to risks associated with climate change. *Arctic*, *57*(4), 389–400.

Hanesiak, J., Stewart, R., Barber, D., Liu, G., Gilligan, J., Desjardins, D., Dyck, R., Fargey, S., Hochheim, K., Martin, R., Taylor, P., Biswas, S., Gordon, M., Melzer, M. A., Moore, K., Field, R., Hay, C., Zhang, S., McBean, G., Strapp, W., Hudak, D., Scott, J., Wolde, M., Goodson, R., Hudson, E., Gascon, G., Greene, H., Henson, W., & Laplante, A. (2010). Storm Studies in the Arctic (STAR). *Bulletin of the American Meteorological Society*, *91*(1), 47–68.

Horsburgh, K. J., & Wilson, C. (2007). Tide-surge interaction and its role in the distribution of surge residuals in the North Sea. *Journal of Geophysical Research*, *112*(C8), 1–13.

Hovelsrud, G. K., White, J. L., Andrachuk, M., & Smit, B. (2010). Community Adaptation and Vulnerability Integrated. In *Community Adaptation and Vulnerability in Arctic Regions*, (pp. 335–348).

Irvine, M. (2010). *Living on Unstable Ground: Identifying Physical Landscape Constraints on and Planning and Infrastructure Development in Nunavut Communities*. Master's thesis, M.Sc. Thesis, Memorial University of Newfoundland, St. John's.

Jorgenson, T. (2001). Topography and flooding of coastal ecosystems on the Yukon-Kuskokwim Delta, Alaska: implications for sea-level rise. *Journal of coastal research*, *17*(1), 124–136.

Leech, S. (1998). *The transport of materials by ice in a subarctic macrotidal environment, Koojesse Inlet, southeast Baffin Island*. Master's thesis, M.Sc. Thesis, University of Regina, Regina.

Martini, I. (1991). *Sedimentology of subarctic tidal flats of western James Bay and Hudson Bay, Ontario, Canada*, chap. Memoir 16, (pp. 301–312). Canadian Society of Petroleum Geologists.

McCann, S., & Dale, J. (1986). Sea ice breakup and tidal flat processes, Frobisher Bay, Baffin Island. *Physical Geography*, *7*(2), 168–180.

McCann, S., Dale, J., & Hale, P. (1981). Subarctic Tidal Flats in Areas of Large Tidal Range, Southern Baffin Island, Eastern Canada. *Géographie physique et Quaternaire*, *35*(2), 183–204.

Mitasovä, H., & Drake, T. (2004). Quantifying Rapid Changes in Coastal Topography using Modern Mapping Techniques and Geographic Information System. *Environmental & Engineering Geoscience*, *X*(1), 1–11.

Pethick, J. S., & Crooks, S. (2002). Development of a coastal vulnerability index: a geomorphological perspective. *Environmental Conservation*, *27*, 359–367.

Roberts, E., Nawri, N., & Stewart, R. (2009). On the Storms Passing Over Southern Baffin Island During Autumn 2005. *Arctic*, *61*(3), 309–321.

Ruz, M., Allard, M., & Michaud, Y. (1998). Sedimentology and evolution of subarctic tidal flats along a rapidly emerging coast, eastern Hudson Bay, Canada. *Journal of Coastal Research*, *14*(4), 1242–1254.

Smit, B., & Wandel, J. (2006). Adaptation, adaptive capacity and vulnerability. *Global Environmental Change*, *16*(3), 282–292.

Solomon, S. (2005). Spatial and temporal variability of shoreline change in the Beaufort-Mackenzie region, Northwest Territories, Canada. *Geo-Marine Letters*, *25*(2), 127–137.

St-Hilaire-Gravel, D., Forbes, D. L., & Bell, T. (2012). Multitemporal Analysis of a Gravel-Dominated Coastline in the Central Canadian Arctic Archipelago. *Journal of Coastal Research*, *280*(2), 421–441.

Webster, T., Forbes, D., MacKinnon, E., & Roberts, D. (2006). Flood-risk mapping for storm-surge events and sea-level rise using LiDAR for southeast New Brunswick. *Canadian Journal of Remote Sensing*, *32*(2), 194–211.

Webster, T. L., Forbes, D. L., Dickie, S., & Shreenan, R. (2004). Using topographic lidar to map flood risk from storm-surge events for Charlottetown, Prince Edward Island , Canada. *Canadian Journal of Remote Sensing*, *30*(1), 64–76.

Appendix A

Geoscience field work report, Iqaluit Nunavut 2010-2011 (Open File)

A.1 Cruise Information

Dates	13/08/2010 - 26/08/2010 12/02/2011 - 16/02/2011 12/07/2011 - 05/08/2011 21/11/2011 - 28/11/2011
Area of Operations	Koojesse Inlet off the shores of Iqaluit, Nunavut
Operating from:	Iqaluit, NU.
GSC Personnel:	Donald Forbes (senior scientist) Gavin Manson (systems specialist) Scott Hatcher (volunteer student)
Ship personnel:	Alex Flaherty (boat operator)

A.2 Introduction

This cruise report describes field operations in and around Koojesse Inlet during two field seasons in 2010 (BIO 2010307) and 2011 (BIO 2011303 & 2011307). Koojesse Inlet sits on the northwest coast of Frobisher Bay on southern Baffin Island in Canada's Subarctic. It is macro-tidal with an 11.3 m spring tidal range. It spans 4 km at its mouth, and runs 4 km long. It is located between Tarr Inlet and Laird Peninsula to the east and Peterhead Inlet the west.

A.2.1 Objectives

To collect evidence of erosional and depositional processes at work on and just beyond the extensive tidal flats in the bay, measure current and wave energy in the system, and map the offshore substrate and bedforms. The work was partially in support of Scott Hatcher's M.Sc. thesis aimed at understanding coastal hazards in the city of Iqaluit in the context of climate change. Lack of an adequate baseline required the collection of data over the years reported here in order to better understand how this physical setting might affect the cultural and infrastructural hazard landscape into the future.

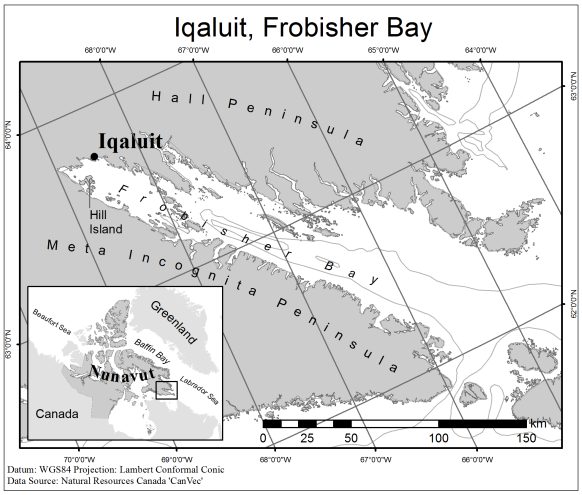

(a) Location of Iqaluit in Frobisher Bay

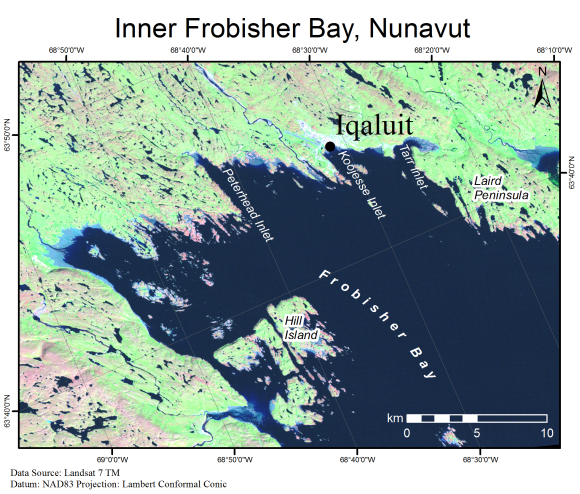

(b) Inner Frobisher Bay

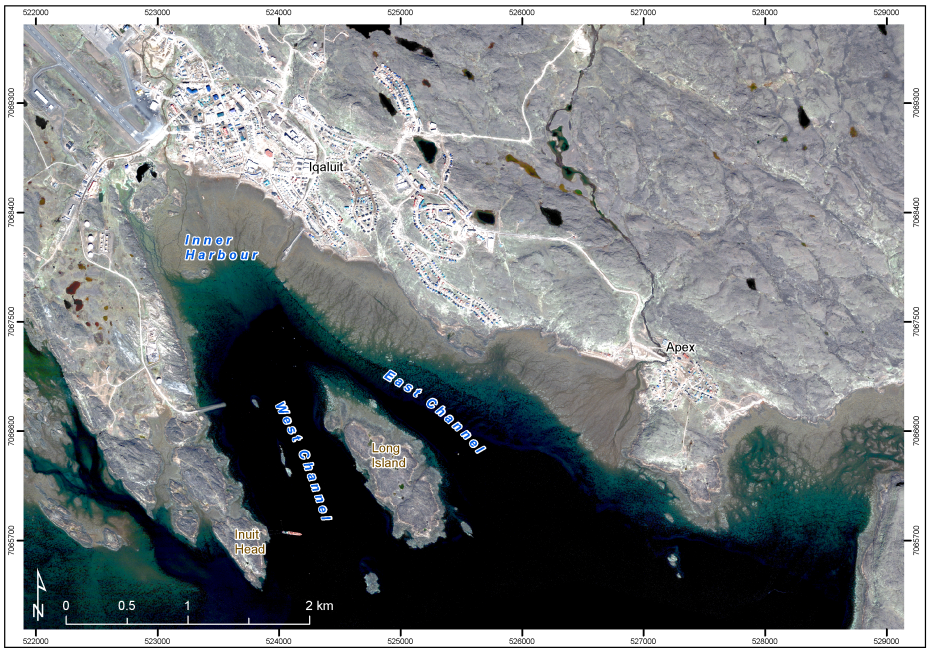

(c) Overview of Koojesse Inlet, with Frobisher Bay to the south and the city of Iqaluit on the northern shore. The projection is NAD83 CSRS UTM zone 19.

Figure A.1: Study area

A.3 Data Collected

A.3.1 RTK Surveys

Real-time Kinematic GPS surveys were conducted throughout the study area using an Ashtech Z-Extreme survey-grade receiver to collect high-precision coordinates at

locations of interest in the bay (See Figure A.3).

Survey control was provided by local CCRS benchmarks, and correction to tidal surfaces was done by surveying in the FB1968 coast guard tidal benchmark. During both 2010 and 2011 benchmarks M009000 and CCM24 (Table A.1) provided local control. A temporary benchmark were established closer to the survey sites at CAP (Table A.1), with check points on the east and west flukes of the anchor mounted at the Iqaluit cemetery (Table A.1). All surveys were corrected to M009000, with listed horizontal and vertical root-mean-square errors averaging 0.013 m and 0.017 m respectively.

Table A.1: Control positions used to correct RTK-GPS surveys in 2010 and 2011.

ID	Easting (m)	Northing (m)	Elevation (Ellipsoidal) (m)	Elevation (CGVD28) (m)
M009000	522372.23	7068886.14	22.34	32.506
CCM24	524629.620	7069268.499	118.234	128.4
CAP	524511.59	7068063.94	3.524	13.69

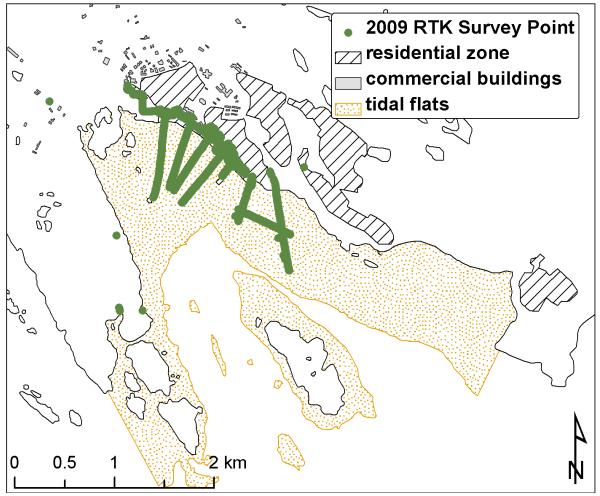

(a) 2009 RTK Field Surveys.

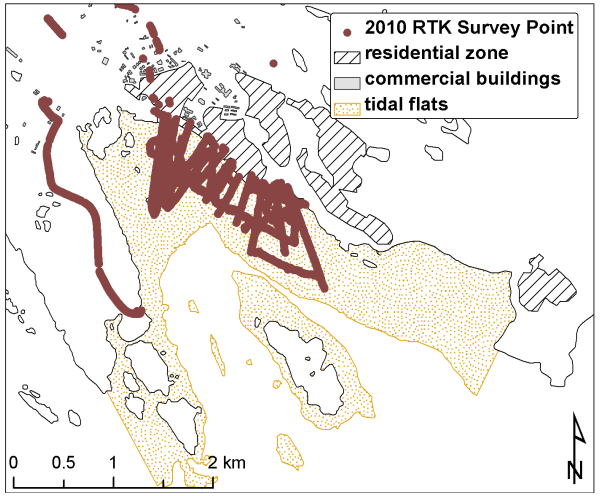

(b) 2010 RTK Field Surveys.

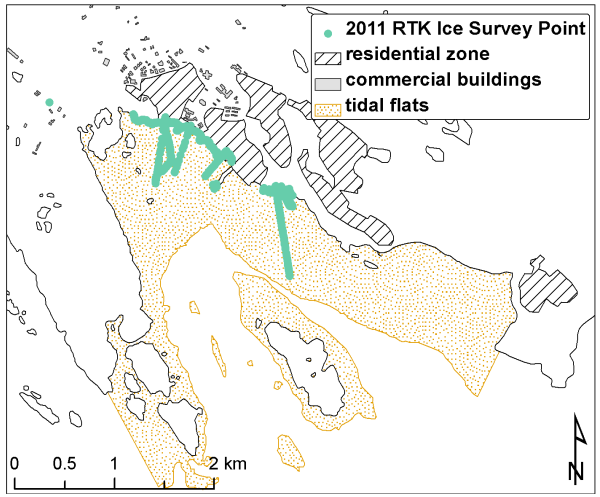

(c) 2011 RTK Field Surveys from February 2011.

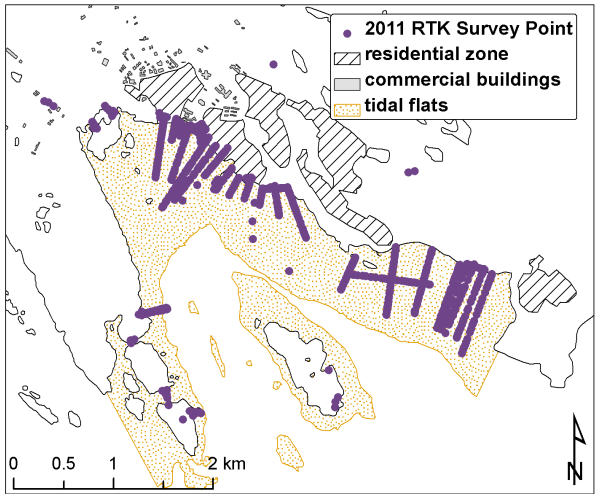

(d) 2011 RTK Field Surveys from July/August 2011.

Figure A.2: RTK-GPS survey points from 2009, 2010, and 2011 field seasons.

A.3.1.1 Tidal Flat Transects

Twenty shore-normal transects were collected along the flats, with two additional shore-parallel transects used to map shore-parallel sediment transport. The initial plan was to re-survey the transect lines drawn in the 2009 surveys conducted by Don Forbes and Dominic St.Hilaire. Once this was finished, further shore-normal transects were established in order to a) be re-surveyed in 2011, and b) provide a robust overview of shore-normal topography on the tidal flats in the absence of DEM or Bathymetric information. The transects were drawn approximately shore-normal using Quickbird satellite imagery of the area to create 'endpoints', which were then transferred to a handheld GPS for navigation during the kinematic RTK survey.

A.3.1.2 Tidal Flat Topography Kinetic Surveys

Kinetic surveys meant to 'fill in' topography on the flats in order to extend the DEM. These surveys used the RTK GPS system in kinematic mode sampling points every 1 m and running roughly transverse to the defined shore-normal transects.

A.3.1.3 Coastal Infrastructure

Surveys of foundation heights of coastal infrastructure were conducted in order to provide information of inundation potential from sea level rise and storm water inundation in the future.

A.3.1.4 Ice surveys

In February of 2011 ice surveys were conducted on the winter sea ice. These included re-occupying three of the established shore-normal transects, as well as mapping the edge of the icefoot along Iqaluit beach.

A.3.1.5 Other

- Water level elevations with time stamp to validate RBR tide measurements, as well as predicted water elevations.
- High water debris lines on Long Island and around the sewage pond.
- Control point surveys used to establish local control, as well as tie the surveys into the CSRS network.
- Vegetation lines on the beach in order to measure shore-normal orientation.
- High water limit kinetic surveys to orient transects deviation from shore normal.

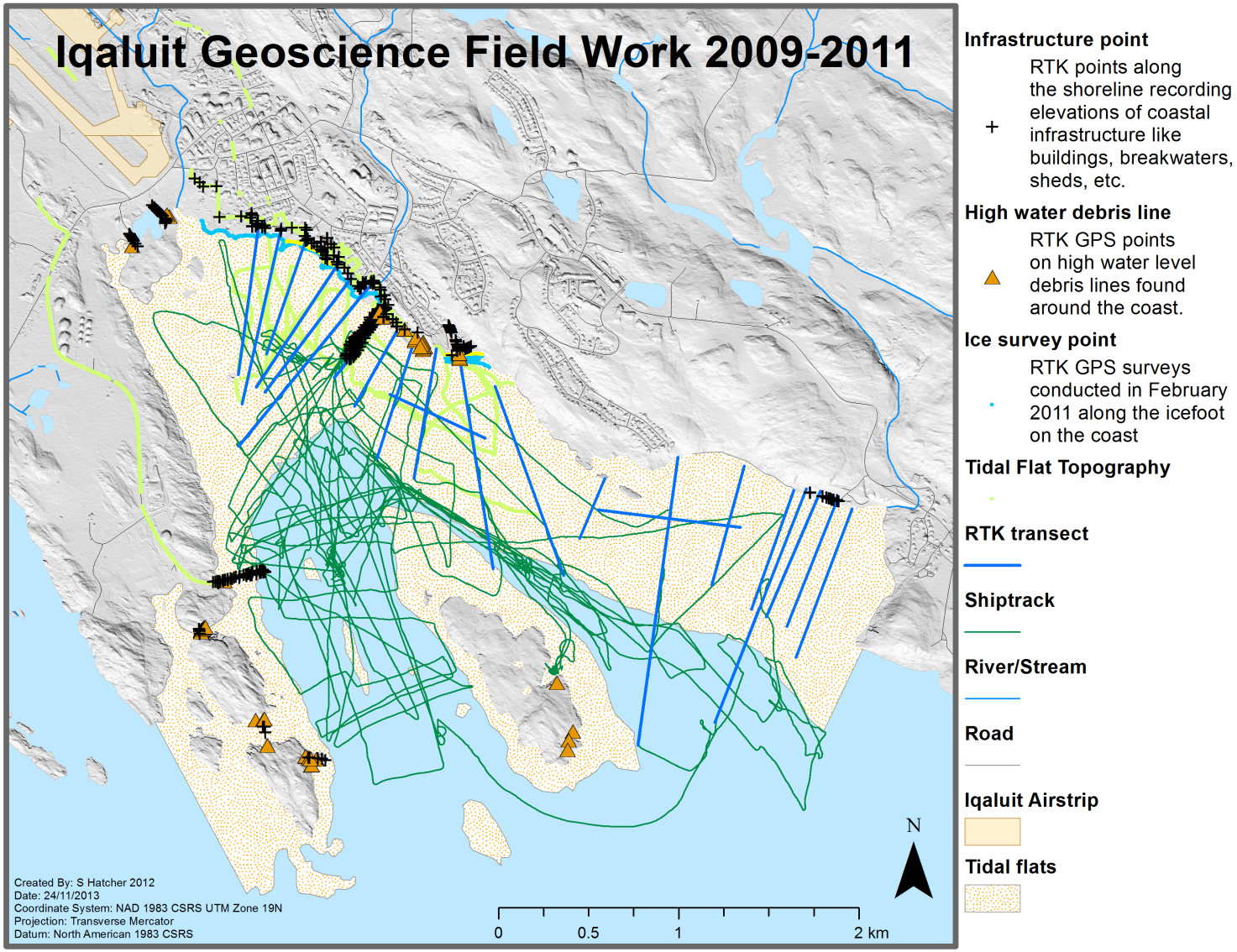

Figure A.3: Map of surveys conducted during the 2009, 2010, and 2011 field seasons in Iqaluit, Nunavut.

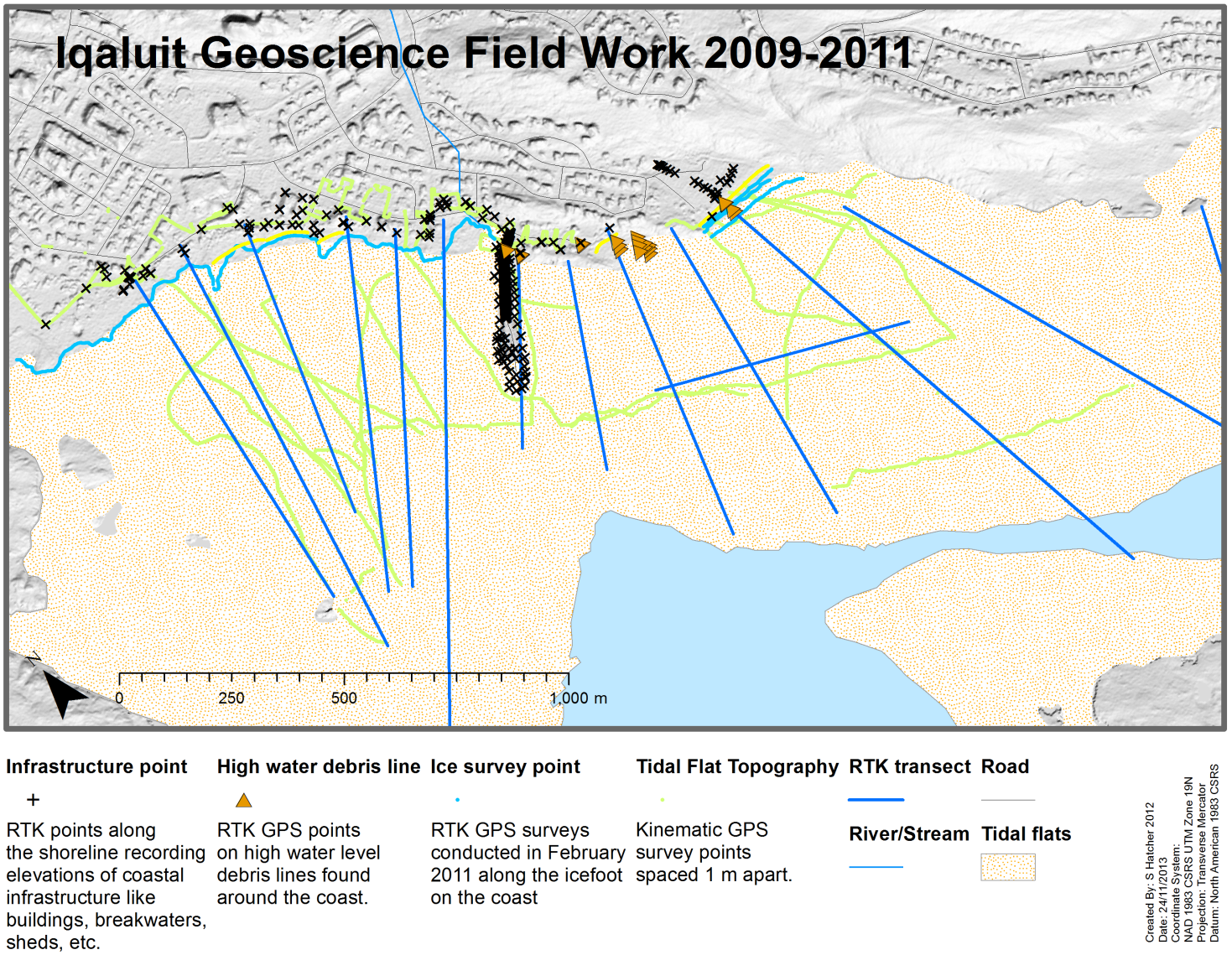

Figure A.4: Map of surveys conducted along the Iqaluit shoreline during the 2009, 2010, and 2011 field seasons.

A.3.2 RBR Deployments

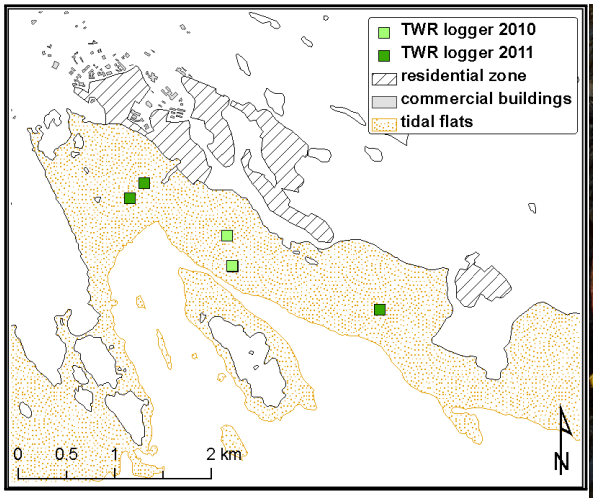

(a) Map showing location of Tide and Wave data loggers on the tidal flats in Koojesse Inlet.

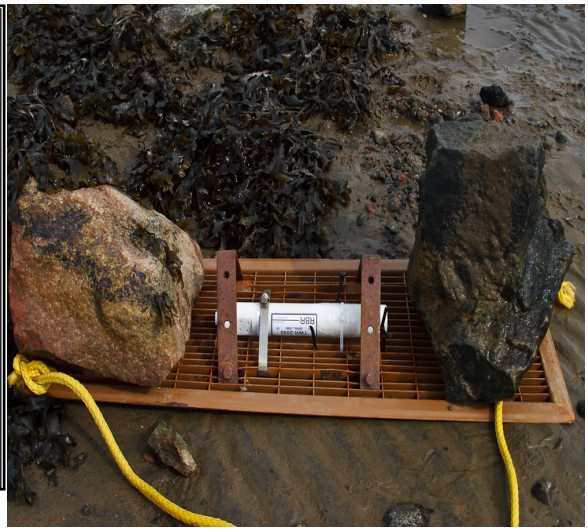

(b) RBR moorings were made either from bolted strap ties, or from flooring grates.

Figure A.5: RBR tide and wave recorders

A total of six RBR TWR-2050 pressure transducer tide and wave recorders were deployed over the two year span. These instruments have a published accuracy of 0.05% in the depth channel (± 5mm at 10 m depth) and ± 0.005 ℃ in the temperature channel.

A.3.2.1 Time Periods

Year	Period of Observation
2010	Aug 18 - Oct 19
2011	Jul 16 - Sep 18

Table A.2: Schedule of RBR tide and wave recorder (TWR) deployments

A.3.2.2 Locations

In 2010, the TWR's were deployed on a surveyed transect line. They were placed on the flats at the farthest end of the transect (near LLW) as well as approximately three-quarters of the way along the transect. This was done to allow comparison between the instruments in order to look at wave attenuation over the tidal flats. In 2011, the deeper deployment from 2010 was used, as well as three new deployments. Two were used to mirror the study from 2010 (two points along a shore-normal transect), only on a line directly in front of the city (See Figure A.6). The last deployment was used on the Apex side, near the outlet of Tarr Inlet, to look at differing wave climate due to increased SE exposure on the Apex side.

A.3.2.3 Separation on 0 m depth points

The loggers were placed at roughly 2 m CD elevation on the flats to record waves over the flats. Because of this there was a period during low spring tides where the instruments were dry. All records were separated into 'wet' and 'dry' irregular time series in order to facilitate analysis.

A.3.2.4 Measured Parameters:

- Depth (m)
- Chart Datum water level through RTK GPS surveyed position
- Water Temperature (℃)
- Air Temperature on surface of flats after exposure (℃)
- Tidal Slope (m/hr)
- Wave Statistics (m)
  - Average Wave Height
  - Maximum Wave Height

- 1/10 Wave Height
- Significant Wave Height
- Wave Energy (J/m^2)

A.3.3 ADCP Deployments

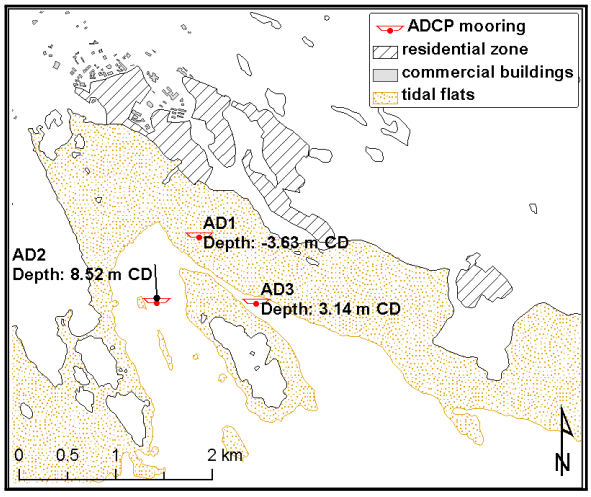

Figure A.6: Map showing location of Acoustic Doppler Current Profilers (ADCP) on the tidal flats in Koojesse Inlet.

The first (AD1) was set on the tidal flats near the LLW line. This was done in order to show current velocity on the flats, and to be able to compare that with the velocities recorded during a spring tidal cycle in the channels within Koojesse inlet, running between Long island and the mainland.

AD 2 was deployed in the channel running between the Western side of Long island and Polaris reef. This is the deeper channel running into Koojesse inlet, and was a good place to measure the current velocities found in the deeper channel during a spring tidal cycle.

AD3 was deployed in the channel running between the tidal flats in between Apex and Iqaluit and Long Island's northern coast. This is a shallower channel, which was hypothesized to have a stronger current signature than AD2 due to constriction.

A.3.3.1 Time periods and locations

Deployment	Time Period
AD1	July 24 2011 11:40 - July 26 2011 13:28
AD2	July 26 2011 18:18 - July 29 2011 17:05
AD3	July 29 2011 17:25 - Aug 3 2011 15:40

Table A.3: Schedule of Nortek Aquadopp Acoustic Doppler Current Profiler (ADCP) deployments

A.3.3.2 Separation on 0 m depth on AD1

AD1 was on the flats, and so was subject to periodic exposure. The record was split at these points of 0 depth to produce an irregular time series.

A.3.3.3 Measured Parameters

- Depth (m)
- Temperature (℃)
- Current Velocity (m/s) and Direction (up to surface in 50 cm cells)

A.3.4 Sediment Samples

Surface sampling consisted of trowel samples ranging in depth from 2-5 cm below the surface. Forty-six samples spread over tidal flats and upper beachface were taken. Marine grab sampling was done from in the offshore using an Ekman grab sampler, with depths ranging between 2-5 cm. Nine grab samples were taken from within Koojesse Inlet.

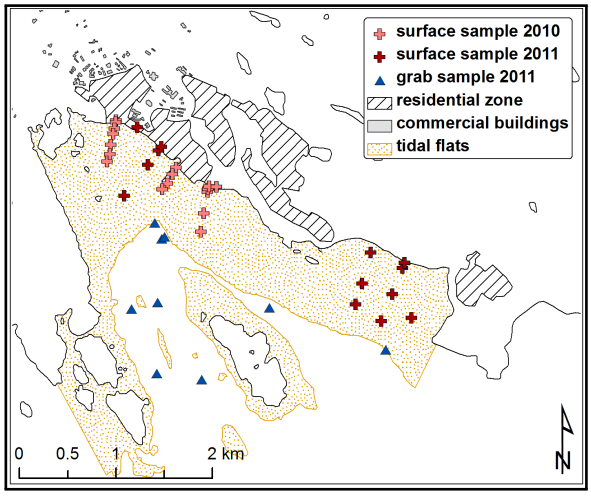

Figure A.7: Map showing location of surface samples on the tidal flats in Koojesse Inlet and offshore grab samples in the bay.

A.3.4.1 Surface Sediment Samples

46 samples spread over tidal flats and upper beachface. Depths ranging from 0-2 to 0-5 cm

A.3.4.2 Marine Grab Samples

9 Ekman grab samples from various locations within Koojesse Inlet. Depths of 0-4 cm

A.3.5 Boat Survey Logistics

The small vessel survey logistics were determined by the timing of the tides in Koojesse Inlet. The small 18' wooden freighter canoe (Figure A.8b) was chosen as a survey vehicle with the macro-tides in mind. The "drying" of the tidal flats during spring low tides, however, made survey work impossible at these times. Therefore, boat-work was conducted at mid to high tide at whatever hours of the day that was. Because of this, as well as the multiple sensors being used for surveying, the mount had to be

removable at the end of each working day.

The boat was set up to accommodate the sensor mount and three or four crew. The crew included Scott Hatcher, Gavin Mansion, Alex Flaherty, and occasionally one deckhand. The sensor mount was made-fast across the gunnels, and had a right angle steel pipe mount reaching down to 20 cm depth below surface (Figure A.8a). This system provided the safest way to conduct shallow water surveys, but had inherent problems with systematic boat-motion induced noise. It also severely limited the travel speed of the boat while surveying was underway - a cost in ground covered for the benefit of shallow water capability.

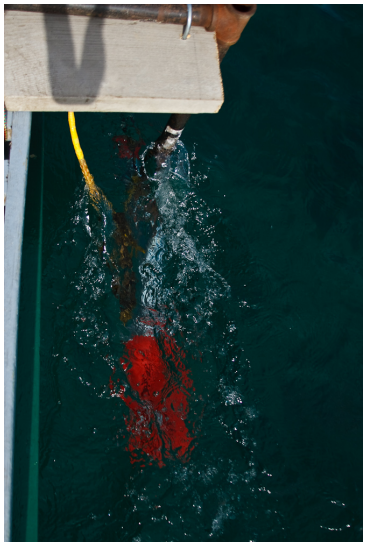

(a) Sensor mount setup with the Sidescan Sonar

(b) View from the stern of the 18' wooden freighter canoe

Figure A.8: Photographs showing the layout of the survey boat

A.3.6 Boat Survey Planning

Navigation was provided by two basic map grade GPS receivers on-board. Planning navigation was done using a handheld Garmin®GPS-Map 76. Uploaded waypoints from the projects GIS provided bearings for continuing coastal transects done with

ground-based surveying, and collected waypoints gave position information for deployed instruments and grab samples. An integrated GPS antenna and receiver in the Lowrance®single beam echosounder provided position information to the depth surveys. This echosounder was used as a live depth monitor as well as a depth data logger for all boat-work.

There were a number of goals for the ship surveys, which included:

1. Extending GPS transect lines over the tidal flat edge and into the deeper bathymetry of the bay.

2. Providing preliminary single beam sounding lines in a roughly spaced grid throughout the inlet in order to extend the elevation information from land into the seabed.

3. Sample seabed substrate and sediment in areas of interest to the morphology of the overall area.

4. Provide underwater video tows that would further show morphological differences in substrate make up within and around the inlet.

A.3.7 Sidescan Sonar

The sidescan survey system employed was an Imagenex dual frequency SportScan© digital sonar transducer array. The two transducers operate at 330/800 kHz with beam widths of 1.8°×60°(330 kHz) and 0.7°×30°(800 kHz). This results in relative range resolutions of 0.06 m (15 m "shallow" mode), 0.12 m (30 m "medium" mode), and 0.24 m (60 m "deep" mode). The system was hard-mounted to the boat by a fastened arm running down the starboard gunnel, which put it at a depth of 0.5 m. This translates into a swath width of 160 m in 30 m depths, and 110 m in shallow coastal waters (like on the flats).

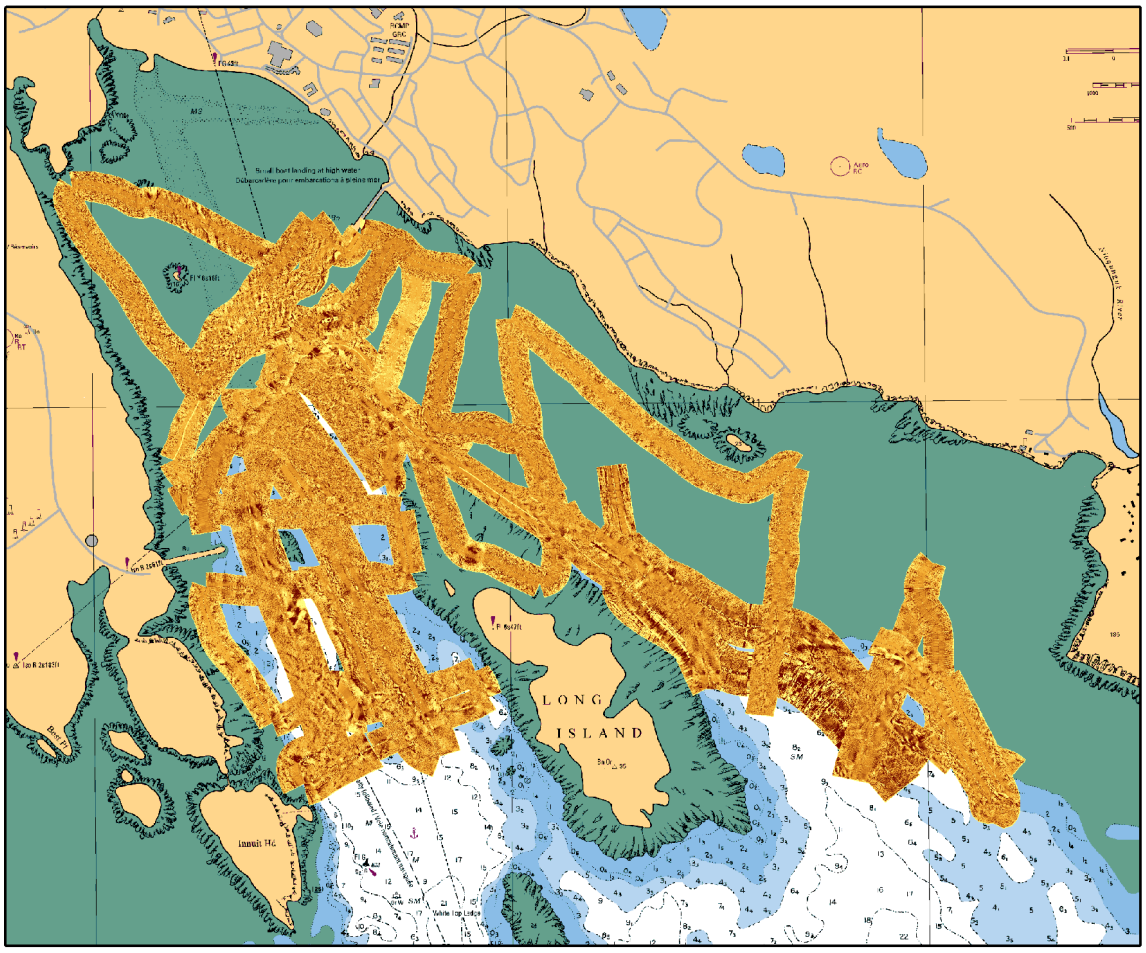

Figure A.9: Sidescan sonograph mosaic within Koojesse Inlet.

A.3.8 Strata Box Sub bottom profiler

The sub-bottom profiler used was a SyQwest StrataBox© low frequency sound profiler. The unit operates at 10 kHz, which provides a vertical resolution of 0.06 m with 40 m bottom penetration. It was mounted on the same arm as the sidescan system, and so was hard mounted at 0.5 m depth. Lines were run travelling over the flats, as well as off the edge of the flats. Also, a line over the Apex flats was done for use in comparison, as well as one through the Apex channel toward Long Island. The abundance of boulders and outcrops of coarse substrate made it hard to resolve sub-bottom stratigraphy on the flats. The only place that gave data was over the "sealift"

road; the road on the flats cleared annually to allow barge unloading at low tide.

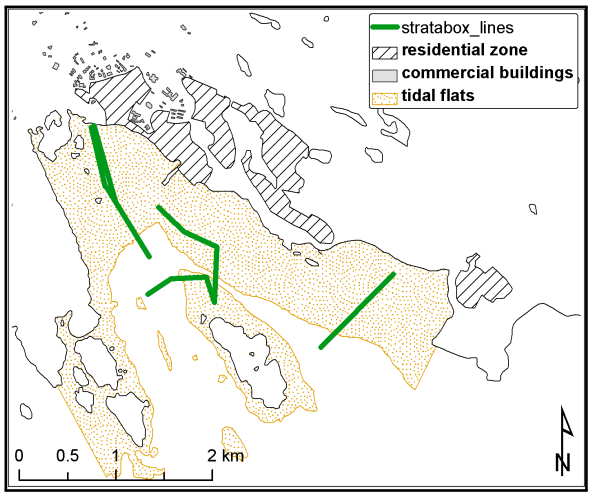

Figure A.10: Map showing strata box lines in Koojesse Inlet.

A.3.9 Marine drop video camera

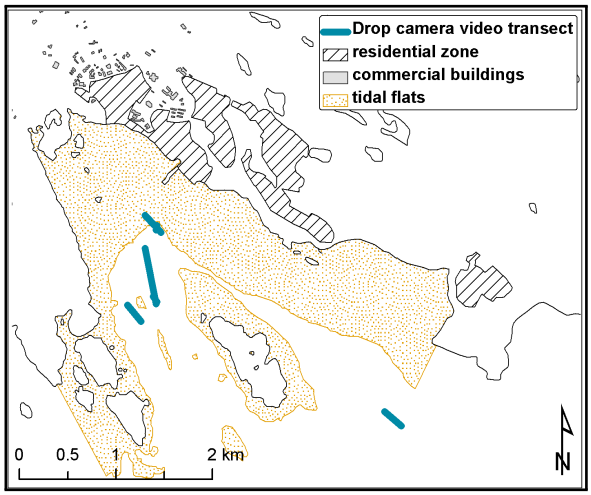

Figure A.11: Map showing location of drop camera underwater video transects in Koojesse Inlet.

Table A.4: Marine video camera files and dates

Transect file	Start time
DVR010101_0005_001.avi	July 26 2011 21:02 UTC
DVR010101_0022_001.avi	July 26 2011 21:18 UTC
DVR010104_1830_001.avi	July 30 2011 15:26 UTC
DVR010101_1906_001.avi	Aug 1 2011 16:03 UTC
DVR010106_2142_001.avi	Aug 1 2011 18:38 UTC
DVR010106_2226_001.avi	Aug 1 2011 19:22 UTC

A.4 Scientific Summary

A.4.1 Study Area and Related Work

The study area is Koojesse Inlet, a small inlet located at the head of Frobisher Bay on the southeastern end of Baffin Island in the Canadian subarctic. Koojesse houses the city of Iqaluit, the capital of the territory of Nunavut and home to 6,700 people (Statistics Canada, 2012). The inlet is east of the Sylvia Grinnell river, and in between Tarr Inlet and Peterhead Inlet (See Figure A.1a). Surrounding bedrock is pre-Cambrian gneiss with outcrops of Paleozoic sediments (Hodgson, 2005). This material is the source for the boulders that were deposited on the tidal flats in the area.

Tidal flats are quite common on most of the coast in Frobisher bay, due mainly to the macro-tides found in the bay. Semi-diurnal tides here have a spring range of 11.3 m and a neap range of 7.8 m (Dale et al., 2002) In Koojesse Inlet specifically, it appears the flats were formed proglacially during the last glaciation, the base layer deposited in brackish coastal waters at the edge of the “Iqaluit” river delta formed on a paleotributary of the Sylvia Grinnel river (Hodgson, 2005; McCann et al., 1981; McCann & Dale, 1986)

Field seasons conducted in 1981 and 1982 in and around Koojesse Inlet by McCann,

Dale, and Hale from McMaster University established the current geomorphological understanding of the tidal flats near Iqaluit. There work focused on sedimentary zonation and processes on the low-slope flats, as well as the process and dynamics of the break up and freeze up of the annual sea ice cover on the flats (McCann et al., 1981). Aerial surveys of these ice processes revealed their importance in both the transportation of sediment on the flats through rafting and entrainment, but also the importance of offshore drift ice in containing the fractured ice, and its entrained sediment, on the flats (McCann & Dale, 1986). This cycling of sediment is an important part of the sediment budget on the flats, and is a key aspect in looking at how things might change in a different sea ice climate.

Measurement of boulder movement on the flats, along with a theoretical treatment in Drake & McCann (1982) of boulder movement, came out of studies on the Iqaluit tidal flats. The movement of boulders on the flats is a variable that is both constant, and surprisingly dynamic. In some cases boulders with a diameter of 0.5 m were moved greater than 30 m over a single ice season (McCann & Dale, 1986). The lack of a cohesive boulder barricade on the Iqaluit tidal flats, as is found in other analogous environments (McCann et al., 1981), remains a mystery. It appears, however, that given the extent of the Koojesse Inlet flats, small quasi-barricades have formed intermittently along the lower flats. Why they have not been connected over time by ice processes is unknown.

The process of sea ice freeze up and break up, as said earlier, formed a substantial aspect of previous work on the flats. The ice surveys conducted in 2010 and 2011, over top of the summer time surveys, will be able to provide a better measurement of mean thicknesses found over the flats, as well as describe the motion of the ice overtop the flats with the daily tide floating and resting a large amount of ice.

A.4.2 Morphology of Koojesse Inlet

A.4.2.1 Tidal flat topography

Within Koojesse Inlet the tidal flats cover an area of 6.4 km ^{2} delineated shoreward by the lower beachface and seaward by the slope leading into the tidal channels running out of the inlet A.12. They are characterized by a low slope gradient with extensive boulder cover and fine silt surface material with discontinuous sandy pebble outcrops in ebb tide channels. Tidal flat width varies considerably throughout the inlet, with the greatest widths on the eastern side (1100 m) and the smallest widths on the western side (150 m). Within the inlet, the flats run 4.6 km on the eastern side and 3.7 km on the western side. Three main channels flow offshore of the flats; a narrow shallower channel running between Long Island and the Apex trail running east of Iqaluit, and two deeper channels running between Long Island and Inuit head, divided by Polaris reef A.12.

The inlet has three channels leading in and out. One leads between Long Island and the shoreline east of the city, and the others lead out between Long Island and Inuit head, and are divided by Polaris reef and Black ledge in the middle. The Apex channel is narrower and shallower than the other two (See Figure A.12). The Apex channel has a minimum depth of 1 m CD, and on the western side of Long Island the channels have a minimum of 2.6 m CD on the east and 7.6 m CD on the west. The latter, however, appears to have been dredged in the past.

Given the high tidal range of the inlet, and the limited channels leading into it, there was an initial hypothesis that currents would be strong in the channels, and that the bottom would be current scoured. The findings from the ADCP's did not confirm this, instead showing current levels not greater than 1 m/s, and almost entirely focused on the top 1 m of the water column and decreasing with depth. Because of this, the

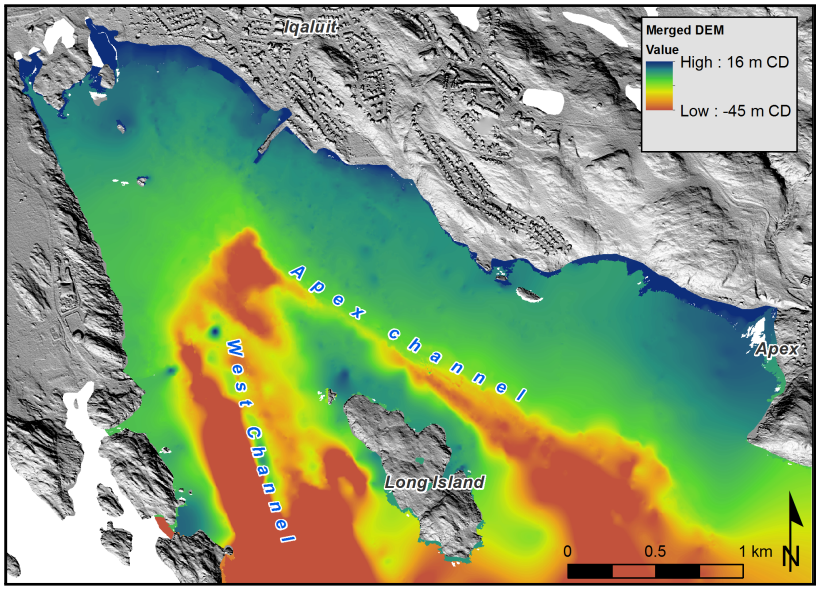

Figure A.12: Digital elevation model for Koojesse Inlet constructed from RTK GPS points in the intertidal zone and single beam echo soundings in the offshore channels. A constrained spline interpolation was used to create the model from elevation points of differing densities throughout the region.

bottom substrate found within the inlet was of very fine silt composition with little evidence of current scouring found in the drop-camera transects.

A.4.2.2 Surficial sediments

The surficial material found on the flats ranges from boulders to fine silty sediments. The sediments found on the surface of the flats are a mixture of fine silty sand with coarser sand and pebble clasts intermixed within ebb tide channels and areas of ice scour and deposition (Leech, 1998). Multiple studies of the sedimentology of the flats surface have shown no fining landwards trend (Leech, 1998; McCann et al., 1981; Dale et al., 2002), which is a common characteristic of temperate tidal flats (Dionne, 1992; Dionne & Poitras, 1998). Boulders are plentiful on the flats [*add boulder flat photograph], and are arranged in varying densities and groupings across the flats. They seem to be concentrated more on the eastern end of the flats, perhaps because of

the typical circulation of ice during freezeup. There exists only discontinuous and faint boulder barricades on the outer flats that correspond roughly to LLWLT, although they are far less defined than in other subarctic settings (McCann et al., 1981).

The substrate materials found off the flats in the offshore channels varies widely as well. Drop camera transects have shown the existence of boulders similar to those found on the flats, although they were very rare and were found amongst angular clasts near the western breakwater and so likely a product of human construction. Elsewhere there exists very fine draped silt substrate which seems to be affected very little by the tidal currents found in the inlet. This description, however, holds only for the inner inlet. Offshore of Apex to the east of Long Island the substrate was found to be an arrangement of cobbles with silt filled cracks. These were found at roughly the same depths as the inner channel fine materials, and could be due to increased exposure to southerly swell or increased tidal current influence (the ADCP measurements were not taken nearby to where cobbles were found). Sidescan imagery indicates a similar outcrop just west of Polaris reef in similar depths, but this could not be verified with the drop-camera.

The sidescan sonar imagery revealed significant iceberg wallow marks at the mouth of the inlet on both sides of Long Island in about 30 - 40 m depth. Residents describe seeing icebergs at about that location, usually in mid summer and in the past.

Sub-bottom profiling carried out in this field study has corroborated previous interpretations of the tidal flats' origins. Previous studies have sampled the underlying dense clay sediments of the flats (McCann et al., 1981; Dale et al., 2002). These are interpreted to be of glacio-marine origin (Hodgson, 2005), deposited during the last postglacial high stand roughly 6500 BP about 45 m above current sea level. Sub-bottom profiles collected in 2011 show draping of this sediment underlying the flats. Irregularities in this configuration could be due to boulder placement or underlying

geology. The proliferation of boulders and cobble clasts on the substrate of the flats made it hard to collect meaningful sub-bottom data, and so this interpretation is only based on a single resolved image taken over an area where boulders are annually cleared to allow barge unloading. It is, therefore, rather weak.

A.4.2.3 Backshore

Within Koojesse inlet there exists bedrock coast and sand beach coast. Both the Iqaluit beach and the Apex beach are products of postglacial deltaic deposition by the two rivers running through Iqaluit and the Apex river respectively (Hodgson, 2005). Iqaluit is built primarily on this deltaic plain, terminated seaward by a poorly sorted sand beach system, which provides coarse material for reworking on the flats surface. Apex beach differs from Iqaluits beach in that it is constrained by bedrock cliffs on the backshore. It is also of greater slope and less extensive in the littoral direction.

A.4.3 Erosion

Simple differencing of concurrent yearly transects over the flats was not able to resolve any significant erosion or deposition over the flats, assuming a combined error estimate of ± 20 cm. Previous studies have shown that a significant amount of sediment is entrained by basal adfreezing to sea ice on the flats, but McCann & Dale (1986) describes a process by which offshore ice contains the sediment laden pack ice during breakup. The net result is significant sediment recycling over the flats, and the interpretation that erosional depositional bedforms on the flats are largely a product of reworking by ice (in winter) and currents (in summer) during high tide. Historical aerial photos support this interpretation, showing little coastline movement, except in areas where it was caused by humans. Observations, along with ADCP measurements

of currents on the flats and scatterometer TSS profiles in the channels, show very little suspended sediment in the water column on both flood and ebb spring tides. No measurements were taken during high wind events, however, which could significantly alter the suspension load.

A.4.4 Significant Findings

- Currents recorded during spring tidal cycles showed low velocities, and concentration of velocity on the top 2 m of the water column. Consequently, scatterometer profiles showed little suspended sediment in the channels due to tidal currents, with only local reworking in shallow water on the flats themselves.
- The seaward edge of the flats was found to correspond closely with the LLWLT water level, and thus represents the areas of 0% aerial exposure.
- The substrate found off the tidal flats varies depending on depth and position in the inlet. More sheltered areas on the inner inlet show very fine draped silt material, with sporadic cobble. There appears to be boulders similar to those found on the flats, but with much less density.
- Sub-bottom profiles seemed to support the earlier interpretation of a glaciomarine origin of the sub-flat marine clay material, showing draped stratigraphy up to a depth of 4 m.
- Transect differencing on the flats showed no resolvable erosion during the three year study period.

A.5 Summary of Operations

2010

Cruise BIO 2010307

Day **230** (Aug 18 2010)

- Set up base on M009000 Pillar (near EC climate station).
- Surveyed tidal bm 'FB-1968' (20:23).
- Kinematic survey on road leading out to the dump in order to validate DEM in this area.
- Tagged temporary bm near M009000 (bm_7966) at 21:38

Day **231** (Aug 19 2010)

- Iqaluit Control:
- CORRECT CAP COORDINATES
- 524511.5914 E 7068063.9359 N 3.524 Z (WGS84 Ellips)
- ptnum 232-236, kinetic on waterline off by 0.25 m due to ant. height error.
- Set up base (CAP)
- Got TR-6 (tn11) and TR-5 (tn9) from 2009 surveys (going from deep to shallow).
- Did deep part of tr-6 (tn11) then whole of tr-5 (tn9) then back to finish tr-6 (tn11).
- Points along small breakwater.
- kinematic waterline survey
- trundle around cemetary

Day **232** (Aug 20 2010)

- Set up BASE at CAP (near cemetary). Corrected to known points from Aug 19 survey.

- Surveyed spot elevations at base of main breakwater, then followed outline of breakwater road.
- Took 4 surface sediment samples along the east side of the main breakwater.
- Due to timing, we surveyed the outer sections of tn6, tn4, tn3, and tn1. In between lines we ran kinematic topo.
- Later in the day we returned and surveyed the inner parts of tn6, tn4, tn3, and tn1. There was a gap in the middle of the lines that needed to be filled.
- Surveyed culvert elevations near 2nd pumping station.

Day **233** (Aug 21 2010)

- Set up BASE on CAP using corrected coords from Aug 19.
- Surveyed Geophysics line with sampling along the line (smpl 5-11).
- Ran midpoints of tn1, followed by extending tn1 on the outer end.
- Ran midpoints of tn3, tn4, and tn6.
- Ran tn10 off cemetary, with samples 12-16.
- Took sample 17 on cemetary beach (14:16)
- Ran inner points of tn7 and tn8.
- Got foundation heights (RTK) on Fisheries building and the Museum.

Day **234** (Aug 22 2010)

- Set up BASE at CAP using Aug 19 survey.
- Took photos of sample sites (smpl 1-17)
- Finished tn7 and tn8
- Surveyed identified features from the Quickbird imagery
- Surveyed Coast Guard Station fence line, as well as pumping station 1.
- Surveyed water line
- Tagged cemetary anchor fluke for control.

Day **235** (Aug 23 2010)

- Set up BASE at pillar M009000
- Topo survey on the airstrip curtain.
- Surveyed tn2 and tn5
- Surveyed shallow RBR (12540) position.
- Tagged CAP and cemetary anchor fluke for survey control.

Day **236** (Aug 24 2010)

- Downloaded RBR's (12539, 12540)
- Ran tn12 and end of tn10.

2011

Cruise BIO 2011303

Day **43** (Feb 13 2011)

- Set up BASE at autonomous point on cemetary beach (to be post-processed).
- Surveyed tn11 on top of the ice.
- Ran shore-parallel surveys of a) icefoot hinge line, b) upper extent of chunk ice line, and c) the uppermost water level line (slush line).
- Surveyed small portions of tn10 and tn12.
- Captured two shore-normal linear features in the ice.
- Sunny, 5 knt SE wind, -28 degC.

Day **44** (Feb 14 2011)

- Set up base at temp rock on the end of the main breakwater. Provided control by taggin pillar M009000, then surveying the cemetary anchor fluke and the basestation from feb 13 2011.
- Surveyed ice pile up on the western side of the end of the main breakwater.

- Surveyed ice sitting above tn6, tn3, and tn1.
- Topo kinematic on top of ice near tn1.
- Surveyed the pile-up line running the entire length of the city shoreline.

Day **196** (July 16 2011)

- Deployed RBR's (21504, 21503)
- 21503: WP004, 18:00
- 21504: WP005, 18:55

Day **197** (July 17 2011)

- Set up BASE over pillar M009000.
- tagged bm_7966 near pillar.
- Surveyed in RBR 21504 and 21503 elevations.
- Spot elevations on the corners of the end of the main breakwater.
- Surveyed tidal benchmark FB_1968.
- Established second temporary benchmark (CAP2) near cemetary.
- Surveyed in CCM24 on top of the hill for control.
- Tagged bm_7966 again.

Day **199** (July 19 2011)

- Set up base on CCM29 on top of the hill by the francophone school. BASE point was autonomous with tie in at M009000.
- Tagged M009000
- Ran Apex transects tn13, tn14, tn16, tn18, tn19, and tn20.

Day **200** (July 20 2011)

- Set up BASE on CCM29 on top of the hill. Used horizontal coordinates from July 19 survey, and vertical coordinates from CSRS database.

- Ran tn22 (shore-parrallel).
- Ran tn15, took samples 003-006
- Ran tn17, took samples 007-011
- Surveyed base heights of the monument sitting on the beach.
- Tagged bm_7966 for control.

Day **201** (July 21 2011)

- Set up BASE on M009000
- tied in to bm_7966
- Collected infrastructure elevations along shore:
- Navaid base
- Seacans
- Seashacks
- Manhole near pumping station
- Surveyed tn1
- Surveyed tn3, took smpl 0012
- Collected infrastructure
- Seacans
- Courthouse
- Water Booster station
- Small temp transect off eastern side of minor breakwater.
- Ran tn4
- Ran tn5 with smpl 013-016
- Surveyed sewage pond containment causeway elevations and storm debris lines near causeways.

Day **202** (July 22 2011)

- Deployed two additional RBR's (21560, 21561)
- 21560: off Apex,
- 21561: off Breakwater, deployed 22:13.

Day **203** (July 23 2011)

- Set up BASE on CCM29.
- Captured smpl003 site, as well as the two RBR locations from July 22.
- Tied in to bm_7966, as well as M009000.

Day **204** (July 24 2011)

- Set up BASE at CAP2 near cemetary.
- Deployed AD1 on tidal flats off cemetary.
- Tied in to cemetary anchor fluke, and M009000.

Day **205** (July 25 2011)

- Set up BASE at M009000
- Tied in to bm_7966
- Captured elevation on pumping station 2
- Ran inner part of tn2
- ran inner part of temp line 2
- Ran two kinematic surveys along the seaweed line on the beachface in front of the city in order to orient transect distance to shore-normal.
- Ran inner part of tn6
- Tied in to bm_7966

Day **206** (July 26 2011)

- Boat work

- Lowrance transducer depth: 0.3 m
- AD2 deployed 18:18, 14m dut. WP: 'AD2 actual'
- SV1 -¿ up at 21:10, 14-16 m dut.
- SV2 -¿ down at 21:17.
- Grab sample. 16 m dut. WP: 'wp0022'
- ES lines running off main breakwater towards causeway. Then causeway to long island, then on to Inuit head.
- ES lines across tn from cemetary to Long island.

Day **207** (July 27 2011)

- Boat work
- ES + SS line across flats at ln1 -¿ 230 deg true bearing.
- CTD 0024 - Start 20:20, End 20:23 FAILED
- CTD 0025 - Start 20:38, End 20:41. FAILED
- Grab sample 20:45. WP: "G0026". 19 m dut.
- ES line on 270 deg bearing. Start 21:02.
- ES line on 90 deg bearing. Start 21:10.
- ES line on 240 deg bearing. Start 21:15.

Day **208** (July 28 2011)

- Sidescan and Echosounder line to fill in hole of flats.
- Line 1 at 310 deg True, 1435h.

Day **209** (July 29 2011)

- Echosounder and Sidescan lines on 3 cross channel transects, then 3 parrallel to channel
- CTD cast at AD2, stn 0027

- Start: 15:05:13
- End: 15:06:19
- AD3 deployed off Apex.
- Deployed 17:25
- Recovered: 15:40 Aug 3 2011
- CTD cast off AD3 stn 0029
- S: 17:27:40
- E: 17:28:05
- 4.6 m depth
- CTD cast off AD3 stn 0030
- S: 17:30:30
- E: 17:31:20

Day **210** (July 30 2011)

- Launched from breakwater on a falling spring tide. Went to AD3 site to do a drop camera and make sure it was sitting upright.
- Grab sample 0031 off AD3
- Grab sample 0032 at WP"HOLE"
- CTD cast WP"HOLE" stn0033
- S: 15:36
- E: 15:36:30
- Ran Stratabox lines parrallel with ln10 then ln5 onto the flats. (Echosounder as well)
- Stratabox lines up both channels East of Long Island.
- Called it a day due to poor weather.

Day **211** (July 31 2011)

- Set up Basestation on CAP2 near cemetary. Used coords from July 19th survey.
- Tied in to cemetary anchor fluke.
- Surveyed:
- ln13
- ln6
- ln8
- beach kinematic on pocket beach near cemetary.
- beach kinematic on cemetary beach
- tied into to cemetary anchor fluke

Day **212** (Aug 1 2011)

- Sidescan and Echosounder for ln4-ln6
- Echosounder deployed at 13:30
- reboot, new file: 15:04
- Drop camera stn0035 off Apex.
- CTD stn0036
- Grab sample stn0037
- CTD cast in inner stn0038
- Grab sample 0039
- CTD cast off west channel stn0040
- Drop camera through West channel stn0041
- Grab sample West channel stn0042
- CTD cast West channel stn0043
- S: 19:00:30
- E: 19:01:30
- 16 m depth
- Grab sample stn0044

- Drop camera stn0045 off edge of flats near ln9

Day **213** (Aug 2 2011)

- CTD cast in WP"HOLE" stn0046
- 15 m depth
- rising spring tide.
- CTD cast off Inuit head stn0047 & stn0048
- 35 m depth
- CTD cast stn0049
- further north in channel than stn0048
- shallower water
- Set up basestation at M009000
- Surveyed out Inuit head
- Control on BM7966

2011307

Day **325** (Nov 22 2011)

- Survey RBR's for recovery
- Rod height = 1.219 m
- Recovered RBR 21561 "rbrapex"
- GPS session 1001 static
-
- s: 15:07
-
- e: 15:14
- RBR recording in EDT?
- Recovered RBR 21560 "rbrnew2"

- session 1002 static
-
- s: 16:03:30
-
- e: 16:15
- GPS session 9000 at M009000
- s: 17:08
- e: 17:14

Day **326** (Nov 23 2011)

- 15:00 - walked out over ice to recover RBR 21504 ”rbrdeep” off of cemetary
- 15:35 - recovered RBR21504 from an ice cover 3 cm thick.
- GPS session 2001
- 16:00 - Went out off west side of breakwater to recover RBR 21503 ”rbrnew”.
- Again, thcik ice chucnks on nearshore with think (5cm) veneer of flating puck ice in the windward catch of the breakwater.
- Once past this line there was very little ice, only frozen veneer over sediment and along rocks.
- This is a place only exposed to air during spring tides.
- 16:20 - recovered RBR21503
-
- GPS session 2002
- 18:15 - GPS session on pillar M009000 (site: 9000)
- 19:50 - Static survey on beach near monument (Apex).
- GPS session 2003, SW corner of monument.

A.6 RTK-GPS data

Shown here are graphs of all the RTK-GPS coastal transect data plotted with elevation on the vertical axis and distance cross-shore in the horizontal axis. A amp of showing the location of these transects is shown in A.3. The legend shows the year the surveyed line was collected, with additions showing "ext" (boat mounted single beam sonar extension of the line) and "ice" (on-ice survey directly over transect line during the February 2011 field visit).

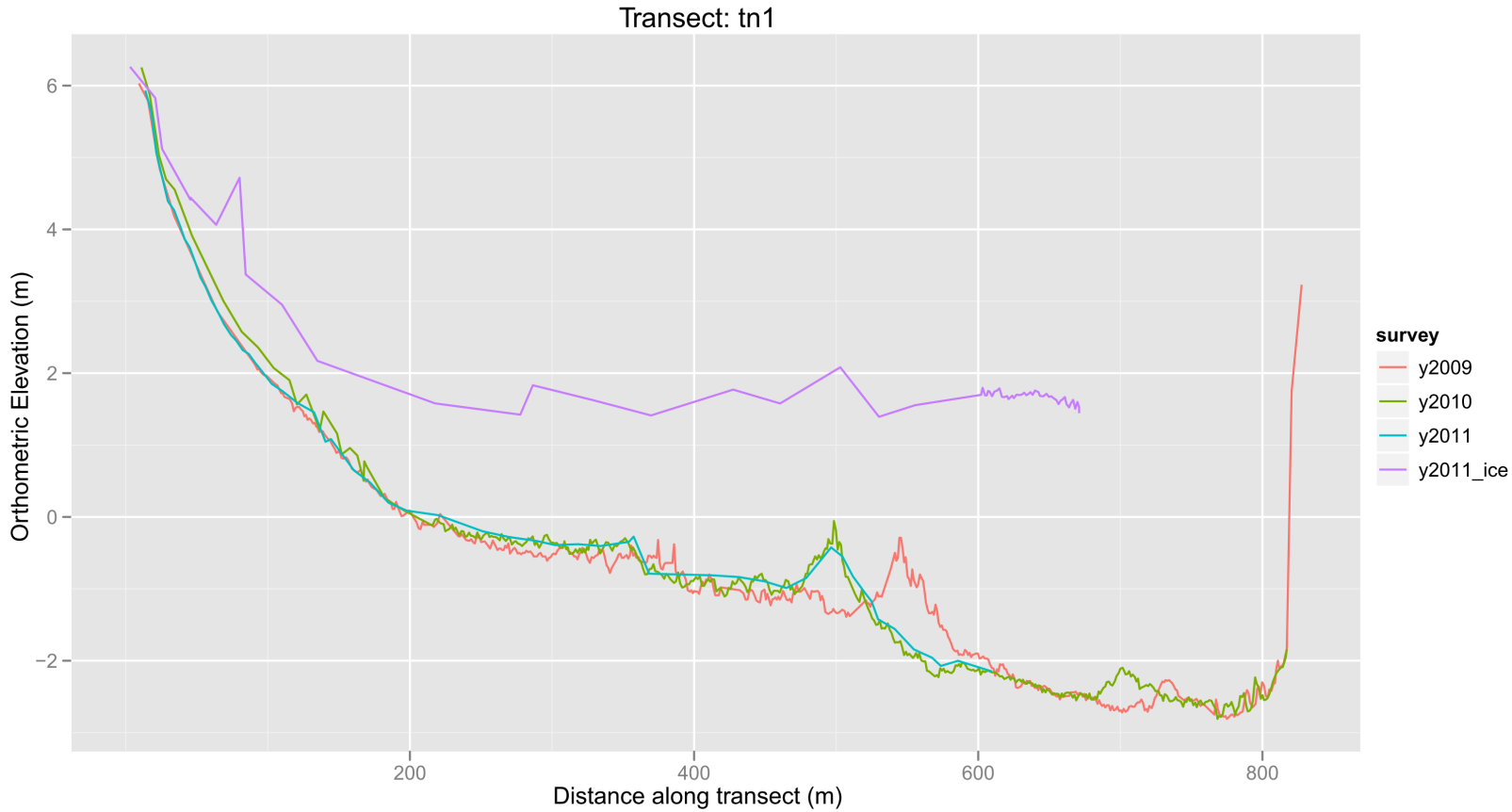
Transect: tn1
Orthometric Elevation (m)
6
4
2
0
−2
200
400
600
800
Distance along transect (m)
survey
y2009
y2010
y2011
y2011_ice


Transect: tn2
Orthometric Elevation (m)
4
2
0
−2
−4
200
400
600
800
1000
Distance along transect (m)
survey
y2010
y2011

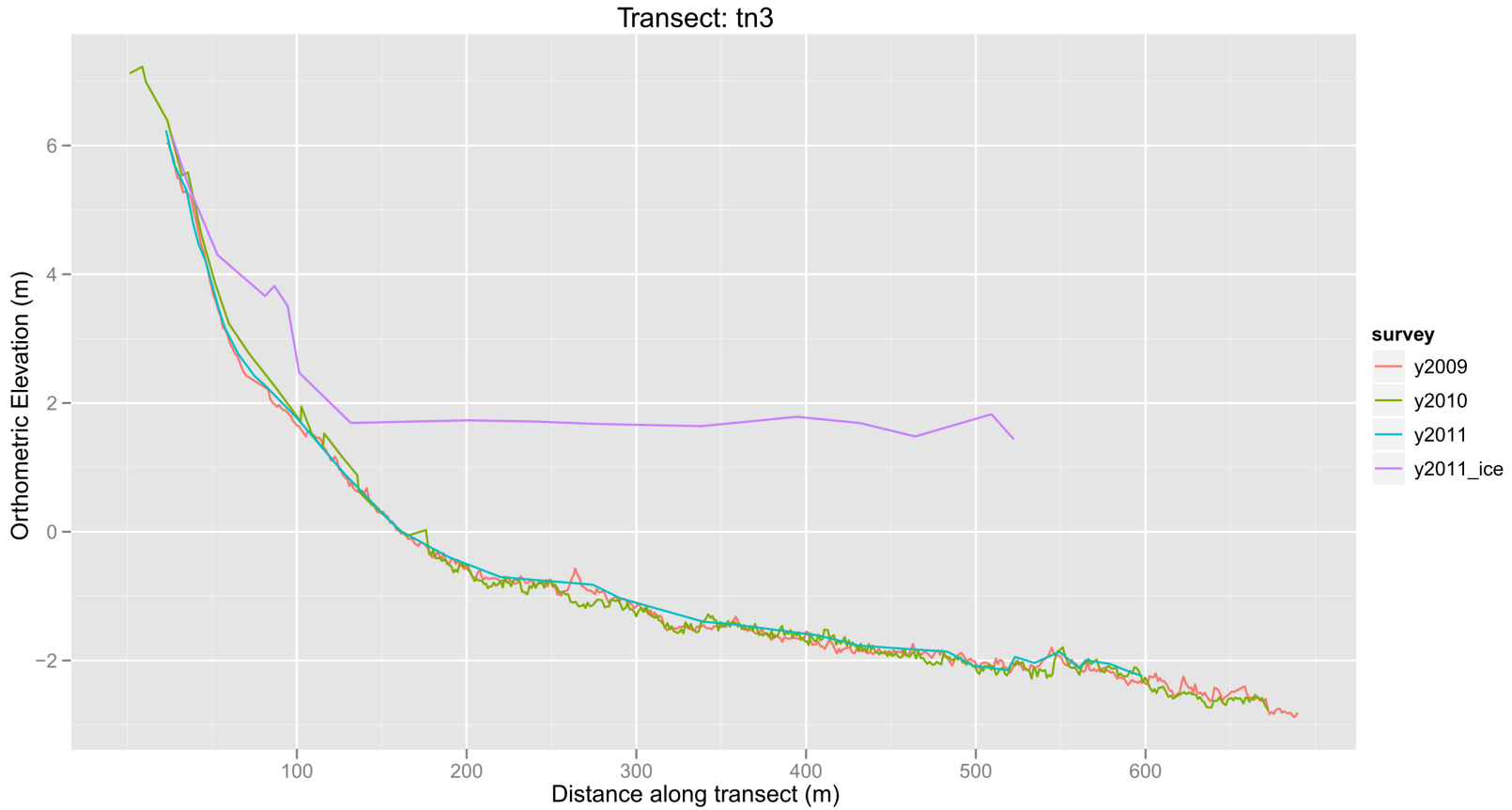
Transect: tn3
Orthometric Elevation (m)
6
4
2
0
−2
100
200
300
400
500
600
Distance along transect (m)
survey
y2009
y2010
y2011
y2011_ice

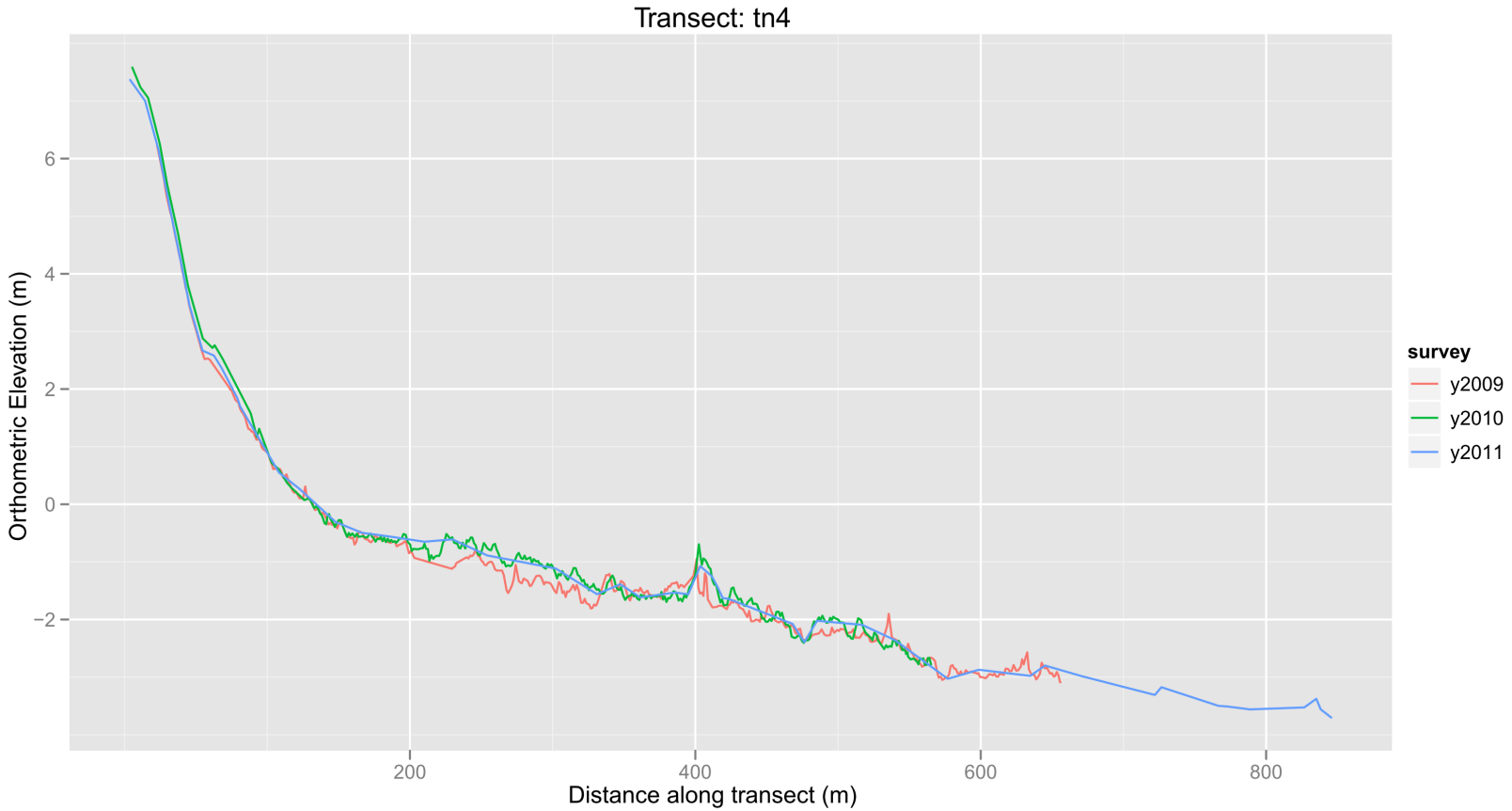
Transect: tn4
Orthometric Elevation (m)
6
4
2
0
−2
200
400
600
800
Distance along transect (m)
survey
y2009
y2010
y2011

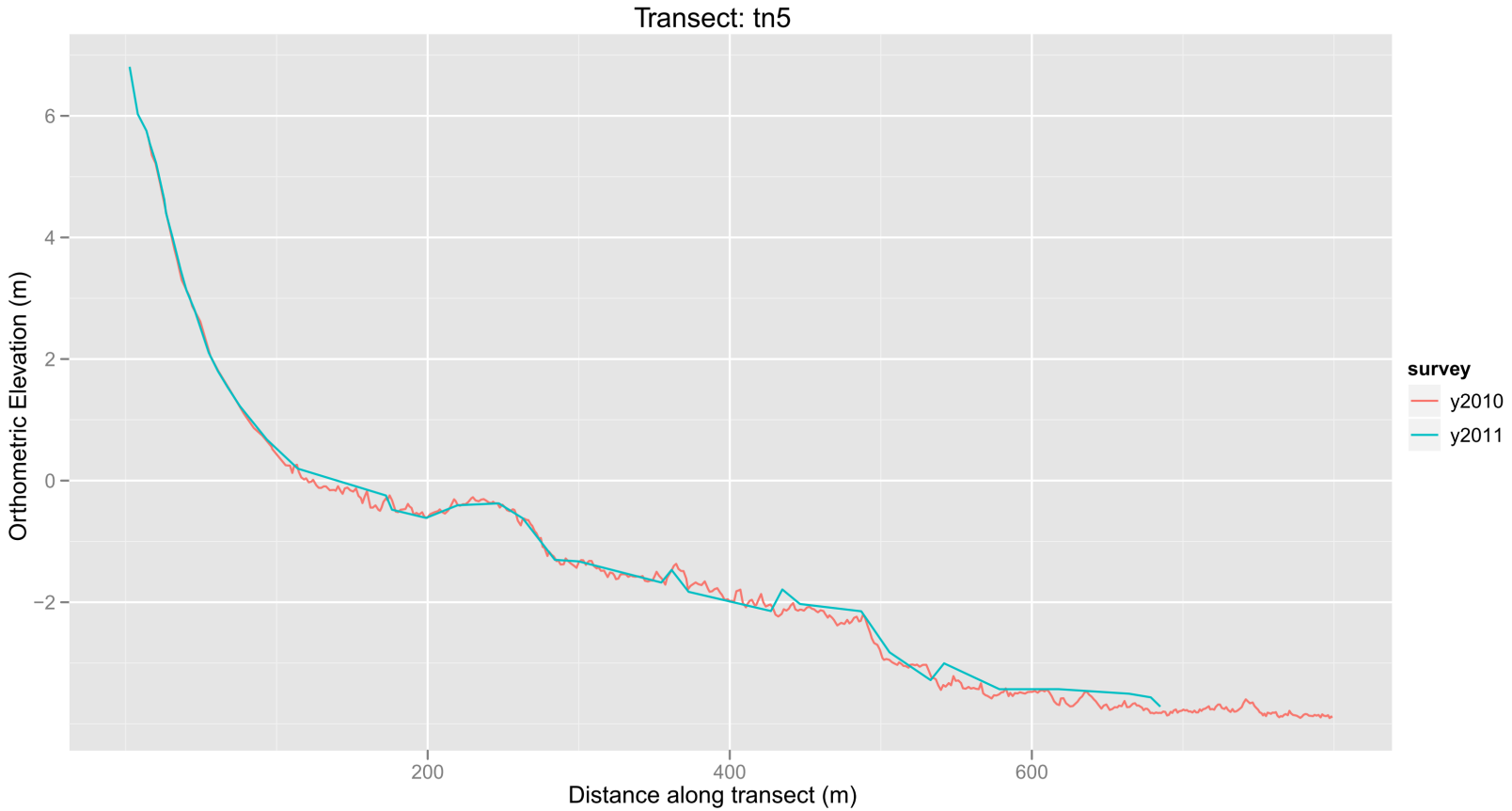
Transect: tn5
Orthometric Elevation (m)
6
4
2
0
−2
200
400
600
Distance along transect (m)
survey
y2010
y2011

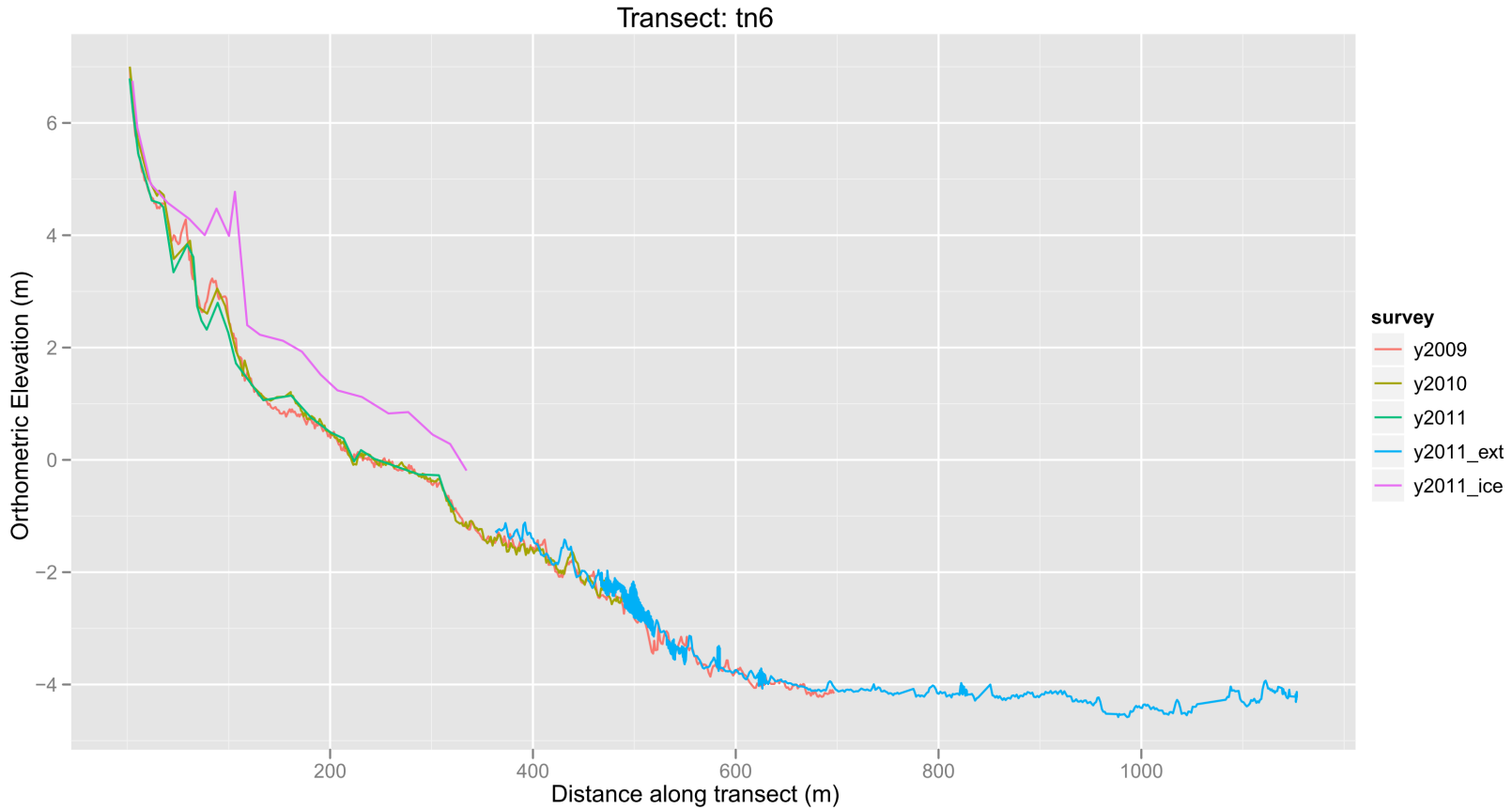
Transect: tn6
Orthometric Elevation (m)
6
4
2
0
−2
−4
200
400
600
800
1000
Distance along transect (m)
survey
y2009
y2010
y2011
y2011_ext
y2011_ice

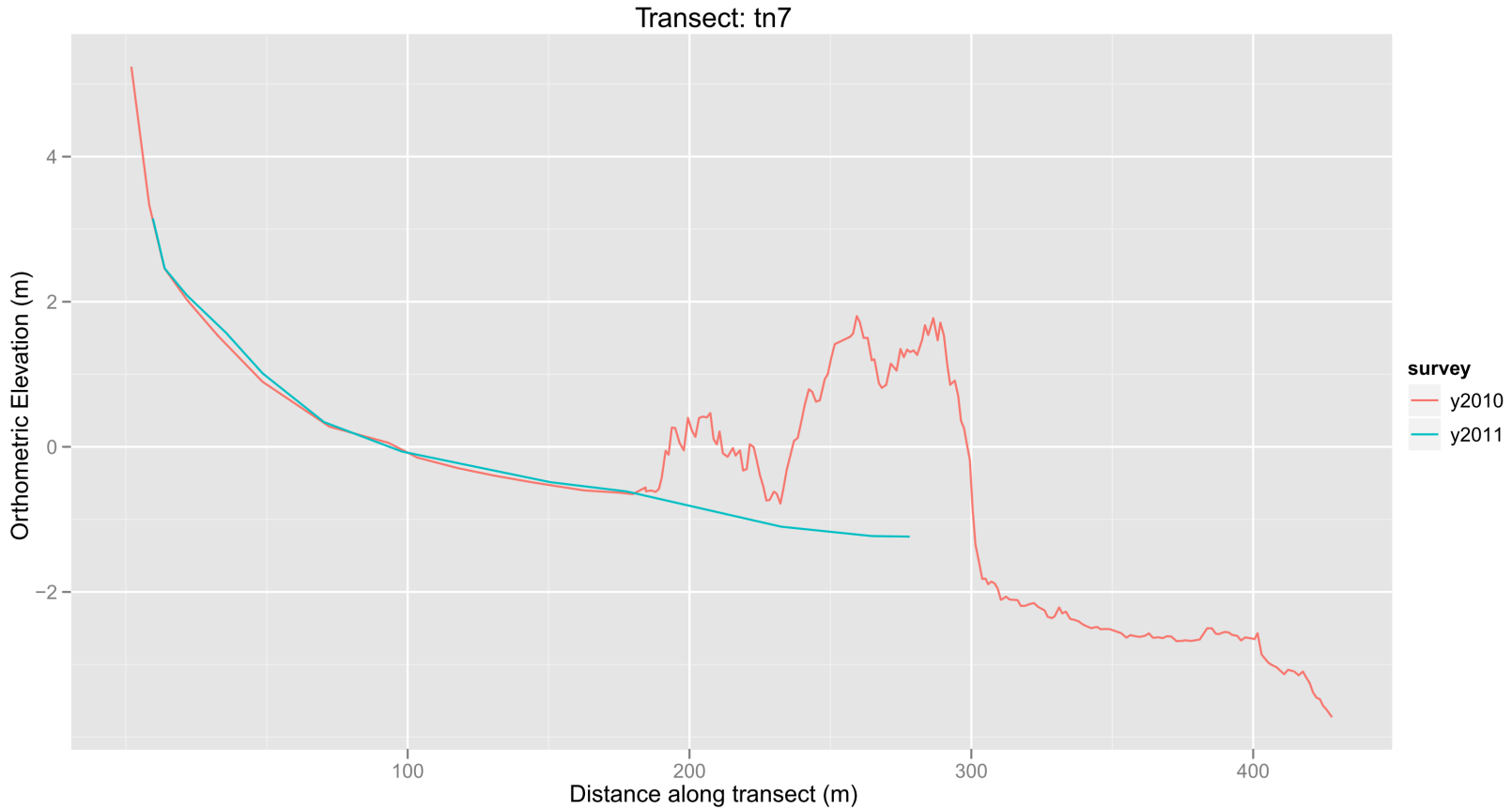
Transect: tn7
Orthometric Elevation (m)
4
2
0
−2
100
200
300
400
Distance along transect (m)
survey
y2010
y2011

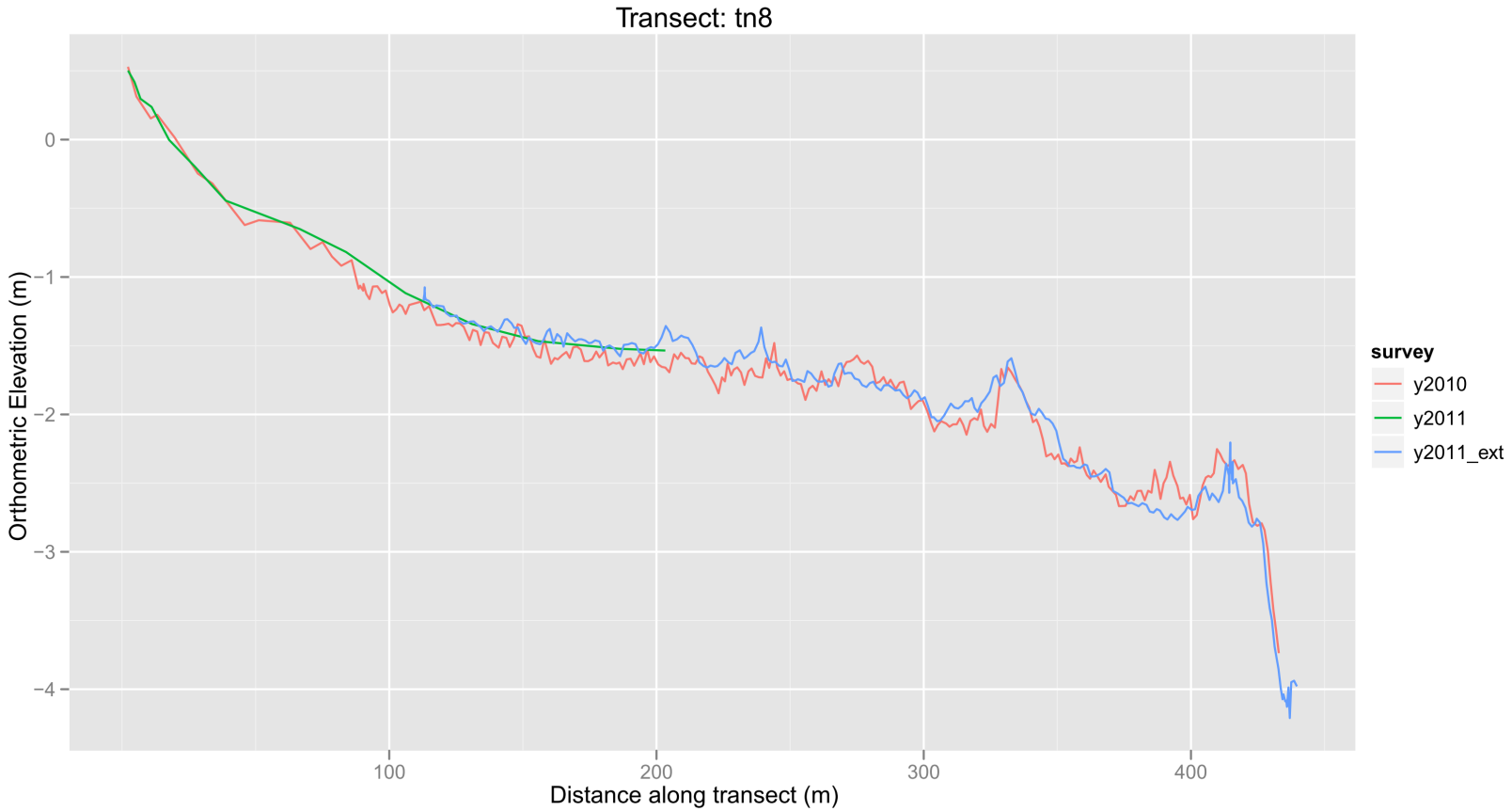
Transect: tn8
Orthometric Elevation (m)
0
−1
−2
−3
−4
100
200
300
400
Distance along transect (m)
survey
y2010
y2011
y2011_ext

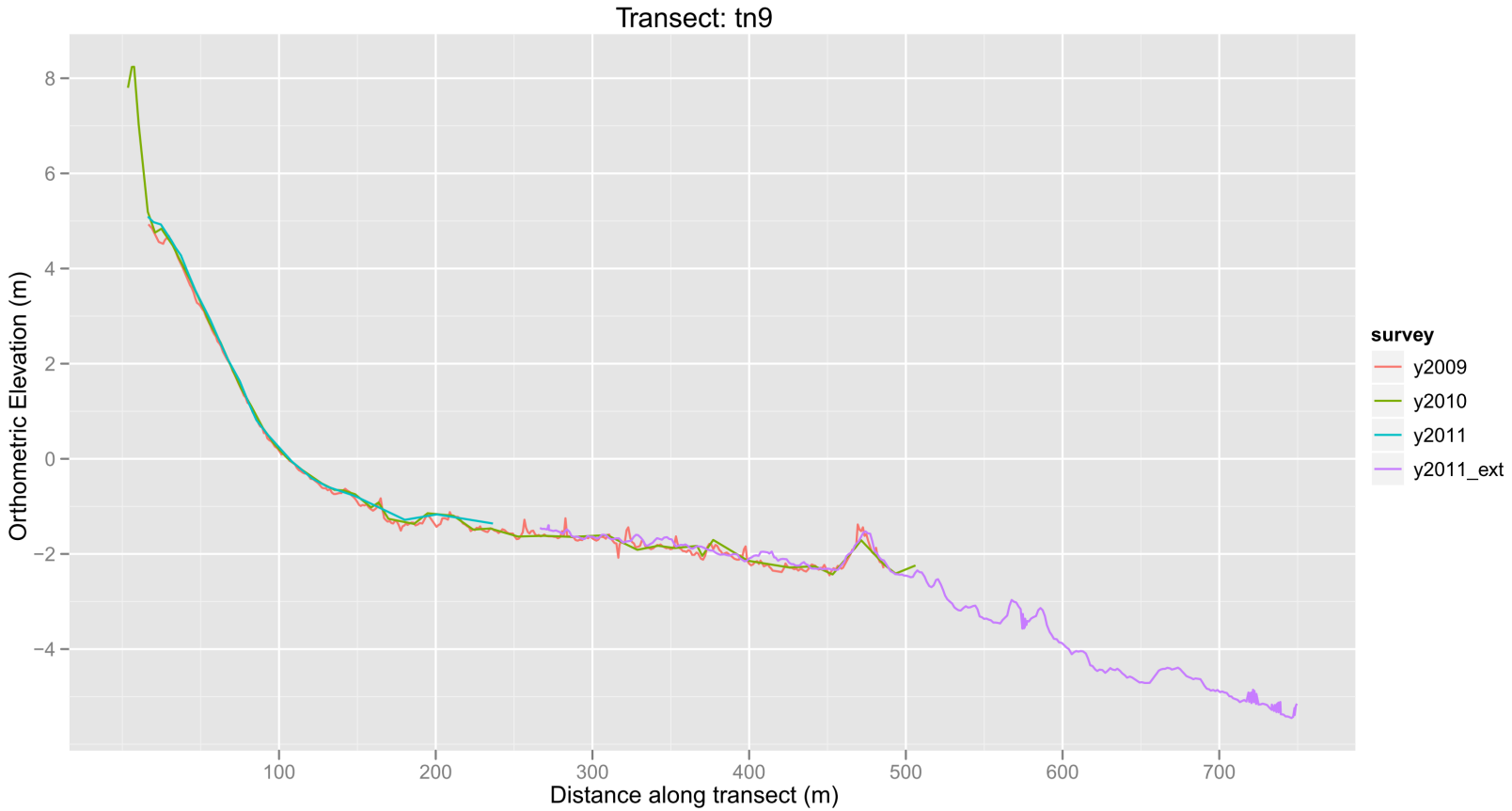
Transect: tn9
Orthometric Elevation (m)
8
6
4
2
0
−2
−4
100
200
300
400
500
600
700
Distance along transect (m)
survey
y2009
y2010
y2011
y2011_ext

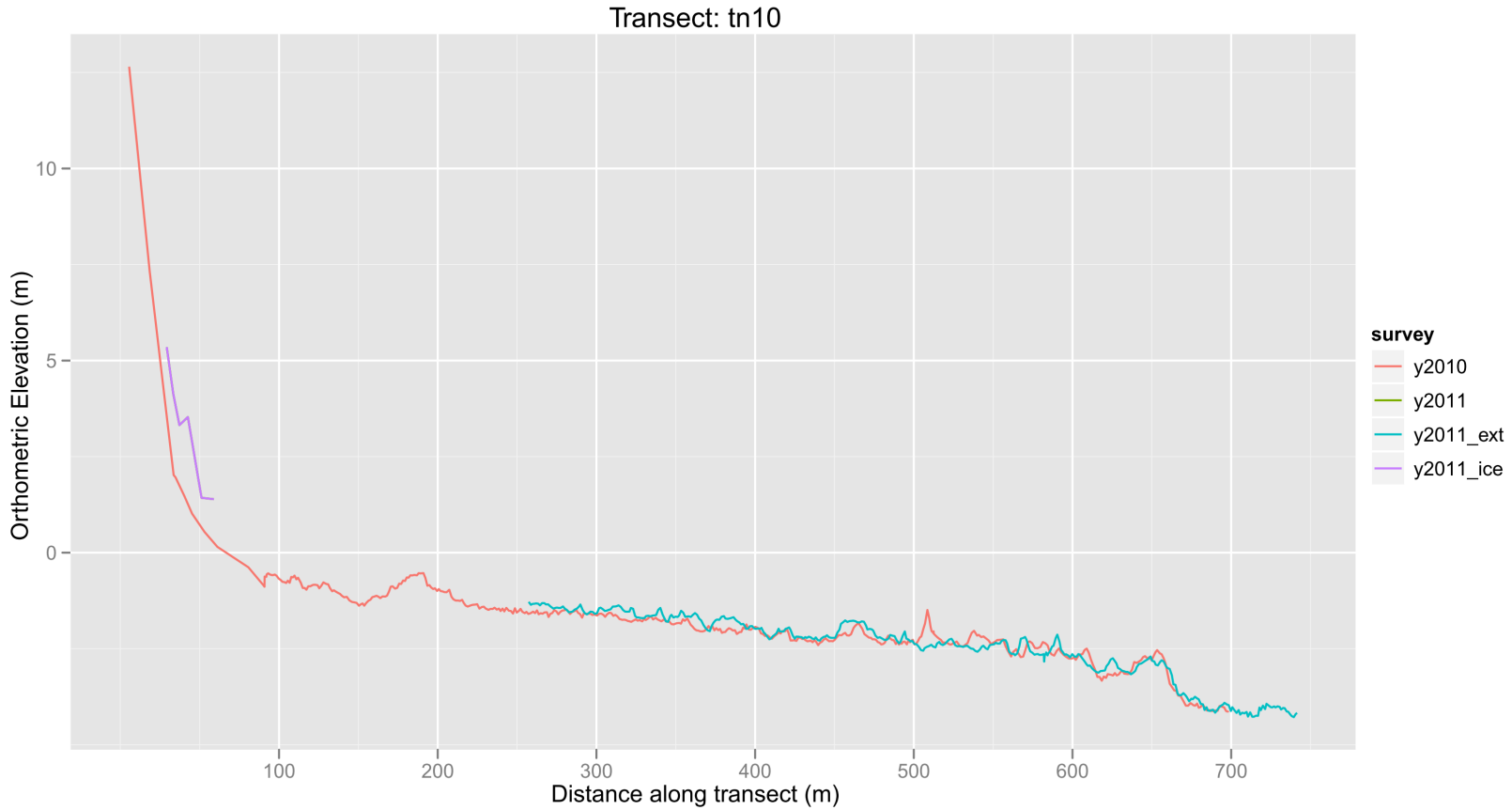
Transect: tn10
Orthometric Elevation (m)
10
5
0
100
200
300
400
500
600
700
Distance along transect (m)
survey
y2010
y2011
y2011_ext
y2011_ice

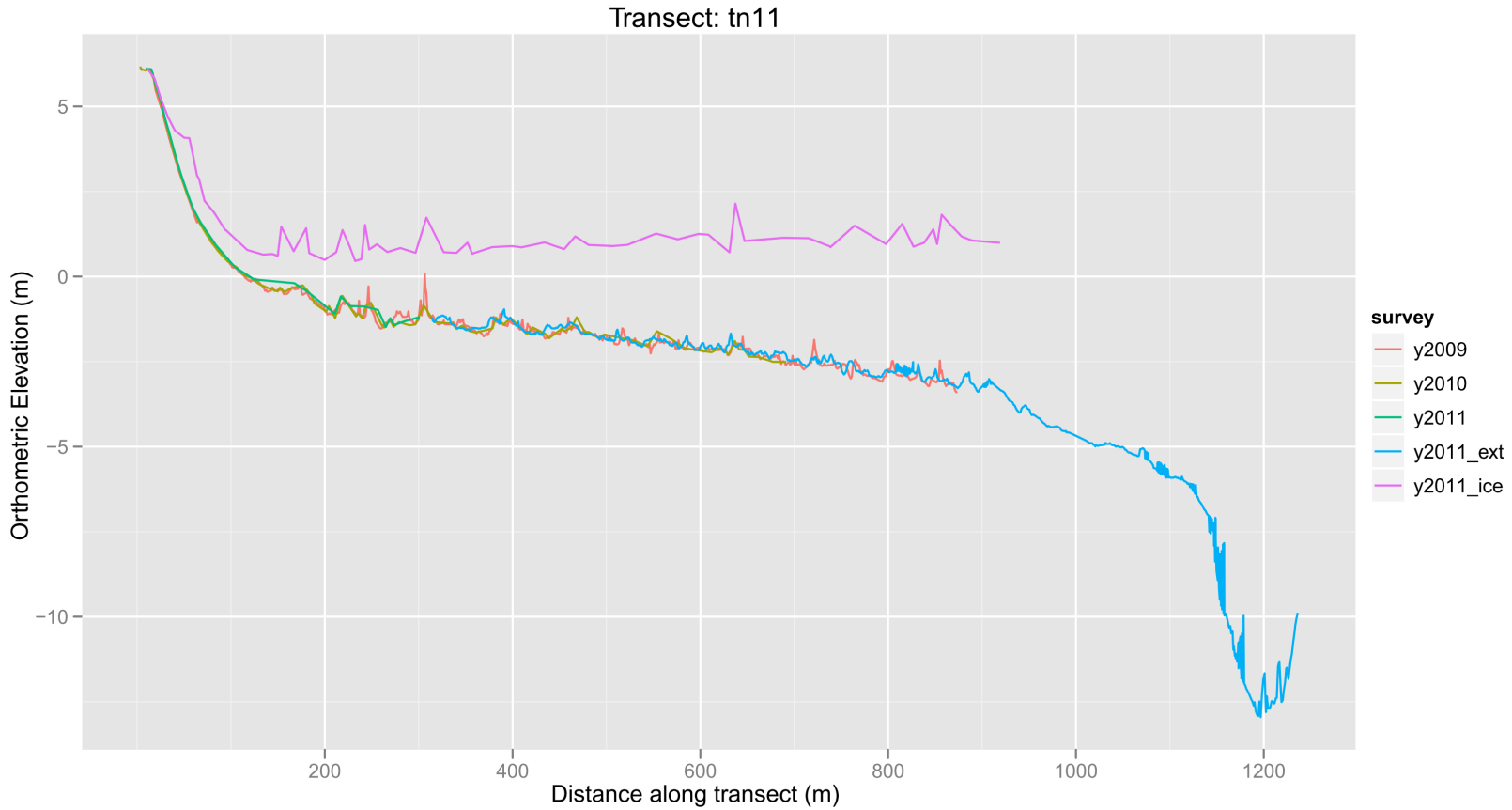
Transect: tn11
Orthometric Elevation (m)
5
0
−5
−10
200
400
600
800
1000
1200
Distance along transect (m)
survey
y2009
y2010
y2011
y2011_ext
y2011_ice

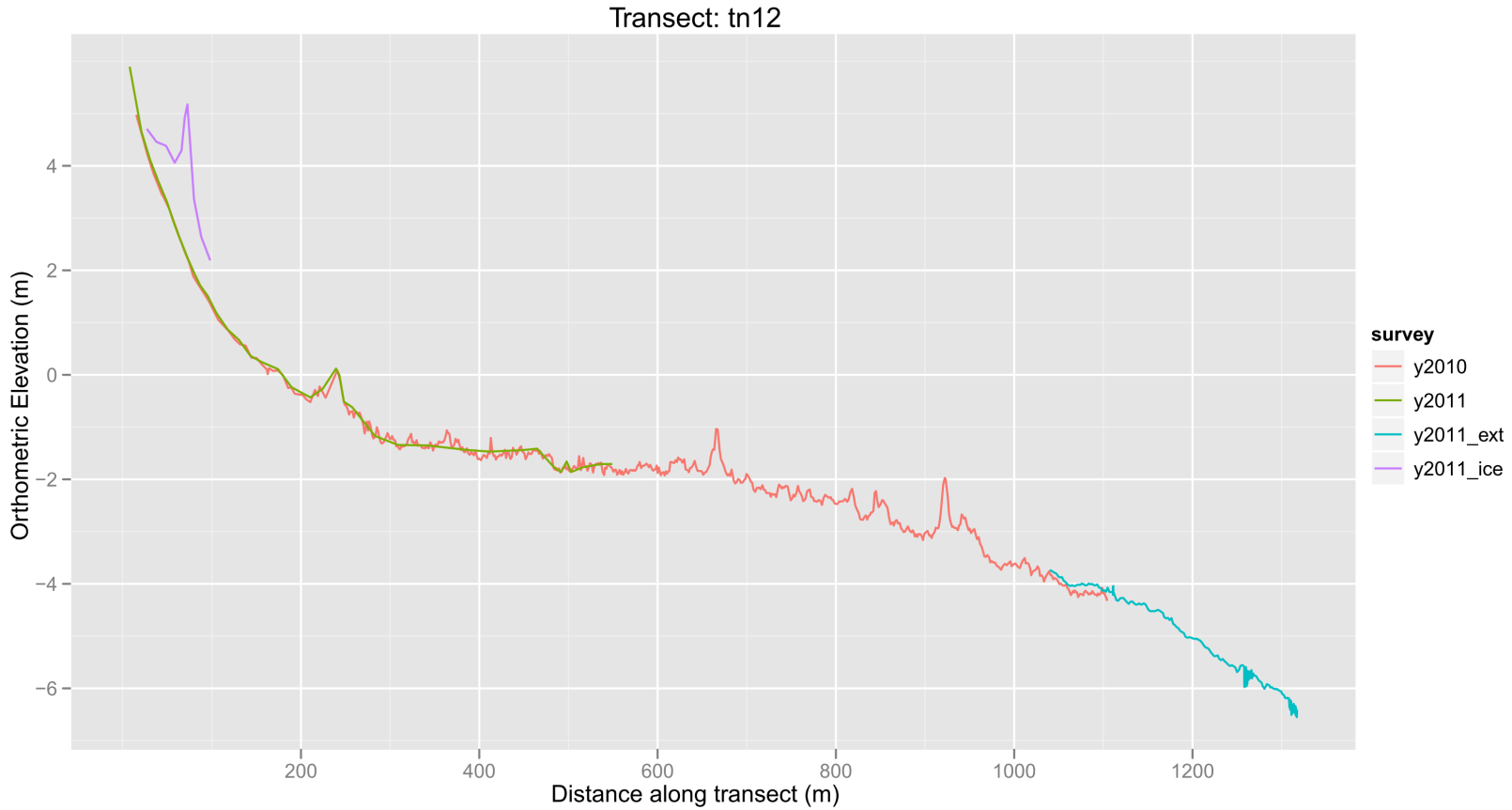
Transect: tn12
Orthometric Elevation (m)
4
2
0
−2
−4
−6
200
400
600
800
1000
1200
Distance along transect (m)
survey
y2010
y2011
y2011_ext
y2011_ice

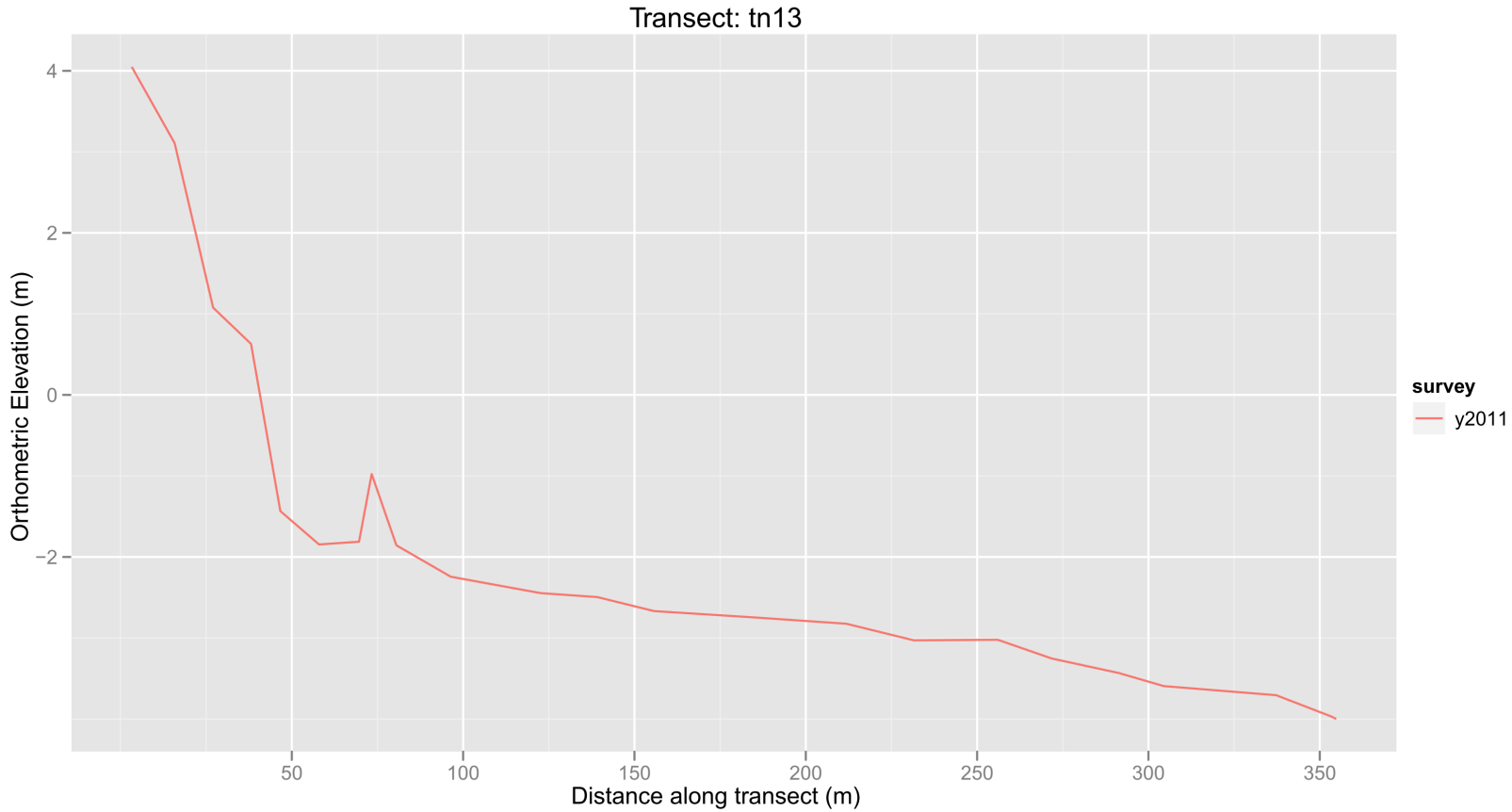
Transect: tn13
Orthometric Elevation (m)
4
2
0
−2
50
100
150
200
250
300
350
Distance along transect (m)
survey
y2011

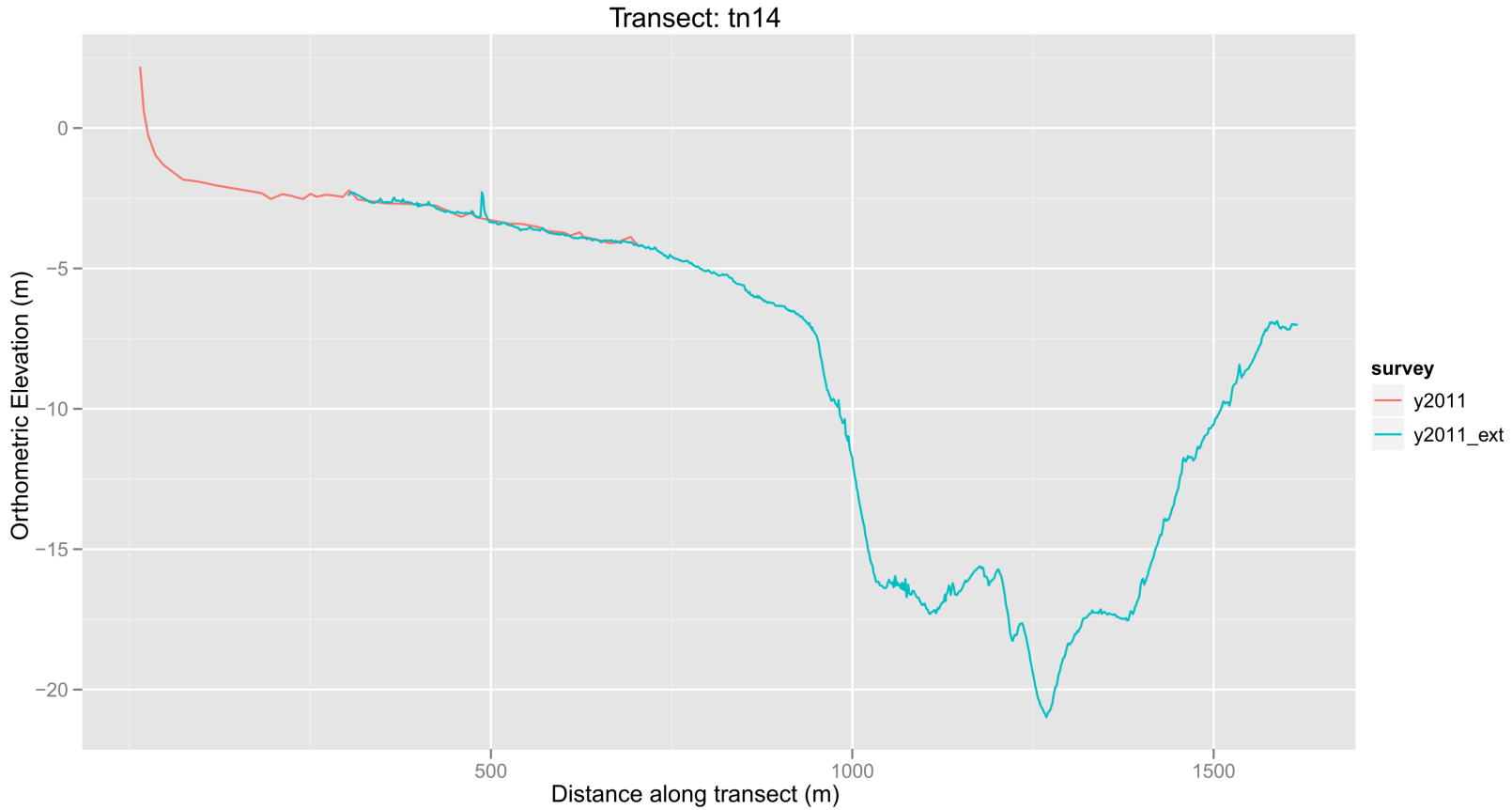
Transect: tn14
Orthometric Elevation (m)
0
−5
−10
−15
−20
500
1000
1500
Distance along transect (m)
survey
y2011
y2011_ext

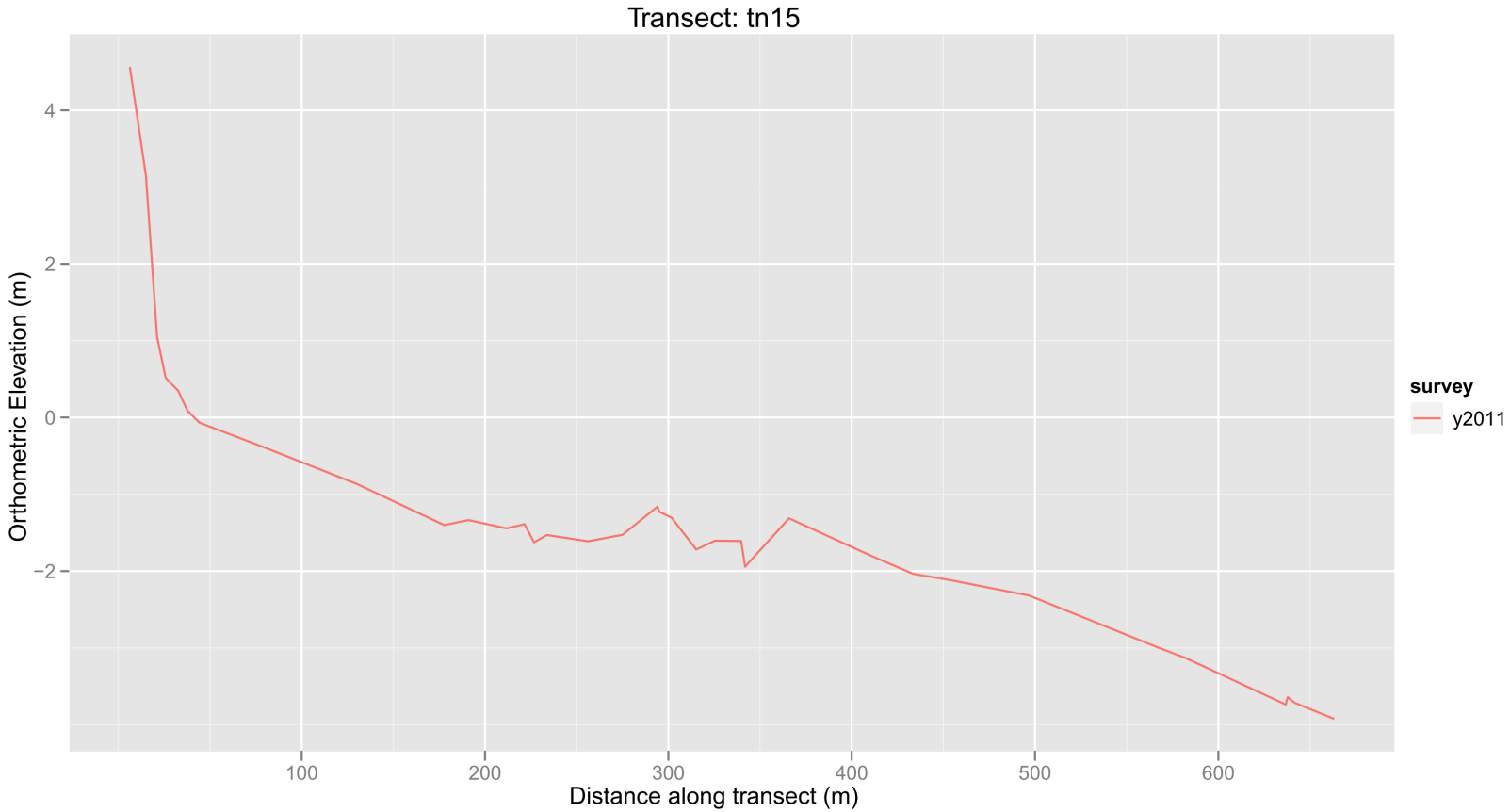
Transect: tn15
Orthometric Elevation (m)
4
2
0
−2
100
200
300
400
500
600
Distance along transect (m)
survey
y2011

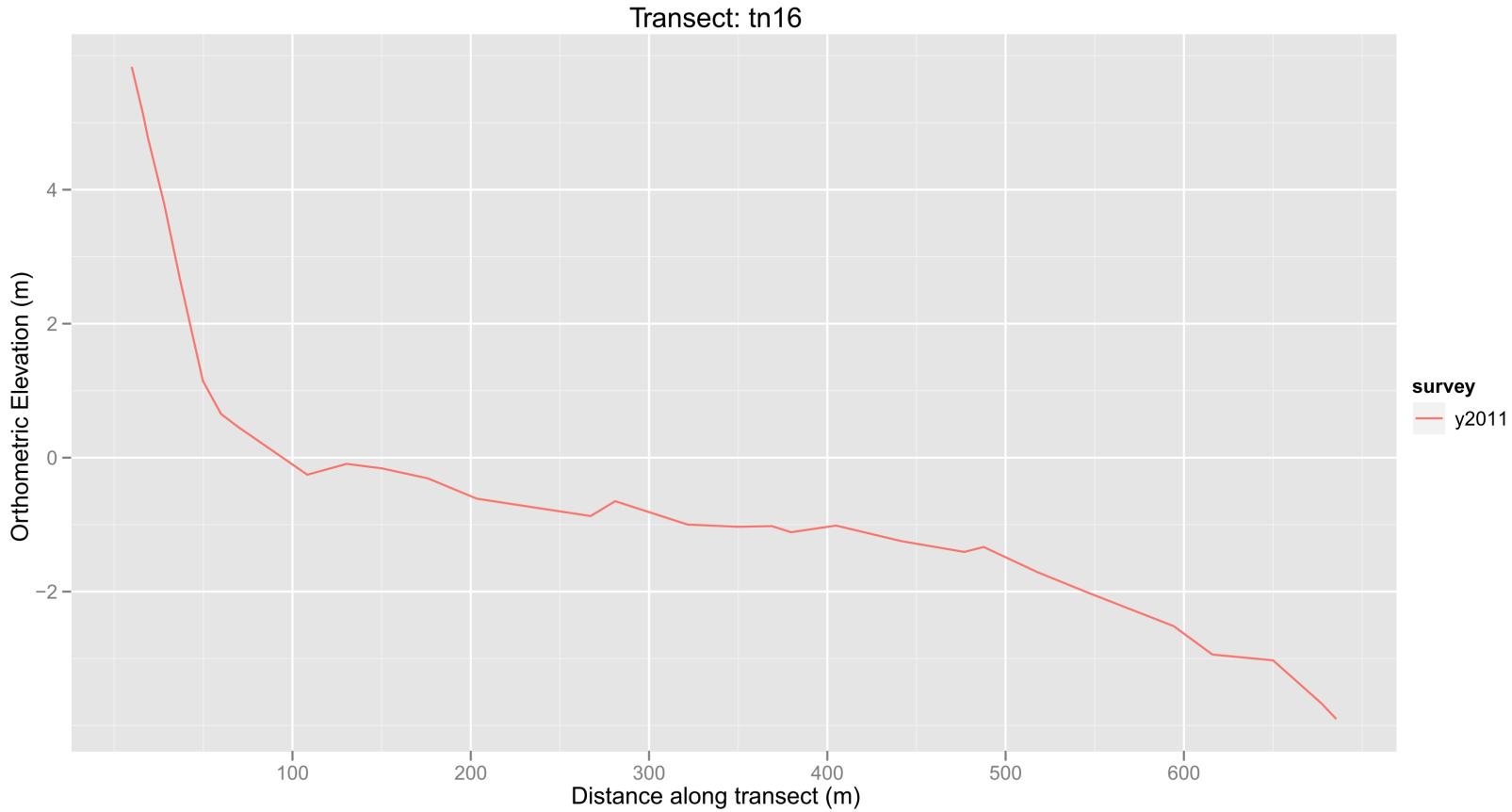
Transect: tn16
Orthometric Elevation (m)
4
2
0
−2
100
200
300
400
500
600
Distance along transect (m)
survey
y2011

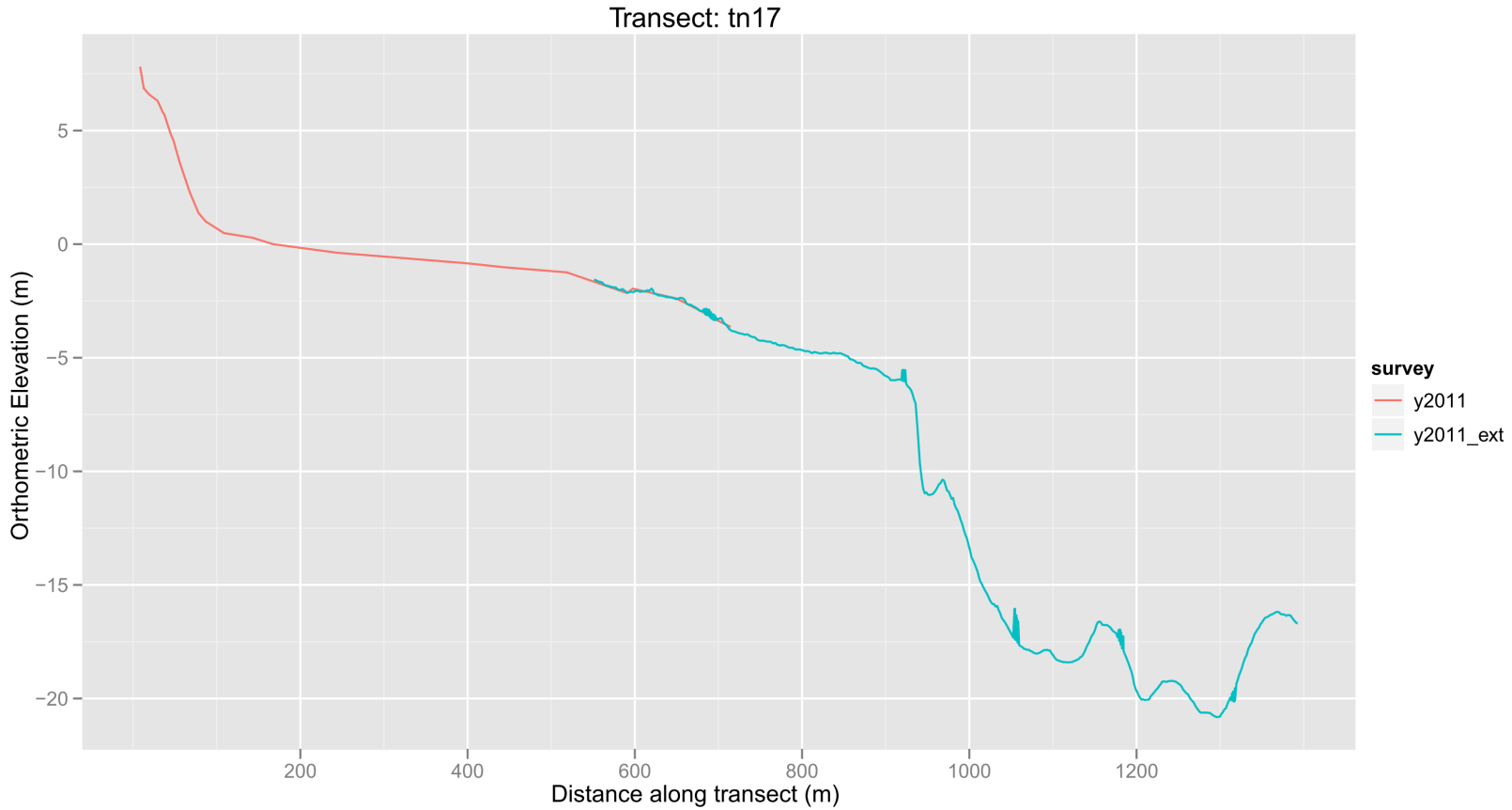
Transect: tn17
Orthometric Elevation (m)
5
0
−5
−10
−15
−20
200
400
600
800
1000
1200
Distance along transect (m)
survey
y2011
y2011_ext

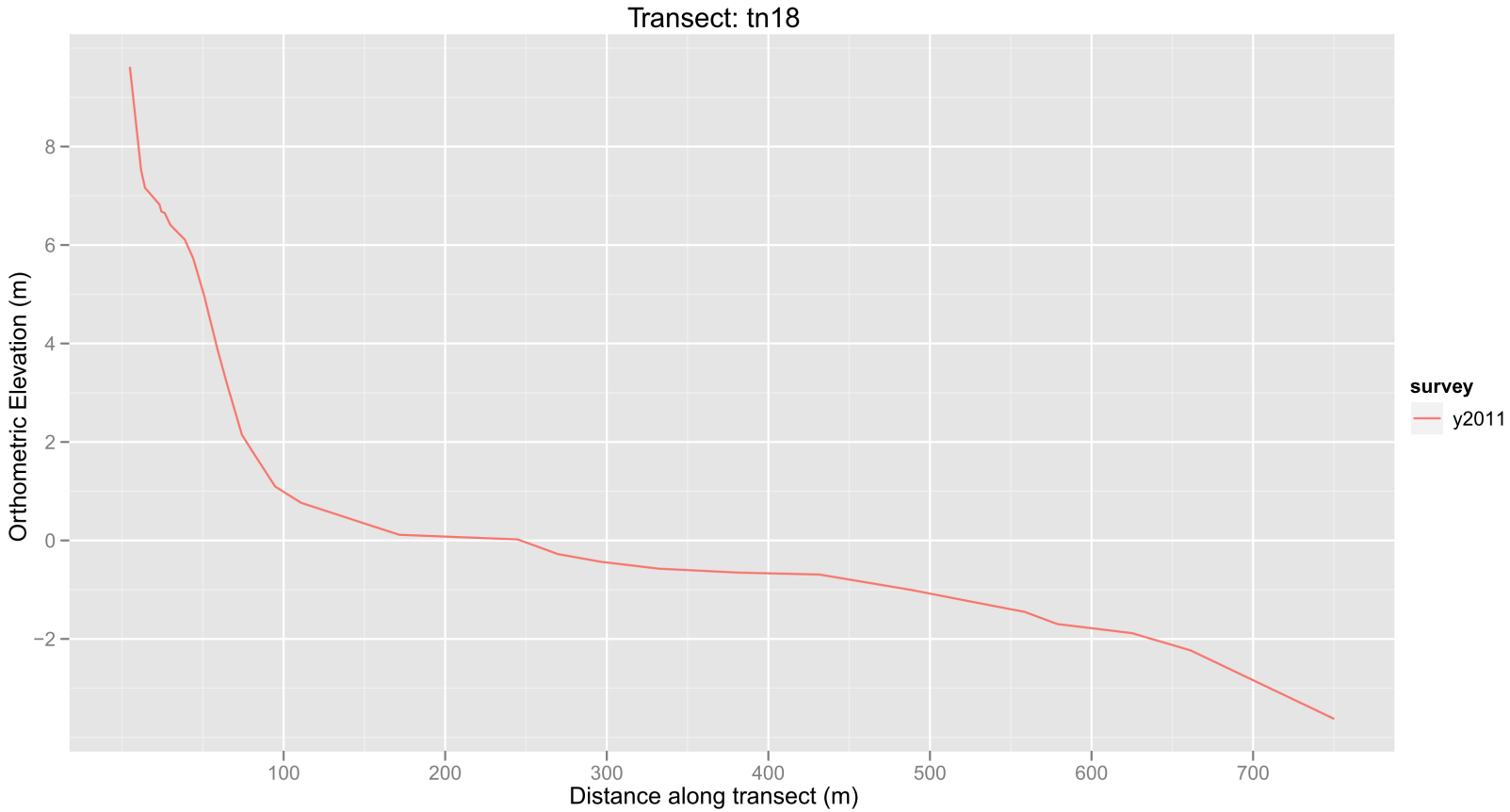
Transect: tn18
Orthometric Elevation (m)
8
6
4
2
0
−2
100
200
300
400
500
600
700
Distance along transect (m)
survey
y2011

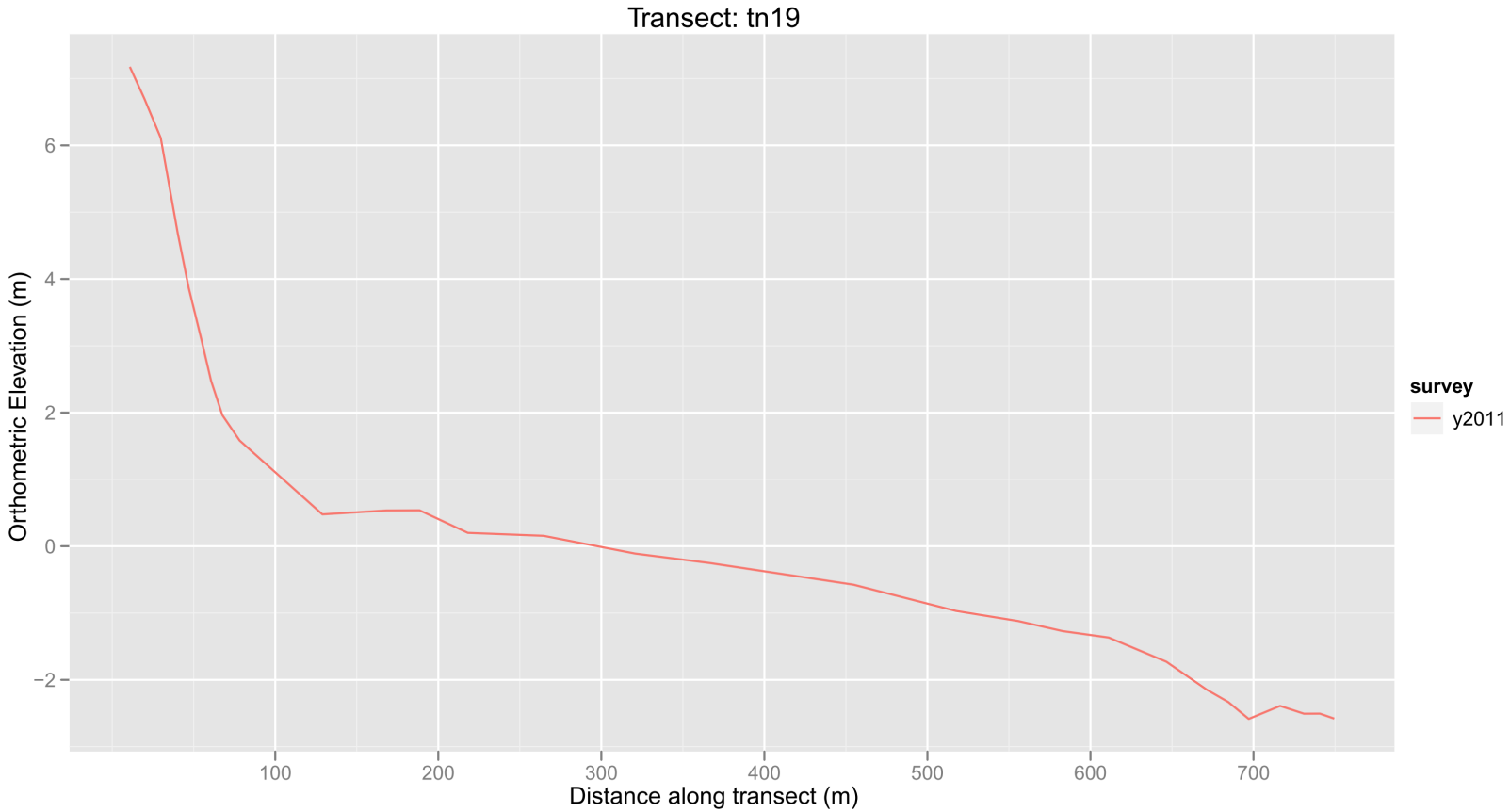
Transect: tn19
Orthometric Elevation (m)
6
4
2
0
−2
100
200
300
400
500
600
700
Distance along transect (m)
survey
y2011

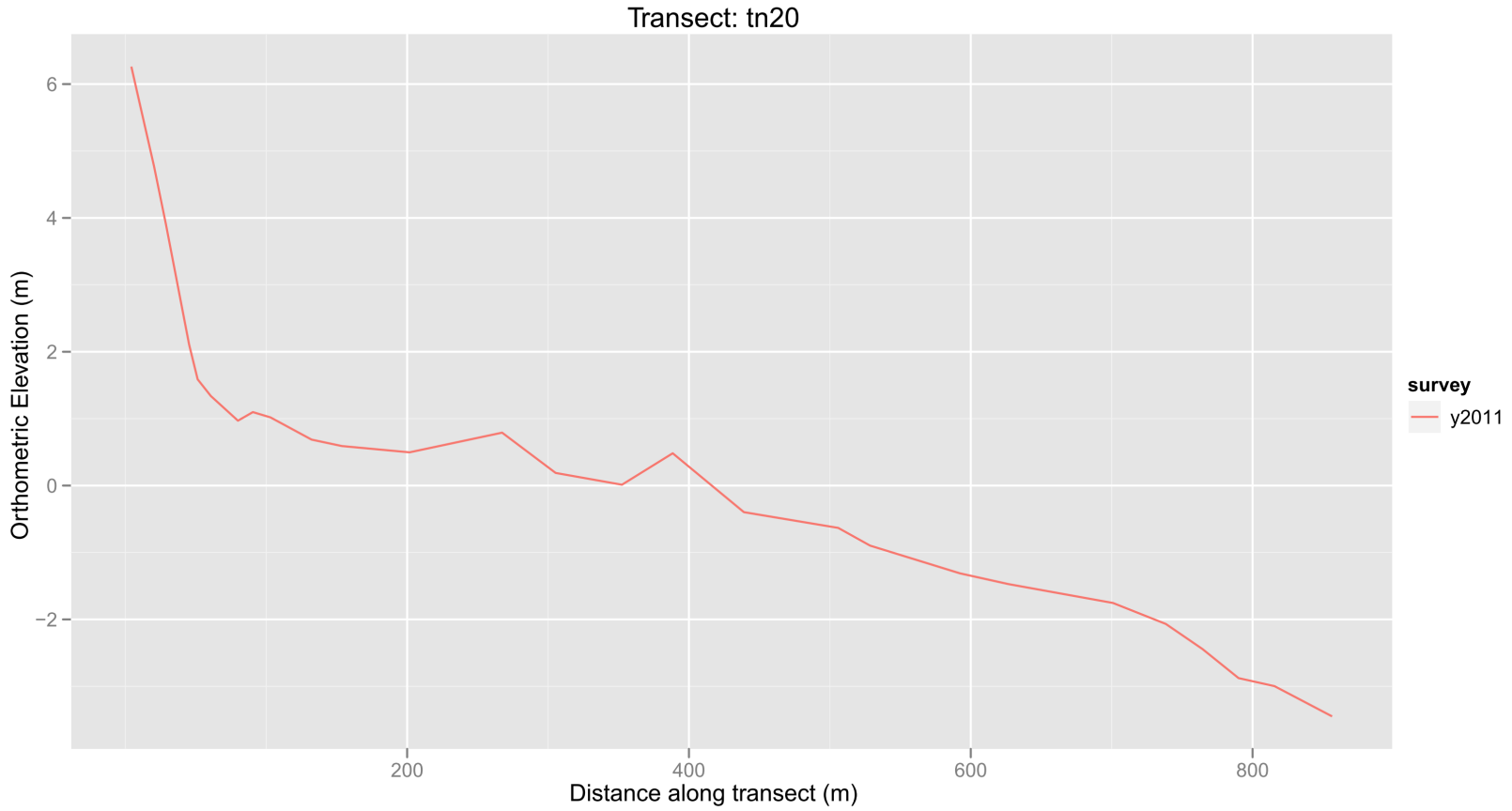
Transect: tn20
Orthometric Elevation (m)
6
4
2
0
−2
200
400
600
800
Distance along transect (m)
survey
y2011

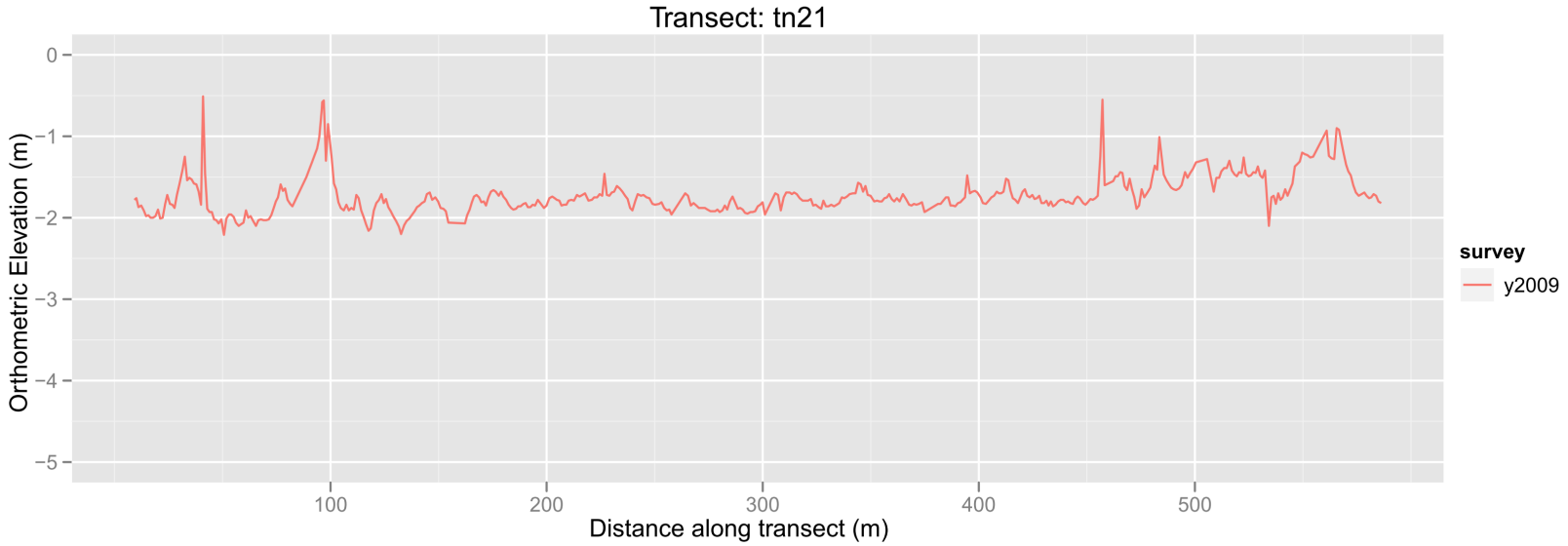
Transect: tn21
Orthometric Elevation (m)
0
−1
−2
−3
−4
−5
100
200
300
400
500
Distance along transect (m)
survey
y2009

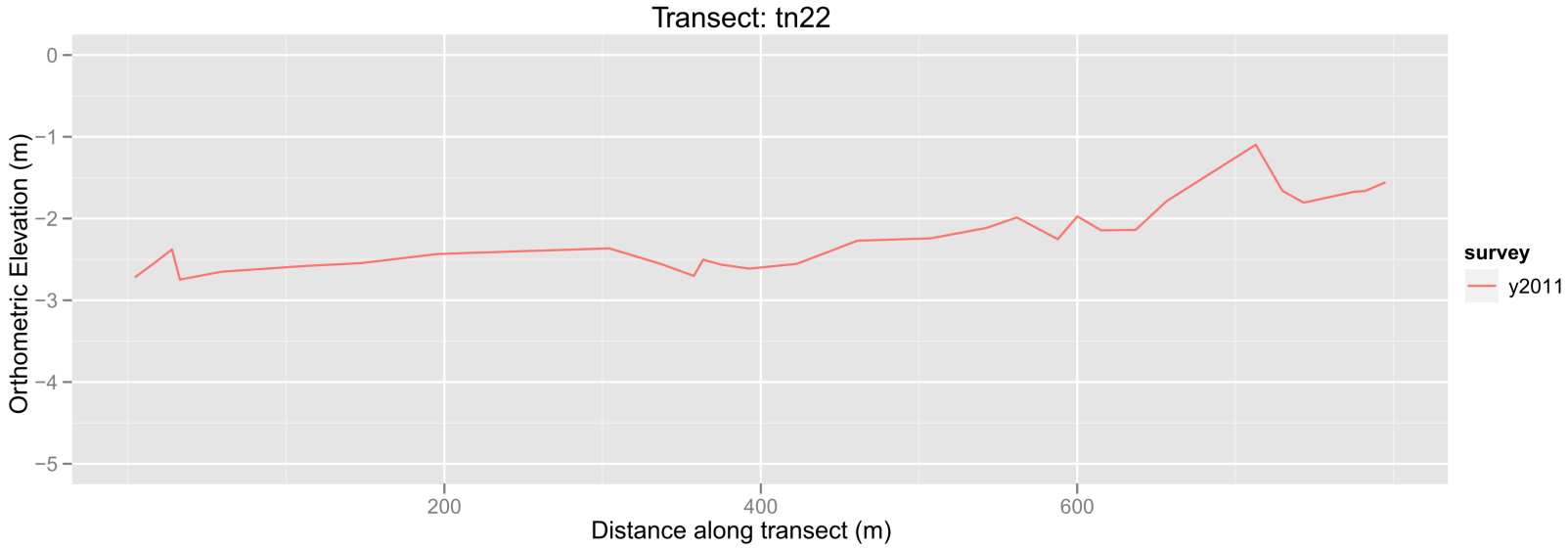
Transect: tn22
Orthometric Elevation (m)
0
−1
−2
−3
−4
−5
200
400
600
Distance along transect (m)
survey
y2011

A.7 RBR tide and wave recorder data

RBR TWR-2050 Tide and Wave recorders Sampling period: 00:15:00 Averaging period: 00:01:00 Wave sampling period: 00:30:00 Wave burst rate: 2 hz

A.7.1 TWR 012539

Deployment 1 - Start: 2010-08-14 12:00:00 End: 2010-08-24 19:30:00

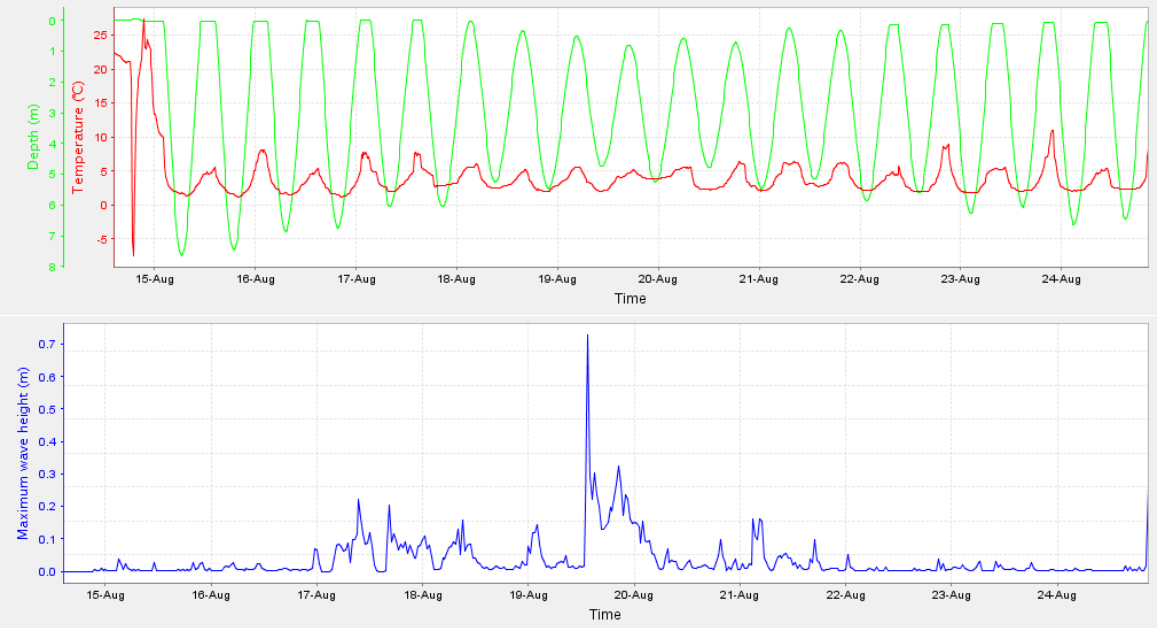

Deployment 2 - Start: 2010-08-24 20:00:00 End: 2010-10-19 20:00:00

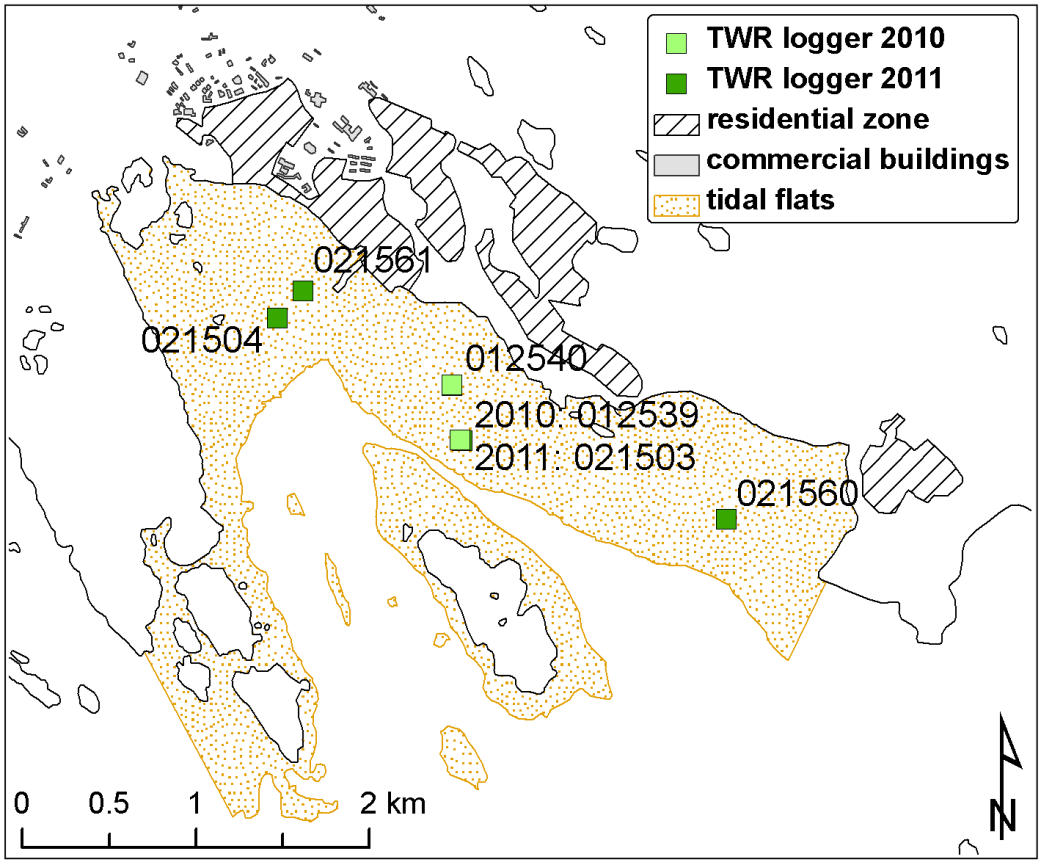

Figure A.13: Location of the RBR TWR-2050 tide and wave recorder instruments on the Iqaluit tidal flats. All instruments were deployed on foot, and so were dry for part of the tidal cycle.

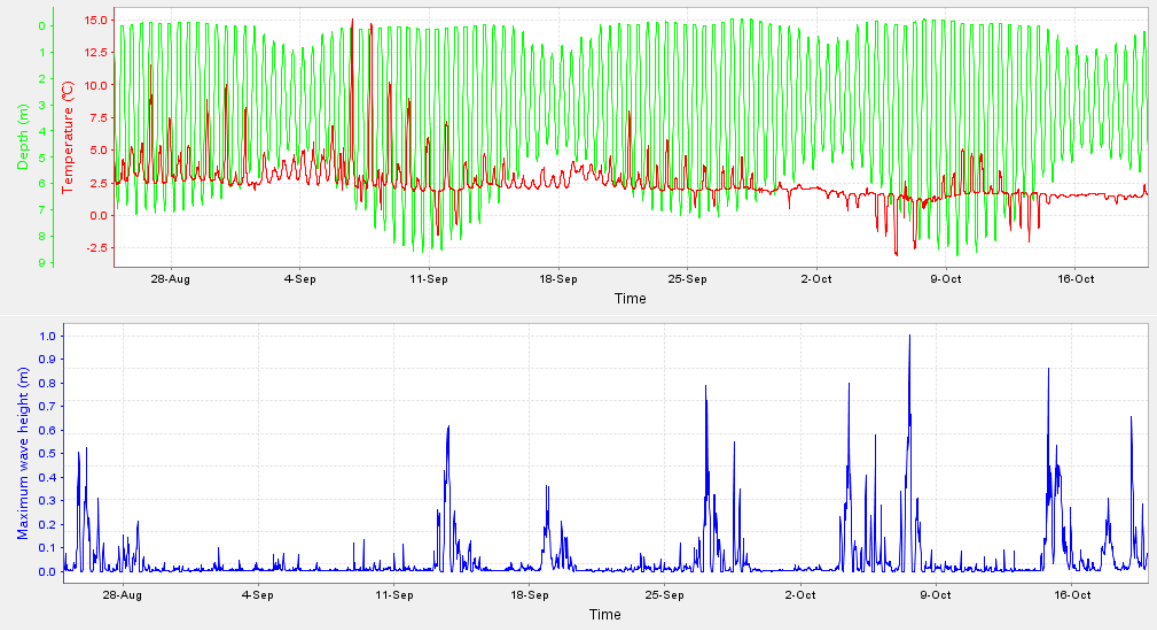

A.7.2 TWR 012540

Deployment 1 - Start: 2010-08-14 12:00:00 End: 2010-08-24 19:30:00

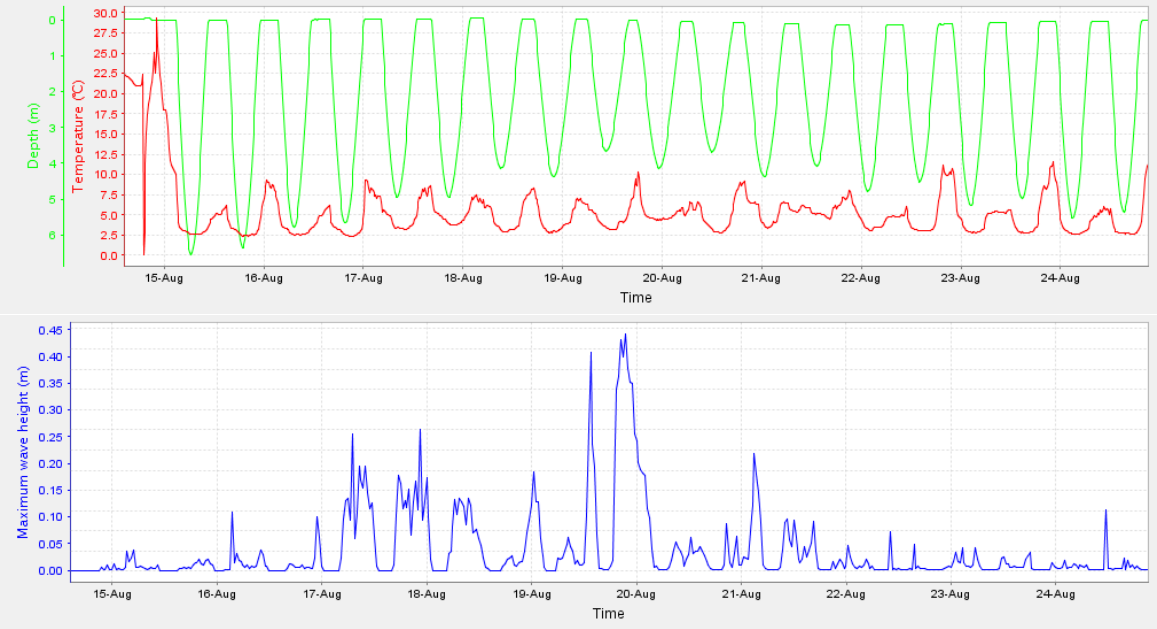

Deployment 2 - Start: 2010-08-24 20:00:00 End: 2010-10-19 20:00:00

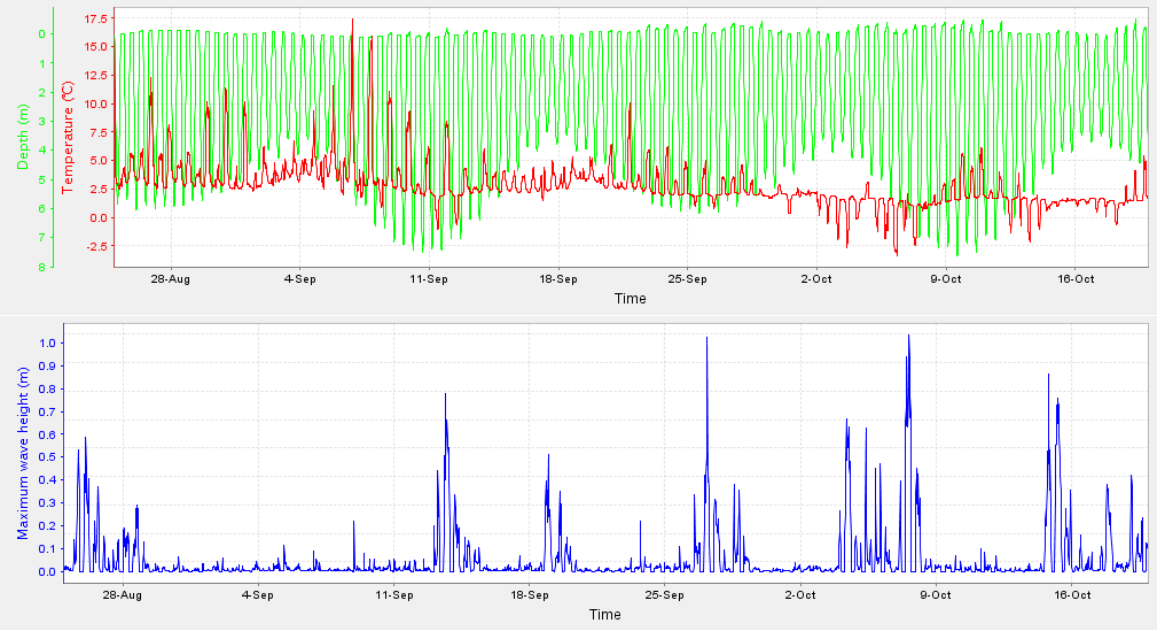

A.7.3 TWR 021503

Deployment 1 - Start: 2011-07-16 20:00:00 End: 2011-09-11 00:00:00

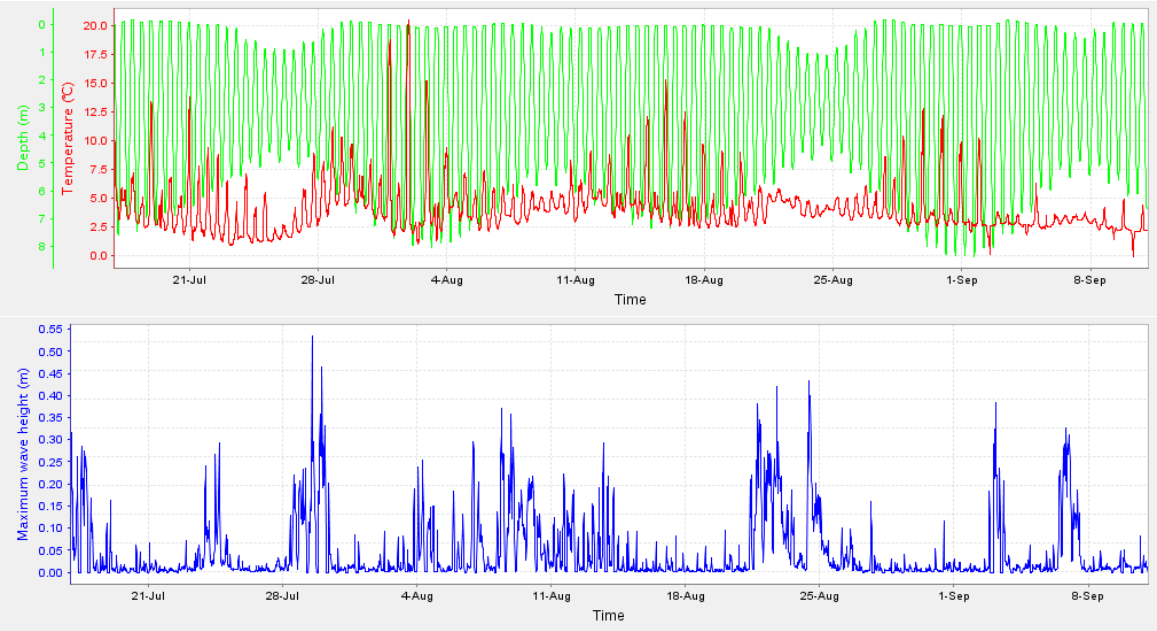

Deployment 2 - Start: 2011-09-28 12:44:42 End: 2011-11-23 15:44:29

A.7.4 TWR 021504

Deployment 1 - Start: 2011-07-16 20:00:00 End: 2011-09-11 00:00:00

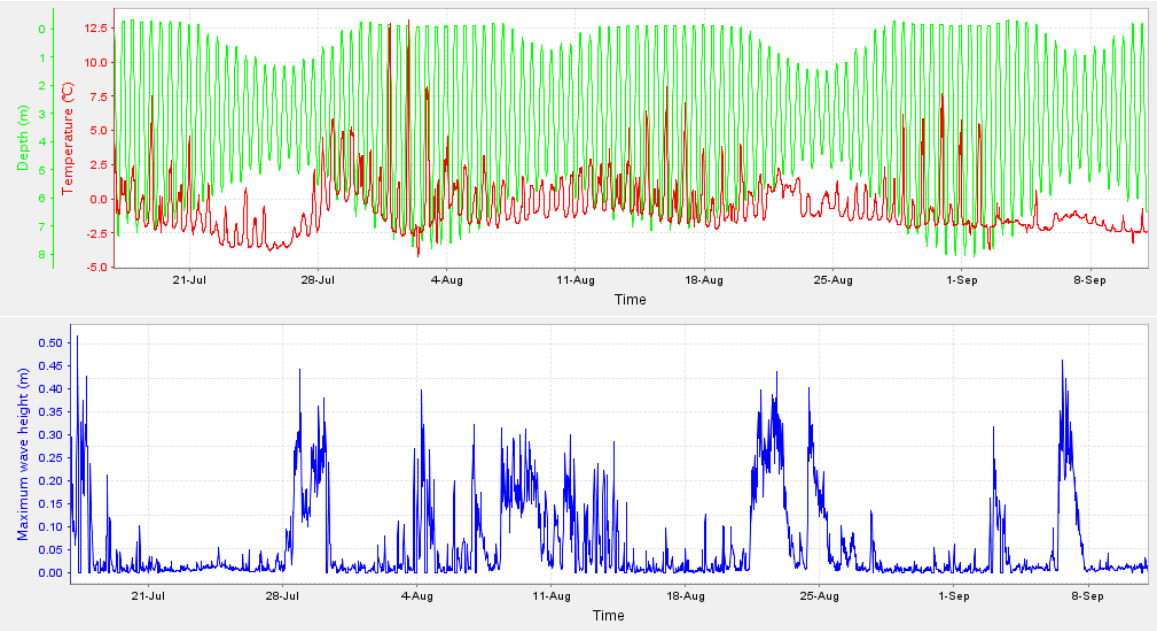

Deployment 2 - Start: 2011-09-28 12:40:00 End: 2011-11-23 15:39:09

A.7.5 TWR 021560

Deployment 1 - Start: 2011-07-24 00:00:00 End: 2011-08-21 03:15:00

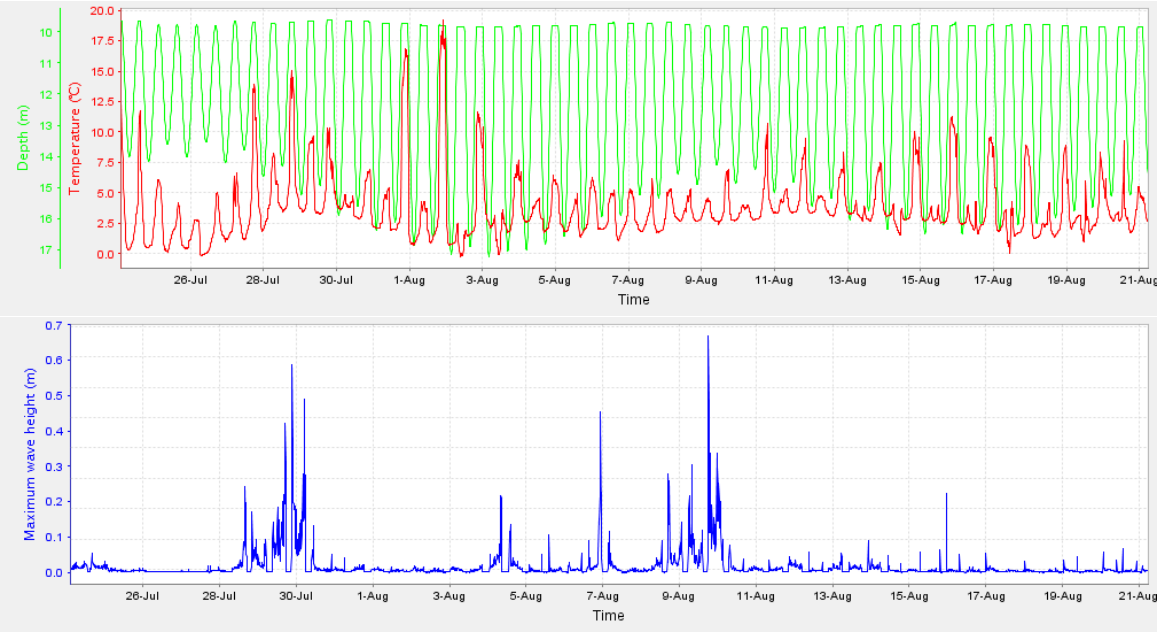

Deployment 2 - Start: 2011-09-28 12:42:50 End: 2011-11-23 15:42:33

A.7.6 TWR 021561

Deployment 1 - Start: 2011-07-23 23:00:00 End: 2011-09-18 03:00:00

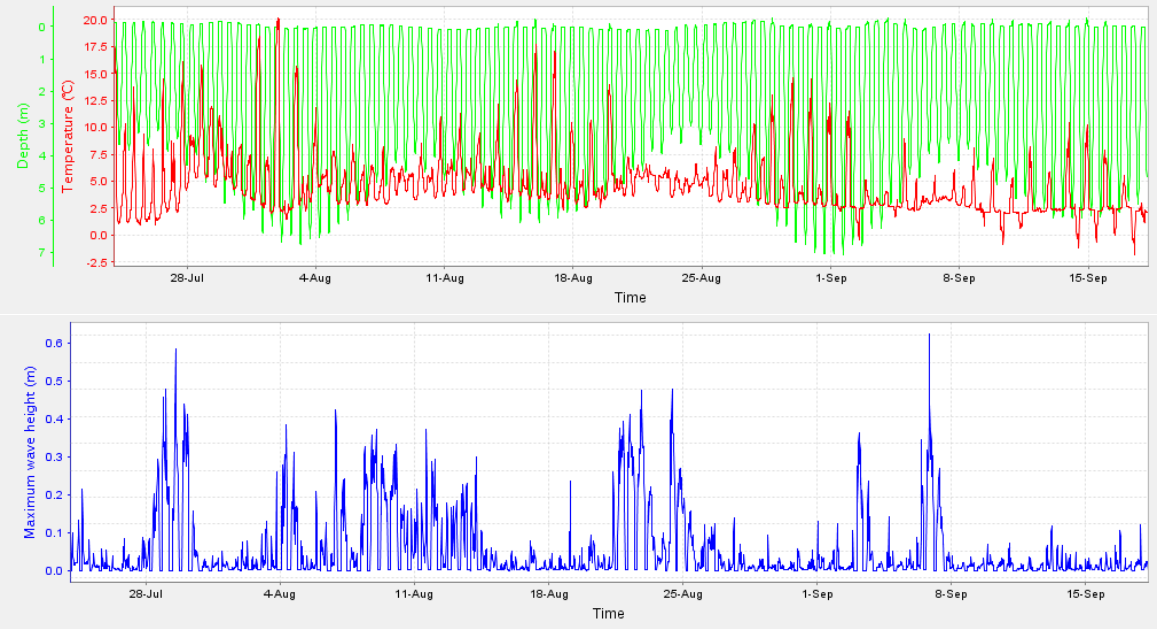

A.8 CTD and turbidity casts

The CTD profiler used was an RBR XR-620 CTD and turbidity profiler. Casts were taken during rising and falling tides during spring tides on July 29/30 2011 and Aug 02 2011. Table A.5 shows the tidal stage and spring/neap conditions for each profile.

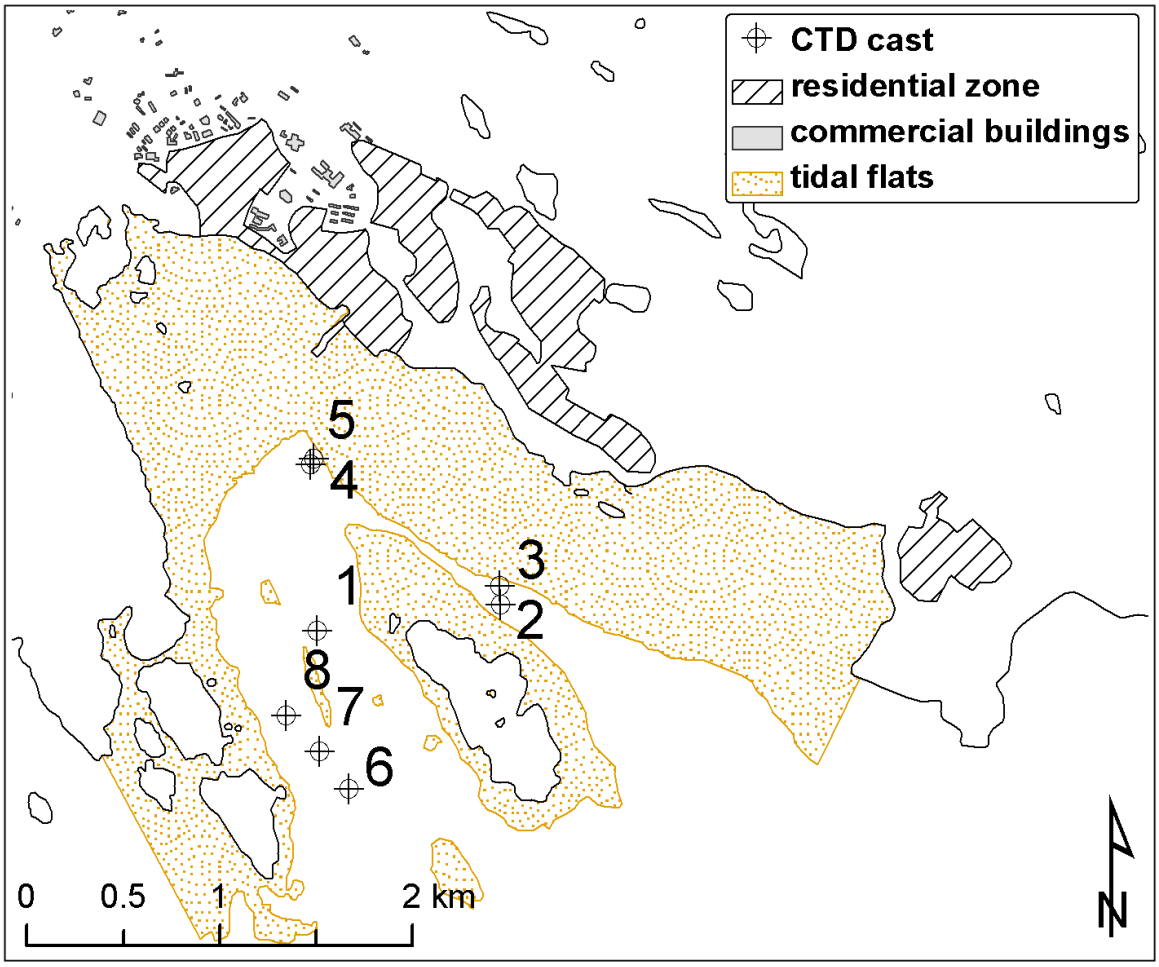

Figure A.14: Map showing location of CTD profile casts in Koojesse Inlet.

CTD Profile	Time (UTC)	Tidal stage	Tidal cycle
1	2011-07-29 15:05	Late-falling	Mid-spring
2	2011-07-29 17:27	Early-rising	Mid-spring
3	2011-07-29 17:30	Early-rising	Mid-spring
4	2011-07-30 15:36	Late-falling	Mid-spring
5	2011-08-02 12:55	Late-rising	Spring
6	2011-08-02 15:12	Mid-falling	Spring
7	2011-08-02 15:21	Mid-falling	Spring
8	2011-08-02 15:40	Mid-falling	Spring

Table A.5: Table showing the times and tides for each CTD profile.

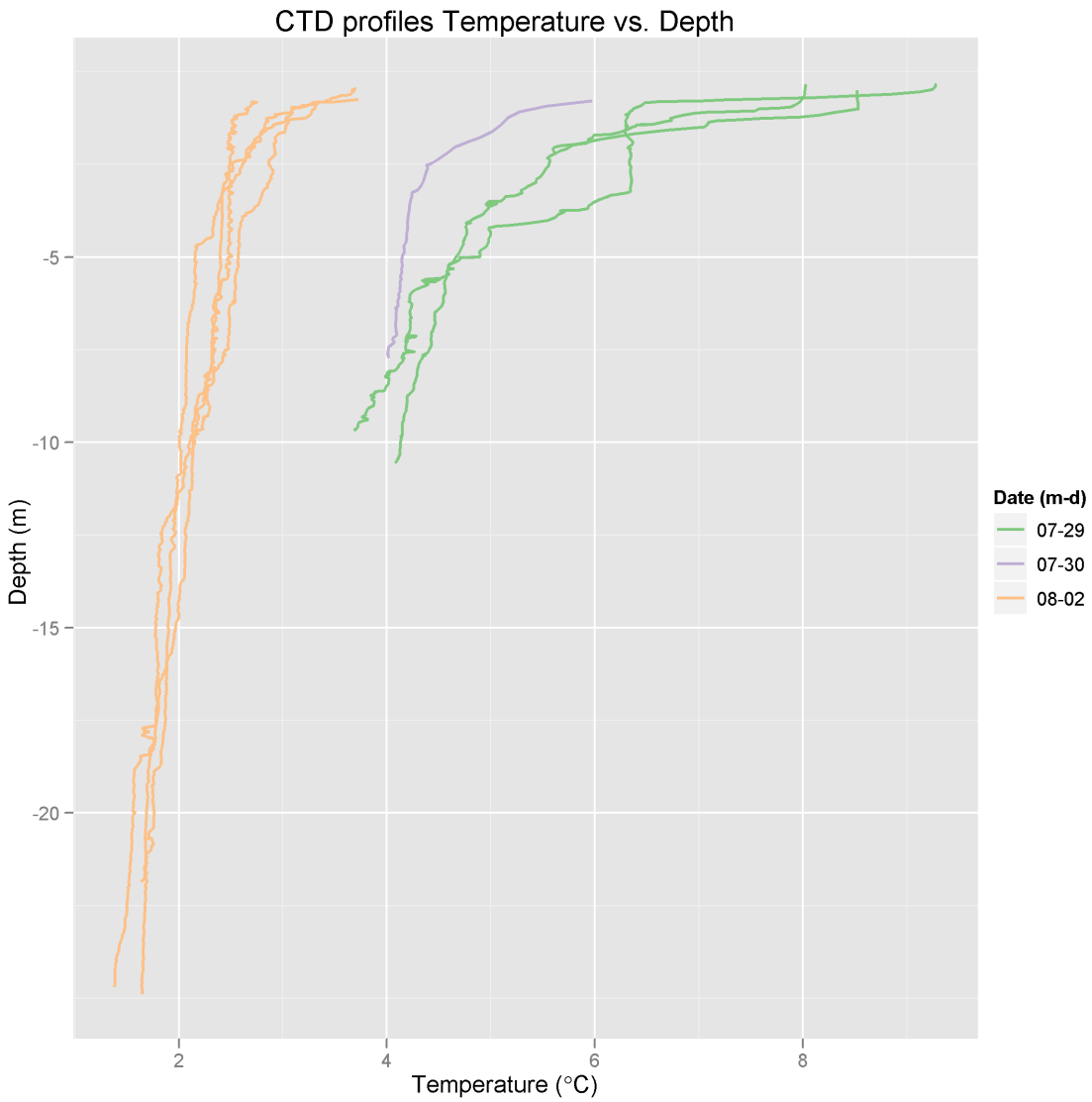

Figure A.15: Plot of temperature with depth grouped by the three sampling days.

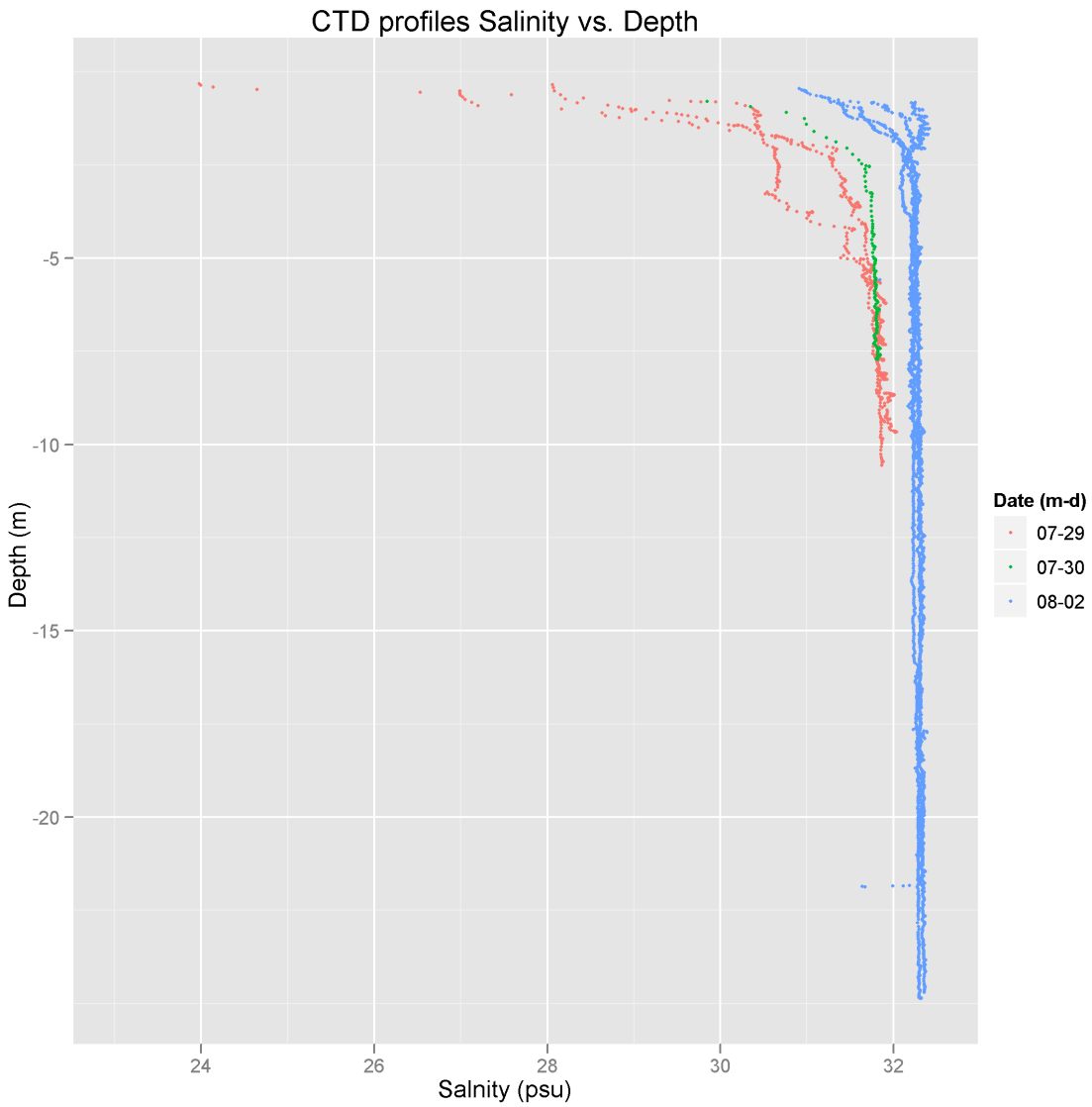

Figure A.16: Plot of salinity with depth grouped by the three sampling days.

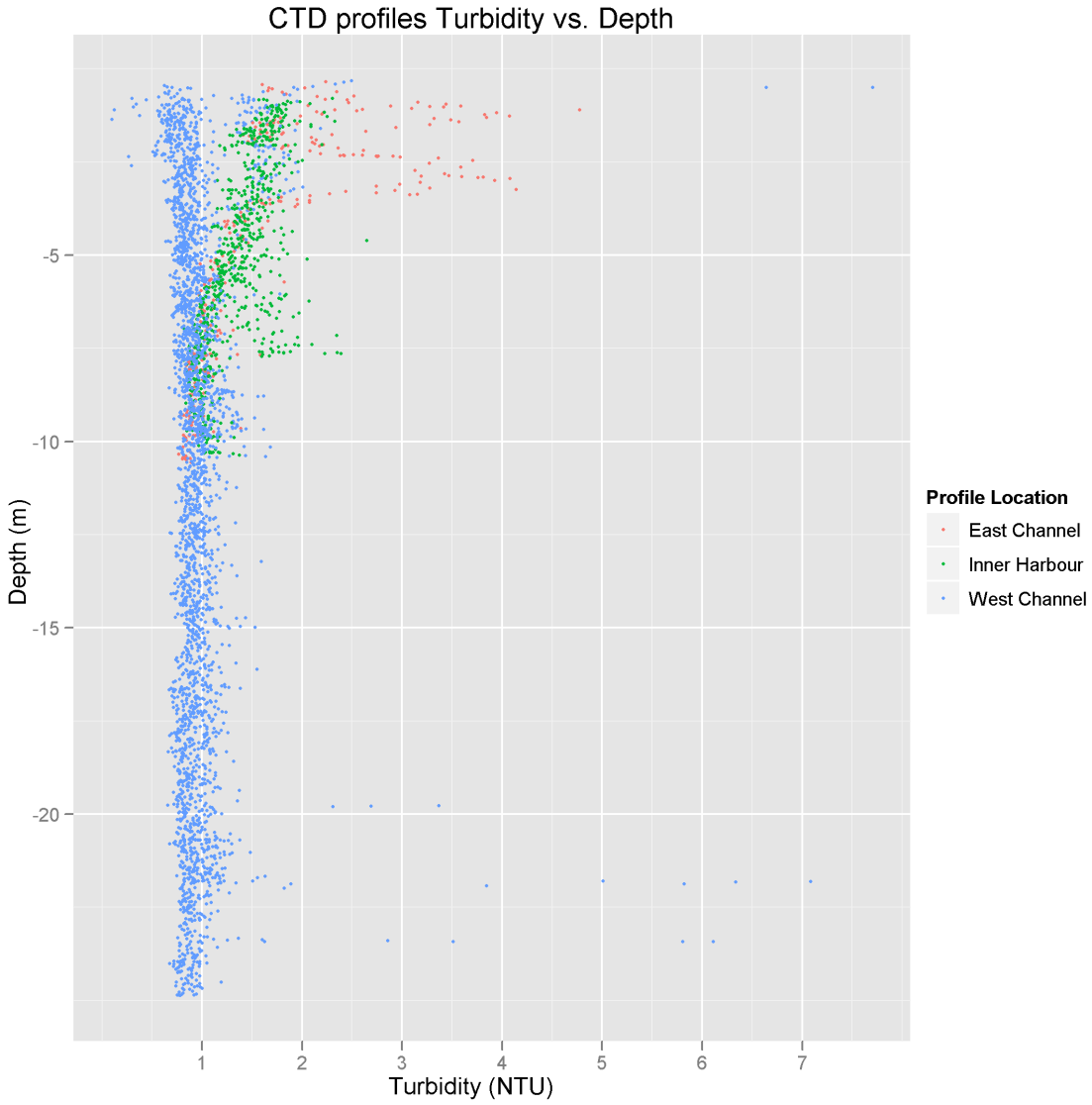

Figure A.17: Plot showing turbidity with depth grouped by the position in Koojesse Inlet of the profile. The water is generally extremely clear during the sampling times (all ¡ 10 NTU), but there seems to be a slight increase in turbidity in the eastern channel during both rising and falling tides. This could be due to the nearby river input off Apex, or the bathymetry of the narrow channel.

A.9 data directory structure

- /
  - video
    - underwater_video ..... *.dvi files of drag camera deployments
  - marine
    - ADCP
      - AD1 ..... raw Nortek aquadopp ADCP files
      - AD2+3
    - CTD
      - profiles ..... csv profile files
      - raw ..... *.hex files. Need RBR Ruskin software
    - TWR ..... *.hex files. Need RBR Ruskin software
  - surveys
    - RTK_GPS
      - 2009 ..... csv files. 2009 surveys
      - 2010
        - processed ..... csv files
        - raw ..... receiver raw files
          - base
          - rover
      - 2011
        - summer
          - processed ..... csv files
          - raw ..... receiver raw files
            - receiver
              - base
              - rover
        - winter
          - Processed ..... csv files
          - Raw ..... receiver raw files
    - shiptrack
      - garmin_gps ..... ESRI shapefiles
      - sounder
        - processed ..... csv files
        - raw ..... raw echosounder files
    - sidescan_sonar
      - CSF ..... *.csf files of all lines
      - mosaic ..... geoTiff mosaic of all lines
      - nav ..... ASCII navigation files
      - XTF ..... *.xtf files for all lines
  - sub_bottom ..... *.sgy files for all lines

A.10 Geodatabase structure

The geodatabase serves as a GIS data repository for the layers creted from raw data collected during this project. The benefit of housing all the data in a shared geodatabase is a common reference coordinate system shared between all GIS layers, as well as ease of access and security in future editing.

All data layers share the NAD83 CSRS reference datum and are projected into UTM coordinates in zone 19.

- Iqaluit.gdb
  - Survey_Other
    - ADCP_moorings_2011
    - bkwtr ..... RTK-GPS point elevation data on the main breakwater
    - bldgs ..... RTK-GPS survey points coastal infrastructure foundations
    - camera_transects_2011_line ..... underwater drop camera transects
    - ctd_2011 ..... CTD profile locations
    - RBR ..... location of TWR recorders 2010 deployments
    - RBR_2011 ..... location of TWR recorders 2011 deployments
    - smpl ..... location of 2010 sediment sampling sites
    - smpl_2011 ..... location of 2011 sediment sampling sites
    - smpl_grab2011 ..... location of 2011 grab sampling sites
    - stratabox_lines ..... location of sub-bottom profile lines
  - Surveys_Raw ..... RTK-GPS surveys for each day of surveying
  - Transects_2009 ..... RTK-GPS transect lines 2009
  - Transects_2010 ..... RTK-GPS transect lines 2010
  - Transects_2011 ..... RTK-GPS transect lines 2011
    - *_ext ..... transect extensions offshore using sounder
    - *_ice ..... transect lines on ice February 2011
  - iqaluit_ss_mosaic ..... Sidescan mosaic in Iqaluit harbour, 2011

A.11 References

Dale, J., Leech, S., McCann, S., & Samuelson, G. (2002). Sedimentary characteristics, biological zonation and physical processes of the tidal flats of Iqaluit, Nunavut. In

K. Hewitt, M. Byrne, M. English, & G. Young (Eds.) *Landscapes in Transition: Landform Assemblages and Transformations in Cold Regions*, vol. 111, (pp. 205–234). Dordrecht: Kluwer.

Dionne, J. (1992). Ring structures made by shore ice in a muddy tidal flat, St. Lawrence estuary, Canada. *Sedimentary geology*, *76*(3-4), 285–292.

Dionne, J., & Poitras, S. (1998). Lithologie des cailloux de la baie de Mitis, rive sud de l'estuaire maritime du Saint-Laurent (Québec): un exemple de transport glaciaire et glaciel complexe. *Géographie physique et Quaternaire*, *52*, 107–122.

Drake, J., & McCann, S. (1982). The movement of isolated boulders on tidal flats by ice floes. *Canadian Journal of Earth Sciences*, *19*(4), 748–754.

Hodgson, D. A. (2005). Quaternary Geology of Western Meta Incognita Peninsula and Iqaluit area, Baffin Island, Nunavut. Tech. rep., Geological Survey of Canada.

Leech, S. (1998). *The transport of materials by ice in a subarctic macrotidal environment, Koojesse Inlet, southeast Baffin Island*. Master's thesis, M.Sc. Thesis, University of Regina, Regina.

McCann, S., & Dale, J. (1986). Sea ice breakup and tidal flat processes, Frobisher Bay, Baffin Island. *Physical Geography*, *7*(2), 168–180.

McCann, S., Dale, J., & Hale, P. (1981). Subarctic Tidal Flats in Areas of Large Tidal Range, Southern Baffin Island, Eastern Canada. *Géographie physique et Quaternaire*, *35*(2), 183–204.

Statistics Canada (2012). Census Profile. 2011 Census. Online.

URL `http://www12.statcan.gc.ca/census-recensement/2011/dp-pd/prof/details/page.cfm?Lang=E&Geo1=POPC&Code1=0306&Geo2=PR&Code2=`

62&Data=Count&SearchText=Iqaluit&SearchType=Begins&SearchPR=01&B1=

All&Custom=&TABID=1